The Cell-Intrinsic and Microenvironmental Basis of Impaired B-Lymphopoiesis in Trisomy 21 Fetal Bone Marrow



Arundhati Wuppalapati

New College

University of Oxford

A thesis submitted for the degree of

Doctor of Philosophy

Long Vacation 2025

Acknowledgements

First and foremost, I would like to express my sincere and heartfelt gratitude to my supervisors, Anindita Roy, Irene Roberts and Bethan Psaila. Many thanks to Andi for her incredible dedication, patience and kindness, supporting me academically and personally over the past three years. Thank you to Irene for her infectious enthusiasm and pearls of wisdom. Thanks to Beth for the insight and sage advice. I feel very lucky to have had the opportunity to be supervised by such inspiring clinician scientists.

A heartfelt thanks goes to the members of the Roy lab past and present, for their help, guidance, and camaraderie; it has been a pleasure to work with them. Special thanks to Natalina Elliott, for taking me under her wing; Rebecca Ling and Joe Cross, for the best coffee dates; and Tom Jackson, Emily Neil, Lucy Hamer, Ananya Mahadevan and Alia Welsh for all the laughs between the lab work.

I have also benefitted greatly from the collaborative environment at the WIMM. Many thanks go to the FACS team, Paul Sopp, Craig Waugh, Sally-Ann Clark and Kevin Clark, for their all their help and expertise with FACS. Thanks to Alastair Smith, for his advice on bioinformatics. Many thanks to Abdullah Khan, Yuqi Shen, Natalie Jooss, Aideen O'Neill and Andrew MacIntyre for their insightful technical perspectives when optimising experiments.

I would also like to thank the HDBR team, and those that donated fetal samples, without whom this research could not take place. I am also extremely grateful for the funding provided by Cancer Research UK, which made this work possible.

Finally, I would like to thank my loved ones. Thank you to Emma, for being my closest friend from the first day as an undergraduate and always encouraging me to follow my dreams. Thank you to Paras, who never fails to cheer me up after a tough day. Thanks to my parents, Priti and Siddhartha, whose passion for medicine and dedication to their clinical practice always reminds me of why medical research matters. Many thanks to my sister, Aarushi, for always being in my corner. Lastly, I would like to express my deepest thanks to Matthew, for his endless patience, kindness, and unfailing support through the highs and lows of this PhD.

Declaration

I would like to gratefully acknowledge all collaborators who have generated data contributing to this project. The following is a comprehensive list of all data included in this thesis that was generated by others.

1. **Figures 3.7 - 3.15; Figures 3.17 - 3.18; Figures 3.22 - 3.25; Figures 3.28 - 3.30; Appendix Figures 1-8; Appendix Tables 1-14; and Appendix Tables 15 and 16**. These figures and tables show the results from an analysis of an integrated RNA-Seq dataset that includes some libraries previously generated by members of the Roy lab: Sorcha O'Byrne, Kate Murnane and Lucy Hamer; details are provided in Table 2.5 and Figure 2.8.

2. **Figures 3.16 - 3.20; and Appendix Tables 17-19**. These show the results of an analysis of an integrated NM and T21 fetal BM ATAC-Seq dataset, which includes some libraries previously generated by Sorcha O'Byrne and Kate Murnane, members of the Roy Lab. Details of this are provided in Table 2.6 and Figure 2.9.

Abstract

Background: Children with Down syndrome, which is caused by trisomy of chromosome 21 (T21), have an increased risk of developing B cell acute lymphoblastic leukaemia (ALL) and an increased frequency and severity of infections. Individuals with Down syndrome also have B lymphopenia and an increased frequency of autoimmune diseases often in association with circulating self-reactive antibodies. Our lab has previously shown this striking reduction in B cell frequency can be traced back to fetal life. B lymphopoiesis is severely reduced in fetal liver and, to an even greater extent, in fetal bone marrow (BM) which is the principal site of B cell production during fetal life. However, the molecular mechanisms of exactly how T21 impairs fetal B lymphopoiesis remain unclear. Additionally, B lymphopoiesis is supported by the BM haematopoietic niche, but in Down syndrome these niche cells also harbour T21, and very little is known about the fetal BM haematopoietic niche. Understanding the mechanisms underpinning impaired B lymphopoiesis in T21 fetal BM are an important step in understanding why children with Down syndrome are predisposed to ALL, infection and autoimmune disease.

Aims: The aims of this project were to investigate the cellular and molecular mechanisms underpinning impaired B lymphopoiesis in T21 fetal BM, by addressing the following questions:

1. What are the HSPC-intrinsic factors contributing to impaired B lymphopoiesis in T21 fetal BM?

2. How does the T21 fetal BM microenvironment contribute to impaired B lymphopoiesis in T21?

HSPC-intrinsic differences in T21 fetal bone marrow. Detailed multi-parameter flow cytometry identified a striking decrease in the frequency of fetal-specific lymphoid progenitors (Early Lymphoid Progenitors, PreProB progenitors and an early myelolymphoid population recently identified in our lab that we have named "PreELP/GMP") in T21 BM. There was a concurrent expansion in myeloid progenitors, pinpointing a block in B lymphopoiesis and a lineage skew downstream of lymphomyeloid progenitors LMPP. Functionally, T21 fetal BM HSC, MPP and LMPP showed a striking reduction in B lymphoid output *in vitro*. Transcriptomically, T21 fetal lymphoid progenitors failed to activate B lymphoid

programmes normally and to repress alternative lineage programmes. Additionally, T21 fetal BM lymphoid progenitors showed an increased inflammatory response signature by Gene Set Enrichment Analysis (GSEA).

Effects of T21 fetal BM stromal cells on B cell production *in vitro*. Functionally, T21 fetal BM mesenchymal stromal cells (MSC) were less able to support B lymphopoiesis *in vitro* compared to their normal counterparts. However, normal fetal BM MSC failed to rescue the intrinsic defects in T21 fetal BM HSPC. Transcriptomic profiling and GSEA of fetal BM MSC expanded *in vitro* showed that T21 fetal BM MSC had an increased inflammatory response signature compared to normal fetal BM MSC. This may explain the differences in the functional behaviour of T21 BM MSC but taken together my data suggest that T21 fetal BM MSC are likely to play a modest role in the impaired B lymphopoiesis in T21 fetal BM.

Differences in haematopoietic niche composition in T21 fetal bone marrow. Multiparameter flow cytometry of the whole fetal BM stromal compartment identified a possible reduction in osteoMSC frequency, and by scRNA-Seq, T21 MSC appeared to be primed towards adipogenesis rather than osteogenesis. Single cell RNA sequencing (scRNA-Seq) suggests that osteoMSC may be a major source of supportive B lymphopoietic cytokines IL7, IGF2 and CXCL12 in normal fetal BM. Although T21 fetal BM osteoMSC also expressed these genes, they were all expressed at significantly lower levels compared to normal fetal BM suggesting that reduced niche-derived support for B lymphopoiesis in T21 fetal BM may be due to quantitative and qualitative changes in the osteoMSC population. Analysis of the scRNA-Seq data also showed that macrophages were overrepresented in T21 fetal BM by scRNA-Seq, and that these cells were a source of the proinflammatory cytokine TNFα. In preliminary experiments I was able to show that TNFα severely reduced B lymphoid output from normal fetal BM HSPC in co-culture assays even at low concentrations.

Conclusions: B lymphopoiesis is severely impaired in T21 fetal BM. This work has uncovered three potential contributing mechanisms to this: a concurrent failure to activate B lymphoid programmes and silence non-B lymphoid differentiation programmes in T21 fetal BM lymphoid progenitors; decreased osteoMSC-derived B lymphopoietic support, and increased TNFα signalling originating from increased myeloid cells in T21 fetal BM.

Contents

List of Figures **xi**

List of abbreviations **xv**

1 Introduction **1**
1.1 Haematopoiesis through ontogeny 1
1.1.1 The haematopoietic hierarchy 2
1.1.2 Overview of lymphopoiesis in fetal and adult life 5
1.1.3 B lymphopoiesis in fetal and adult life 8
1.1.4 T lymphopoiesis in fetal and adult life 13
1.1.5 NK lymphopoiesis in fetal and adult life 15
1.1.6 Myelopoiesis in fetal and adult life 18
1.2 The haematopoietic niche 21
1.2.1 The fetal liver haematopoietic niche 21
1.2.2 The BM haematopoietic niche 22
1.2.3 The cellular components of the BM niche 25
1.3 Down syndrome 32
1.3.1 Trisomy of chromosome 21 33
1.3.2 Haematological abnormalities in Down syndrome 34
1.3.3 T21 and autoimmune disease 38
1.3.4 Haematological malignancies in Down syndrome 38
1.3.5 The haematopoietic niche in Down syndrome 40
1.4 Hypothesis and aims 42

2 Methods **43**
2.1 Fetal bone marrow samples 43
2.2 Sample processing, cryopreservation and thawing 45
2.3 Flow cytometry analysis and sorting 46
2.3.1 FAC-Sorting (FACS) of fetal BM HSPC 46
2.3.2 Flow cytometry of whole fetal bone 48
2.3.3 Intracellular flow cytometry 49
2.4 Co-cultures on MS5 stroma to assess B lymphoid potential of fetal BM HSPC 52

2.4.1 TNFα ELISA 54
2.5 Derivation and characterisation of fetal BM MSC 54
2.6 Osteolineage differentiation of fetal BM MSC 56
2.6.1 Alizarin Red staining 56
2.7 MSC co-cultures to assess stromal support of B lymphopoiesis . . . 56
2.8 Analysis of MSC-secreted cytokines 58
2.9 Bulk RNA-Seq of derived MSC 59
2.10 Bulk RNA-Seq of fetal BM HSPC populations 59
2.11 RNA-Seq analysis 62
2.11.1 Differential expression analysis and and GSEA (Gene Set Enrichment Analysis) 62
2.11.2 Weighted Gene Correlation Network Analysis 63
2.11.3 Differential exon usage analysis 63
2.12 Assay for Transposase-Accessible Chromatin using sequencing (ATAC-Seq) of fetal BM HSPC 64
2.13 ATAC-Seq Analysis 65
2.13.1 Differential accessibility analysis 65
2.13.2 Motif enrichment analysis 66
2.13.3 Visualisation of peaks 66
2.14 Analysis of scRNA-Seq datasets 66
2.14.1 Integration of scRNA-Seq datasets 66

3 Results I: the impact of T21 on the gene expression and chromatin accessibility of fetal BM progenitors 73
3.1 Background and aims 73
3.2 Immunophenotypic characterisation of T21 fetal BM HSPC 75
3.3 T21 HSPC show a B lymphopoietic defect and skewed differentiation towards myeloid and NK fates 79
3.4 Trisomy 21 results in altered gene expression and chromatin accessibility in fetal BM HSPC 80
3.4.1 Expression of key lymphoid genes 80
3.4.2 Expression of B lymphoid genes 82
3.4.3 Expression of T/NK lymphoid genes 86
3.4.4 Expression of myeloid genes 91
3.4.5 Differential gene expression and chromatin accessibility . . . 97
3.4.6 Differences in chromatin landscape in T21 fetal BM HSPC . 106
3.4.7 Differences in gene expression in T21 fetal BM HSPC 112
3.4.8 Inflammatory signalling in T21 fetal BM 120
3.5 Summary and discussion 124
3.5.1 Future work 127

4 Results II: Characterising the haematopoietic support provided by T21 fetal BM MSC 129
4.1 Background and aims . . . 129
4.2 Haematopoietic support of fetal BM MSC *in vitro* . . . 130
4.2.1 Optimising an *in vitro* MSC co-culture system . . . 130
4.2.2 The impact of T21 fetal BM MSC on normal B lymphopoiesis 138
4.2.3 Molecular profiling of NM and T21 fetal BM MSC . . . 141
4.2.4 Crossover fetal BM MSC co-culture assays . . . 148
4.3 Summary and discussion . . . 152
4.3.1 Future work . . . 154

5 Results III: The T21 fetal BM microenvironment 155
5.1 Background and aims . . . 155
5.2 Comparative single cell transcriptome profiling of NM and T21 fetal BM cells . . . 156
5.3 Differences in niche composition between NM and T21 fetal BM . . 158
5.3.1 Differences in osteolineage differentiation in T21 fetal BM . 163
5.3.2 Functional validation of transcriptomic findings . . . 168
5.4 Understanding the role of haematopoietic cells that form part of the fetal BM microenvironment . . . 171
5.4.1 Inflammatory TNFα signalling in T21 fetal BM . . . 174
5.4.2 Functional validation of the role of TNFα in human fetal B lymphopoiesis . . . 179
5.5 Summary and discussion . . . 182
5.5.1 Future work . . . 184

6 Discussion 185
6.1 The impact of T21 on fetal BM B lymphopoiesis . . . 186
6.2 The impact of T21 on stromal support for fetal BM B lymphopoiesis 189
6.3 The impact of inflammation in T21 fetal BM on B lymphopoiesis . 190
6.4 Future work . . . 191
6.5 Conclusions . . . 192

Appendices
.1 Expression of lineage-specific genes by RNA-Seq in NM fetal BM . 195
.2 Differential gene expression in fetal BM HSPC . . . 203
.2.1 Top 50 DEG between NM and T21 fetal BM HSPC . . . 203
.2.2 Differentially expressed genes between NM and T21 HSPC on chromosome 21 . . . 215

.2.3 Genes associated with the B lymphopoietic module by WGCNA in NM and T21 fetal BM HSPC 220
.3 Differential chromatin accessibility in T21 fetal BM HSPC 222
.4 Differential gene expression in fetal BM MSC 233

References **239**

List of Figures

1.1 Models of the haematopoietic hierarchy 4
1.2 Lymphopoiesis in adult life 7
1.3 A proposed model of fetal B lymphopoiesis 10
1.4 Myeloid fate decisions 19
1.5 The BM niche for haematopoiesis 23

2.1 Sort gating for fetal BM HSPC 47
2.2 Flow cytometry analysis of whole fetal BM 48
2.3 Intracellular flow cytometry for TNFα 49
2.4 Gating strategy for MS5 co-culture assays. 53
2.5 Characterisation of derived MSC. 55
2.6 Gating strategy for MSC differentiation into osteolineage cells . . . 56
2.7 Gating strategy used to analyse output from MSC co-culture experiments 57
2.8 Initial analysis of RNA-Seq libraries to check for a batch effect . . . 62
2.9 Initial analysis of ATAC-Seq libraries to check for a batch effect . . 65
2.10 Integration of scRNA-Seq datasets using Harmony 67
2.11 Reannotation of published datasets 68
2.12 Composition of integrated scRNA-Seq dataset 69
2.13 Correcting for dropout with ALRA 70

3.1 Frequency of HSPC in the fetal-like pathway of B lymphopoiesis in fetal BM 75
3.2 Frequency of HSPC in the adult-like pathway of B lymphopoiesis in fetal BM 76
3.3 Frequency of CD19+ B cells in fetal BM 77
3.4 Frequency of myeloid progenitors in fetal BM 77
3.5 Proposed model of altered B lineage differentiation in T21 fetal BM HSPC 78
3.6 *In vitro* differentiation assay of NM and T21 fetal BM HSC, MPP and LMPP 79
3.7 Expression of genes with a known role in lymphoid specification . . 81

3.8 Expression genes with a known role in B lymphopoiesis 83
3.9 Expression genes with a known role in B cell development 85
3.10 Expression of genes with a known role in T lymphopoiesis 87
3.11 Expression of genes with a known role in NK lymphopoiesis 89
3.12 Expression of genes with a known role in myeloid specification . . . 92
3.13 Expression of genes with a known role in monopoiesis 94
3.14 Expression of genes with a known role in granulopoiesis 95
3.15 PCA of the top 1000 most variably expressed genes by RNA-Seq . . 99
3.16 PCA of the top 1000 most variably accessible peaks by ATAC-Seq . 100
3.17 T21 results in genome wide changes in gene expression and chromatin accessibility 102
3.18 Differential chromatin accessibility and gene expression on chromosome 21 in T21 HSC, MPP and LMPP 104
3.19 Differentially accessible peaks in T21 HSC, MPP and LMPP 106
3.20 RUNX1 chromatin in T21 HSC, MPP and LMPP 107
3.21 Differentially accessible transcription factor motifs in T21 HSPC . . 108
3.22 Differential *RUNX1* exon usage in T21 fetal BM HSC, MPP and LMPP 110
3.23 Differentially expressed genes in T21 HSPC 112
3.24 Changes in gene expression along the lymphoid differentiation trajectory in NM and T21 fetal BM 114
3.25 Weighted gene correlation network analysis of RNA-Seq data from NM and T21 fetal BM HSPC 116
3.26 HSC, MPP, LMPP and ELP clusters by scRNA-Seq 117
3.27 Differential inferred transcription factor activity in fetal BM LMPP and ELP 119
3.28 Inflammatory response gene sets are enriched in T21 HSPC 120
3.29 T21 lymphoid progenitors have increased expression of genes associated with TNFα signalling 121
3.30 Fold change in expression of TNFα response genes on NM and T21 fetal BM LMPP 123
3.31 Potential mechanisms of impaired B lineage commitment in T21 fetal BM 126

4.1 Fetal BM MSC co-cultures support a mostly myeloid cell output . . 133
4.2 Optimisation of the MSC co-culture system 134
4.3 Optimisation of the MSC co-culture cytokines 135
4.4 Supplementation of MSC co-cultures with SCF improves B cell output from HSC, MPP and LMPP 137

4.5 Haematopoietic cell output of NM fetal BM HSC, MPP and LMPP on NM and T21 fetal BM MSC. 139
4.6 Absolute numbers of B cells, Lin+ myeloid cells and NK cells produced by NM fetal BM HSC, MPP and LMPP co-cultured with either NM or T21 fetal BM MSC. 140
4.7 PCA of the top 500 most variably expressed genes in derived fetal BM MSC 141
4.8 The impact of T21 on fetal BM MSC gene expression. 142
4.9 T21 fetal BM MSC show an enrichment for inflammatory response gene sets. 143
4.10 T21 fetal BM MSC overexpress the Notch ligand JAG1 145
4.11 Differences in cytokine secretion in T21 fetal BM MSC compared to NM fetal BM MSC 146
4.12 NM fetal BM MSC are unable to rescue T21 haematopoiesis. 149
4.13 NM fetal BM MSC are unable to rescue T21 haematopoiesis. 150
4.14 T21 cell-intrinsic differences in lymphoid potential of fetal BM HSC, MPP and LMPP predominate over extrinsic effects mediated by T21 fetal BM MSC 151

5.1 scRNA-Seq analysis of NM and T21 fetal BM 157
5.2 UMAP of NM and T21 fetal BM by refined clusters. 158
5.3 Frequency of stromal and endothelial cells in NM and T21 fetal BM 159
5.4 Subsets of stromal cells in native NM and T21 fetal BM 160
5.5 Frequency of osteoMSC and osteoblasts assessed by flow cytometry in gestation matched NM and T21 fetal BM. 162
5.6 scRNA-Seq trajectory inference analysis for fetal BM MSC towards osteogenic and adipogenic fates 164
5.7 Inference of transcription factor activity governing osteogenic or adipogenic fate from gene regulatory networks in fetal BM MSC . . 165
5.8 Gene expression of lymphopoietic cytokines by fetal BM stromal cells 167
5.9 Osteo-lineage differentiation of NM and T21 fetal BM MSC *in vitro* 169
5.10 Frequency of haematopoietic cells in NM and T21 fetal BM 171
5.11 Differences in composition of haematopoietic cells in T21 fetal BM . 172
5.12 Frequency of NK cells and monocytes in NM and T21 fetal BM mononuclear cells 173
5.13 TNF signalling in fetal BM as inferred by gene expression 175
5.14 Sources and targets of TNFα in fetal BM 176
5.15 TNFα production in fetal BM 177
5.16 Co-cultures of NM fetal BM HSC, MPP and LMPP in the presence of TNFα 180

5.17 Secreted TNFα in NM and T21 fetal BM LMPP co-culture supernatants 181

1 Appendix: Expression of genes with a known role lymphoid specification 195
2 Appendix: Expression genes with a known role in B lymphopoiesis . 196
3 Appendix: Expression genes with a known role in B cell development 197
4 Appendix: Expression of genes selected for their role in T lymphopoiesis 198
5 Appendix: Expression of genes selected for their role in NK lymphopoiesis 199
6 Appendix: Expression of genes with a known role in myeloid specification 200
7 Appendix: Expression of genes with a known role in monopoiesis . . 201
8 Appendix: Expression of genes with a known role in granulopoiesis . 202

List of abbreviations

αMEM . . . . α-Minimum Essential Medium

AGM . . . . . Aorta-Gonad-Mesonephros

ALL . . . . . Acute Lymphoblastic Leukaemia

ANOVA . . . . Analysis of Variance

ATAC-Seq . . Assay for Transposase-Accessible Chromatin Sequencing

BCR . . . . . B Cell Receptor

BM . . . . . Bone Marrow

CLP . . . . . Common Lymphoid Progenitor

CMP . . . . . Common Myeloid Progenitor

DAP . . . . . Differentially Accessible Peak

DEG . . . . . Differentially Expressed Gene

DS . . . . . Down Syndrome

ELISA . . . . . Enzyme-Linked Immunosorbent Assay

ELP . . . . . Early Lymphoid Progenitor

FACS . . . . . Fluorescence Activated Cell Sorting

FBS . . . . . Fetal Bovine Serum

FC . . . . . Fold Change

FDR . . . . . False Discovery Rate

FMO . . . . . Fluorescence Minus One

GMP . . . . . Granulocyte/Macrophage Progenitor

GSEA . . . . . Gene Set Enrichment Analysis

HDBR . . . . Human Developmental Biology Resource

HSC . . . . . Haematopoietic Stem Cell

HSC . . . . . Haematopoietic Stem and Progenitor Cells

IFN . . . . . Interferon

IL . . . . . Interleukin

ILC . . . . . Innate Lymphoid Cell

iPSC . . . . . induced Pluripotent Stem Cell

LMPP . . . . . Lymphoid-primed Multipotent Progenitor

LPS . . . . . Lipopolysaccharide

MEP . . . . . Megakaryocyte/Erythroid Progenitor

MFI . . . . . Mean Fluorescence Intensity

ML-DS . . . . Myeloid Leukaemia of Down Syndrome

MLP . . . . . Multi-Lymphoid Progenitor

MNC . . . . . Mononuclear Cell

MPP . . . . . Multipotent Progenitor

MSC . . . . . Mesenchymal Stromal Cell

NES . . . . . Normalised Enrichment Score

NK . . . . . Natural Killer

NM . . . . . non T21; Normal

PBS . . . . . Phosphate Buffered Saline

PCA . . . . . Principal Component Analysis

PCR . . . . . Polymerase Chain Reaction

PMA . . . . . Phorbol 12-Myristate 13-Acetate

RNA-Seq . . . RNA-Sequencing

scATAC-Seq . Single Cell Assay for Transposase-Accessible Chromatin Sequencing

scRNA-Seq . . Single Cell RNA-Sequencing

SD . . . . . Standard Deviation

SEM . . . . . Standard Error of the Mean

TAM . . . . . Transient Abnormal Myelopoiesis

TNFα . . . . . Tumour Necrosis Factor-α

T21 . . . . . Trisomy 21

UMAP . . . . Uniform Manifold Approximation and Projection

VST . . . . . Variance Stabilising Transformation

WGCNA . . . Weighted Gene Correlation Network Analysis

1 Introduction

1.1 Haematopoiesis through ontogeny

The yolk sac is the earliest site of haematopoiesis in humans, generating erythroblasts to meet the increasing oxygen demands of the growing embryo. Early studies imaging human embryos observed primitive nucleated erythroblasts, developing megakaryocytes and macrophages[1, 2] at day 18 post conception. Recent single cell studies in human embryos at around 2-3 post-conception weeks (PCW) supports and extends these early observations[3].

The second wave of haematopoiesis in the yolk sac generates erythro-myeloid progenitors (EMP)[4]. Whether yolk sac haematopoiesis contributes to lifelong haematopoiesis in humans has been a matter of debate for many years[5–7]. These EMP seed the developing embryonic organs[8, 9], and some of their progeny may become lifelong tissue-resident macrophages in some tissues[10, 11], reviewed in [12]. The presence of haematopoietic CD34+CD45+ cells in the human fetal liver at 3-4 PCW, prior to the emergence of haematopoietic stem cells (HSC), was first described almost thirty years ago[13]. More recently, scRNA-Seq of human yolk sac cells has suggested that yolk sac-derived myeloid progenitors may seed the fetal liver prior to HSC emergence[14].

The next wave of haematopoiesis occurs at 4-5 PCW in humans, and generates HSC, as recently reviewed in [15]. The aorta-gonad-mesonephros (AGM) region is the anatomical site at which HSC emergence occurs. Definitive HSC develop within intra-aortic haematopoietic clusters[13]. The gene *RUNX1* is essential in the emergence of HSC from haemogenic endothelial cells[16, 17].

These definitive HSC generated in the AGM migrate to the fetal liver, the main site of haematopoiesis in the first and second trimesters[18]. The fetal BM is colonised from 11 PCW, and contributes to fetal haematopoiesis from then onwards[19]. The fetal BM is the primary site for B lymphopoiesis from the second trimester onwards[20, 21].

After birth, the primary site of haematopoiesis is the BM. There are a few models of the transition between fetal and adult haematopoiesis based on murine and human data, reviewed in [22, 23]. Briefly, the switch to adult haematopoiesis may come from distinct developmental waves of HSPC emergence, and that fetal HSPC are gradually replaced by postnatal HSPC in postnatal life[24–27]; or a progressive maturation of HSC gene expression programmes, resulting in the gradual loss of fetal-like gene expression programmes in postnatal life[28–30].

There are a number of molecular and functional differences between HSC in fetal and adult life. Fetal HSC are more proliferative[21, 31–33], and show an increased capacity for self-renewal[34, 35]. HSC also show biases in differentiation through ontogeny, with fetal liver HSC being biased towards erythroid output[18, 21], fetal BM HSC showing a B lineage bias in comparison[20, 36], while adult BM HSC show a myeloid lineage bias[37].

1.1.1 The haematopoietic hierarchy

The accepted definition of a HSC is that these cells are able to self-renew, to differentiate into all haematopoietic lineages and to reconstitute long-term haematopoiesis *in vivo* when transplanted into immunodeficient mice[38, 39]. Using this definition, HSC have been demonstrated both in fetal liver and in fetal BM in humans[40–45]. HSC are found at the apex of the traditional haematopoietic hierarchy, and give

rise to multipotent progenitors (MPP), which do not have the capacity to self renew[46, 47]. The traditional haematopoietic hierarchy (Figure 1.1A) is a step-wise differentiation model in which different stages are defined by specific cell surface markers, and validated by functional, often colony forming unit and transplantation, assays[48]. In this classical hierarchical model, HSC can self-renew, or differentiate in a stepwise manner from multi-, to oligo-, to bi- and uni-potent progenitors, before terminally differentiating. The lymphoid and myeloid differentiation pathways are described in more detail in sections 1.1.3-1.1.6 below.

The advent of high throughput single cell methods has complemented our understanding of haematopoiesis. Gene expression data and chromatin accessibility of single cells can be aligned to the classical model of haematopoiesis with the use of technologies such as CITE-Seq. These multiomic approaches applicable at a single cell level have revealed substantial heterogeneity within populations once assumed to be uniform by traditional functional experiments and immunophenotyping, resulting in the continuous refinement of the haematopoietic hierarchy[49, 50]. This has led to a more flexible perspective of haematopoiesis in which cells exist along a continuous differentiation trajectory, and stages of the classical haematopoietic hierarchy reflect a snapshot within this continuum. Elements of this too have been reported to change through ontogeny, with a progressive reduction in the ratio of multi- and oligo- to uni-potent progenitors over the course of human development, with adult BM containing negligible numbers of oligopotent progenitors[51].

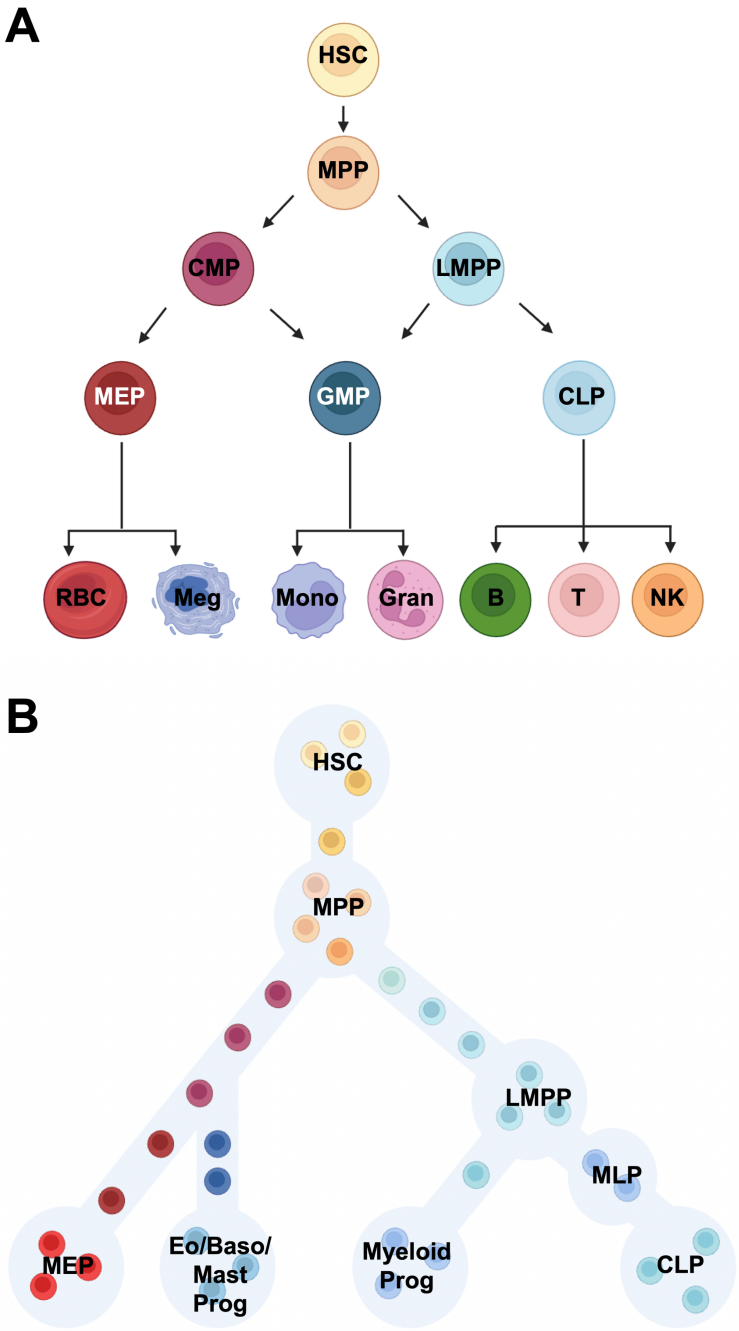

Figure 1.1: Models of the haematopoietic hierarchy. (A) The classical model of the adult haematopoietic hierarchy based on functional human and murine studies, adapted from [52]. (B) A more refined model of the haematopoietic hierarchy in HSPC, characterised by gradual transitions between HSPC and a gradual loss of multipotency, adapted from [52]. HSC, haematopoietic stem cell; MPP, multipotent progenitor; LMPP, lymphoid primed multipotent progenitor; CMP, common myeloid progenitor; MEP, megakaryocyte erythroid progenitor; GMP, granulocyte macrophage progenitor; CLP, common lymphoid progenitor; RBC, red blood cell; Meg, megakaryocyte; Mono, monocyte; Gran, granulocyte; B, B lymphocyte; T, T lymphocyte; NK, Natural Killer Lymphocyte; Prog, Progenitor; Eo/Baso/Mast, Eosinophil/Basophil/Mast.

Lineage fate decisions in haematopoiesis

Haematopoietic lineage commitment is orchestrated by the interplay between transcription factors and extrinsic cytokine signals which together govern commitment to a certain lineage. Transcription factors play central roles in the activation of lineage specific differentiation programmes, and the concurrent repression of alternative cell fate differentiation programmes. Cytokine signalling can result in the transcription of lineage associated transcription factors and contribute to haematopoietic fate[53]. This multi-stage process governed by transcription factors and their associated gene networks results in gene expression changes leading to lineage specification, and ultimately commitment[54–58].

Data from bulk and scATAC-Seq has suggested that changes in chromatin accessibility precede changes in gene expression in HSPC[59, 60]. These multiomic studies provide evidence that despite the undifferentiated state of multipotent HSPC, low-level changes in chromatin accessibility and gene expression of lineage associated genes can prime them to differentiate towards a specific lineage, upstream of the classical lineage commitment decision point[61–64].

1.1.2 Overview of lymphopoiesis in fetal and adult life

Lymphopoiesis in adult life

The lymphopoietic hierarchy in adult life in humans is summarised in Figure 1.2; HSC differentiate into multipotent progenitors (MPP), lymphoid-primed multipotent progenitors (LMPP)[65, 66], multi-lymphoid progenitors (MLP)[67, 68], and common lymphoid progenitors (CLP). CLP can give rise to B, T, NK and dendritic cells[54]. B and NK lymphopoiesis occurs in the BM in adult life, while T lymphopoiesis is restricted to the thymus.

LMPP were first described in humans in cord blood and BM mononuclear cells, with the immunophenotype Lin-CD34+CD38-C90-CD45RA+[47], and are present in fetal[18, 69, 70] and adult life[18, 68–71]. More detailed characterisation of this population refined the LMPP immunophenotype to Lin-CD34+CD38-C90-CD45RA+CD10-[68, 71].

LMPP are thought to give rise to MLP (Lin-CD34+CD38-CD90-CD45RA+CD10+) in adult life, though this has not yet been demonstrated functionally[67, 68]. MLP have been characterised well *in vitro* and *in vivo*, giving rise to B, T and NK lineages, while retaining myeloid potential[67, 68].

CLP were first described in human adult BM thirty years ago as a population that could give rise to B, T, NK and dendritic cells *in vitro*[54], and have since been extensively characterised in human and murine adult BM[72–75]. We, and others[54, 73, 76] use the immunophenotype Lin-CD34+CD38+CD10+ to define CLP. While CLP have been described in human cord blood[76, 77], there is limited functional evidence about their existence in human fetal life[54].

Lymphopoiesis in fetal life

Several studies have shown that there are very significant differences between lymphopoiesis in fetal life compared to post-natal life[20, 23, 78, 79]. In human fetal liver and BM, an IL7R-expressing lymphoid progenitor, termed early lymphoid progenitor (ELP), has been described, and shown functionally to produce B, T and NK cells[20, 80–83]. These ELP in fetal liver and BM differ immunophenotypically from CLP by the lack of expression of CD10[20], and are exceedingly rare in postnatal life[20]. In addition to ELP, recent unpublished work in our research group has characterised a novel lymphoid progenitor upstream of ELP and downstream of LMPP, with the immunophenotype Lin-CD34+CD38+CD127-CD10-CD123-CD45RA+. Based on their functional output *in vitro*, they have provisionally been named PreELP/GMP. The main fetal B lymphoid differentiation pathway is shown in Figure 1.3.

In fetal life, B and NK lymphopoiesis occurs in both the fetal liver[18] and the BM[36], while T lymphopoiesis occurs in the thymus, following migration of lymphoid progenitors from the fetal liver and BM to the thymus[84].

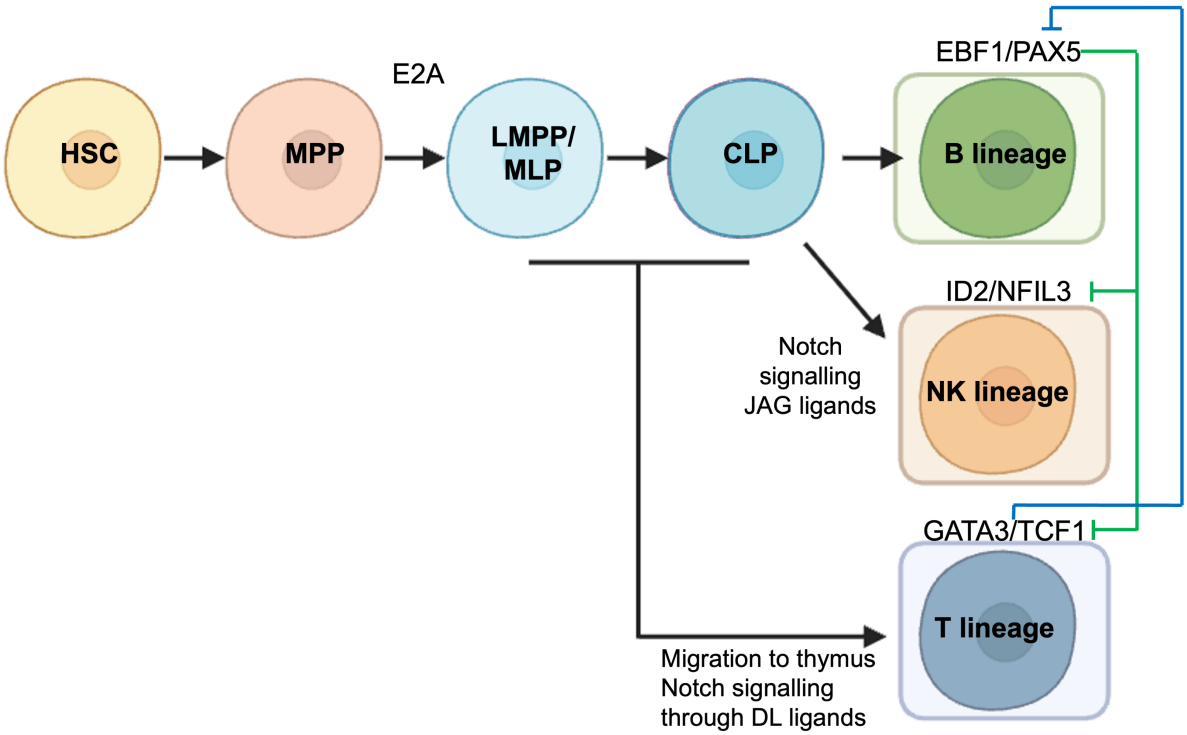

Figure 1.2: Lymphopoiesis in adult life, with the key transcription factors governing lymphoid fate decisions. Adapted from [85]. Lymphoid progenitors can differentiate into B cells, NK cells or T cells. T cell differentiation requires migration to the thymus and Notch signalling in the thymus activates the T cell programme, orchestrated by GATA3 and TCF1. The central transcription factors in the B lymphoid programme are EBF1 and PAX5. The key transcription factors in the NK lineage programme are ID2 and NFIL3, which can also be activated by Notch signalling. Activation of one programme represses alternative lineage programmes. Citations in text.

1.1.3 B lymphopoiesis in fetal and adult life

Adult B lymphopoietic progenitors

In adult BM, commitment to the B lineage occurs immediately downstream of CLP with ProB progenitor cells representing the first B lineage restricted population, as reviewed in [86]. ProB progenitors are defined both by their immunophenotype (CD45+CD34+CD19+CD10+) and by their functional output (solely B cells)[86].

Transcriptional control of adult B lymphopoiesis

CLP are directed towards B lineage fates by the action of transcription factors EBF1 and PAX5 as reviewed extensively in [56, 85]. Lymphoid specification transcription factors such as RUNX1, Ikaros and TCF3 act upstream of this to create a chromatin landscape permissive for the action of EBF1 and PAX5, which subsequently activate B lymphoid programmes[56, 64, 87–89].

B lymphopoiesis also depends on the action of cytokines. Of these the best studied are FLT3L and IL7. In mice, the combined loss of the receptors to both these cytokines, *Flt3* and *Il7r* respectively, results in a complete block in fetal and adult B lymphopoiesis[90]. Signalling through FLT3 upregulates the expression of *Il7ra* in murine HSPC[91], and signalling through IL7Rα in adult mice results in the upregulation of *Ebf1*, facilitating the differentiation of CLP to ProB[92–95]. In humans, though IL7 supports B lymphopoiesis, it is not essential for B lymphopoiesis to occur. Patients with SCID arising from mutations in *IL7RA*, have normal numbers of B cells, though B cell function is impaired[96, 97]. Additionally, *in vitro* supplementation of IL7 to human cord blood and adult BM derived HSPC increases B lymphoid output[98].

Fetal B lymphopoiesis

There are some important differences between fetal and adult B lymphopoiesis, notably, the sites of B lymphopoiesis, the B lymphoid progenitors, and in cytokine control of B lymphopoiesis.

Fetal B lymphopoiesis occurs in the fetal liver and BM in humans. By 7 PCW, B progenitors are present in the embryonic liver, and four weeks later, in fetal BM[20]. The BM is the primary site of B lymphopoiesis from the second trimester onwards, as evidenced by a much greater frequency of B progenitors and B cells compared to fetal liver[20].

Fetal B lymphopoietic progenitors and B cells

Our lab has previously identified a fetal-specific B progenitor, that we termed a PreProB progenitor, that lies immediately upstream of ProB progenitors, and downstream of ELP. PreProB progenitors were defined immunophenotypically as CD34+CD19+CD10-[69, 70, 99]. Their functional output both *in vitro* and *in vivo* was restricted to B cells and their gene expression pattern was consistent with this, expressing B lymphoid programmes[20].

This, alongside, ongoing work in our lab has led to the refinement of the fetal B lymphopoietic hierarchy. We propose that PreELP/GMP (a yet to be fully characterised fetal-specific lymphoid progenitor identified in our group), ELP, PreProB represent the main fetal B lymphopoietic pathway. A more adult-like pathway, featuring MLP and CLP is also active in fetal life, but the fetal-like pathway dominates fetal B lymphopoiesis[20]. This proposed model, alongside the key transcription factors governing B lymphoid fate decisions are summarised in Figure 1.3.

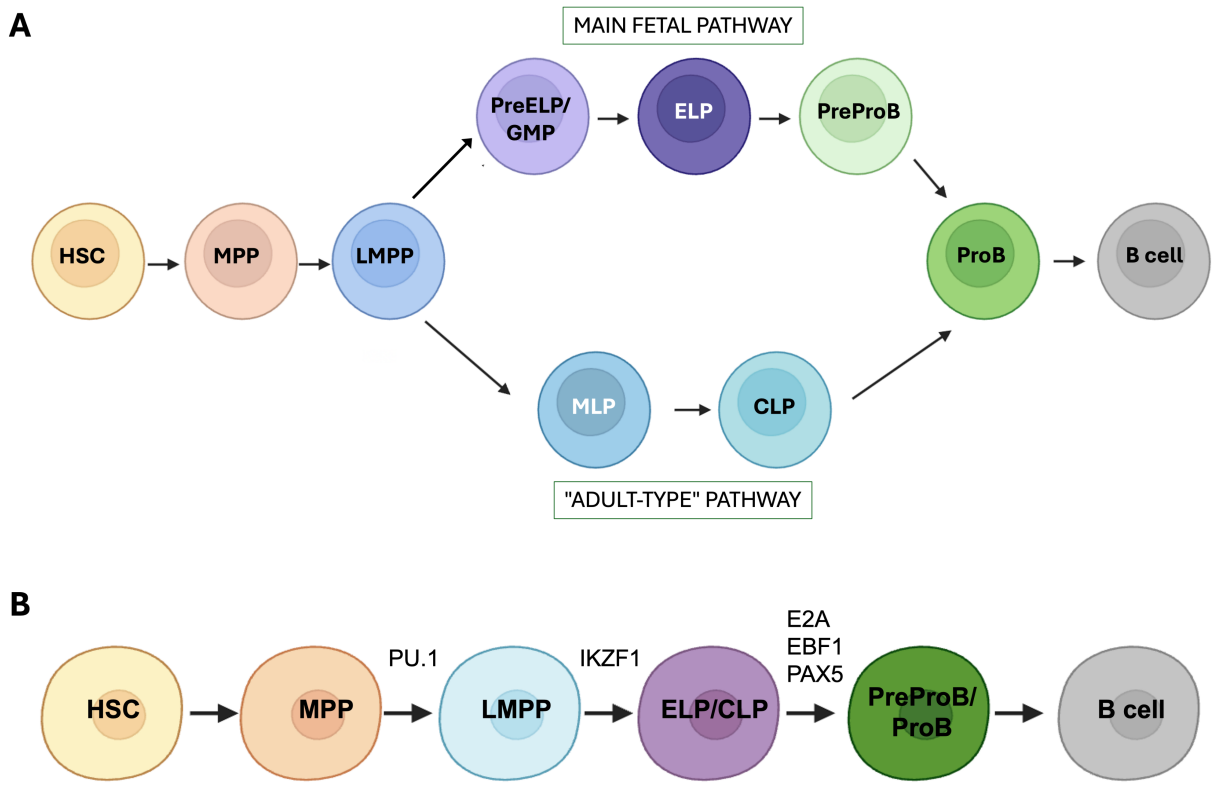

Figure 1.3: A proposed model of fetal B lymphopoiesis. (A) Fetal-like and adult-like pathways are active in fetal life but the fetal pathway dominates fetal B lymphopoiesis. (B) Transcription factors governing B lineage fate decisions, citations in text. HSC, haematopoietic stem cell; MPP, multipotent progenitor; LMPP, lymphoid-primed multipotent progenitor; MLP, multilymphoid progenitor; PreELP/GMP, pre-early lymphoid progenitor/ granulocyte macrophage progenitor; ELP, early lymphoid progenitor; CLP, common lymphoid progenitor.

Additionally, B cells specific to fetal life (B-1 cells) have been described in mice. These B-1 cells are innate B cells, capable of spontaneously secreting IgM[100]. In murine development, B-1 cells have been described in the yolk sac[101], prior to definitive HSC emergence and in fetal liver and BM after definitive HSC have emerged[102–104], with their frequency decreasing in postnatal life, being virtually undetectable in adult BM[105, 106]. Efforts have been made to characterise B-1 cells in humans. Cells with the immunophenotype CD20+CD27+CD43+CD38low/int were found in cord blood and adult peripheral blood and met functional definitions of B-1 cells[107]. These were later described in human fetal liver and fetal BM[108, 109], with their frequency decreasing with age postnatally[100, 110, 111].

B cells are found in both fetal liver and fetal BM[20, 108, 112, 113]. B cells found in fetal life show early features of maturation, with IgM+ B cells being described in fetal liver[114]. Conversely, B cells in fetal BM are largely CD10+ and IgM/IgD-, consistent with a Pre-B cell stage, with a smaller proportion of more mature populations[114].

Transcriptional control of fetal B lymphopoiesis

Most of our understanding of the B cell development programmes has been delineated from experiments in murine models and human adult B cells. However, there are some important differences in gene signatures between fetal and adult lymphoid and B lymphoid progenitors.

A hallmark of B cell maturation is B cell receptor diversification. In fetal life, this process begins in fetal-specific progenitors ELP and PreProB, which show partial IgH rearrangement[20]. Full V(D)J rearrangement is typically complete at the ProB stage in fetal life[20]. The molecular machinery underpinning this process RAG recombinase, comprised of the proteins encoded by *RAG1* and *RAG2*, which are regulated by Ikaros in mice[115]. RAG recombinase binds and cleaves genomic DNA at specific regions flanking variable (V), diversity (D) and joining (J) gene segments. These breaks in DNA are repaired by DNA repair machinery, particularly through non-homologous end joining. This process is error prone, and the joining of segments may include small insertions or deletions, thereby contributing to junctional diversity. Additional diversity at this step is generated by the enzyme terminal deoxynucleotidyl transferase, TdT, encoded by the gene *DNTT*, which adds nucleotides at these joints between gene segments. While, *DNTT* and *RAG1* are highly expressed in fetal specific B progenitors[20], some differences in BCR structure in fetal life have been described. BCRs developed in fetal life have been shown to have shorter complementarity determining region (CDR) 3 lengths, and preferential use of different immunoglobulin gene segments[114, 116–120].

Transcriptionally, fetal HSPC differ from their adult counterparts, and these changes have been described in some transcriptional analyses of fetal and adult

HSPC, B progenitors and B cells[121], though this is still an area of active research. The gene *Lin28b* has been functionally investigated for its role in regulating the switch in production of B-1 cells to conventional B cells postnatally in mice[122]. Recent work in our lab has shown that *LIN28B* in humans is essential for fetal B lymphopoiesis, and acts by stabilising key B lymphoid specification genes such as *IKZF1* and *IKZF2* in fetal liver CD34+ HSPC[123].

Additionally, recent work has implicated ERG, a transcription factor promoting B lymphoid specification in mice[124], in promoting the switch to adult haematopoiesis in mice, in the context of B lymphopoiesis but also in the wider context of haematopoiesis[125]. LIN28B has been shown to repress *Erg* expression in murine HSPC[126]. This recent work has shown that *Erg* expression increases in murine HSPC through ontogeny, and that adult *Erg* haploinsufficient mice retain fetal phenotypes[125].

Cytokine control of fetal B lymphopoiesis

As discussed earlier, IL7 is an important cytokine in providing B lymphopoietic support. However, while IL7 supplementation to *in vitro* cultures with cord blood HSPC improves B lymphoid output, cord blood derived HSPC are still able to produce CD19+ cells in the presence of FLT3L alone. However, adult BM derived HSPC are unable to do this, suggesting that there is increased dependence of B lymphopoiesis on IL7 in adult life[98]. This was also described in adult *Il7*-/- mice, in which B lymphopoiesis in adult BM was abrogated, while fetal B lymphopoiesis could still occur, although at a reduced rate[127].

Thymic stromal lymphopoietin (TSLP) is another cytokine that has been posited to play a role in supporting B lymphopoiesis. TSLP signals through IL7Rα, but not the common γ chain (encoded by *IL2RG*), which IL7 does, and early observations comparing knockout mice for *Il7ra* and *Il2rg* showed that *Il7ra*-knockout mice had a much more severe impairment in B lymphopoiesis compared to *Il2rg* knockout mice, providing indirect evidence that TSLP may be more important in murine B lymphopoiesis[90, 128, 129]. Given that fetal B lymphopoiesis has

been demonstrated to occur in the absence of IL7 in humans and mice[98, 127], the increased severity of impairment of B lymphopoiesis in *Il7ra*-/- mice compared to *Il2rg*-/- mice suggests that TSLP may also be more important in a fetal context. In *Il7*-/- mice, TSLP has been shown to rescue the block in B lymphopoiesis associated with *Il7* knockouts[130], and this has been also been described *in vitro* in assays with IL7 neutralising antibodies in human cord blood HSPC[131]. TSLP has also been shown to support the survival and proliferation of B progenitors, but to a lesser extent after stimulation with IL7[132]. Together, these experiments point to a role for TSLP in IL7 independent B lymphopoiesis in human fetal life.

In summary, B lymphopoiesis in fetal life occurs through distinct cellular differentiation pathways, is sensitive to different cytokine signalling, and employs different gene expression programmes to adult B lymphopoiesis.

1.1.4 T lymphopoiesis in fetal and adult life

T lymphopoiesis in adult life

In addition to differentiating into the B lineage, CLP can give rise to T cells. In contrast to B lymphopoiesis, lymphoid progenitors must migrate to seed the thymus in order to receive the signals that commit them to a T lymphoid fate. Most of our mechanistic knowledge of T lymphopoiesis has been delineated in murine models.

A series of recent lineage tracing experiments, in which murine LMPP and CLP were barcoded and transplanted into mice, provided direct evidence for both LMPP and CLP homing to and seeding the thymus, with LMPP appearing to be more efficient at this process[133]. LMPP and CLP in adult BM have been suggested to be primed by BM-derived Notch signals[134], and knockout experiments in adult mice suggest that chemokine receptors CCR7 and CCR9 are essential for migration of these BM LMPP and CLP to the thymus[135].

In humans, cells resembling CLP immunophenotypically and transcriptionally have been shown to seed the thymus[136]. Additionally, a population of CD10-CD24-CD62L+ adult BM progenitors that transcriptionally and functionally resemble LMPP have been implicated to migrate to the thymus[65]. Whether human MLP can

migrate to the thymus has not been tested directly, despite being able to produce T cells *in vitro*. However, analysis of the BM of a patient lacking MLP and committed B and NK precursors has showed that T lymphopoiesis was modestly affected, suggesting that MLP contribute to T lymphopoiesis alongside other cells[67]. More recent work characterising the adult human thymus identified three transcriptomic subsets of thymic seeding populations, which corresponded to transcriptomically defined HSC, MPP, and LMPP and CLP in adult BM[137]. The authors speculated that the HSC-like thymic subset may represent an intra-thymic HSC population, as it is largely quiescent[137]; and, rather, it is the LMPP/CLP-like subset that gives rise to committed thymocytes much more quickly *in vitro*.

It is within the thymus that commitment to the T lineage occurs. The thymus provides a specialised environment particularly rich in Notch ligands, which are central to T lymphoid commitment and shutting down alternative (B lymphoid, myeloid, dendritic cell) fates; inducible inactivation of *Notch1* in mice results in a block in T lymphopoiesis, accompanied by ectopic B lymphopoiesis in the thymus[138, 139].

Notch signalling triggers a cascade of events resulting in T lineage commitment, with the upregulation of *TCF7*, which encodes TCF1, and *GATA3* which are central to the activation of the a gene regulatory network governing T lymphoid commitment and development[140–144], as reviewed extensively in [145]. Once committed to the T lineage, maturation of T cells occurs in three well documented stages: first, thymocytes begin as negative for both CD4 and CD8 (double negative, DN), before upregulating both CD4 and CD8 (double positive, DP), before maturing into either a CD4+ or CD8+ T cell (single positive, SP), a sequence preserved across humans and mice[146, 147].

T lymphopoiesis in fetal life

The thymus develops from the third pharyngeal pouch at 6 PCW in fetal life and is seeded by haematopoietic cells derived from the fetal liver from 8 PCW onwards, and from the fetal BM once haematopoiesis is established there[148, 149]. T progenitors

are detected in the human fetal thymus as early as 9 PCW, with mature T cells being detected from 12-13 PCW[150]. T cells have been described in secondary lymphoid organs (the spleen and lymph nodes) later in gestation, from 24 PCW onwards[150].

There are some interesting distinctions between fetal and adult T lymphopoiesis, as discussed in depth in [23], notably that the output of T lymphopoiesis in human fetal life is biased towards T regulatory cells[151, 152] and more innate inflammatory-like tissue-associated memory effector cells, which are suggested to be important for maintaining materno-fetal tolerance in fetal life[153–155], while also preparing to regulate the immune response at birth, upon exposure to novel antigens[23].

1.1.5 NK lymphopoiesis in fetal and adult life

NK lymphopoiesis in adult life

In addition to B and T lymphocytes, CLP can give rise to innate lymphoid cells (ILC), a family of lymphocytes characterised by their lack of somatically rearranged antigen receptors. NK cells are a sub-category of ILC, characterised by their cytotoxic activity, and play an important role in the anti-viral and anti-tumour response. In human adult life, the primary (but not exclusive[156]) site of NK lymphopoiesis is the BM.

The transcription factors that control NK lineage commitment have been extensively reviewed in [157]. NFIL3 and ID2 are the apical transcription factors that govern commitment to ILC fate. NFIL3 has been shown to bind to and upregulate *Id2* expression in murine ILC progenitors[158], and its knockout mouse demonstrates a severe reduction in NK cells[159, 160]. ID2 is another apical transcription factor in ILC lymphopoiesis, with *Id2*-/- mice failing to develop NK cells, as well as peripheral lymphoid organs[161, 162].

IL2 and IL15 are both important in NK development, both of which were first described for their role in T lymphopoiesis[163]. IL15 is central in NK lymphopoiesis, with mice lacking IL15 or its receptors reported to demonstrate a striking reduction, or complete absence of NK cells[164–166]. IL15 is required for NK differentiation and maturation in humans[167–169], but not NK lineage commitment, as CD122, a

subunit of the IL15 receptor, is only expressed on NK-committed progenitors and not before commitment to the NK lineage[170]. IL2 plays a supportive role in NK lymphopoiesis, enhancing NK survival, expansion, and effector function[171–174].

A number of parallels have been drawn between T lymphopoiesis and ILC lymphopoiesis. ILC are often classified into "helper" (ILC1, ILC2 and ILC3) and "effector" (NK cells) subsets, much like T cells - with CD4+ helper T cells and CD8+ cytotoxic T cells[175]. NK cells are often subdivided into CD56-bright and CD56-dim NK subsets, representing populations poised for cytokine production and cytotoxicity respectively[176–178]. Additionally, there is significant overlap in the transcriptional programmes associated with ILC lymphopoiesis and T lymphopoiesis, with transcription factors GATA3, TCF1, T-bet, Eomes, RORγT and PLZF playing parallel roles in differentiation into different subsets of ILC and helper T cell from ILC progenitors and DP T cells respectively, as reviewed extensively in [157, 179]. Notch signalling is also suggested to be important in NK lineage commitment, specifically, signals from JAG1[180]; and the loss of Notch signalling dramatically reduces NK progenitors in mice[181] and *in vitro* from human cord blood[182].

There are multiple pathways involved in NK fate in humans, reviewed in[183–185]. Briefly, CLP can give rise to NK progenitors, which are sub-classified into three stages of maturation: NK progenitors, preNK cells, and immature NK cells, which are immunophenotypically marked by CD34+CD10+CD45RA+ CD34+CD117+CD7+CD122+, and CD34-CD10-CD117+CD122+NKG2D+ respectively[183–185]. In addition to CLP directly giving rise to NK cells, CLP can also differentiate into a common ILC precursor which can then commit to the NK lineage, reviewed in[156, 157, 184, 186].

NK lymphopoiesis in fetal life

In human fetal life, NK progenitors have been described in the fetal liver and BM[187]. NK cells have been described in the fetal liver from 6 PCW[188] and fetal spleen from 15 PCW[188], and in the second trimester human fetal BM at a lower frequency[189].

Additionally, primitive NK cells have been reported to arise from EMP in the murine yolk sac from recent lineage tracing studies[190]. In humans, the evidence for this is limited, though lympho-myeloid progenitors from the human embryonic yolk sac have been reported to show NK potential *in vitro*[191].

Early work showed that human fetal NK express cytoplasmic CD3δ and CD3ϵ, unlike adult peripheral blood NK cells leading to the hypothesis that NK and T cells shared a common differentiation pathway[188]. Bipotent NK/T progenitors were also described in the murine fetal liver[192]. Similarly, recent single cell analyses propose that the ILC/T lineage in human fetal liver have a shared differentiation trajectory that is distinct from B lymphopoiesis[18]. There are a number of lines of evidence to suggest that bipotent NK/T progenitors commit to an NK fate in the absence of T-lineage specifying signals. For example, in murine fetal life, a DN population in the fetal thymus has been described, which, if maintained in a thymic microenvironment would produce CD8+ T cells, but if removed from the thymus would produce NK cells *in vitro* or *in vivo*[193]. The transcription factor BCL11B plays a key role in suppressing NK fate to favour T lineage commitment: *Bcl11b*-/- mice fail to undergo V(D)J rearrangement[194], while conditional *Bcl11b* deletion in postnatal murine DN thymocytes results in a reprogramming towards NK fate[195–197].

The NK lymphopoietic differentiation pathways in fetal life are an area of active research. However, a greater deal of plasticity has been described fetal NK lymphopoiesis, with the observation that cord blood-derived CMP and GMP could give rise to NK cells *in vitro*[198], this was also observed in fetal BM to a greater extent, from which a GMP-derived myeloid-NK precursor with the immunophenotype CD33+CD56+CD36+ could give rise to mature NK cells when transplanted into mice[199]. Notably, this myeloid-NK precursor was very rare in adult BM[199].

A number of differences have been described in fetal NK cells compared to their adult counterparts. Crucially, fetal NK cells are less mature[200], and respond well to cytokines and antibody-mediated stimulation, but less robustly to class

I HLA negative target cells compared to their adult counterparts, perhaps as a mechanism of materno-fetal tolerance[189].

1.1.6 Myelopoiesis in fetal and adult life

In addition to generating lymphocytes, HSPC can differentiate along a myeloid branch of haematopoiesis, which includes megakaryocytic/erythroid, granulocyte/macrophage and eosinophil/basophil/mast cell pathways (see Figure 1.1). The common myeloid progenitor (CMP) arises from MPP in traditional models of haematopoiesis, and the transcription factor PU.1 (encoded by *SPI1*), restricts HSC fate towards a lympho-myeloid fate. *Spi1* knockout mice die soon after birth, with severe defects in granulocyte-macrophage and B lymphoid lineages, while megakaryocytic/erythroid development is mostly intact[201, 202]. Conditional disruption of *Spi1* in mice results in a complete loss of CMP and GMP, while MEP frequency is increased[203, 204], suggesting PU.1 is important in the HSC to CMP transition. PU.1 is thought to act in a dose-dependent manner, with higher doses favouring myelopoiesis along the granulocyte/monocyte trajectory, and lower doses favouring lymphopoiesis in mice[204, 205].

PU.1 and the master erythro-megakaryocytic transcription factor GATA1 reciprocally antagonise each other [206–209]; the balance of PU.1 and GATA1 activity in CMP is a determinant of megakaryocytic-erythroid fate versus granulocytic-macrophage fate decisions[210, 211]. Although the traditional hierarchy of CMP, MEP and GMP[212] are a useful framework, advances in single cell -omics experiments have challenged some of the aspects of this model. Single cell experiments performed in mice suggest that instead of separating lymphoid and myeloid HSPC, the first lineage bifurcation step separates cells with lympho-myeloid potential from cells with megakaryocytic/erythroid potential[213], in line with more recent observations from single cell -omics experiments on human cord blood suggesting that different programmes underpinning this bifurcation are apparent at a HSC stage[214]. Additionally, LMPP, while associated with lymphoid fate also give rise to GMP[20, 215].

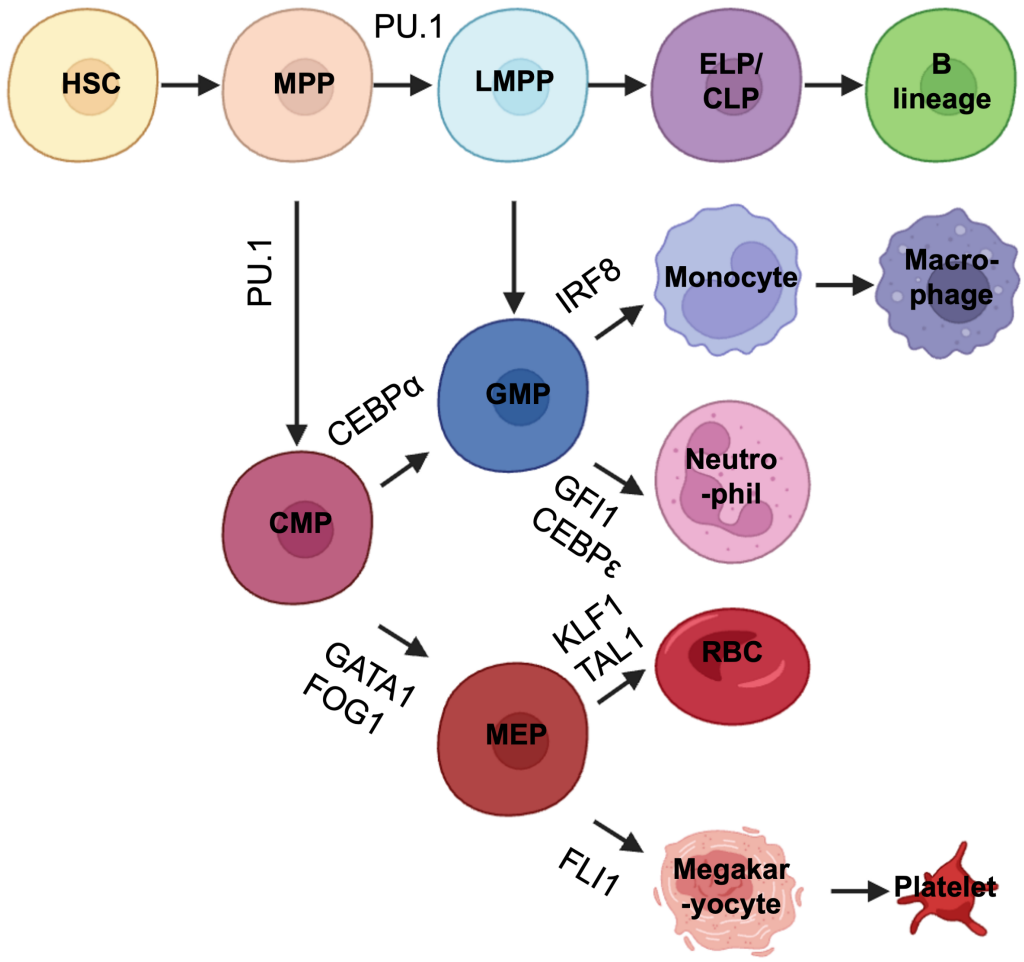

Figure 1.4: Myeloid fate decisions and the transcription factors that govern them. Adapted from [216, 217]. HSC, haematopoietic stem cell; MPP, multipotent progenitor; LMPP, lymphoid-primed multipotent progenitor; ELP, early lymphoid progenitor; CLP, common lymphoid Progenitor; CMP, common myeloid progenitor; GMP, granulocyte macrophage progenitor; MEP, megakaryocyte erythroid progenitor; RBC, red blood cell.

Granulocyte and monocyte development in fetal and adult life

Granulocytes and macrophages arise from a single progenitor, GMP, which in turn can arise from CMP in traditional haematopoietic models[212], and LMPP[215]. C/EBPα is necessary for GMP development, with its conditional deletion in mice resulting in a loss of GMP, and downstream, a lack of granulocytes but normal levels of lymphoid and erythroid/megakaryocytic cells[218]. In line with this phenotype, C/EBPα, downstream of GMP, acts in a dose-dependent way to favour granulocytic commitment, with knockdown experiments in human HSPC *in vitro* showing an increased monocyte: granulocyte ratio upon *CEBPA* knockdown[219]. The transcription factor IRF8 plays a role in monocytic lineage commitment, with murine knockouts lacking BM resident macrophages and dendritic cells[220], and mutations in *IRF8* in humans being associated with a complete lack of circulating monocytes and dendritic cells[221]. These transcriptional networks are supported by cytokines: G-CSF supports granulopoiesis[222], while M-CSF biases differentiation towards macrophages[223].

Cells derived from GMP: monocytes, macrophages, DCs, neutrophils, eosinophils, basophils and mast cells, make up most of the innate immune system, playing a major role in the initial response to infection, and modulating the adaptive immune response. These cells also play major roles in mediating, modulating and responding to inflammation. In response to inflammatory stimuli, HSPC activate emergency myelopoietic pathways, as reviewed extensively recently in [224].

Recent work in mice suggests that emergency myelopoiesis in fetal life is restricted by maternal IL10[225], with fetal liver HSPC responding to emergency-myelopoietic stimuli *in vitro* but not *in utero in vivo*. Loss of maternal IL10 restored the ability of fetal HSPC to activate emergency myelopoietic pathways, however, this resulted in the loss of the pregnancy – emphasising the importance of the immunosuppressive mechanisms in fetal life.

1.2 The haematopoietic niche

Haematopoiesis occurs in multiple niches through ontogeny, from the yolk sac, to the AGM, the fetal liver and BM[226], and emerging work with single cell -omics experiments have provided new perspectives on how haematopoiesis is supported by cells of the haematopoietic niches in these tissues.

1.2.1 The fetal liver haematopoietic niche

As HSC from the fetal liver are more proliferative than their postnatal BM counterparts, it has been hypothesised that the microenvironment of the fetal liver promotes expansion while maintaining their stemness[227]. The key cell types in fetal liver studied for their role in providing haematopoietic support include hepatoblasts and hepatocytes, endothelial cells, perivascular stromal cells and macrophages. Early work comparing human fetal liver and adult BM stroma identified an increased proliferative capacity of fetal liver stromal cells, and an increased expression of Wnt signalling pathway regulators and decreased expression of Notch signalling pathway regulators in fetal liver, which the authors suggested may contribute to the increased proliferation of fetal liver HSC[227].

Recent characterisation of human fetal liver haematopoiesis by sc-transcriptomics has demonstrated that fetal liver haematopoiesis shows an increased HSC frequency and an erythroid bias compared to fetal BM, especially at earlier gestation[18, 21]. Hepatoblasts in fetal liver provide a niche for erythropoiesis, with studies in mice showing they are close in proximity to developing erythroblasts[228], and secrete SCF and EPO[229]. Additionally, murine fetal hepatoblasts secrete IGF2, a growth factor for HSC[230], ANGPTL2 and ANGPTL3, which also support HSC expansion *in vitro*[231], CXCL12, a chemoattractant for HSC[232], and TPO, which when deleted from murine fetal liver depletes HSC[233]. Macrophages form a very heterogeneous population both in BM and fetal liver. In murine fetal liver, specialised erythroblast island macrophages have been described (EBI)[234] both transcriptomically[235] and using spatial transcriptomics[236]

Perivascular stromal cells have been shown to secrete similar cytokines to hepatoblasts in murine fetal liver[237, 238], and have been well described as an important component of the fetal liver HSC niche in humans [239, 240], being able to support haematopoiesis *in vitro* [227]. In comparison to their adult counterparts, human fetal liver MSC are much more proliferative *in vitro*[227, 241] and recent *in vitro* co-cultures suggest that human fetal liver MSC inhibit NK and T cell proliferation, unlike their adult BM counterparts[241–244], potentially promoting a more tolerogenic environment during fetal life.

Endothelial cells in fetal liver also come into direct contact with HSPC and form part of the haematopoietic niche[236]. Fetal liver endothelial cells are also an important source of membrane-bound SCF, an isoform of SCF important in erythropoiesis; depletion of membrane-bound SCF in murine fetal liver endothelial cells results in a marked anaemia[245].

Taken together, these studies highlight the importance of the cellular components of the fetal liver haematopoietic niche and their molecular features in providing a specialised niche capable of supporting HSC survival and expansion, and also lineage specific differentiation of HSPC during development, particularly supporting erythropoiesis and megakaryopoiesis.

1.2.2 The BM haematopoietic niche

The BM microenvironment plays a central role in supporting and regulating haematopoiesis throughout the human lifetime. The BM niche is much more complex than the fetal liver microenvironment, and is comprised of haematopoietic- and non-haematopoietic-derived cells that provide haematopoietic support and regulatory cues to HSPC. Key cellular constituents of the BM niche include mesenchymal stromal cells (MSC), osteoblasts, adipocytes, endothelial cells, megakaryocytes, macrophages, sympathetic nerves and Schwann cells[246]. These components are not uniformly distributed throughout the BM; rather, they assemble into spatially and functionally distinct niches that differentially regulate HSPC fate according to developmental stage[247], lineage commitment[248, 249], and physiological

demand[250, 251]. This spatial organization gives rise to anatomically distinct domains, and the current model, based on murine BM architecture, proposes two niches: the endosteal niche and central BM niche, each characterized by different cellular compositions and signalling landscapes, as recently reviewed in [252]. Most of our understanding of the BM environment comes from imaging and functional experiments conducted in murine BM, and more recently this has been supplemented with scRNA-Seq and spatial transcriptomic atlases from human BM.

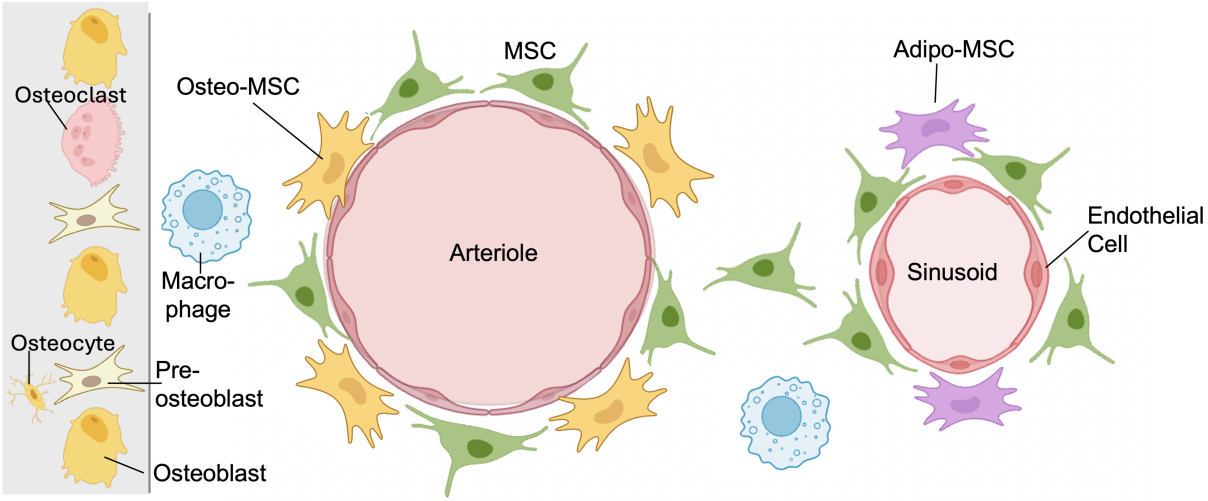

Figure 1.5: The BM niche for haematopoiesis. A simplified schematic representing the cells comprising the central and the endosteal (shaded in grey) BM niches, adapted from [253].

The central BM niche

Early work characterising the BM HSC niche identified that immunophenotypic HSC localised to regions adjacent to sinusoidal vessels in murine BM[254–256]. The key cellular constituents of this central BM niche, which in murine BM harbours over 85% of HSC[257], are sinusoidal and arteriolar endothelial cells, and their associated MSC, which together secrete supportive cytokines CXCL12 and SCF to create a niche for HSC[257, 258]. Within the central BM, the niches provided by sinusoidal and arteriolar vessels may also have different functions.

The arteriolar niche is suggested to promote HSC quiescence[259, 260], however, this is debated, with opposing evidence also reported from different murine

models[261], perhaps as a result of inconsistencies in the inducible knockout mice models used[252]. Additionally, it has been suggested that the specialised NG2+ MSC found in the periarteriolar space may provide a niche for lymphoid-primed HSC in murine BM[249, 262].

In addition to providing a niche for HSC, the perisinusoidal niche has been implicated in myelopoiesis, with imaging studies in murine BM showing localisation of granulocytic and monocytic precursors exclusively to sinusoids, a source of M-CSF. Deletion of *Csf1*, which encodes M-CSF, results in a failure of monocyte-dendritic cell progenitors to localise to sinusoids, and an overall decrease in monocytes and dendritic cells[263].

The sinusoidal niche also provides support for erythropoiesis, with the observation that erythroid progenitors localise near perisinusoidal LEPR+ MSC in murine BM[261].

Megakaryocytic maturation has also been reported to be localised to the sinusoidal niche in mice[264] , and megakaryocytes have been shown to contribute to the haematopoietic niche in human BM, particularly with respect to regulating HSC quiescence, through TGFβ, as reviewed recently[265]. In mice, HSC in close contact with megakaryocytes are more myeloid biased, and their depletion in fetal BM can reprogramme these HSC to have a more balanced lineage output[249].

The endosteal BM niche

The endosteal niche is much smaller, comprising around 10% of the BM, and provides a specialised niche for HSC quiescence[266–271]. The endosteal and central BM HSC niches have been suggested to be functionally different. The central BM niche for HSC is the site of day-to-day haematopoiesis[252] and is more sensitive to stress from irradiation or myeloablation compared to the endosteal niche in mice[266, 272]. Additionally, HSC from the endosteal niche show higher reconstitution activity when compared to their counterparts from the central BM niche[273]. Therefore, HSC from the endosteal niche have been suggested to be important in haematopoietic regeneration following genotoxic stress[252, 266].

The endosteal BM niche has also been reported to provide specialised support for lymphopoiesis. This was shown by imaging studies in rat and mouse BM identifying lymphoid progenitors near the surface of the bone[248, 274–278]. Additionally, imaging of femurs of *Il7*-GFP reporter mice showed that a population of IL7-producing cells were localised to the endosteum, in addition to the central BM niche[279].

The key cellular components of this niche include osteoblasts, osteoclasts and endothelial cells associated with transition zone vessels[253]. Additionally, different subsets of MSC are also found in the endosteal niche in mice, albeit at a lower frequency compared to the central BM niche in mice (CXCL12 abundant reticular (CAR) cells, Nestin+ MSC)[280] and in human adult BM (osteoMSC, fibroMSC)[281].

1.2.3 The cellular components of the BM niche

Mesenchymal Stromal Cells (MSC)

Much of our understanding of MSC and their importance in supporting haematopoiesis also derives from murine experiments. Subcutaneous or subrenal injection of MSC (from human and murine BM, respectively) into mice was capable of generating an ectopic environment for haematopoiesis[282, 283]. In the context of B lymphopoiesis, histological examination of murine BM identified the association of B progenitors with MSC[284–286].

MSC give rise to cells of adipocytic, chondrocytic and osteoblastic lineages in the BM. MSC have been best characterised in murine BM. These studies have identified a number of subtypes of BM including CAR cells, LEPR+ MSC, Nestin+ MSC, NG2+ MSC, and PDGFRα+ MSC. Though there is significant overlap between these populations[258], there are some important distinctions, in that NG2+ MSC, which highly express Nestin, are found exclusively in the periarteriolar space[259] and by transitional zone vessels[287], and are thought to represent the apical MSC progenitor, at least in murine BM[288].

Another subtype of MSC are CXCL12-abundant reticulocytes (CAR cells), which were initially identified in *Cxcl12*-GFP reporter mice, based on their high expression

of CXCL12 and their morphology[267, 289]. CAR cells are located primarily in the central BM niche, though some are found in the endosteal niche[267, 289, 290]. These form an important niche for HSC, with most HSC in adult murine BM being in close proximity to CAR cells when imaged[267], and their conditional ablation causing a loss of cycling B lymphoid progenitors and erythroid progenitors[289].

CAR cells are bipotent, being able to give rise to adipocytes and osteoblasts[289]. Recent scRNA-Seq analysis of murine BM has identified transcriptomic subsets of CAR cells, a more abundant adipoCAR population, localised to sinusoids, and a rarer osteoCAR population, associated with arterioles, or in avascular regions[288], and probably also associated with transition zone vessels[252], though this has not yet been demonstrated. Both of these subtypes of CAR cells expressed high levels of *Cxcl12*, *Il7*, *Scf* and *Csf1*[288]. Specifically, based on gene expression, adipoCAR made a higher contribution to *Scf* and *Cxcl12* pools, while osteoCAR made a greater contribution to the *Il7* pool; both populations made a similar contribution to the *Csf1* pool[288]. These data suggest that these subsets of MSC in murine BM are important contributors to supporting haematopoiesis.

In human adult BM, there are some differences in marker gene expression for MSC populations compared to murine BM. CD271 has been reported to be a pan-MSC marker[291], and CD146 expression has been suggested to distinguish perisinusoidal (CD146+) and endosteal (CD146-) MSC[292]. Recent scRNA-Seq of adult BM, with a focus on the stromal compartment, has shown that adult BM MSC are also a highly heterogenous group, identifying five different transcriptomically defined MSC subsets: adipoMSC, APOD+MSC, THY1+MSC, fibroMSC, and osteoMSC[281]. A newly characterised population of MSC in this study, fibroMSC, defined by expression of *NT5E* (CD73), *CXCL12*, *DPT*, *PDPN* and *HAS1* has been reported to be the apical MSC progenitor in adult BM, matching the ICST mesenchymal stem cell definition[293] and functionally giving rise to osteoblasts, adipocytes and chondrocytes *in vitro*. This population was also the primary source of *IGF1*, at least, transcriptomically[281]. Imaging of adult BM in this study showed

that THY1+ and adipoMSC were largely in the central BM niche, unlike fibroMSC and osteoMSC, which were more generally endosteal in location.

Characterisation of human fetal BM MSC is limited, in comparison to adult and murine BM MSC. Though CD146 and CD271 have been established as adult human BM MSC markers, these were undetectable at a protein level in fetal BM; instead LIFR and PDGFRA were detected[294]. Recent sc-transcriptomics of human fetal BM has also identified heterogeneity in the MSC compartment, identifying different subsets of CAR cells and MSC, though these studies did not focus specifically on characterising the stromal compartments[36, 45].

MSC-derived cytokines and haematopoiesis

MSC in BM are an important source of cytokines that play a role in HSC maintenance and B lymphopoiesis, including CXCL12, SCF and IL7, as reviewed extensively in [295].

MSC are also an important source of SCF, a cytokine which plays an important role in HSC survival and maintenance[255, 261, 296, 297]. Conditional deletion of *Scf* in *Il7-Cre* transgenic mice results in a striking reduction in HSC and MPP in the BM[298].

CXCL12 is essential for the early stages of B lymphopoiesis, by guiding lymphoid progenitors to their niche[298]. Conditional ablation of *Cxcl12*-expressing MSC reduces CLP and ProB numbers[289]; while deletion of *Cxcl12* in LEPR+ MSC, CAR cells and osteoblasts result in a reduction in B progenitors[248, 298]. CXCL12 also regulates HSC and quiescence and maintenance of BM HSC, with conditional knockouts of *Cxcl12* in MSC that co-express *Cxcl12* and *Il7* resulting in a loss of HSC and MPP[290].

IL7 also plays a major role in B lymphopoiesis, promoting B lymphoid commitment, and the survival and expansion of B progenitors, as discussed earlier (page 8) and reviewed in[299, 300]. The contribution of MSC-derived IL7 to B lymphopoiesis has been demonstrated by conditional deletion of *Il7* in a *Lepr-Cre* transgenic model. This led a significant depletion of CLP and downstream B

progenitors[298], while deletion of *Il7* using a *Prx1-Cre* transgenic murine model, which deletes *Il7* from LEPR+ MSC, CAR cells and osteoblasts, also affected B cell development at a ProB stage[298].

While most of these results were first investigated in mice, recent single cell atlases of human BM have validated some of these observations, with populations of MSC expressing *CXCL12*, *SCF* and *IL7* mRNA identified in adult[281] and fetal BM[36, 45].

Osteolineage Cells

Osteolineage cells are derived from MSC, and represent a heterogenous population along a differentiation trajectory from osteoMSC to mature osteoblasts and osteocytes, marked by the progressive expression of ALPL, type I collagen, BSP, OPN, and osteocalcin[301]. Osteoprogenitors, including osteoMSC, are found in the perivascular space in the central BM[302], while osteoblasts are found in the endosteal niche. Osteolineage cells at different stages of differentiation provide different haematopoietic support, with earlier stages of osteoblast differentiation being more important in haematopoiesis: early murine osteoblasts better support LSK expansion than mature murine osteoblasts in *in vitro* co-culture assays[303].

Osteolineage cells have been well studied for their role in supporting B lymphopoiesis, as reviewed in [304], and are a source of CXCL12 and IL7 in murine BM[275, 305, 306]. Deletion of *Cxcl12* from osteoblasts using *Col2.3-Cre* resulted in a modest reduction in CLP frequency, while conditional deletion of *Cxcl12* from mature (osteocalcin-expressing) osteoblasts in murine BM had no effect on frequency of lymphoid progenitors[290], in line with the observation that earlier osteoblasts are more important for supporting lymphopoiesis.

Osteoprogenitors and early osteoblasts are also an important source of IL7 in the BM, and a number of experiments targeting pre-osteoblast-derived IL7 using *Osx-Cre* transgenic mice have described impaired B lymphopoiesis at various stages[276, 307, 308]. In addition to providing IL7 and CXCL12, pre-osteoblasts and osteoblasts are also a source of IGF1[309, 310], a cytokine that supports ProB cell development

from human HSPC *in vitro*[311]. In line with this, conditional deletion of *Igf1* from *Osx*-expressing pre-osteoblasts impaired the ProB to PreB transition[309], suggesting the importance of this population in supporting B lymphopoiesis.

Adipocytes

MSC can also give rise to adipocytes. Adipocytes are virtually undetectable in fetal BM, and increase in frequency during ageing[312–314]. In murine adult BM, adipocytes have been described to have a largely inhibitory role in B lymphopoiesis, with mice fed high-fat diets, who develop an increased frequency of BM adipocytes, having fewer B cells and decreased *Il7* expression[315]. Adipocytes derived from human BM have been shown to secrete adipokines that inhibit B lymphoid commitment at a CLP stage *in vitro*[316] directly, and indirectly, with murine BM adipocytes preferentially promoting myelopoiesis of a CD11b+ population that inhibit B lymphopoiesis[317, 318]. More recent work in imaging adult human BM has described HSPC localising to an adipocytic niche in the central BM, proposing that this niche promotes myeloid priming of HSPC[281]. These findings have been hypothesised to contribute to the decrease in B lymphopoiesis and concurrent myeloid skew observed with ageing[317].

Endothelial Cells

Endothelial cells are also an important source of cytokines that support HSC and haematopoiesis. Advances in scRNA-Seq have allowed the identification of gene signatures associated with arteriolar or sinusoidal endothelial cells[281, 288, 310], which differ structurally and functionally in their support for haematopoiesis, as reviewed in [319].

The haematopoietic support offered by BM endothelial cells has been best characterised in murine BM. Murine BM endothelial cells have been identified as an important source of CXCL12[248, 290] and IL7[298]. A few studies have demonstrated that conditional deletion of *Cxcl12*[248, 290] and *Scf*[255, 261] from endothelial cells using *Tie2-Cre* transgenic mice impairs HSC survival and maintenance. Additionally, conditional deletion of *Il7* in *Tie2-Cre* transgenic mice

resulted in a reduction of frequency B progenitors, suggesting the importance of endothelial-derived *Il7*, at least in mice[298].

In human fetal BM, endothelial cells have been categorised as sinusoidal and non-sinusoidal "tip" endothelial cells based on their gene expression profiles[36], both of which express *SCF*, *FLT3L* and Notch ligands *DLL4*, *JAG1* and *JAG2*[36], though the support offered by tip and sinusoidal endothelial cells in human fetal BM and how they may differ has not been functionally tested. FLT3L has been previously described to be secreted by human endothelial cells *in vitro*[320], and plays a critical role in B lymphopoiesis, as discussed previously (page 8). It does so by promoting lymphoid commitment and synergising with IL7 signalling in B lymphopoiesis[321, 322]. Endothelial cells are the main source of delta-like Notch ligands in murine BM[310]; Notch signalling is essential for T lymphopoiesis, as discussed earlier (page 14), and in the BM is important for priming CLP towards T lineage fate[323]. Conditional deletion of *Dll4* in endothelial cells in murine BM resulted in a loss of CLP and an induced myeloid bias in HSPC[310].

Taken together, endothelial cells are a key component of the haematopoietic niche in both fetal and adult BM, providing haematopoietic support through secretion of FLT3L, SCF, IL7, and CXCL12, as well as providing Notch signalling, which plays a role in HSC maintenance and lymphopoiesis.

Macrophages

BM macrophages are a dynamic and diverse population of cells, with different developmental origins. Tissue resident macrophages in some tissues have an embryonic yolk-sac origin; however, in murine BM, initial lineage tracing and functional experiments suggest so far that only osteoclasts are yolk-sac derived[324–326], and that macrophages in adult murine BM are derived from monocytes[327]. More recent work published earlier this year has shown that a subset of adult murine BM macrophages expressing F4/80 was embryonic in origin[328].

Early work used imaging to observe macrophages associated with red blood cells. This was first described in the 1950s in murine BM[329] and later in humans[330].

These macrophages were termed stromal macrophages, expressing FcR1, HLA-DR, CD11a, CD11c, CD14 and CD16 by flow cytometry in humans. Later work identified CD163, an endocytic receptor, as a marker for stromal macrophages[331, 332]. These specialised stromal macrophages, erythroblast island macrophages, can provide specialised support for erythropoiesis, reviewed in [333].

Such early imaging studies laid the foundations for the identification of three overlapping subpopulations of stromal macrophages in the BM, based on their spatial location and the cell types with which they associated: erythroblast island macrophages, as described above; HSC-supportive macrophages, identified recently[334, 335]; and osteo-macrophages (osteomacs), a macrophage population found in the endosteal niche that promotes osteoblast survival and ossification[336].

The HSC-supportive macrophage population were described more recently in human and murine BM[337]. This population was characterised by its expression of CD169 in murine BM[334], and conditional ablation of these macrophages in mice resulted in a loss of HSC in the BM[334, 335]. These HSC were mobilised to the blood and secondary lymphoid organs; the depleted populations of stromal macrophages promote HSC retention by regulating the stromal cells comprising HSC niche to promote CXCL12 secretion[334, 335, 338]. Importantly, murine osteomacs also express CD169 (encoded by the gene *Siglec1*)[336], and so it is likely that this population was also depleted in the conditional ablation of *Siglec1*-expressing cells[334].

In humans, CD163 is used as a marker of stromal macrophages, with recent imaging studies of adult BM reporting all stromal macrophages expressed CD163[281]. Though very little is known about human fetal BM macrophages, a recently published scRNA-Seq atlas had a stromal macrophage cluster, marked by *CD163* expression[36].

In addition to tissue-resident stromal macrophages in BM, monocytes can also give rise to macrophages *in situ*, for instance, under inflammatory conditions[339]. Macrophages are also highly dynamic and can polarise in response to inflammatory stimuli to give rise to pro-inflammatory M1 or anti-inflammatory

M2 macrophages[340, 341]. M1 macrophages secrete TNFα, IL6 and IL1β, and immunophenotypically express CD80, CD86 and TLR4, while M2 macrophages secrete IL10, and immunophenotypically express CD163, CD206 and CD209 - this has been reviewed in depth in [341] and [342] . Murine M1 and M2 macrophages have been reported to have opposing effects on murine HSC expansion and self renewal *in vitro* and *in vivo*, with M2 macrophages promoting HSC expansion and renewal, while M1 macrophages oppose this[343]. Additionally, M1 macrophage-derived cytokines, such as TNFα, IL6 and IL1β have been shown to promote myelopoiesis in human and murine HSPC[344–348].

Overall, macrophages are a heterogenous population in the BM that may influence haematopoiesis through a number of mechanisms, including supporting HSC niches, regulating lineage commitment and erythropoiesis, and regulating inflammatory signalling.

1.3 Down syndrome

Down syndrome is caused by trisomy of chromosome 21 (T21), and is the most common aneuploidy in humans, with a prevalence of 29.7 per 10,000 births [349, 350]. Its clinical characteristics were first described in 1866[351], and it was not until 90 years later, that these were linked to an additional copy of chromosome 21[352]. Since then, the clinical features of Down syndrome have been described in much more detail, and include an increased frequency of congenital cardiac and gastrointestinal abnormalities, and neurodevelopmental problems, in addition to the well-characterised craniofacial abnormalities and intellectual disability (reviewed in [353]). Additionally, children with Down syndrome have a broad range of haematological abnormalities, and have an increased risk of developing haematological malignancies compared to children without Down syndrome[354–356].

T21 is most commonly caused by non-disjunction in meiosis, and results in 90% of cases of Down syndrome[357, 358]. Other causes of Down syndrome include mitotic errors after zygote formation, which are responsible for around 5% of T21

cases[359], and translocations most commonly t(14;21) or t(21;21)[358]. Finally, partial T21 is very rare, accounting for <1% of cases[360–362].

1.3.1 Trisomy of chromosome 21

Chromosome 21 is the smallest human chromosome, encoding 222 protein coding and 683 non-coding genes[363], which may explain why T21 causes the least disruption during development, compared to Trisomy 18 and Trisomy 13, which have much poorer prognoses[364, 365].

Studies correlating the phenotype of individuals with partial T21[366] have contributed to the definition of a so-called Down Syndrome Critical Region (DSCR). This definition also relies heavily on genotype-phenotype correlations from Down syndrome mouse models (reviewed extensively elsewhere[367]) and T21 iPSC[368], and maps to a region on the long arm of chromosome 21, 21q22 [366, 369, 370]. However, the precise relationship of the number of genes in this region and specific Down syndrome phenotypes yet remain unclear, and for this reason the concept of the DSCR is debated [361, 371, 372].

Other approaches to understanding the relationship between T21 and the phenotypic characteristics of Down syndrome have used CRISPR-Cas9 to silence the second maternal copy of chromosome 21 in iPSC derived from fibroblasts to see whether this can rescue the T21 phenotype[373]. Although this resulted in the rescue of the T21 gene expression profile in iPSC, this mostly reflected a significant reduction in expression of chromosome 21 genes alongside an increase in neural development gene sets[373]. Others have used *XIST* to silence the extra copy of chromosome 21 in T21 iPSC, which appeared to correct the erythro-megakaryocytic skew observed *in vitro*[374]. iPSC represent an interesting platform on which such experiments can be conducted and provide interesting insights, however, in the context of haematopoiesis, which requires carefully controlled gene regulation to activate and repress lineage differentiation programmes, studies of gene expression in primary tissue are very important.

T21 has been reported to result in global changes in the epigenetic landscape in a number of studies,[375–380], including in fibroblasts from monozygotic twins discordant for T21[381, 382]; this is also observed in the context of haematopoiesis[36, 376–380]. A number of epigenetic regulators are encoded on chromosome 21, summarised in Table 3.3 (page 105), which may be responsible for this global epigenetic and transcriptional dysregulation in T21[358]. These changes may also represent a broader epigenetic and transcriptional response adapting to aneuploidy[383].

Additionally, there is variation between individuals with Down syndrome, with a recent study suggesting there are three distinct groups of individuals with Down syndrome based on which genes on chromosome 21 are overexpressed, and that this translates into different haematological phenotypes in T21[384].

1.3.2 Haematological abnormalities in Down syndrome

There are a number of haematological and immune abnormalities described in Down syndrome. Children with Down syndrome are more susceptible to infections, and have poorer outcomes[385]; infection is reported to be the most common cause of mortality in individuals with Down syndrome at all ages[386]. Additionally, individuals with Down syndrome are more likely to develop autoimmune disease[353].

Abnormalities in fetal haematopoiesis in Down syndrome

Many of the haematological abnormalities in Down syndrome can be traced back to fetal life[36, 69, 387, 388]. In the T21 fetal liver, there is an increased frequency of MEP, and increased HSC, coupled with a decreased frequency of GMP and B progenitors[69, 387], and increased clonogenicity and increased megakaryocyte and megakaryocyte-erythroid colonies from HSC, CMP and MEP[69]. Additionally, in T21 fetal liver, B lymphopoiesis is impaired, with B lymphoid output from fetal liver HSC and lymphoid progenitors *in vitro* being severely impaired, and this is accompanied by a reduction in expression of some early lymphoid genes in T21 fetal liver HSPC[69].

More recent scRNA-Seq studies supported these functional observations[36, 388], with Marderstein et al. suggesting T21 fetal liver HSC are primed to differentiate into erythroid cells[388].

HSPC abnormalities have also been described in T21 fetal BM. scRNA-Seq of T21 fetal BM has identified a reduction in B cell frequency and increased erythroid frequency, and functionally, T21 fetal BM HSC/MPP produced significantly more erythroid colonies and fewer myeloid colonies *in vitro*[36].

Preliminary work previously done in our research group also showed that fetal specific lymphoid progenitors ELP and PreProB were reduced in T21 fetal BM[389]. An *in vitro* failure to produce B cells has also been recapitulated in T21 iPSC[390, 391].

Taken together, these reports suggest haematopoiesis is abnormal in T21 fetal life. There is much less known about T and NK lymphopoiesis in T21 fetal life. Some reports have found a reduced T cell and NK frequency in T21 fetal blood[392], while others report normal T cell frequency but an increased frequency of NK cells[393]. However, both of these studies were small.

Postnatal abnormalities in haematopoiesis in Down syndrome

As haematopoiesis changes through ontogeny, it is unsurprising that the T21 haematopoietic phenotype changes through development and postnatal life; haematological abnormalities in children and adults with Down syndrome have recently been reviewed[394, 395].

Neonates with Down syndrome show a number of haematological abnormalities, mirroring the abnormalities in haematopoiesis observed in T21 fetal life[396, 397]. Dyserythropoiesis is common in neonates with Down syndrome, with abnormal red blood cell morphology, including macrocytosis, target cells and basophilic stippling, accompanied by increased circulating erythroblasts and haemoglobin[396]. Concurrently, platelet frequency is decreased in neonates with Down syndrome, and these too have morphological abnormalities, including circulating megakaryocytes/ fragments of megakaryocytes, and giant platelets[396]. Additionally, neonates

with Down syndrome have increased circulating monocytes and granulocytes, in which some morphological abnormalities are more common (including hypogranular neutrophils and stellate monocytes) [396]. Finally, total lymphocyte frequency in neonates with Down syndrome is reduced[396].

Within the first year of life in disomic children, there is an expansion of T and B lymphocytes, however, this is not observed in children with Down syndrome[398]. While T cell frequencies recover during childhood, B cell frequency remains lower[399–401], especially affecting memory B cells[401, 402]. This deficit of B cells in individuals with Down syndrome continues into adulthood, with a similar reported reduction in memory B cells[401–408]. Additionally, recent work has identified an expanded population of atypical CD11c+, T-bet+ and CD21-expressing B cells in the blood of adults with Down syndrome[403–405], a subset of B cells thought to contribute to autoimmunity[395, 409].

A number of studies report that NK cells are more abundant in children with Down syndrome[410–413], and that this persists into adulthood[404],becoming more marked with age[413].

Monocyte frequency is also affected in children with DS, with reports of classical monocytes (CD14+CD16-) being reduced in frequency, while non-classical monocytes (CD14dimCD16+) being increased in frequency[404, 410], although the findings in adults are less clear[403].

Premature aged haematopoiesis in Down syndrome

These haematological abnormalities observed during fetal life and childhood of individuals with Down syndrome, specifically, decreased B lymphocyte frequency, coupled with a myeloid skew, are reminiscent of haematopoiesis in older adults[72, 414]. This has led to some speculation that T21 haematopoiesis shows a premature ageing phenotype, as seen in other tissues in individuals with Down syndrome, including the skin, hair, endocrine organs, and the central nervous system[415, 416]. Early quantitative evidence in the haematopoietic system considered telomere length as a marker of molecular ageing, and showed that T21 leucocytes had

shorter telomere length[417]. More recently, computationally-modelled 'epigenetic clocks' have shown that T21 peripheral blood leucocytes show an accelerated ageing phenotype in childhood and adult life[405, 418]. This is supported by recent studies of neonatal dried bloodspots[419].

Evidence of altered inflammatory signalling in Down syndrome

Many studies have reported increased circulating inflammatory cytokines in the blood of individuals with Down syndrome[403, 420–425]. In particular, IL6, TNFα and IFNγ have consistently been shown to be elevated[426]. More recently, studies in adults with Down syndrome have shown inter-individual variability, identifying three distinct subgroups with different inflammatory profiles: a high-cytokine (overexpressing 22/29 cytokines tested, including TNFα and IFNγ), intermediate cytokine (overexpressing IL13, IL4, TNFβ, IL6 and IL1α) and a low cytokine group, which clustered with disomic adults. In this study, most (16/21) individuals with Down syndrome fell into high or intermediate groups, suggesting cytokine dysregulation is a common feature of Down syndrome[403]. This heterogeneity in circulating cytokines has been described independently, with similar high- and intermediate- groups identified in a separate cohort, attributing this variability to patterns of overexpression of chromosome 21 encoded genes[384].

It is notable that four of six interferon receptors are encoded on chromosome 21 (*IFNAR1*, *IFNAR2*, *IFNGR2* and *IL10RB*)[427], and increased gene dosage of these receptors has been suggested to be responsible for the overactive interferon response observed in T21 cells[404, 428–431], with knockdown of *IFNAR1* and *IFNAR2* in T21 cell lines resulting in a rescue of the T21 interferon response phenotype to levels comparable to disomic cell lines[430]. Additionally, triplication of the interferon receptor genes in a T21 mouse model was necessary for multiple hallmark phenotypes of Down syndrome, including cognition, craniofacial abnormalities, cardiac malformations and antiviral responses, however, the haematological phenotypes were not directly assessed in this model[432]. Finally, constitutive trisomies themselves have been shown to activate interferon signalling, through

the accumulation of double-stranded DNA in the cytoplasm, and activation of the cGAS-STING pathway[429, 433].

1.3.3 T21 and autoimmune disease

Individuals with Down syndrome have an increased risk of developing a number of autoimmune diseases, including a 4-6-fold increase in autoimmune thyroid disease, type I diabetes and coeliac disease[398, 434–437], as reviewed in [438]. This may reflect the altered inflammatory cytokine landscape, increased CD11c+ B cell frequency and elevated interferon sensitivity. There is also an increase in circulating autoantibodies[403, 439], reacting to the antigens found in the pancreas, gastrointestinal tract, central nervous system, immune system and against rheumatoid factor[395, 403, 439], in individuals with Down syndrome suggesting that B cell dysfunction is an important contributor to autoimmunity in T21.

1.3.4 Haematological malignancies in Down syndrome

Children and adults with Down syndrome, while being less cancer-prone in general, have an increased risk of developing acute leukaemia, with children with Down syndrome having approximately a 30 fold increased risk of acute lymphoblastic leukaemia (DS-ALL) and a 150 fold increased risk of developing a distinct myeloid leukaemia (ML-DS) before their 4th birthday[354, 356, 440], reviewed recently[441, 442].

ML-DS

ML-DS is classified separately to non-DS associated myeloid and megakaryoblastic leukaemias[443], and is virtually unique to individuals with Down syndrome[444–448]. ML-DS is preceded by a stage of transient abnormal myelopoiesis (TAM) in the neonatal period, first described in the 1980s[449], which was later found to be caused by somatic mutations in the *GATA1* gene[450–455]. This mutation results in the production of a truncated GATA1 protein lacking the N-terminal activation domain (GATA1 short, GATA1s), which impairs the role of GATA1 as a key regulator

of erythro- and megakaryopoiesis[452–455]. These *GATA1* mutations have been traced back to prenatal life, most likely originating in the second trimester[456–459], and these mutations are only acquired during fetal life[459]. While most cases of TAM resolve without treatment within three to four months, a small subset of these transforms into full-blown ML-DS, as a result of accumulating secondary mutations, most frequently in cohesin genes, epigenetic regulatory genes, or tyrosine kinase signalling genes[460, 461]. ML-DS responds well to chemotherapy[462] and in the majority of cases is cured[397], however some patients may relapse, which is associated with poor outcomes [463].

DS-ALL

DS-ALL has a less favourable prognosis compared to ML-DS, and compared to ALL in non-DS children, due mainly to treatment-related morbidity and toxicity[464–466], though long term survival has more recently been improving with advances in treatment regimes[467]. DS-ALL is most common in children aged 1-5, and has never been reported in children under the age of 1[356, 465]. Immunophenotypically, DS-ALL most commonly resembles PreB cells; T-lineage DS-ALL is exceedingly rare[468–470].

DS-ALL differs genetically and molecularly from its non-DS counterparts, with "good prognosis" non-DS ALL cytogenetic groups (e.g. *ETV6-RUNX1*, high hyperdiploidy) or "poor prognosis" cytogenetic groups (e.g. *BCR-ABL* translocations or *KMT2A* gene rearrangements) being much less common in DS-ALL[465]. Instead, the most common genetic abnormality in DS-ALL is a rearrangement in *CRLF2*[465, 471–474], a gene encoding part of the receptor to TSLP. In non-leukaemic contexts, signalling through the TSLP receptor induces the JAK/STAT pathway[475]; it is therefore interesting that secondary mutations in JAK/STAT pathway genes are the commonest secondary genetic events in *CRLF2*-rearranged DS-ALL[471, 472, 474].

Unlike ML-DS, the mechanism of leukaemia initiation in DS-ALL is currently unknown. However, the profound impairment in fetal B lymphopoiesis[36, 69, 388], and global changes in the epigenetic landscape in neonates with Down syndrome[379]

may provide a chromatin landscape in fetal life that is more amenable to leukaemic transformation. Additionally, many types of non-DS ALL have been shown to have a prenatal origin[476, 477], including *CRLF2*-rearranged non-DS ALL, in which *CRLF2* rearrangement has been traced back to neonatal bloodspots[478]. A current model of childhood leukaemogenesis proposes that mutations may arise in fetal HSPC, resulting in an abnormal clonal expansion, and after birth further mutations, potentially secondary to infection/ inflammation-related DNA damage, could be the switch to developing an overt leukaemia[476].

Single cell whole genome sequencing studies considering mutation rate in HSPC through ontogeny have found that mutation rate in fetal HSPC is higher than HSPC post-infancy[479]. Importantly, the mutation rate in T21 fetal life was higher than in normal fetal HSPC from very early in development, possibly due to oxidative stress[479]. Oxidative stress was also recently suggested to be increased in T21 fetal liver CD34+CD38+ HSPC[388]. Genes associated with mitochondrial function, such as *SOD1* and *RCAN1* are encoded on chromosome 21, and oxidative stress and mitochondrial dysfunction is reported to be higher in a number of T21 tissues[480–486]. Therefore, this too may be another contributor to leukaemia initiation in T21 fetal life.

There are a number of genes encoded on chromosome 21 involved in the pathology of ALL; this is reflected by the most common acquired chromosomal abnormality in paediatric B-ALL being the complete or partial gain of chromosome 21 (most commonly in high hyperdiploidy B-ALL or iAMP21ALL)[487, 488]. Chromosome 21 encoded genes with a role in leukaemia have been summarised in Table 3.3 (page 105).

1.3.5 The haematopoietic niche in Down syndrome

Much less is known about the haematopoietic niche in Down syndrome. Previous work in the lab investigating T21 fetal liver MSC has shown that they preferentially promote erythropoiesis *in vitro* compared to NM fetal liver MSC[489]. Additionally, co-culture experiments of TAM blasts on murine stromal layers have shown fetal

liver derived stromal cells preferentially support TAM blast expansion compared to adult BM-derived stromal cells[490].

Even less is known about the fetal BM haematopoietic niche in T21. A recent scRNA-Seq analysis provided some initial evidence suggesting Notch ligands are increased in expression in T21 fetal BM endothelial cells, and that *NOTCH1* expression is increased in T21 HSC/MPP[36]. Notch signalling plays a key role in HSC maintenance, as reviewed previously[491]. Additionally, the scRNA-Seq study of T21 fetal BM reported the upregulation of multiple proinflammatory pathways (including TNFα, Type I IFN, IFNγ, IL1 and IL6) in niche cells[36].

One cellular component of the BM haematopoietic niche affected in T21 is the osteoblast population, which has largely been studied in the context of bone development rather than haematopoiesis. Impaired osteoblast differentiation and function in Down syndrome has been reviewed in [492]. Postnatally, individuals with Down syndrome have reduced bone mineral density and an increased risk of fractures and osteoporosis, suggestive of impaired osteoblast function[493]; this phenotype is also recapitulated by murine models of T21[494, 495]. Reduced osteoblast frequency has been shown histologically in an adult with Down syndrome[496]. Similarly, this has been reflected in murine models[497]. These defects may originate in fetal life, as T21 fetuses have decreased long bone length[498, 499], and murine models of Down syndrome have reduced bone volumes during development[494].

1.4 Hypothesis and aims

The main aim of this project was to investigate the cellular and molecular mechanisms underpinning impaired B lymphopoiesis in T21 fetal BM. I refined this into two main research questions:

What are the HSPC-intrinsic factors contributing to impaired B lymphopoiesis in T21 fetal BM?

I addressed this question by:

1. Characterising T21 fetal BM HSPC frequency and functional output
2. Performing bulk RNA-Seq and ATAC-Seq of immunophenotypically defined T21 fetal BM HSPC

How does the T21 fetal BM microenvironment contribute to impaired B lymphopoiesis in T21?

I addressed this question by:

1. Characterising T21 fetal BM stromal cells molecularly, immunophenotypically and functionally
2. Integrating and interrogating published scRNA-Seq datasets of NM and T21 fetal BM
3. Investigating the role of niche-derived inflammatory signals in impairing B lymphopoiesis

2 Methods

2.1 Fetal bone marrow samples

Fetal limbs were collected after elective termination of pregnancy after maternal informed consent was obtained by the Human Developmental Biology Resource (HDBR, REC ref 23/LO/0312 and 23/NE/0135). Tissues were staged (as per Table 2.1) and distributed by the HDBR. Samples were also tested for chromosomal abnormalities by the HDBR, using SNP array or exome sequencing, which allowed the detection of T21. Samples used in this project ranged between 12-22 PCW for normal fetal BM (median=17 PCW) and 12-19 PCW for T21 fetal BM (median=15 PCW).

PCW	**Foot length (mm)**	**Knee - heel length (mm)**	**Gestational age in weeks**
Late 8	<5 and less than 6	8	10
9	6 or above and less than 8	11	11
10	8 or above and less than 10	13	12
11	10 or above and less than 13	17	13
12	13 or above and less than 17	24	14
13	17 or above and less than 20	31	15
14	20 or above and less than 23	36	16
15	23 or above and less than 25	40	17
16	25 or above and less than 27	43	18
17	27 or above and less than 31	51	19
18	31 or above and less than 33	56	20
19	33 or above and less than 36	60	21
20	36 or above and less than 40	66	22

Table 2.1: HDBR Fetal Staging Guide [500]

2.2 Sample processing, cryopreservation and thawing

Fetal tissue was transported at 4°C and processed immediately on arrival in the lab under tissue culture sterile conditions[20, 69]. Briefly, limbs were dissected to extract long bones. These were flushed with Dulbecco's Modified Eagle Medium (DMEM) with a narrow gauge needle, and this suspension was passed through a 70μm filter to obtain a single cell suspension. Samples were red cell and granulocyte depleted by density gradient using Ficoll-Paque PLUS (GE Healthcare) and mononuclear cells were isolated from the mononuclear layer carefully using a sterile dropping pipette. Freshly isolated mononuclear cells were stained with CD34 microbeads for thirty minutes (Miltenyi) at 4°C, and then magnetically separated using MS or LS columns, depending on sample size (Miltenyi); CD34+ and CD34- fractions were cryopreserved as described below.

To assess stromal composition of fetal BM, dissected long bones were cut into small pieces before grinding with a pestle and mortar. These were incubated at 37°C with agitation in pre-warmed digestion medium: 2.5mg/ml Liberase TM (Sigma-Aldrich, contains collagenase I and II), 20μg/ml DNAseI (Sigma-Aldrich), supplemented with 10% heat-inactivated fetal bovine serum (FBS) (Sigma-Aldrich). Once digested, the material was immediately passed through a 100μm filter and washed with PBS with 1mM EDTA and 2% heat-inactivated FBS.

Cells from processed samples were centrifuged at 300g for 5 minutes, aliquoted and cryopreserved in heat-inactivated FBS supplemented with 10% DMSO and stored in liquid nitrogen until further analysis. Samples were stored in compliance with the Human Tissue Act (HTA, 2004).

Before use in experiments, samples were thawed at 37°C for two minutes, diluted in an excess of pre-warmed heat-inactivated FBS, and centrifuged at 300g for 5 minutes. Sample recovery was assessed by counting. All counts were manually performed using a haemocytometer, with cell suspensions diluted 1 in 10 in Trypan Blue (0.4%, Gibco).

2.3 Flow cytometry analysis and sorting

Cells were stained for flow cytometry in 100μl FACS buffer (PBS with 2% heat-inactivated FBS, and 1mM EDTA) for 30 minutes in the dark with fluorophore-conjugated antibodies and viability dyes. Antibody details are described in Table 2.3. Samples were analysed on BD Fortessa X20, and sorted on BD Fortessa Fusion instruments. Gates were set based on Fluorescence Minus One (FMO) gating on viable cells, and analysed using FlowJo v10.10.

2.3.1 FAC-Sorting (FACS) of fetal BM HSPC

Bead selected CD34+ HSPC were thawed and stained as described above, and HSPC were sorted on a BD Fortessa Fusion instrument. The gating strategy and immunophenotypes for this are described in Table 2.2 and Figure 2.1 respectively.

Population	**Immunophenotype**
HSC	Lin2-CD19-CD34+CD38-CD45RA-CD90+
MPP	Lin2-CD19-CD34+CD38-CD45RA-CD90-
LMPP	Lin2-CD19-CD34+CD38-CD45RA+CD10-
MLP	Lin2-CD19-CD34+CD38-CD45RA+CD10+
PreELP/GMP	Lin2-CD19-CD34+CD38+CD127-CD10-CD45RA+CD123-
ELP	Lin2-CD19-CD34+CD38+CD127+CD10-
CLP	Lin2-CD19-CD34+CD38+CD10+
PreProB	Lin2-CD19-CD34+CD10-CD19+
ProB	Lin2-CD19-CD34+CD10+CD19+
CMP	Lin2-CD19-CD34+CD38+CD127-CD10-CD45RA-CD123+
GMP	Lin2-CD19-CD34+CD38+CD127-CD10-CD45RA+CD123+
MEP	Lin2-CD19-CD34+CD38+CD127-CD10-CD45RA-CD123-
Lin2: CD2/3/14/16/56/235a	

Table 2.2: Immunophenotypes defining HSPC populations.

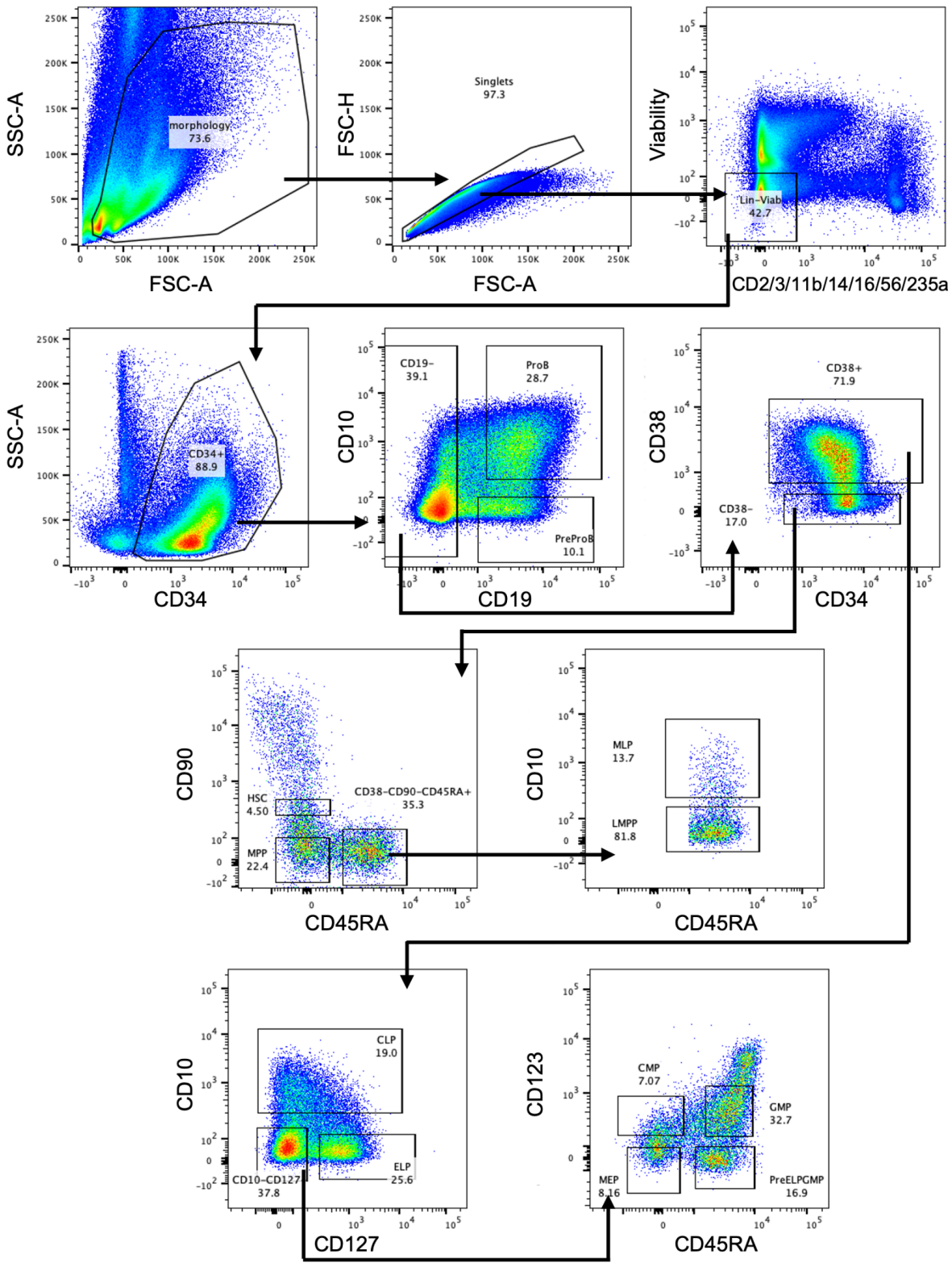

Figure 2.1: Sort gating fetal BM HSPC. Gating strategy to sort cells isolated from Ficoll-separated mononuclear cells and positively selected for CD34+ expression by magnetic beads; representative NM sample from second trimester shown.

2.3.2 Flow cytometry of whole fetal bone

Fetal bones processed by crushing and digestion, as described above, were thawed and stained for flow cytometry. Live, CD45- CD235a- CD71- CD31- cells' unscaled, compensated MFI values were exported and arcsinh transformed, as done in established dimensionality reduction pipelines for multiparameter flow cytometry and mass cytometry [501–503]. PCA was performed on these values, and the top 11 prinicipal components (PCs) were used for UMAP. Kmeans clustering was carried out using the top 11 PCs.

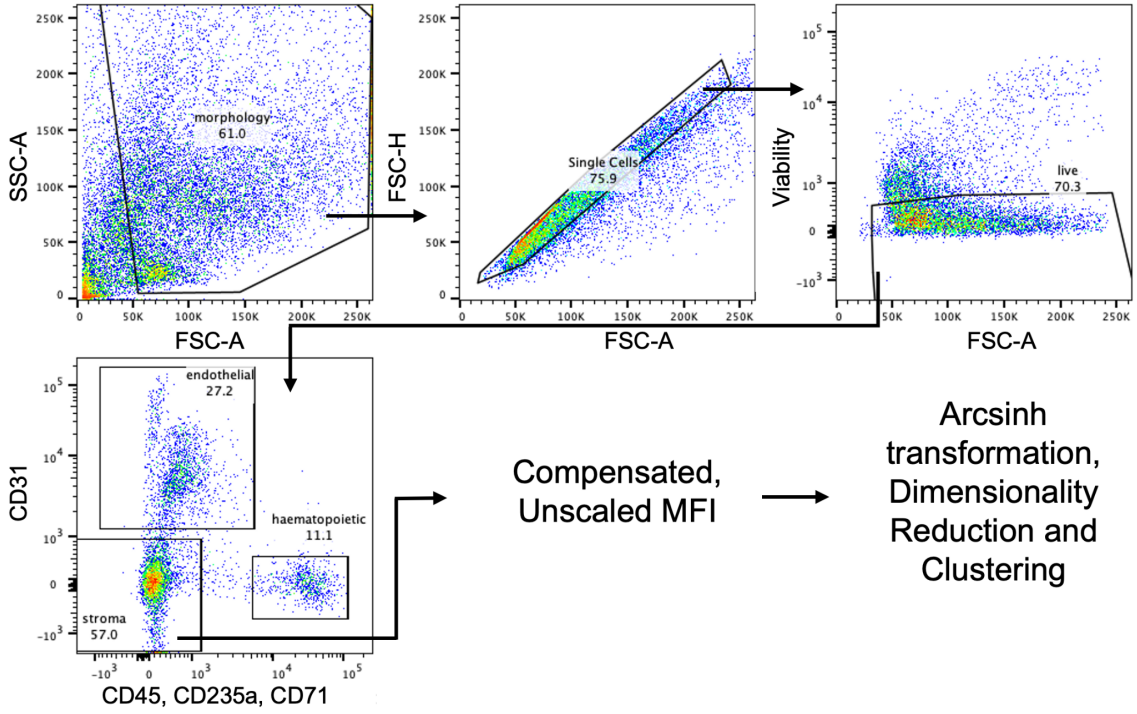

Figure 2.2: Flow cytometry analysis of whole fetal BM. Gating strategy for cells isolated from crushed, digested bone marrow; representative second trimester sample shown.

2.3.3 Intracellular flow cytometry

Cryopreserved samples from crushed and digested fetal long bones were thawed as described earlier and passed through a 100μm filter. Cells were treated with a low concentration of LPS (10ng/ml, Sigma) and a protein transport inhibitor (GolgiPlug, BD Biosciences) for five hours at 37°C. Cells were stained as described earlier, and fixed and permeabilised using the BD Cytofix/Cytoperm Kit according to manufacturer's instructions. Intracellular staining for TNFα was performed for 30 minutes at 4°C; staining with an isotype control with the same fluorophore (BV650) was also used as a negative control. Cells were then washed using the BD Cytofix/Cytoperm wash buffer before analysis by flow cytometry.

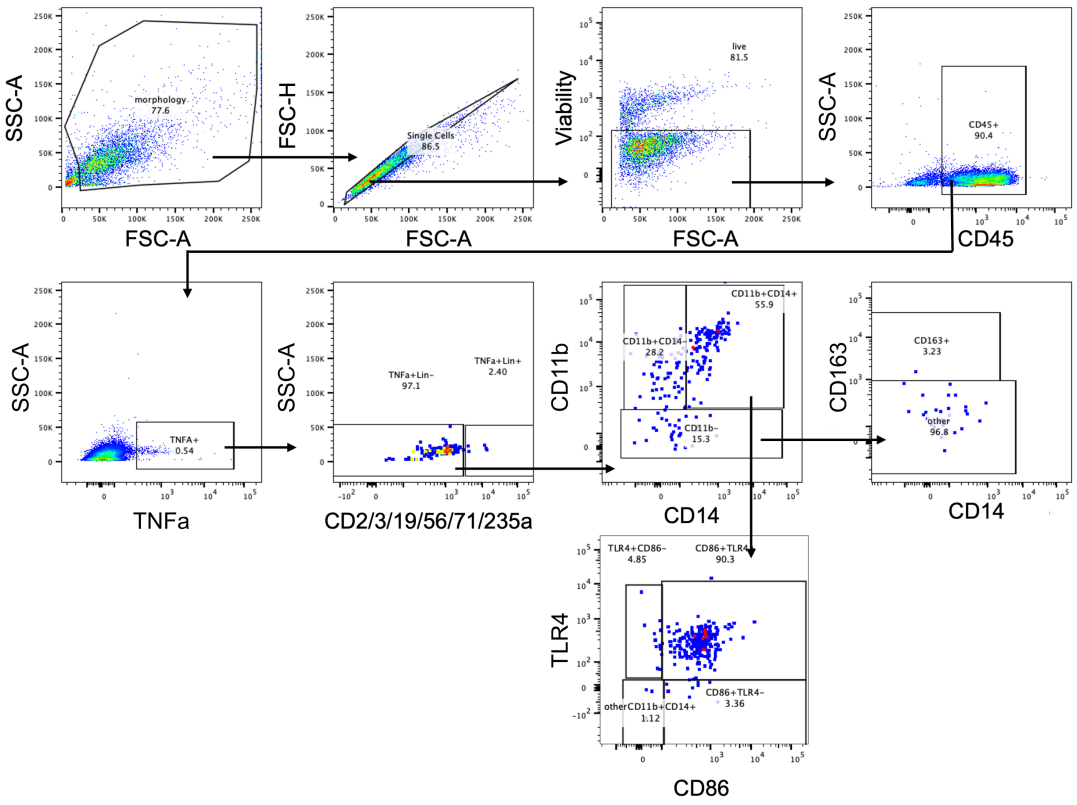

Figure 2.3: Intracellular flow cytometry for TNFα. Gating strategy for cells isolated from crushed, digested bone marrow treated with 10ng/ml LPS and protein transport inhibitor GolgiPlug for five hours, before staining. Representative NM second trimester sample shown.

Table 2.3: Details of antibodies used for flow cytometry

Antibody	**Colour**	**Clone**	**Company**	**Cat No**
ALPL	AF700	B4-78	RnD	FAB1448N-100UG
CD10	FITC	eBioCB-CALLA	Life Tech	11-0106-42
CD10	PECY7	eBioCB-CALLA	Life Tech	25-0106-42
CD10	PECy5	eBioCB-CALLA	Life Tech	15-0106-42
CD11b	FITC	ICRF44	Biolegend	B362416
CD11b	PE-Dazzle	ICRF44	Biolegend	301348
CD11b	PECy7	ICRF44	Biolegend	301322
CD123	BV650	6H6	Biolegend	306020
CD127	PE	eBioRDR5	Life Tech	12-1278-42
CD14	PerCPCy5.5	M5E2	Biolegend	301824
CD14	FITC	61D3	Biolegend	B367422
CD14	AF700	63D3	Biolegend	367114
CD146	PECy7	P1H12	Biolegend	361008
CD15	PerCPCy5.5	W6D3	Biolegend	323020
CD16	PerCPCy5.5	3G8	Biolegend	302028
CD163	BV421	GHI/61	Biolegend	333611
CD19	APC	HIB19	Biolegend	302212
CD19	FITC	HIB19	Life Tech	11-0199-42
CD19	BV421	HIB19	Biolegend	302234
CD2	PerCPCy5.5	RPA-2.10	Biolegend	300216
CD2	FITC	RPA-2.10	Life Tech	11-0029-42
CD20	PE-Dazzle	2H7	Biolegend	302348
CD235	PerCPCy5.5	HIR2	Biolegend	306614
CD235	FITC	HIR2	LifeTech	11-9987-82
CD271	PerCPCy5.5	ME20.4	Biolegend	345111
CD284	APC	HTA125	Biolegend	312816
CD3	PerCPCy5.5	OKT3	Biolegend	317336
CD3	FITC	OKT3	LifeTech	11-0037-43
CD3	BV711	OKT3	Biolegend	317328
CD31	BV711	WM59	Biolegend	303135/303136
CD33	FITC	P67.6	Biolegend	366620
CD33	PE	WM53	Life Tech	12-0338-42
CD339	BV650	MHJ1-152	BD Bioscience	custom
CD34	BV421	561	Biolegend	343610

Antibody	Colour	Clone	Company	Cat No
CD34	PECy7	4H11	Life Tech	25-0349-42
CD38	AF700	HIT2	Life Tech	56-0389-42
CD45	BUV395	HI30	BD Bioscience	563792
CD45	FITC	HI30	Biolegend	304006
CD45	AF700	2D1	Life Tech	56-9459-42
CD45RA	APC ef780	HI100	Life Tech	47-0458-42
CD56	PerCPCy5.5	HCD56	Biolegend	318322
CD56	PE	CMSSB	Life Tech	12-0567-42
CD56	FITC	HCD56	Life Tech	11-0566-42
CD71	FITC	OKT9	Life Tech	11-0719-42
CD73	APCCy7	AD2	Biolegend	344022
CD86	PE	IT2.2	Biolegend	305405
CD90	BV421	5 E10	Biolegend	328122
CD90	BV421	5 E 10	Biolegend	328122
HLA-DR	FITC	L243	Life Tech	11-9952-42
LEPR (CD295)	AF647	52263	BD Bioscience	564376
NG2	PE	7.1	ThermoFisher	MA5-28549
TNFa	BV650	MAb11	Biolegend	502938
viability	ef506	—	Life Tech	65-0866-18

2.4 Co-cultures on MS5 stroma to assess B lymphoid potential of fetal BM HSPC

Murine stromal cell line MS5 cells[504] were a kind gift from Prof. Paresh Vyas, Weatherall Institute of Molecular Medicine, University of Oxford.

MS5 cells were grown in αMEM (Gibco) supplemented with 10% heat-inactivated FBS, 100U/mL Penicillin, 100μg/mL Streptomycin (Gibco), 2mM L-glutamine (Gibco), 50μM 2-Mercaptoethanol (Gibco), 10mM HEPES (Gibco) (hereafter referred to as αMEM-C10), with half media changes being conducted every 3-4 days. When cells reached 80% confluence, cells were split by first washing with sterile PBS and then incubating for 10 minutes at 37°C with 0.05% trypsin. Cells were split 1:5.

MS5 co-cultures were conducted as standard methods in the lab[20, 69]. Briefly, 30,000 MS5 cells were plated per well in a 24 well plate 24 hours prior to the start of a co-culture assay. 100 FAC-sorted HSC/MPP/LMPP were plated on this MS5 layer in αMEM-C10 supplemented with SCF (20ng/ml, Peprotech), FLT3L (10ng/ml, Peprotech), IL2 (10ng/ml, Peprotech) and IL7 (5ng/ml, Peprotech) in 24 well plates.

For TNFα co-culture experiments, recombinant TNFα (Peprotech) was added at concentrations of 0.1ng/ml, 1ng/ml, 10ng/ml, 100ng/ml and 1μg/ml. Half media changes were conducted every 3-4 days. At weekly time points, wells were harvested by manual pipetting, and washing three times with sterile PBS (Gibco), before being passed through a 70μm filter to obtain a single cell suspension. The B, NK and myeloid output of co-cultures were assessed by flow cytometry every seven days, with absolute cell numbers calculated using CountBright beads (Invitrogen). The co-cultures were replated on a fresh MS5 stromal layer after two weeks of in co-culture.

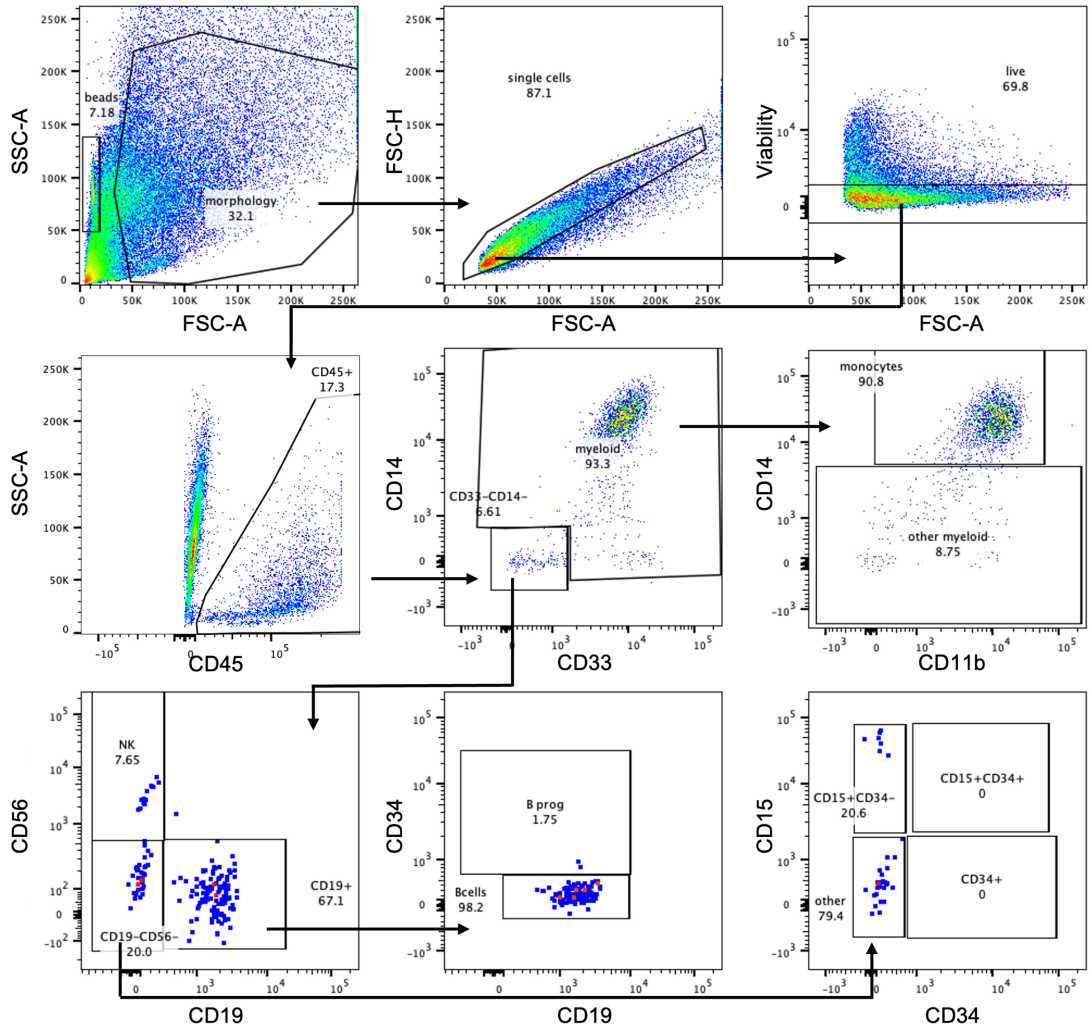

Figure 2.4: Gating strategy for MS5 co-culture assays. Representative plots showing the gating strategy of a NM fetal BM HSC co-cultured on MS5, with SCF (20ng/ml), FLT3L (10ng/ml), IL2 (10ng/ml) and IL7 (5ng/ml).

2.4.1 TNFα ELISA

Media from half media changes were collected from NM and T21 fetal BM HSPC MS5 co-cultures, centrifuged at 400g for 10 minutes at 4°C. The supernatant was collected and stored at -80°C until analysis by ELISA (TNFα DuoSet, R&D Systems), which was performed according to kit instructions.

THP1 monocytic cells[505] were used as a positive control and were a kind gift from the Milne lab, Weatherall Institute of Molecular Medicine, University of Oxford. 1000 THP1 cells per well were plated in a 24 well plate, in RPMI 1640 medium (Gibco), supplemented with 10% heat-inactivated FBS and 100U/mL Penicillin, 100μg/mL Streptomycin (Gibco). These were treated with 50ng/ml Phorbol 12-myristate 13-acetate (PMA) for 48 hours to induce macrophage differentiation *in vitro*. Then, these cells were treated with 10ng/ml lipopolysaccharide (LPS, Sigma) for 12 hours to induce TNFα secretion. The supernatant was collected and used as a positive control for the TNFα ELISA.

2.5 Derivation and characterisation of fetal BM MSC

Normal or T21 fetal BM MSC were derived by plating 1-2 million fetal BM mononuclear cells per well of a six well plate in αMEM-C10. After 48 hours of culture, the non-adherent cells were washed away and the adherent cells were maintained, expanded and passaged as described with MS5. MSC derived in this way matched conventional definitions[293] (Figure 2.5).

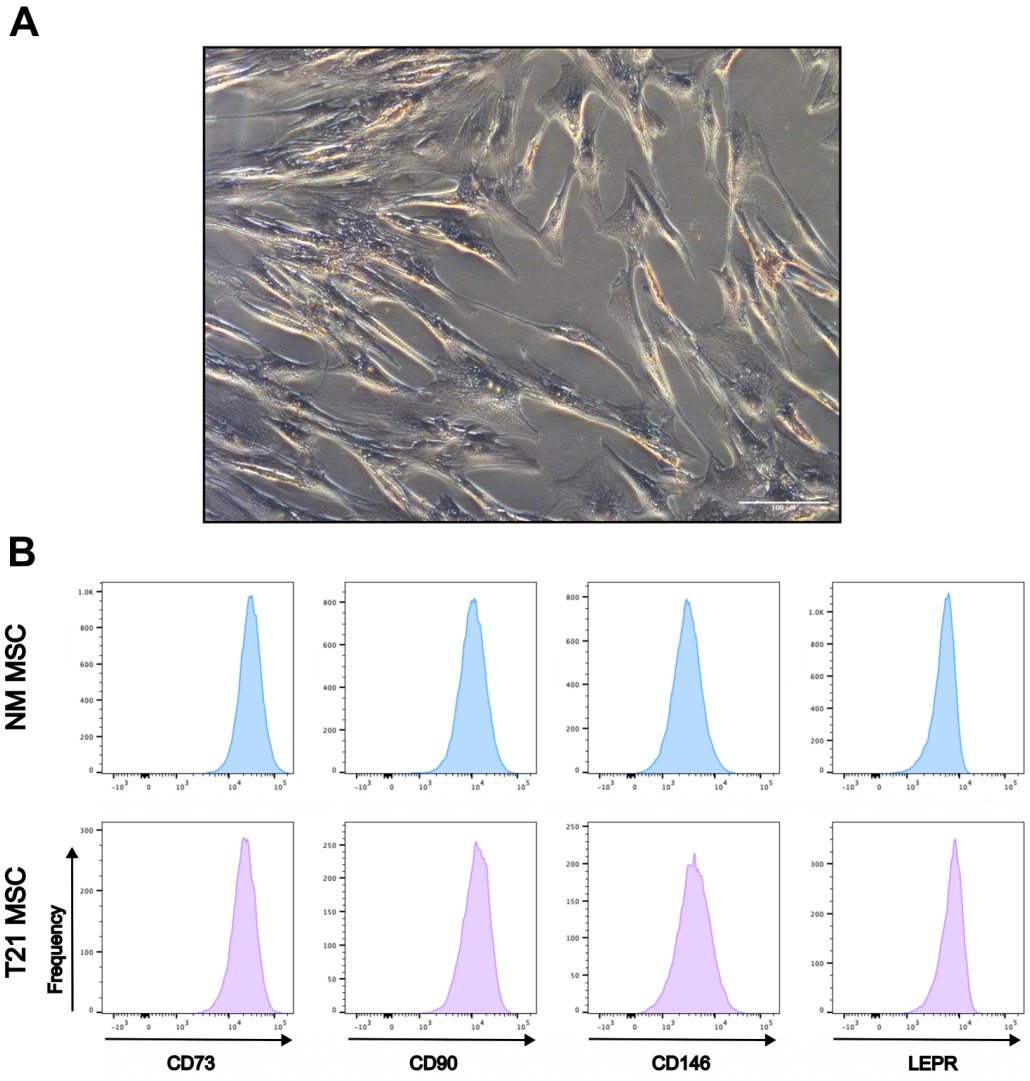

Figure 2.5: Characterisation of derived MSC. Primary fetal BM MSC were derived from MNC. (A) Representative image showing morphology of primary fetal BM MSC, scale bar = 100 μm. (B) Representative histograms showing immunophenotype of primary MSC derived from NM and T21 fetal BM. NM: normal; T21: Trisomy 21.

2.6 Osteolineage differentiation of fetal BM MSC

20,000 fetal BM MSC (passage 4-5) were seeded into a well of a 24 well plate in αMEM-C10 for 24 hours, allowed to adhere, and then cultured in either base medium (αMEM-C10) or osteogenic medium (αMEM-C10 supplemented with 50μM ascorbic acid, 10mM β-glycerophosphate and 100nM dexamethasone) for 14 days. Osteolineage differentiation was assessed qualitatively, by Alizarin Red staining, and quantitatively, by flow cytometry at day 7 and day 14.

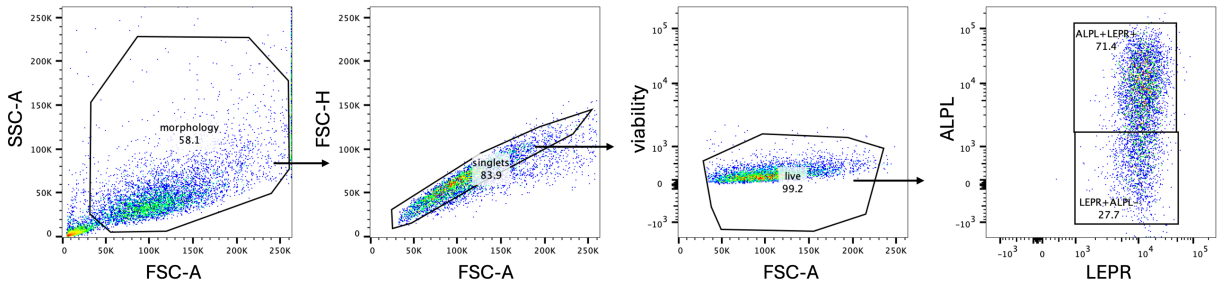

Figure 2.6: Gating strategy for fetal BM MSC differentiation into osteolineage cells. Representative plots showing the gating strategy of fetal BM MSC grown under osteogenic conditions. Expression of ALPL was used to identify osteolineage cells, with ALPL+LEPR+ cells being considered as osteoMSC.

2.6.1 Alizarin Red staining

MSC under base or osteogenic conditions were gently washed with PBS and fixed for 20 minutes with 4% formaldehyde at room temperature. After two gentle washes with deionised water, the fixed cells were stained with 40mM Alizarin Red staining solution (Sigma-Aldrich) for 20 mins. Stained wells were washed four times with deionised water, and imaged with an Olympus BX60 microscope with a Lumenera Infinity 3s camera. Images were analysed using FIJI (v2.9.0).

2.7 MSC co-cultures to assess stromal support of B lymphopoiesis

100 FAC-sorted HSC/MPP/LMPP or 2000 bead-selected CD34+ cells were cultured on 40,000 NM or T21 fetal BM MSC plated 24 hours prior in SFEMII supplemented

with 10% heat-inactivated FBS, 100U/ml Penicillin and 100μg/ml Streptomycin. At the time of HSPC plating, co-cultures were supplemented with IL2 (10ng/ml), IL7 (5ng/ml), FLT3L (10ng/ml) and SCF (20ng/ml). Haematopoietic output was assessed at weekly intervals by flow cytometry, as described above in MS5 co-culture assays.

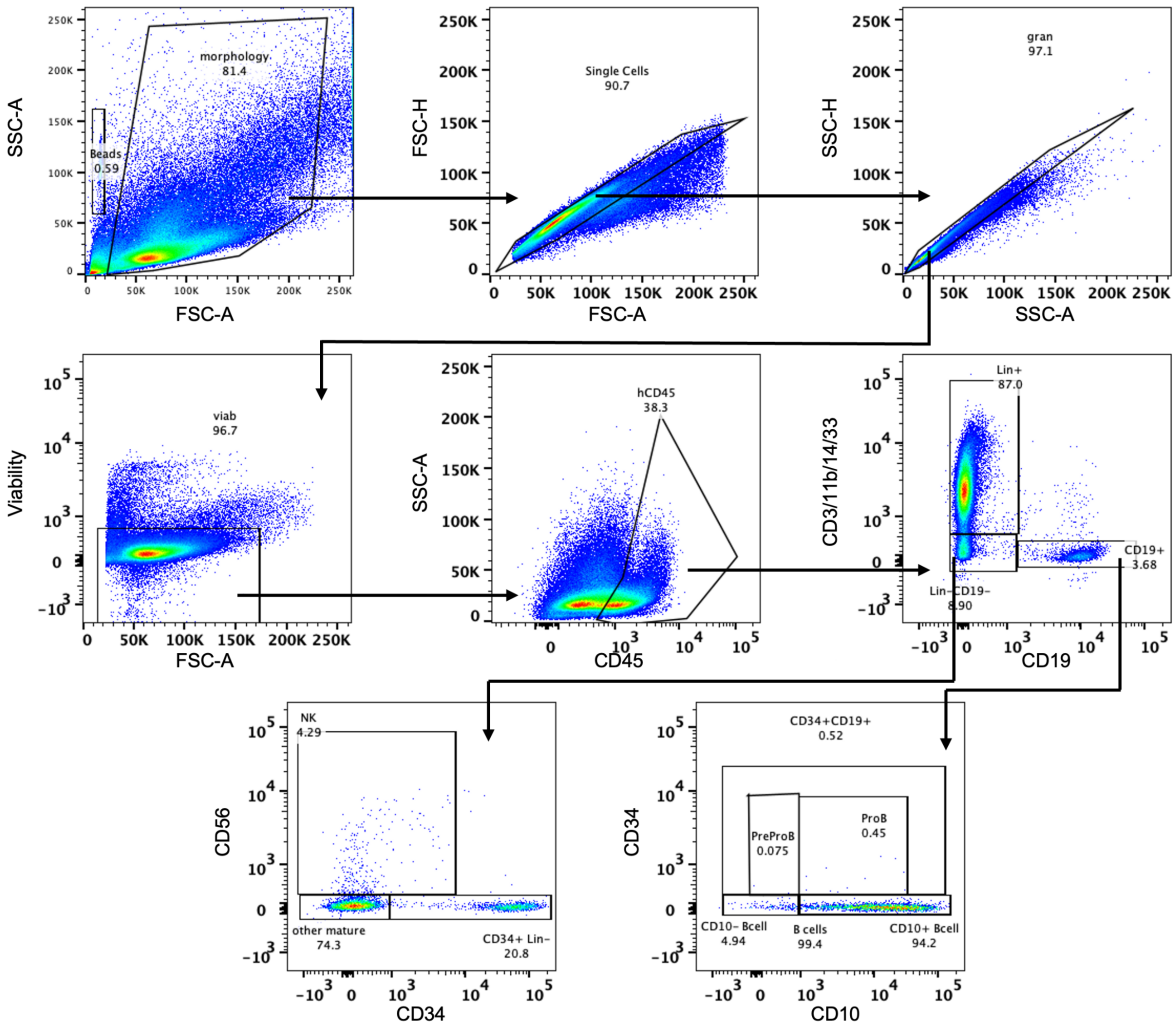

Figure 2.7: Gating strategy used to analyse output from MSC co-culture experiments. One representative sample of NM fetal BM HSC co-cultured on NM fetal BM MSC shown.

2.8 Analysis of MSC-secreted cytokines

500,000 fetal BM derived MSC expanded *in vitro* (passages 3-8) were plated in a 25cm^3 flask in αMEM-C10 and allowed to adhere for 12 hours. After this, αMEM-C10 was removed and replaced with 10ml serum-free medium for 48 hours. This was centrifuged at 400g for 10 minutes at 4°C, and the supernatant was collected and stored at -80°C. ELISA for BMP6 secretion (BMP6 DuoSet kit, R&D systems) and custom human Luminex Discovery Assays (Biotechne, panel provided below in Table 2.4) were performed according to manufacturer instructions on these supernatants.

Luminex Discovery Assay
Angiopoietin-1
FLT3L
HGF
IFNα
IGFBP1
IGFBP6
IL3
IL7
IL11
IL12/IL23 p40
IL15
IL6Rα
LIF
TSLP
IFNγ
IL2
IL6
IL12 p70
IL13
SCF
TNFα
VEGF

Table 2.4: Panel for Luminex Assay

2.9 Bulk RNA-Seq of derived MSC

500,000 fetal BM MSC cultured *in vitro* (passages 2-9) were harvested by incubating for 10 minutes at 37°C with 0.05% trypsin. Total RNA was extracted using the RNeasy mini kit (Qiagen) as per the manufacturer's instructions. RNA quality was assessed by TapeStation (Agilent), and samples with an RNA integrity number (RIN) score of 8/10 or above were taken forward. This RNA was then purified for mRNA, using the NEBNext Poly(A) mRNA magnetic isolation kit as per the manufacturer's instructions. cDNA synthesis, end prep and adaptor ligation was done using the NEBNext Ultra II Directional RNA Library Prep Kit for Illumina according to the manufacturer's instructions. Quality control of these libraries was performed using a TapeStation (Agilent) instrument, and libraries were quantified by KAPA (Roche). Good quality libraries, lacking adapter dimers were pooled for sequencing, and sequenced on an Illumina NextSeq instrument using 75 cycles for paired end sequencing.

2.10 Bulk RNA-Seq of fetal BM HSPC populations

Mini-bulk RNA-Seq of fetal BM HSPC was performed using a protocol modified from SMARTSeq2[506, 507]. 50-100 HSPC (depending on population frequency) were FAC-sorted into 4.15μl lysis buffer containing Triton-X100 (0.18%), RNAse inhibitor (0.96U/μl), dNTPs (2.4mM), oligoDT (2.4μM) and protease (0.026AU/μl) at 4°C, as described in [20]. Once cells were sorted, samples were spun down, immediately snap frozen and stored at -80°C until further processing.

Samples were processed within two weeks of sorting. First, samples were thawed and heat-shocked at 72°C for 15 minutes. Then, mRNA was reverse transcribed. 10μl of master mix containing 5X buffer (Takara, 639538), RNAse inhibitor (1.78U/μL, Takara), Smartscribe Reverse Transcriptase (17.8U/μL, Takara) and LNA-TSO (1.78μM, IDT) was added to the samples. Samples were incubated at

42°C for 90 minutes, followed by ten cycles of two minutes at 50°C then two minutes at 42°C, followed by a fifteen minute incubation at 72°C.

This cDNA was then amplified by PCR. 15μl of mastermix containing 2x buffer (Takara, 638509), ISPCR primers (0.83μM, IDT) and SeqAMP DNA Polymerase (3.33U/μl, Takara) was added immediately. Libraries were incubated at 98°C for three minutes, followed by eighteen (or nineteen, if 50 cells were sorted) cycles of 15 seconds at 98°C, then 20 seconds at 67°C, then six minutes at 72°C; followed by five minutes at 72°C.

Libraries were subsequently cleaned using Ampure XP beads (Beckman Coulter) using a ratio of (0.6 beads: 1 cDNA) by volume and quality control of libraries was conducted by TapeStation. Good quality libraries were quantified by QuBit. Tagment DNA buffer (Illumina) and Amplicon Tagment Mix (Illumina) were added to 1ng of DNA per library, and incubated at 55°C for five minutes. Immediately afterwards, NT buffer (Illumina) was added to stop the reaction.

Libraries were then indexed using Nextera N7 and S5 indexes (Illumina) which were added to libraries with Nextera PCR Mastermix (Illumina). These were incubated at 72°C for three minutes, then 95°C for thirty seconds, followed by twelve cycles of ten seconds at 95°C, then thirty seconds at 55°C, then thirty seconds at 72°C, followed by five minutes at 72°C. Libraries were once again cleaned using Ampure XP beads (Beckman Coulter) and quality control was conducted by TapeStation.

Libraries were quantified by KAPA (Roche) and pooled, and sequenced on an Illumina NextSeq instrument using 75 cycles for paired end sequencing.

Population	**NM n=**	**T21 n=**	**NM (previously generated) n=**	**N T21 (previously generated) n=**	**NM (total) n=**	**T21 (total) n=**
HSC	0	2	10	5	10	7
MPP	0	0	9	6	9	6
LMPP	1	1	5	2	6	3
MLP	2	2	3	2	5	4
PreELP/GMP	1	1	6	2	7	3
ELP	0	2	9	1	9	3
CLP	0	1	9	2	9	3
PreProB	0	0	10	3	10	3
ProB	0	0	9	7	9	7
CMP	0	0	6	5	6	5
GMP	0	0	8	5	8	5
MEP	0	0	6	5	6	5

Table 2.5: Table summarising number of RNA-Seq libraries generated for analysis from FAC-sorted NM and T21 fetal BM HSPC.

2.11 RNA-Seq analysis

Raw paired-end RNA-Seq reads first underwent quality control using Fastqc (v0.11.9) [508], and then were trimmed using TrimGalore (v0.6.10)[509] and mapped to the human genome (hg38) using STAR (v2.7.3a)[510]. Counts tables were generated using featureCounts (v2.0.6)[511].

Counts tables were read into R (v4.2.2). Where counts tables from multiple batches were combined for fetal BM HSPC, batch correction was performed using limma[512] (Figure 2.8).

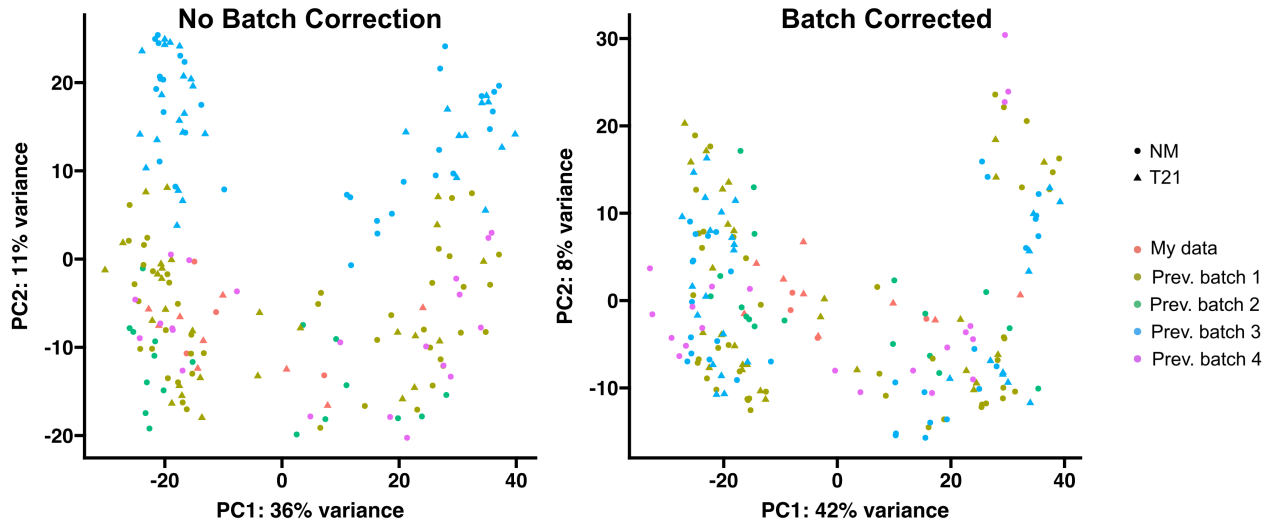

Figure 2.8: Initial analysis of RNA-Seq libraries to check for a batch effect. PCA of previously generated RNA-Seq libraries alongside libraries I generated. Batch correction was performed using limma.

2.11.1 Differential expression analysis and and GSEA (Gene Set Enrichment Analysis)

Pairwise differential expression analysis was carried out for a given population between NM and T21 fetal BM using DESeq2 (v1.38.3)[513]. Additionally, DESeq2 was used to generate normalised counts, using their median of ratios method, and to perform variance stabilising transformations (VST) for principal component analysis[513].

Gene Set Enrichment Analysis (GSEA)[514] was performed using the results of DESeq2 analysis, using the Wald-statistic to rank genes in MSigDB's Hallmark gene sets.

2.11.2 Weighted Gene Correlation Network Analysis

Weighted Gene Correlation Network Analysis (WGCNA) (v1.72.5)[515] was performed on VST-transformed count matrices, generating separate networks for NM and T21 fetal BM HSPC. Modules were annotated based on their the genes most associated with them; the key B lymphoid modules were identified, and the top genes have been listed on pages 220-221.

2.11.3 Differential exon usage analysis

Differential exon use for *RUNX1* was performed using DEXSeq (v1.54.1)[516]. BAM files generated by STAR during mapping were used to quantify reads in non-overlapping exonic parts from a transcript database from Ensembl. Differential exon usage analysis across all exons in the genome was performed using DEXSeq, comparing NM and T21 fetal BM HSC, MPP and LMPP, before focussing on *RUNX1*.

2.12 Assay for Transposase-Accessible Chromatin using sequencing (ATAC-Seq) of fetal BM HSPC

ATAC-Seq of immunophenotypically defined HSPC was performed using our standard lab protocol[20]. Briefly, 900-2000 cells were FAC-sorted into Eppendorf tubes containing 2x TD buffer (Illumina) and digitonin (Promega) at 4 °C. Unfortunately, due to the scarcity of MLP in fetal BM; and PreELP/GMP, ELP and CLP in T21 fetal BM, it was not possible to FAC-sort enough cells from any of these populations for ATAC-Seq. Tn5 transposase (Illumina) was added to cells and incubated at 37 °C with agitation for 30 minutes. Transposed DNA was immediately purified using a Qiagen MinElute Reaction Cleanup Kit and amplified by PCR. Quality control of the libraries was conducted by Tapestation (Agilent) and library quantification was performed using KAPA (Roche). Libraries were pooled and sequenced on an Illumina NextSeq instrument using 75 cycles for paired end sequencing.

Population	**NM n=**	**T21 n=**	**NM (previously generated) n=**	**N T21 (previously generated) n=**	**NM (total) n=**	**T21 (total) n=**
HSC	1	2	2	2	3	4
MPP	1	2	3	1	4	3
LMPP	2	2	3	2	5	4
PreELP/GMP	2	0	2	1	4	1
ELP	0	0	2	0	2	0
CLP	1	1	3	1	4	2
PreProB	0	0	5	5	2	1
ProB	0	1	5	2	5	3
CMP	0	2	3	2	3	4
GMP	0	2	3	2	3	4
MEP	0	1	3	0	3	1

Table 2.6: Table summarising number of ATAC-Seq libraries generated for analysis from FAC-sorted NM and T21 fetal BM HSPC.

2.13 ATAC-Seq Analysis

Raw paired-end RNA-seq reads first underwent quality control using Fastqc (v0.11.9) [508], and then were trimmed using TrimGalore (v0.6.10)[509] and mapped to the human genome (hg38) using BowTie2 (v2.4.2)[517] - SAM files generated from this were indexed and sorted, and saved as BAM files, using SamTools (v1.17)[518]. MACS3 (v3.0.2)[519] was used to call peaks, using an FDR of 0.01. Narrow peaks and BAM files were input into DiffBind (v3.18.0)[520], which was used to define a consensus peak set (using peaks expressed in three or more samples), and to generate a counts table.

There was reasonable concordance between batches of ATAC-Seq data, so no batch correction was performed (Figure 2.9).

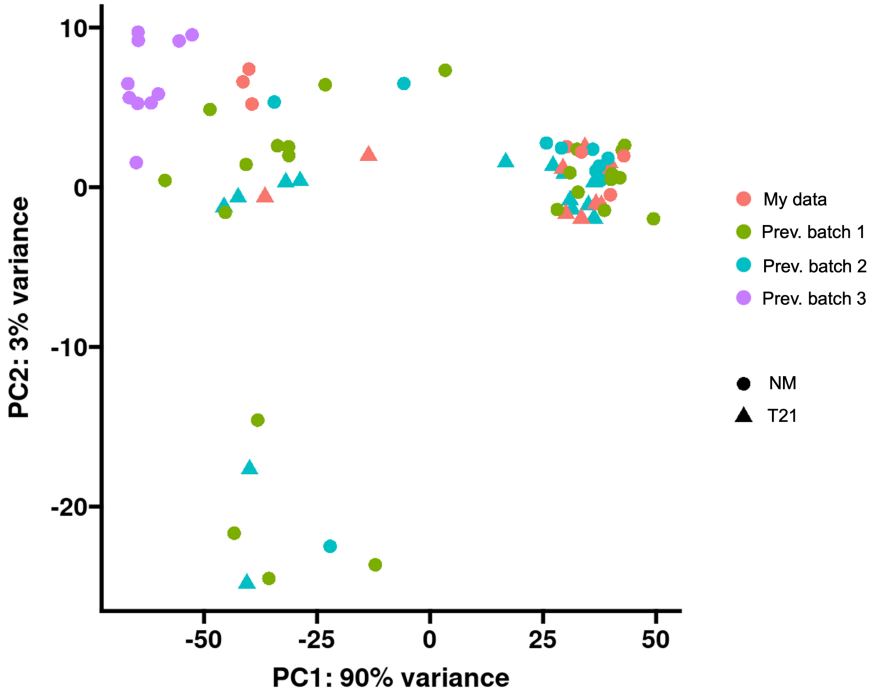

Figure 2.9: Initial analysis of ATAC-Seq libraries to check for a batch effect. PCA of previously generated ATAC-Seq libraries alongside libraries I generated.

2.13.1 Differential accessibility analysis

Differential accessibility analysis was performed for pairwise comparisons between NM and T21 fetal BM HSPC for a given population, using DESeq2 in tandem

with DiffBind, with an FDR of 0.1. Peaks were annotated using ChIPpeakAnno (v3.42.0)[521] based on distance to transcription start site for a given gene, annotated such that they are less than 1000bp upstream of or within this gene.

2.13.2 Motif enrichment analysis

Differentially accessible peaks (FDR <0.1) were saved as BED files, and motif enrichment analysis was performed for a given fetal BM HSPC population comparing NM and T21, using Homer (v4.11) [522]. Non-differentially accessible peaks (FDR >0.1) were set as the background, and known motifs were considered and plotted.

2.13.3 Visualisation of peaks

Chromatin accessibility tracks, saved as BigWig files, were generated from BAM files, normalised to sequencing depth using deepTools (v3.5.2)[523]. These individual normalised BigWig files were averaged to generate a single mean track per condition using WiggleTools (v1.2)[524].

2.14 Analysis of scRNA-Seq datasets

Matrices, or annotated AnnData objects where available, from publicly available datasets [36, 45, 388] were downloaded, and analysed using Seurat (v5.3.0)[525]. Cells with fewer than 200 unique detected genes, and total mitochondrial gene expression exceeding 5% were excluded from further analysis. Genes expressed in fewer than three cells were also removed from further analysis.

2.14.1 Integration of scRNA-Seq datasets

Principal components (PC) were calculated and the top 20 PCs were used for further dimensionality reduction. Data were batch corrected using Harmony [526] to account for technical variation from different datasets. Harmony's k-means-based clustering algorithm was used to iteratively cluster cells in the integrated dataset.

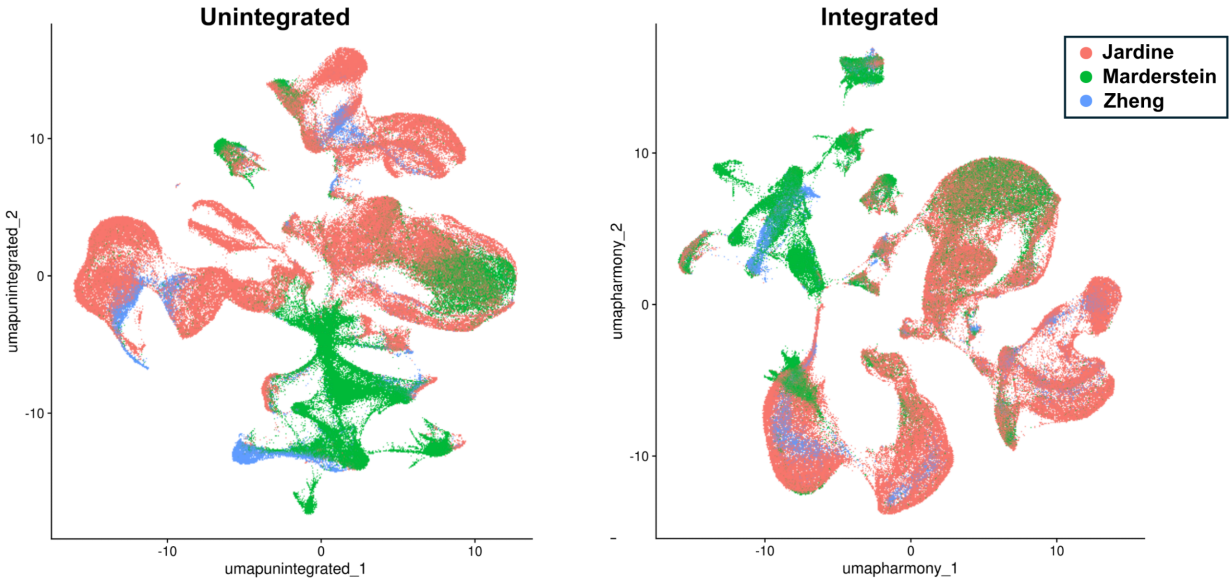

Figure 2.10: Integration of scRNA-Seq datasets using Harmony. Integration and re-annotation of published single cell RNA-Seq datasets of NM and T21 fetal BM[36, 45, 388]. UMAP of cells merged by fetal BM scRNA-Seq dataset without (left) and after integration by Harmony (right). NM fetal BM (n=21, k=129040, gestation age=10-19PCW); T21 fetal BM (n=16, k=67428, gestation age=12-20PCW).

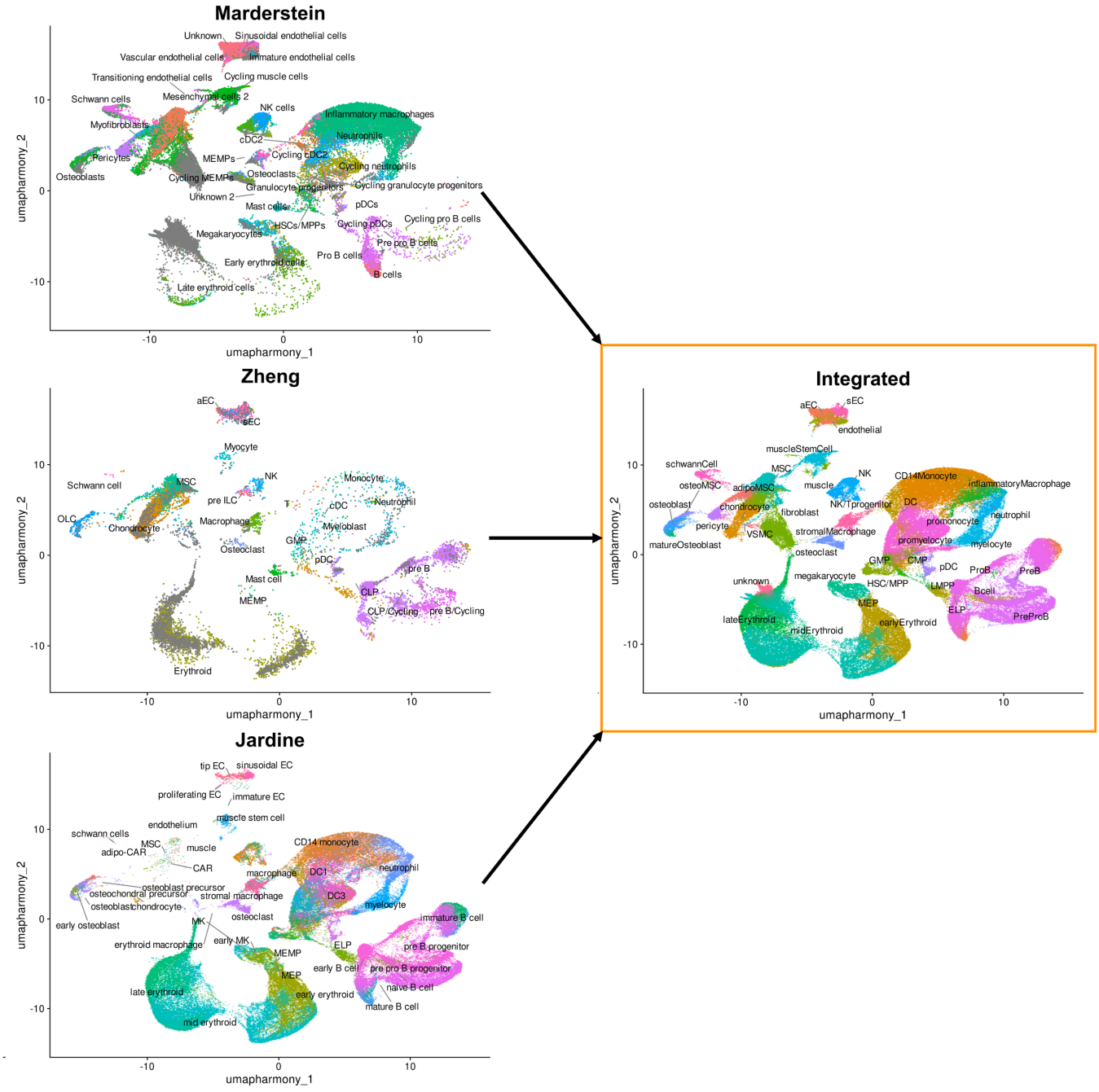

Figure 2.11: Reannotation published datasets. UMAP plots showing original cell type annotations from three published fetal bone marrow scRNA-seq datasets (left panels) [36, 45, 388], alongside integrated annotation derived from my analysis (right panel). NM fetal BM (n=21, k=129040, gestation age=10-19PCW); T21 fetal BM (n=16, k=67428, gestation age=12-20PCW).

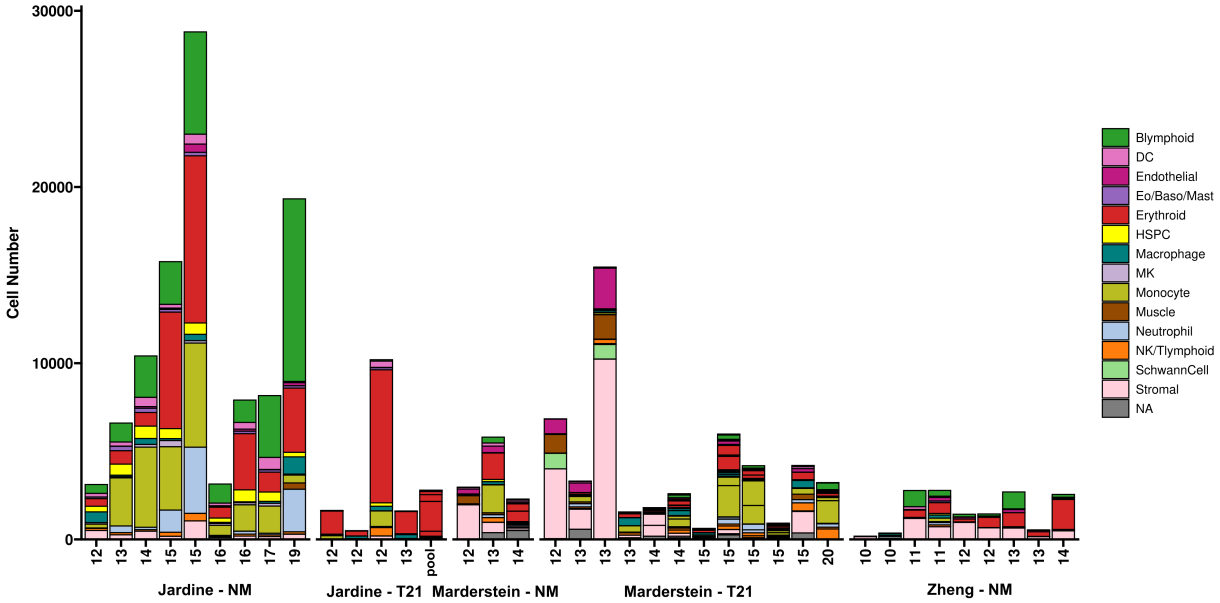

Figure 2.12: Composition of integrated scRNA-Seq dataset. Broad cell lineages of each biological sample from each dataset (ordered by gestation age in PCW). Jardine, fetal BM from [36] (NM: n=9, k=103228, age =12-19 PCW; T21: n=4, k=,16743 age=12-13 PCW), Marderstein, fetal BM from [388] (NM: n=3, k=11058, age=12-14 PCW; T21: n=12, k=50685,age=12-20 PCW), Zheng, fetal BM from [45] (NM: n=9, k=14754, age=10-14 PCW). NB, these datasets were generated by different sorting strategies, which may explain differences in composition across datasets, e.g. Marderstein et al.'s NM fetal BM samples were sorted on all BM CD235a- cells, rather than just haematopoietic cells, which may explain the reduced frequency of erythroid and B lymphoid cells.

Accounting for dropout with ALRA

To account for technical dropout in the integrated scRNA-Seq dataset, the ALRA (Adaptively-thresholded Low Rank Approximation) imputation method [527] was applied to recover missing gene expression values, while preserving biologically non-expressed genes. The ALRA-imputed matrix was used for trajectory analysis, ligand-receptor analysis and transcription factor activity inference.

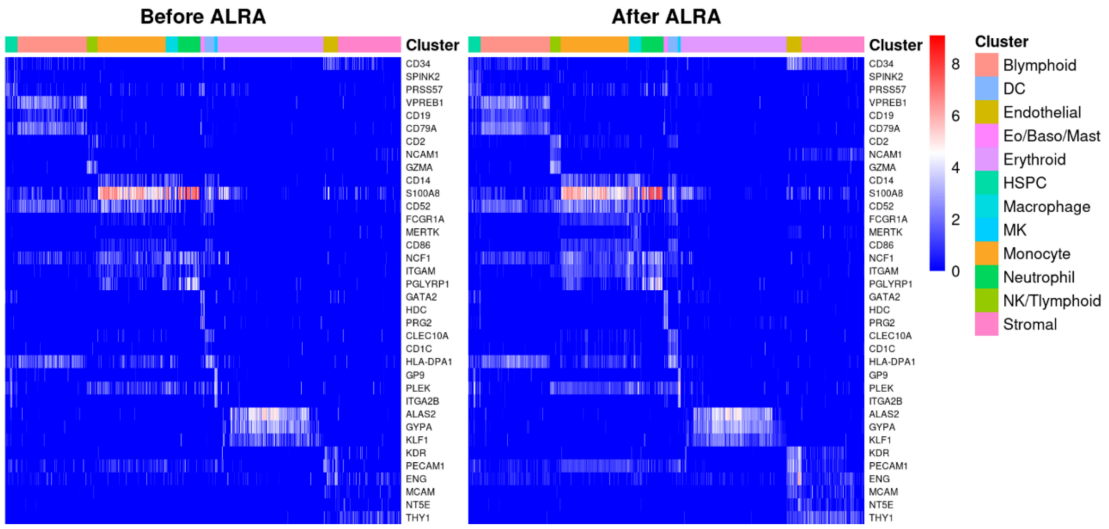

Figure 2.13: Correcting for dropout with ALRA. Heatmap of expression of lineage-associated marker genes in cells, before and after ALRA imputation.(n=21, k=129040, gestation age=10-19 PCW); T21, Trisomy 21 (n=16, k=67428, gestation age=12-20 PCW).

Trajectory analysis using Monocle3

Monocle3 (v1.4.26)[528] was used to infer differentiation trajectories from MSC towards osteoMSC and adipoMSC in normal and T21 fetal BM. For pseudotime analysis, the trajectory root was set to MSC.

Ligand-Receptor analysis using CellChat

CellChat (v2.1.2)[529] was used to identify differentially over-expressed ligands and receptors, as well as identify communication probabilities between different cell types in NM and T21 fetal BM, allowing for the inference and comparison of

intercellular communication networks in NM and T21 fetal BM. Ligand receptor interactions were inferred based on ALRA-imputed gene expression data.

TF activity inference using NetBID2

SJARACNe (v0.2.1)[530] was used to generate transcription factor networks for HSC/MPP, LMPP, ELP and MSC in NM and T21 fetal BM from ALRA-imputed gene expression values. NetBID2 (v2.0.3)[531] was used to perform differential activity analysis for a given population in NM or T21 fetal BM.

3

Results I: the impact of T21 on the gene expression and chromatin accessibility of fetal BM progenitors

3.1 Background and aims

The alterations in haematopoiesis in T21 fetal liver have been well described and are reviewed in the introduction. There is an increase in immunophenotypic HSC, MEP and megakaryocytes, along with a decrease in B progenitors[69, 387]. In the BM, the main site of B lymphopoiesis in the second trimester[20], there is also a profound lack of B lineage cells in T21[36]. Functional differentiation assays of T21 HSPC *in vitro* have recapitulated this B lineage defect, and the bias towards an increased erythroid/megakaryocytic output in fetal liver[69, 387] and fetal BM[36].

However, detailed characterisation of lymphopoiesis in T21 fetal BM and the molecular mechanisms underpinning these abnormalities, particularly in B lymphopoiesis, remain poorly understood. Chromosome 21 contains a number of genes that have an established role in haematopoiesis (Table 3.3) and increased dosage of these genes has been hypothesised to be responsible, at least in part, for altered haematopoiesis in T21[371]. While this may be the case in some cell types or in some model systems[380, 532], this is variable and depends on cell and

tissue context. Rather, there is more evidence to suggest the impact of T21 on gene expression is genome-wide [36, 379, 381, 383, 384]. In that light, it is reasonable to speculate that epigenetic mechanisms may be required to limit the impact of changes in gene expression[441]. Thus, both global changes in chromatin organisation and gene expression may be responsible for the haematological phenotype in T21 fetal BM.

The aim of the experiments in this chapter is to document and analyse perturbations in chromatin landscape and gene expression in T21 fetal BM HSPC, in order to determine how this might impact B lymphopoiesis. I took three approaches to address this:

1. Performing detailed multiparameter flow cytometry and functional differentiation assays to identify the stage at which B lymphopoiesis is disrupted in T21 fetal BM

2. Performing and analysing RNA- and ATAC-Seq on FAC-sorted fetal BM HSPC to understand how changes in gene expression and chromatin landscape may contribute to impaired B lymphopoiesis in T21 fetal BM

3. Integrating and reanalysing published scRNA-Seq atlases of NM and T21 fetal BM[36, 45, 388] to complement my own findings and gain further insight into the molecular basis for perturbation of fetal lymphopoiesis by T21

3.2 Immunophenotypic characterisation of T21 fetal BM HSPC

As a first step, I measured the frequency of HSC and their downstream progenitors in fetal BM using flow cytometry. This showed that the frequencies of many of the HSPC subpopulations were profoundly perturbed in T21 fetal BM. Consistent with what has been described in the T21 fetal liver[69], there was an increase in the frequency of immunophenotypic HSC (p-adj=0.07, T-test with Holm-Sidak correction), and a striking decrease in frequency of three fetal-specific lymphoid progenitors, the previously described Early Lymphoid Progenitors (ELP, p-adj=0.0001) and PreProB progenitors (p-adj=0.0004), as well as a newly identified Lin2-CD34+CD19-CD38+CD127-CD10-CD123-CD45RA+ PreELP/GMP progenitor (p-adj=0.01) which has been partially characterised by two DPhil students in our lab (Kate Murnane and Lucy Hamer), in T21 fetal BM (Figure 3.1).

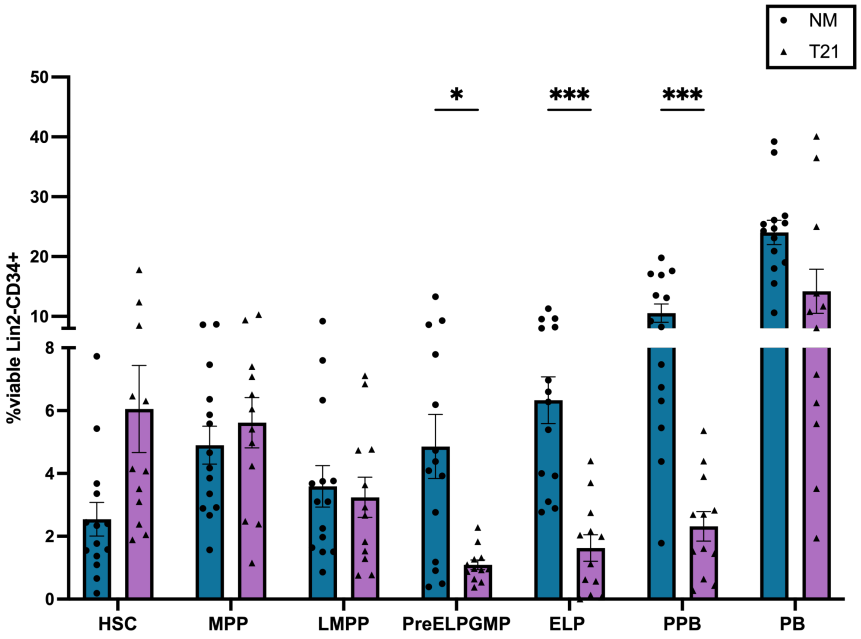

Figure 3.1: Frequency of HSPC in the fetal-like pathway of B lymphopoiesis in fetal BM as assessed by flow cytometry. HSC, haematopoietic stem cell; MPP, multipotent progenitor; LMPP, lymphoid-primed multipotent progenitor; PreELP/GMP, Pre-early lymphoid progenitor/ granulocyte macrophage progenitor; ELP, early lymphoid progenitor; PPB, PreProB progenitor; PB, ProB progenitor. NM, normal, blue bars, n=14; T21, trisomy 21, lilac bars, n=12. Mean ± SEM, T-tests with Holm-Sidak correction, p-adj<0.05 (*), p-adj<0.01(**), p-adj<0.001(***), p-adj<0.0001(****). P-adj HSC = 0.07, p-adj ProB = 0.07. Lin2: CD2/3/14/16/56/235a.

While the fetal-specific B lymphopoietic pathway appeared most strikingly affected in T21 fetal BM, there was also a reduction in frequency of lymphoid progenitors in the adult-like pathway; CLP frequency was significantly reduced (p-adj=0.01). However, MLP, which are a feature of normal adult BM[67, 68, 71] but are virtually undetectable in NM fetal BM, were actually increased in T21 fetal BM (p-adj=0.0006) compared to NM fetal BM. Furthermore, the most mature B progenitors (ProB), which are found in both fetal and adult BM, were not significantly reduced in T21 fetal BM (Figure 3.2).

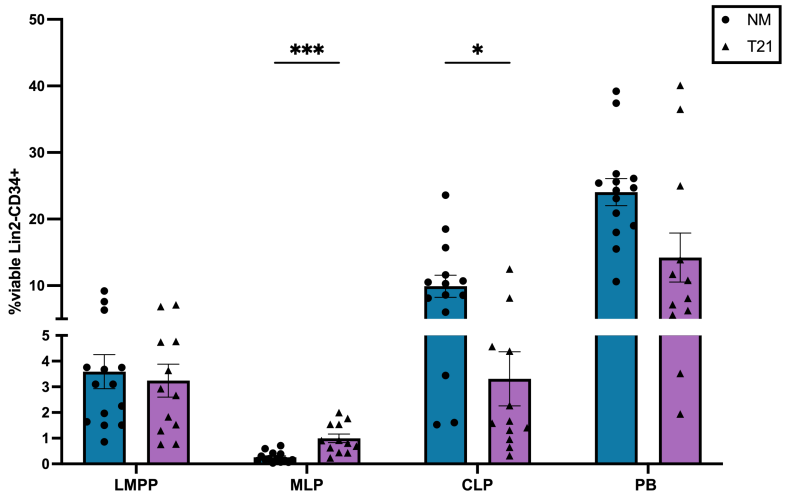

Figure 3.2: Frequency of HSPC in the adult-like pathway of B lymphopoiesis in fetal BM as assessed by flow cytometry. LMPP, lymphoid-primed multipotent progenitor; MLP, multi-lymphoid progenitor; PB, ProB progenitor. NM, normal, blue bars, n=14; T21, trisomy 21, lilac bars, n=12. Mean ± SEM, T-tests with Holm-Sidak correction, p-adj<0.05 (*), p-adj<0.01(**), p-adj<0.001(***). P-adj ProB = 0.07. Lin2: CD2/3/14/16/56/235a.

Taken together, these data suggest that T21 particularly perturbs the fetal type B progenitor pathway. In addition, there is a significant reduction in B cell (CD34-CD19+) frequency in T21 fetal BM (Figure 3.3).

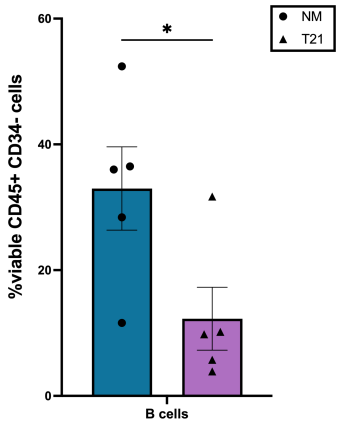

Figure 3.3: Frequency of CD19+ B cells as assessed by flow cytometry on CD34-depleted fetal BM. NM, normal, n=5, gestational age 15-17 PCW; T21, trisomy 21, gestational age 15-17 PCW. Mean ± SEM, T-test, p-adj<0.05 (*).

Alongside a decrease in early lymphoid progenitors, there was a two-fold increase in the frequency of myeloid progenitors (CMP, GMP and MEP, together) in T21 fetal BM compared to NM fetal BM. This reflects an increase in all of the myeloid progenitor populations, particularly CMP and MEP (Figure 3.4).

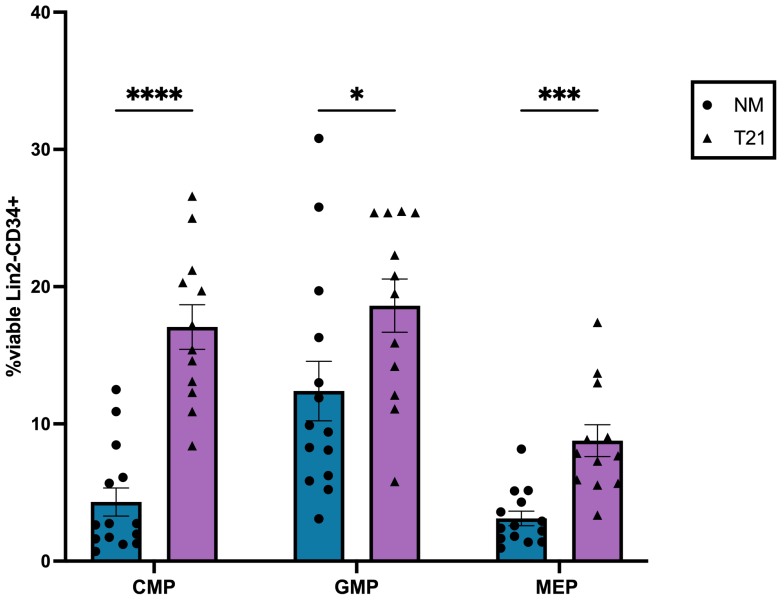

Figure 3.4: Frequency of myeloid progenitors in fetal BM as assessed by flow cytometry. CMP, common myeloid progenitor; GMP, granulocyte/ macrophage progenitor, MEP, megakaryocyte/ erythroid progenitor. NM, normal, blue bars, n=14; T21, trisomy 21, lilac bars, n=12. Mean ± SEM, T-tests with Holm-Sidak correction, p-adj<0.05 (*), p-adj<0.01(**), p-adj<0.001(***). Lin2: CD2/3/14/16/56/235a.

Thus, as reported in fetal liver[69], T21 causes myeloid skewing in fetal BM haematopoiesis; although in contrast to fetal liver, where the increase selectively affects MEP, in fetal BM, all myeloid progenitor types are increased.

Taken together, these frequency data point to a model in which a failure to commit to the fetal B lymphopoietic pathway occurs directly downstream of LMPP in T21 fetal BM, with T21 fetal BM LMPP differentiating preferentially into GMP and adult-like lymphoid progenitor MLP (Figure 3.5).

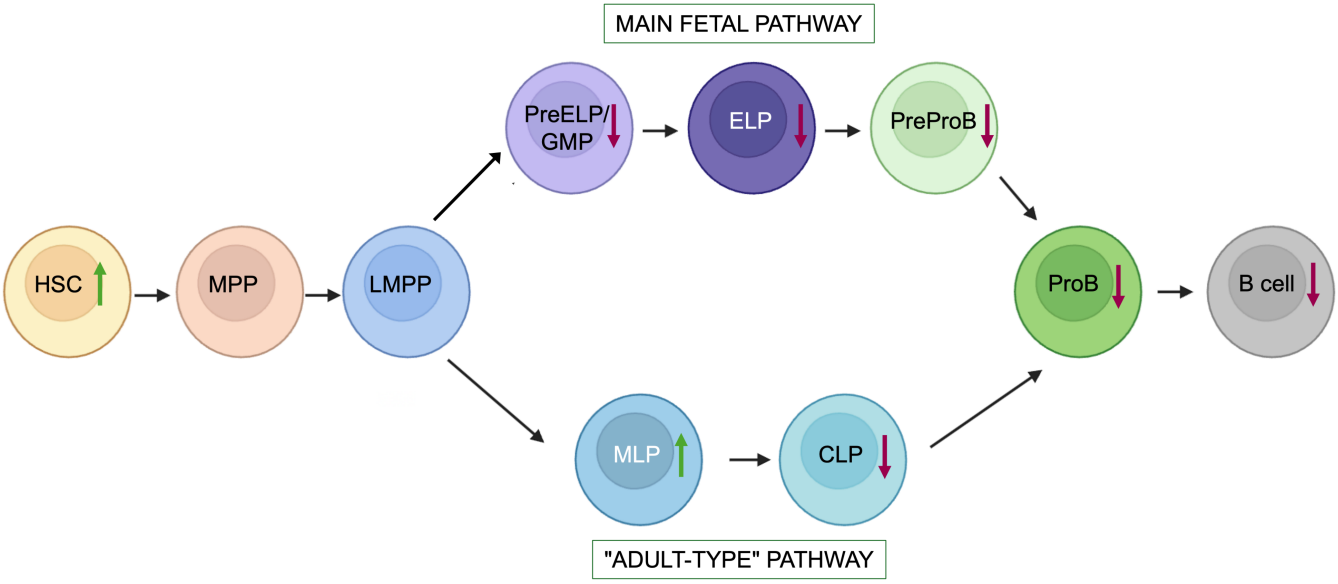

Figure 3.5: Proposed model of altered B lineage differentiation in T21 fetal BM HSPC. Immunophenotypic HSC and MLP are increased in frequency, while lymphoid progenitors, PreELP/GMP, ELP, CLP, and B cells and their progenitors PreProB and ProB are decreased. HSC, haematopoietic stem cell; MPP, multipotent progenitor; LMPP, lymphoid-primed multipotent progenitor; PreELP/GMP, Pre-early lymphoid progenitor/ granulocyte macrophage progenitor; ELP, early lymphoid progenitor; MLP, multi lymphoid progenitor; CLP, common lymphoid progenitor; PreProB, PreProB progenitor; ProB, ProB progenitor.

3.3 T21 HSPC show a B lymphopoietic defect and skewed differentiation towards myeloid and NK fates

To characterise the hypothesised block in B lymphoid differentiation downstream of LMPP, I carried out differentiation assays from sorted NM and T21 fetal BM HSPC upstream of this proposed block (HSC, MPP and LMPP) (Figure 3.6). A failure to differentiate into B cells was evident in all three of these HSPC populations from T21 fetal BM compared to their normal counterparts. Additionally, T21 HSC showed a proportional increase in myeloid output. There was also increased NK cell output from T21 fetal BM MPP and LMPP (Figure 3.6).

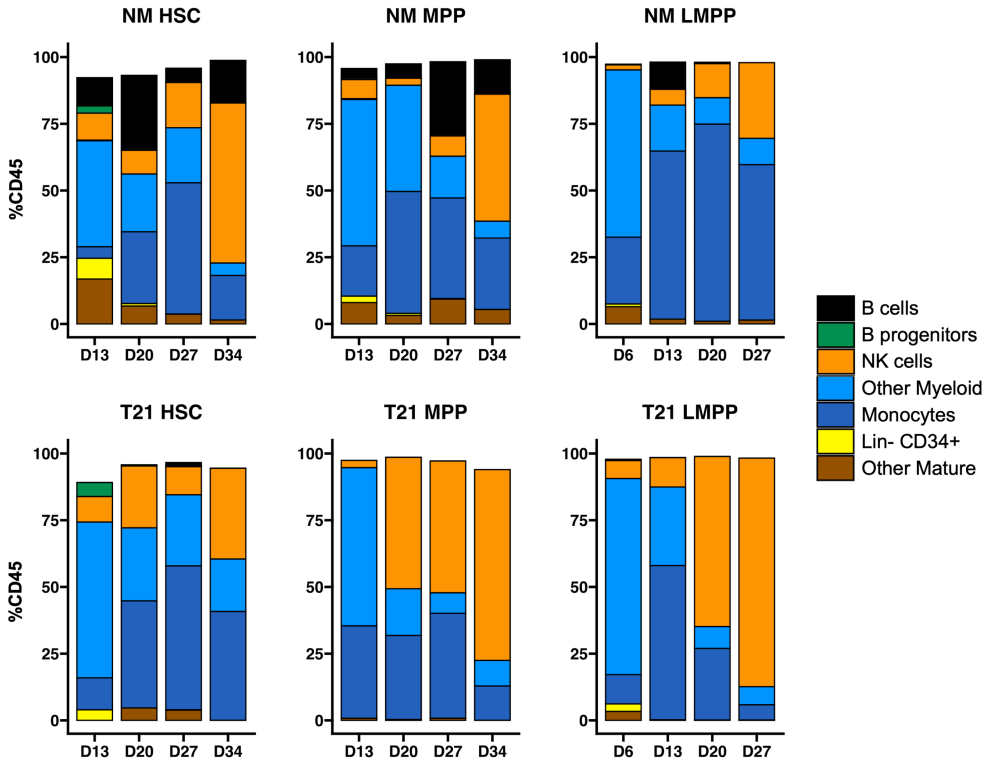

Figure 3.6: *In vitro* differentiation assay of NM and T21 fetal BM HSC, MPP and LMPP. Mean proportional B and NK lymphoid, and myeloid output of sorted HSC, MPP, and LMPP from NM and T21 fetal BM (100 cells each) cultured on MS5 stroma with IL2, IL7, FLT3L and SCF. Output was measured at weekly intervals starting from day 6 (D6) and continuing to day 27 (D27) for LMPP and day 34 (D34) for HSC and MPP cultures. HSC, Haematopoietic Stem Cell, 100 cells, NM, n=3, T21 n=3; MPP, Multipotent Progenitor, 100 cells, NM, n=3, T21, n=2; LMPP, Lymphoid-primed Multipotent Progenitor, 100 cells, NM, n=3, T21, n=2. Other Myeloid: CD11b/CD15/CD33+ CD14-.

3.4 Trisomy 21 results in altered gene expression and chromatin accessibility in fetal BM HSPC

The striking reduction in PreELP/GMP, ELP, CLP, B lineage-committed progenitors and B cells in T21 fetal BM, alongside reduced B lineage output *in vitro* from T21 HSC, MPP and LMPP suggest that there might be a failure of the normal gene regulatory mechanisms that ensure B lineage commitment and differentiation in HSC or their immediate downstream progenitors. To investigate the molecular basis of this, I carried out RNA-Seq and ATAC-Seq on FAC-sorted NM and T21 fetal BM HSPC. I integrated this data with previously generated data in the lab (Table 2.5, page 61), and analysed it.

3.4.1 Expression of key lymphoid genes

I first considered the expression of genes known for their role in lymphoid specification in NM and T21 fetal BM HSPC[56], and compared gene expression alongside patterns of gene expression through differentiation.

Levels of expression of *FLT3*, a gene essential for lymphoid specification, were generally lower in T21 compared to NM fetal BM HSPC (Figure 3.7). *FLT3* encodes the receptor for FLT3L and its crucial role in B lymphoid specification is shown by *Flt3*-knockout mouse models having reduced frequencies of CLP and B lineage cells [533, 534]. In addition to lymphoid specification, FLT3 is thought to play a role in B lineage commitment, with a conditional knockout of *Flt3* in *Rag1*-expressing cells resulting in reductions of ProB, PreB and B cells in murine BM[535]. Interestingly, *FLT3* expression was almost undetectable in T21 fetal BM CLP (Figure 3.7). In NM fetal BM HSPC, expression of *FLT3* is high in HSC and MPP, and peaks in LMPP (Appendix Figure 1, page 195). In T21 fetal BM, the reduced *FLT3* expression in HSC and MPP compared to NM fetal BM HSC and MPP did not reach statistical significance by DESeq2, most likely because of the heterogeneity in the levels of expression between individual samples.

TCF3 is an essential transcription factor for normal B and T cell development and humans with mutations in *TCF3* have severe immunodeficiency, including

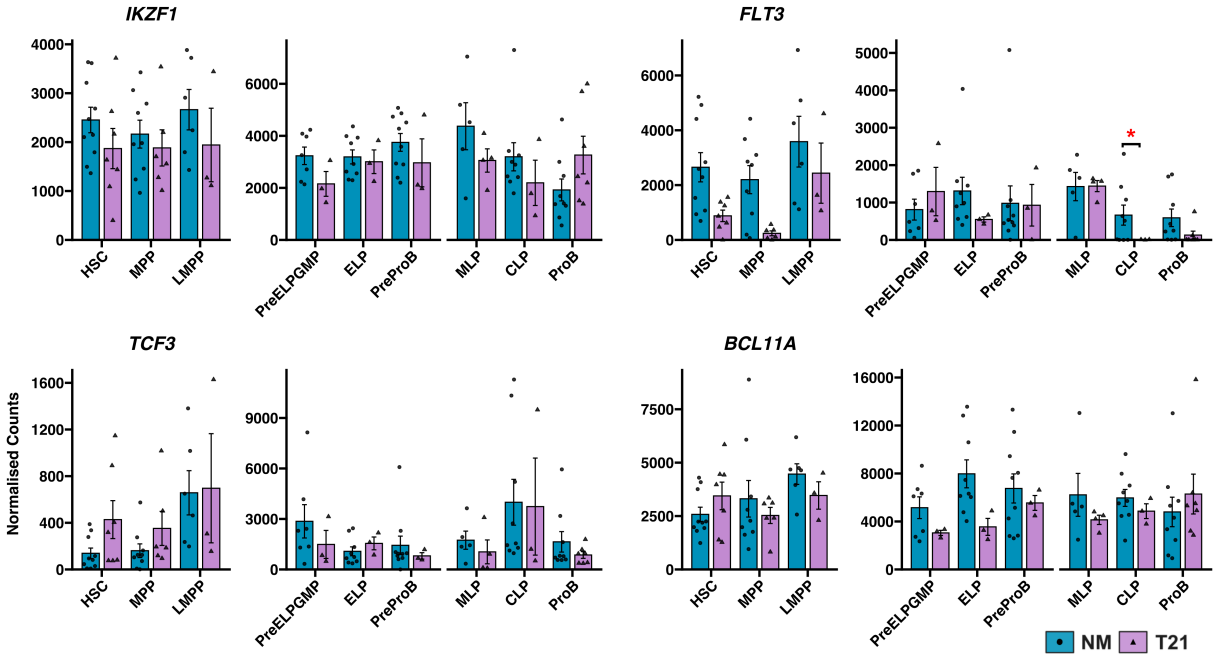

Figure 3.7: Expression of genes with a known role in lymphoid specification in NM and T21 HSPC. Gene expression was measured by RNA-Seq (50-100 cells). For each gene, graphs are grouped (from left to right) for primitive HSPC, fetal specific lymphoid progenitors and adult type lymphoid progenitors. Gene expression data shown as mean normalised counts ± SEM, * denotes significance by DESeq2 (p-adj<0.1). NM (normal, blue bars represent mean expression, dots represent biological samples, n=5-10); T21 (Trisomy 21, lilac bars represent mean expression, triangles represent biological samples, n=3-7).

agammaglobulinaemia[536–538]. However there was no difference in the levels of expression of *TCF3* between NM and T21 fetal BM HSPC suggesting that changes in the expression of this gene are not important in the pathogenesis of the T21-associated B lymphoid defects in fetal BM.

BCL11A is another transcription factor that is essential for lymphopoiesis and lymphocyte survival, with its conditional knockout mouse lacking CLP, and B, T and NK lymphocytes. *BCL11A* expression increases from LMPP to PreELP/GMP, peaks at ELP and decreases thereafter in NM fetal BM HSPC (Appendix Figure 1, page 195). However, in T21 fetal BM, this pattern of upregulation appeared to be impaired, with lower levels of expression in all HSPC apart from HSC and ProB progenitors (though this did not reach statistical significance).

Although these differences in gene expression of lymphoid specification tran-

scription factors *FLT3* and *BCL11A* in T21 HSPC were modest, subtle changes in transcription factor expression may be sufficient to drive the B lymphoid defects in T21 fetal BM.

3.4.2 Expression of B lymphoid genes

I next considered the expression of genes associated with B lineage specification and commitment.

EBF1 was one of the first genes with a key role in B lineage specification to be identified[539]. It is essential for the activation of downstream master regulators of B cell development, in particular *PAX5*[540]. Equally importantly, EBF1 represses commitment programmes to myeloid or T/NK lineages by antagonising C/EBPα, PU.1 and ID2, as identified by knockout experiments conducted in murine BM HSPC[541]. Expression of *EBF1* was significantly reduced in T21 fetal BM PreELP/GMP and ELP, populations that are critical decision points for B lineage commitment.

In addition, V(D)J recombination genes *RAG1*, *RAG2* and *DNTT* were significantly reduced in T21 PreELP/GMP, and the latter two also in T21 ELP (Figure 3.8). V(D)J recombination is a hallmark of B lymphoid lineage progression[20, 542] and depends upon the co-ordinated upregulation of *RAG1* and *RAG2*, which are essential for initiating rearrangement of the immunoglobulin genes. *DNTT* encodes the enzyme terminal deoxynucleotidyl transferase, which adds to diversity generated in V(D)J recombination by adding in non-template nucleotides[543]. While *RAG1*, *RAG2* and *DNTT* are upregulated at the PreELP/GMP and ELP stage in NM fetal BM (Appendix Figure 2, page 196), this fails to occur in these progenitors in T21 fetal BM (Figure 3.8). These data are consistent with failure to activate B lymphopoietic programmes in fetal-specific lymphoid progenitors.

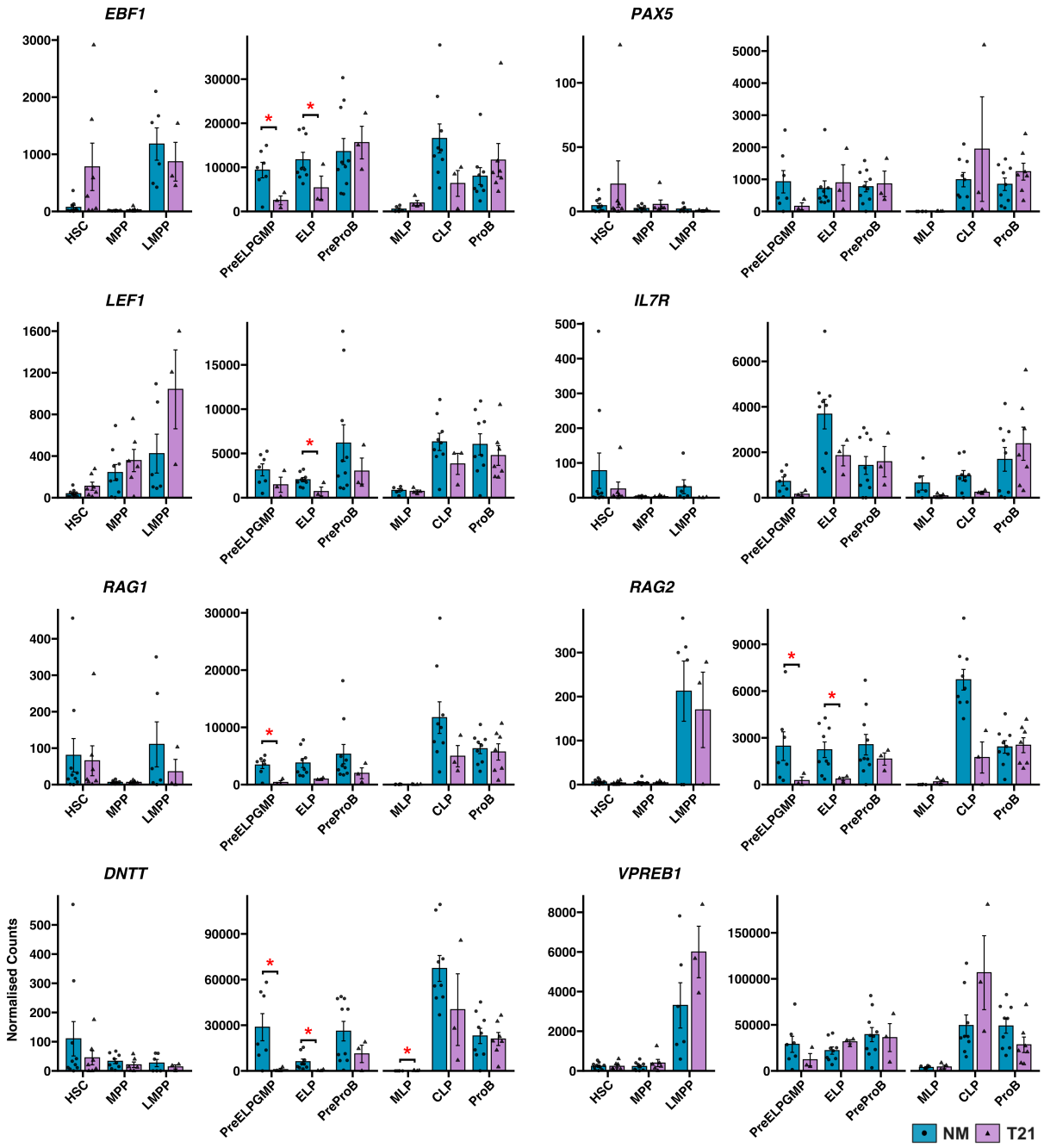

Figure 3.8: Expression genes with a known role in B lymphopoiesis in NM and T21 HSPC. Gene expression was measured by RNA-Seq (50-100 cells). For each gene, graphs are grouped (from left to right) for primitive HSPC, fetal specific lymphoid progenitors and adult type lymphoid progenitors. Gene expression data shown as mean normalised counts ± SEM, * denotes significance by DESeq2 (p-adj<0.1). NM (normal, blue bars represent mean expression, dots represent biological samples, n=5-10); T21 (Trisomy 21, lilac bars represent mean expression, triangles represent biological samples, n=3-7).

By contrast, expression of genes required for normal B cell maturation, including *TCL1A, CD79A, CD79B, MME, CD19* and *MS4A1*, was not significantly different in T21 compared to NM fetal BM HSPC apart from reduced *MME* expression in T21 PreELP/GMP, the significance of which is unclear as PreELP/GMP were FAC-sorted for RNA-Seq as a CD10- population (Figure 3.9). Additionally, expression of hallmark B lineage gene *CD19* was readily detectable in NM fetal BM HSC, MPP and LMPP, but barely detectable in T21 HSC, MPP and LMPP (though immunophenotypically all HSC, MPP and LMPP were CD19-). This may reflect reduced B lymphoid priming in T21 HSC, MPP and LMPP upstream of B lymphoid commitment.

These observations are in line with the hypothesis that a failure to commit to B lymphoid fate drives the B lymphoid defect in T21. Once committed to the B lymphoid fate, as marked by the genes considered in Figure 3.9; there are no significant differences between NM and T21 fetal BM B progenitors PreProB and ProB, suggesting B cell differentiation after commitment to B lymphoid fate is preserved in T21 fetal BM.

Taken together, these changes in gene expression in T21 fetal BM HSPC suggest the impaired lymphoid specification in HSC/MPP/LMPP leads to the failure to upregulate the B cell programmes. Given that activation of B lymphoid programmes occurs in tandem with suppression of non-B lymphoid programmes, it may be that this failure to activate B lymphopoietic programmes may also be accompanied by, or a result of, a failure to silence T/NK and/or myeloid differentiation programmes. To investigate these possibilities, I next examined gene expression patterns across other lineages in T21 fetal BM HSPC.

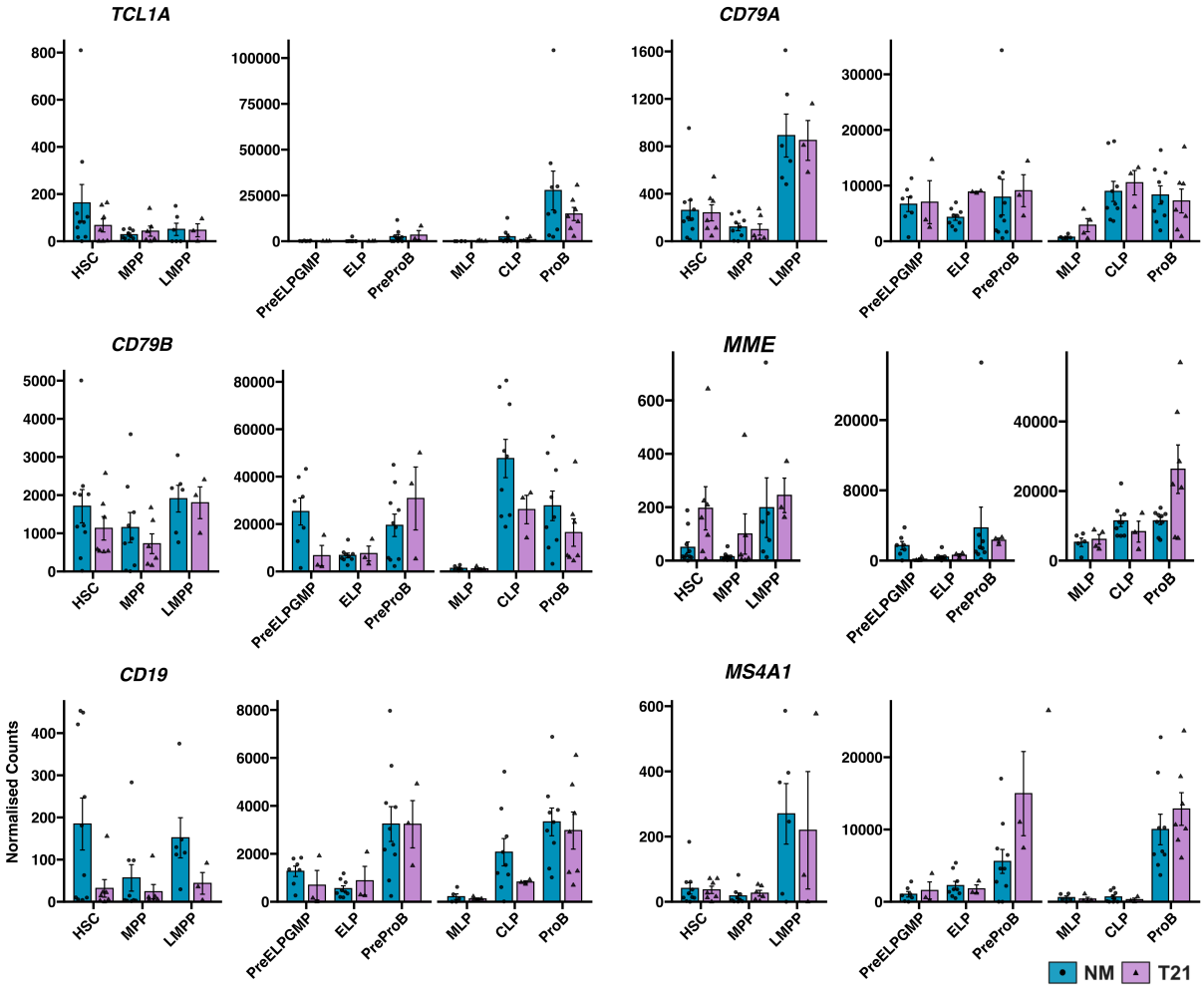

Figure 3.9: Expression genes with a known role in B cell development in NM and T21 HSPC. Gene expression was measured by RNA-Seq (50-100 cells). For each gene, graphs are grouped (from left to right) for primitive HSPC, fetal specific lymphoid progenitors and adult type lymphoid progenitors. Gene expression data shown as mean normalised counts ± SEM, * denotes significance by DESeq2 (p-adj<0.1). NM (normal, blue bars represent mean expression, dots represent biological samples, n=5-10); T21 (Trisomy 21, lilac bars represent mean expression, triangles represent biological samples, n=3-7).

3.4.3 Expression of T/NK lymphoid genes

Expression of T lymphoid genes

I next considered whether alternative lymphoid trajectories - specifically T and NK lymphoid programmes - were similarly affected. Since PreELP/GMP, ELP, MLP and CLP retain the ability to differentiate into T and NK cells, the failure to activate B lineage commitment programmes raised the possibility of either a general block in lymphoid differentiation, or a skewing towards non-B-lymphoid fates. Indeed, the functional data suggests a skew towards NK cell output (Figure 3.6 and unpublished data from the lab). To assess this, I initially compared gene expression of known transcription factors and cytokine receptors associated with T and NK specification (Figure 1.2, page 7), to establish whether these programmes were affected in T21 fetal BM.

Notch signalling is essential for commitment to the T lineage and suppression of B lineage potential[544]; murine models in which *Notch1* or its downstream transcription factor *Rbpj* are inactivated fail to produce T cells and instead produce B cells[545, 546]. Additionally, ectopic Notch signalling in murine BM HSPC inhibits B lineage commitment[547].

In T21 fetal BM, expression of *NOTCH1* is significantly increased in PreELP/GMP, and is elevated in ELP, although this does not reach statistical significance. In addition to its role in T lineage commitment[323], Notch1 has also been shown to play a role in NK lineage specification, with different murine Notch ligands promoting T and NK cell fate *in vitro* human cord blood derived HSPC[180, 548, 549].

TCF7 encodes the transcription factor TCF1, and is a target of Notch signalling. Its overexpression in murine BM HSPC is sufficient to induce T lymphopoiesis through the upregulation of T lymphopoietic factors *Gata3* and *Bcl11b*[140]. *TCF7* expression is significantly higher in T21 fetal BM LMPP, PreELP/GMP and ELP. In addition to its role in T lymphopoiesis, *Tcf7* is also thought to be important in ILC lineage specification, with *Tcf7*-/- mice showing reduced NK cells[550]. Higher *TCF7* expression in T21 fetal BM HSPC is consistent with the *in vitro* NK bias from T21 fetal BM LMPP (Figure 3.6).

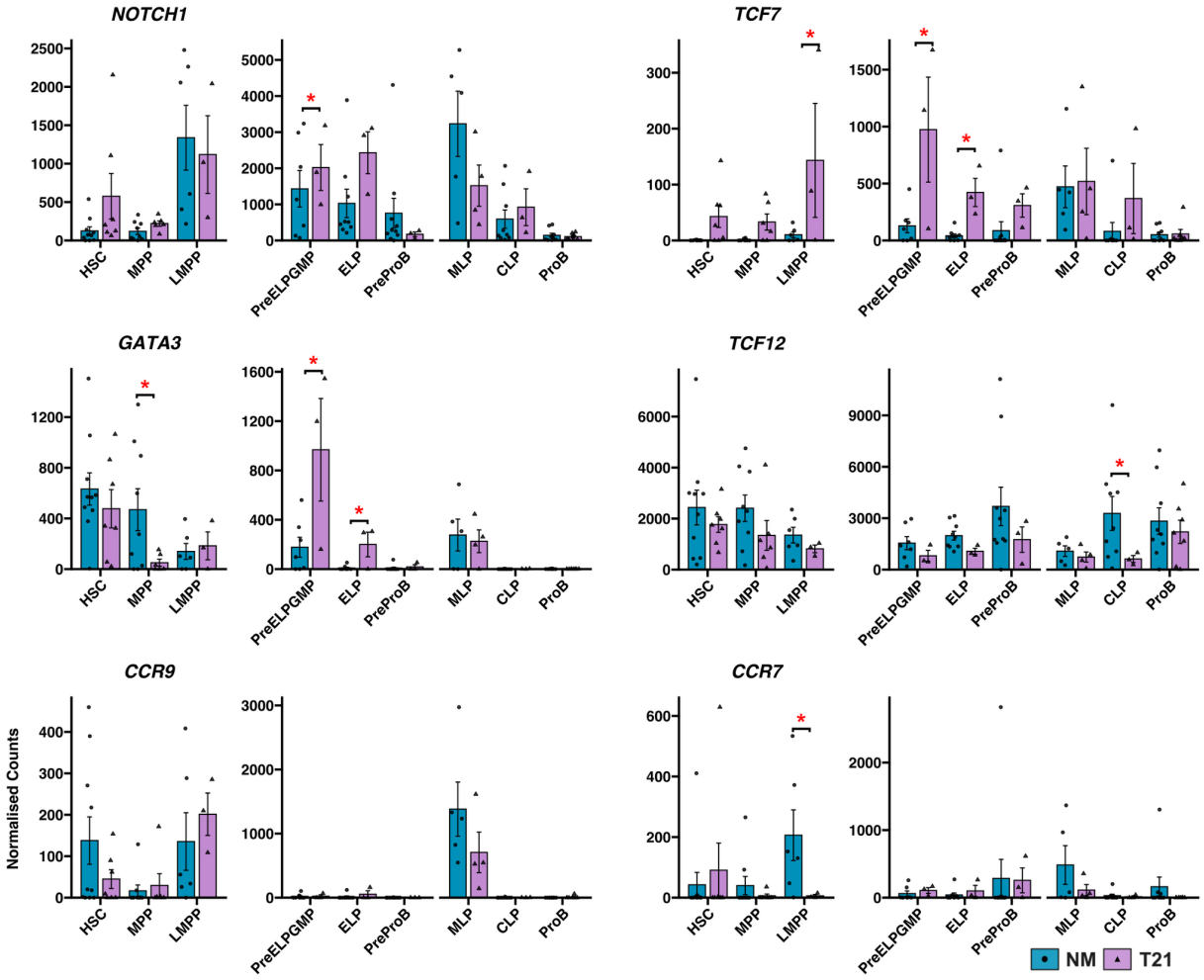

Figure 3.10: Expression of genes with a known role in T lymphopoiesis in NM and T21 fetal BM HSPC. Gene expression was measured by RNA-Seq (50-100 cells). For each gene, graphs are grouped (from left to right) for primitive HSPC, fetal specific lymphoid progenitors and adult type lymphoid progenitors. Gene expression data shown as mean normalised counts ± SEM, * denotes significance by DESeq2 (p-adj<0.1). NM (normal, blue bars represent mean expression, dots represent biological samples, n=5-10); T21 (Trisomy 21, lilac bars represent mean expression, triangles represent biological samples, n=3-7).

Additionally, *GATA3* is a target of TCF1, and its expression is also essential for T lymphopoiesis[551, 552]. GATA3 is also thought to play a role in NK cell maturation [553, 554]. Importantly, GATA3 is also responsible for suppressing B lymphoid potential, with even low levels of expression suppressing B lymphopoiesis[142, 143]. In fetal BM, *GATA3* expression in HSPC is highest in HSC, in line with its role in murine HSC maintenance[555, 556], and reduces such that its expression is very low in ELP and CLP (Appendix Figure 4, page 198). However, in T21 fetal BM,

this did not appear to be the case, with *GATA3* expression being upregulated from LMPP to peak in expression in PreELP/GMP. Indeed, *GATA3* expression was significantly higher in T21 PreELP/GMP and ELP compared to NM counterparts, suggesting that in T21 fetal BM lymphoid progenitors there is a failure to silence *GATA3*, and this may contribute to impaired B lymphoid commitment.

TCF12 plays an essential role in T lineage commitment: *Tcf12*-/- mice have a reduction in T cells, and a developmental arrest in immature single positive thymocytes[557]. However, TCF12 also co-operates with TCF3 to play a role in B lymphopoiesis in mice[558, 559], acting at a CLP stage to induce expression of *Foxo1*[559] and inhibiting NK fate[560]. *TCF12* expression was generally lower in T21 fetal BM HSPC compared to NM progenitors although this only reached statistical significance in the CLP population. Given the dual role of TCF12 in promoting B and T lymphopoiesis, and suppressing NK lymphopoiesis, a reduction in its expression may contribute to an NK lymphoid skew, as observed functionally *in vitro* (Figure 3.6).

As T lymphopoiesis requires the migration of BM lymphoid progenitors to the thymus, I also considered expression of the key chemotactic receptors involved in this process *CCR7* and *CCR9*[135, 561]. Expression of these receptors in NM fetal BM are highest in MLP (Appendix Figure 4, page 198). In T21 fetal BM, expression of *CCR7* in LMPP was reduced. Additionally, T21 fetal BM MLP appeared to have reduced expression of *CCR9* and *CCR7*, though this did not reach significance. This may be a potential explanation for the increased frequency of MLP in T21 fetal BM, if they are unable to migrate to the fetal thymus.

The expression of hallmark T lymphoid specification factors *NOTCH1*, *GATA3* and *TCF7* were significantly increased in T21 fetal BM ELP and PreELP/GMP. This would provide another potential contributory factor to the failure to activate B lineage programs normally in T21 fetal BM. However, confirming this would require functional experiments *in vitro* and *in vivo* which I did not perform in this thesis.

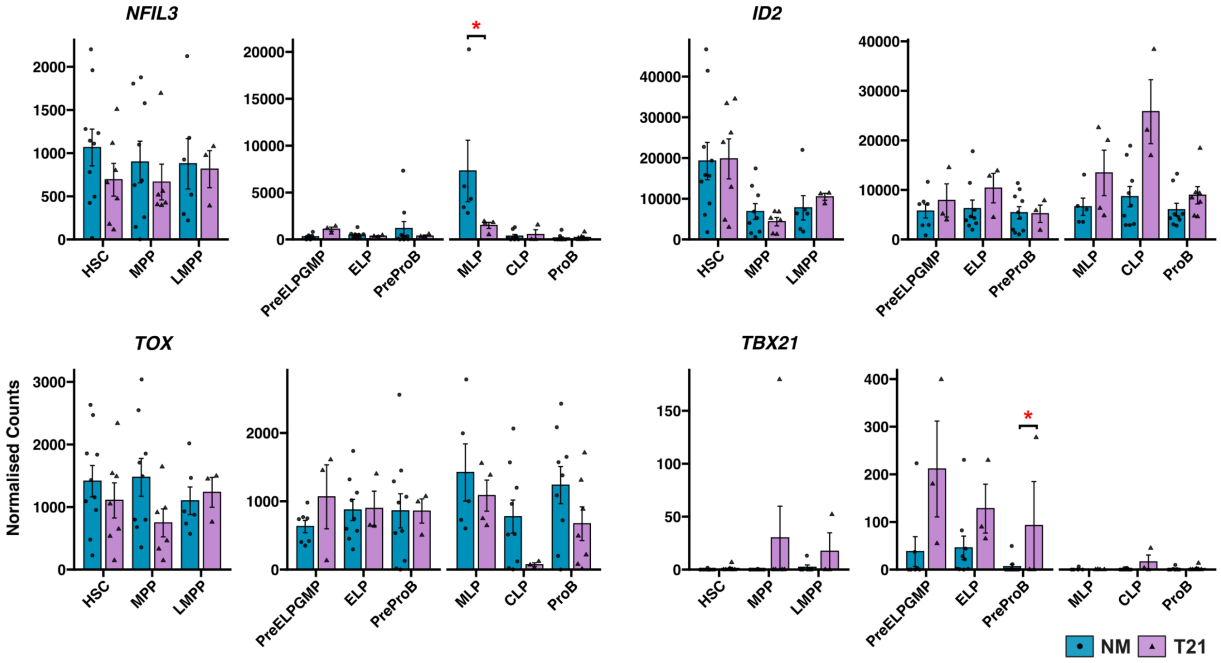

Figure 3.11: Expression of genes with a known role in NK lymphopoiesis in NM and T21 HSPC. Gene expression was measured by RNA-Seq (50-100 cells). For each gene, graphs are grouped (from left to right) for primitive HSPC, fetal specific lymphoid progenitors and adult type lymphoid progenitors. Gene expression data shown as mean normalised counts ± SEM, * denotes significance by DESeq2 (p-adj<0.1). NM (normal, blue bars represent mean expression, dots represent biological samples, n=5-10); T21 (Trisomy 21, lilac bars represent mean expression, triangles represent biological samples, n=3-7).

Expression of NK lymphoid genes

NFIL3 is considered the apex transcription factor associated with innate lymphoid lineage specification[157, 562]. *Nfil3*-deficient mice have no NK cells, but retain T and B lymphocytes[159, 160]. *NFIL3* expression in NM fetal BM peaks in MLP, and this upregulation was not evident in T21 fetal BM MLP, with *NFIL3* expression levels being significantly reduced compared to normal counterparts. NFIL3 activates expression of *ID2*, and both transcription factors act together to specify the NK lineage[563, 564]. Mice lacking *Id2* exhibit an absence of NK cells[161, 162], and ectopic expression of *Id2* in *Nfil3*-deficient mice restores NK cell output[565]. In addition to inducing NK lineage fate, ID2 suppresses the activation of B lymphoid programmes[566].

The transcription factor TOX, which is also activated by NFIL3[567], also specifies the ILC lineage, with *Tox*-/- mice having a marked reduction in NK cells[565].

These apical innate lymphoid genes (*ID2* and *TOX*) in NM fetal BM are expressed at high levels in NM fetal BM HSC, before being downregulated in lymphoid progenitors (Appendix Figure 5, page 199). However, in T21 fetal BM, their expression patterns seemed to differ: *ID2* is expressed at comparable levels in NM and T21 fetal BM HSC, MPP and LMPP, but unlike NM fetal BM, in T21 fetal BM *ID2* is subsequently upregulated and shows highest levels of expression in MLP and CLP (Figure 3.11), while *TOX* expression is not significantly different in T21 compared to NM fetal BM HSPC. Ectopic expression of *Tox* in *Id2* deficient mice does not rescue the defect in NK lymphopoiesis observed which suggests the two act in parallel pathways, rather than in a shared pathway[565]. Therefore, these results suggest increased *ID2* may contribute to the functional NK skew observed in differentiation assays from T21 fetal BM MPP and LMPP, despite *TOX* expression being reduced in CLP.

Finally, *TBX21* encodes a transcription factor promoting NK cell maturation[568, 569], and its expression was higher in many T21 fetal BM populations whereas it was almost undetectable in NM fetal BM.

Taken together, these findings suggest a broad dysregulation of lymphopoiesis in T21 fetal BM, characterised by a failure to activate B lymphoid programmes, accompanied by increased expression of genes associated with the suppression of B lymphoid programmes in lymphoid progenitors, such as *GATA3*, *NOTCH1*, *TCF7* and *ID2*. All of these genes are implicated in both T and NK lineage specification in lymphoid progenitors.

However, expression of other T and NK lymphopoietic genes (*TCF12*, *CCR7*, *CCR9*, *NFIL3*, and *TOX*) was reduced in T21 fetal BM lymphoid progenitors, suggesting that perturbation of lymphopoiesis by T21 extends beyond the B lineage. Direct evidence for this would require analysing gene expression in mature T/NK lymphopoietic progenitors from NM and T21 fetal BM.

3.4.4 Expression of myeloid genes

I next considered whether aberrant expression of myeloid gene programmes might contribute to dysregulated lymphopoiesis in T21 fetal BM especially considering that CMP, GMP and MEP were all increased in T21 fetal BM (Figure 3.4). Key genes with known roles in myeloid specification and priming were considered[217], including transcription factors *SPI1* and *CEBPA*, and markers for myeloid progenitors *IL3RA* and *FUT4*.

SPI1 encodes PU.1, a transcription factor that fine tunes lympho-myeloid specification. *Spi1-/-* mice die soon after birth, and exhibit profound deficits in neutrophils, monocytes and B cells, alongside NK/T cells, although numbers of erythroid cells and megakaryocytes are unaffected[201]. In NM fetal BM, expression of *SPI1* is highest in MPP and myeloid progenitors CMP and GMP (Appendix Figure 6, page 200), which is in line with observations that PU.1 acts in a dose-dependent manner, with higher expression inducing GMP lineage commitment, while downregulation of *SPI1* may be required for megakaryocyte/ erythroid development, as well as lymphopoiesis[205, 570]. In T21 fetal BM, expression of *SPI1* was reduced in MPP, CMP, GMP and CLP, though statistically significant downregulation was observed only in the ELP population. This trend toward lower *SPI1* expression in MPP, CMP, and MEP may contribute to the well-characterised erythroid-megakaryocytic skew observed in T21, as reduced PU.1 expression removes a barrier to erythro-megakaryocytic commitment (as discussed in Chapter 1). Additionally, the significant reduction in *SPI1* expression in T21 MPP, ELP and CLP may impair lymphoid specification in T21, particularly in B lymphopoiesis, which is thought to depend on slightly higher PU.1 levels compared to NK and T cell development[570].

CEBPA is among the most studied transcription factors in haematopoiesis. *Cebpa-/-* mice show a differentiation block in myelopoiesis at the CMP stage, and lack GMP and all subsequent stages of granulocyte and macrophage differentiation[571, 572]. In NM fetal BM, *CEBPA* expression increases from HSC to GMP, with low/absent expression in committed lymphoid progenitors. In T21, expression of *CEBPA* in PreELP/GMP was significantly increased and comparable to that of CMP

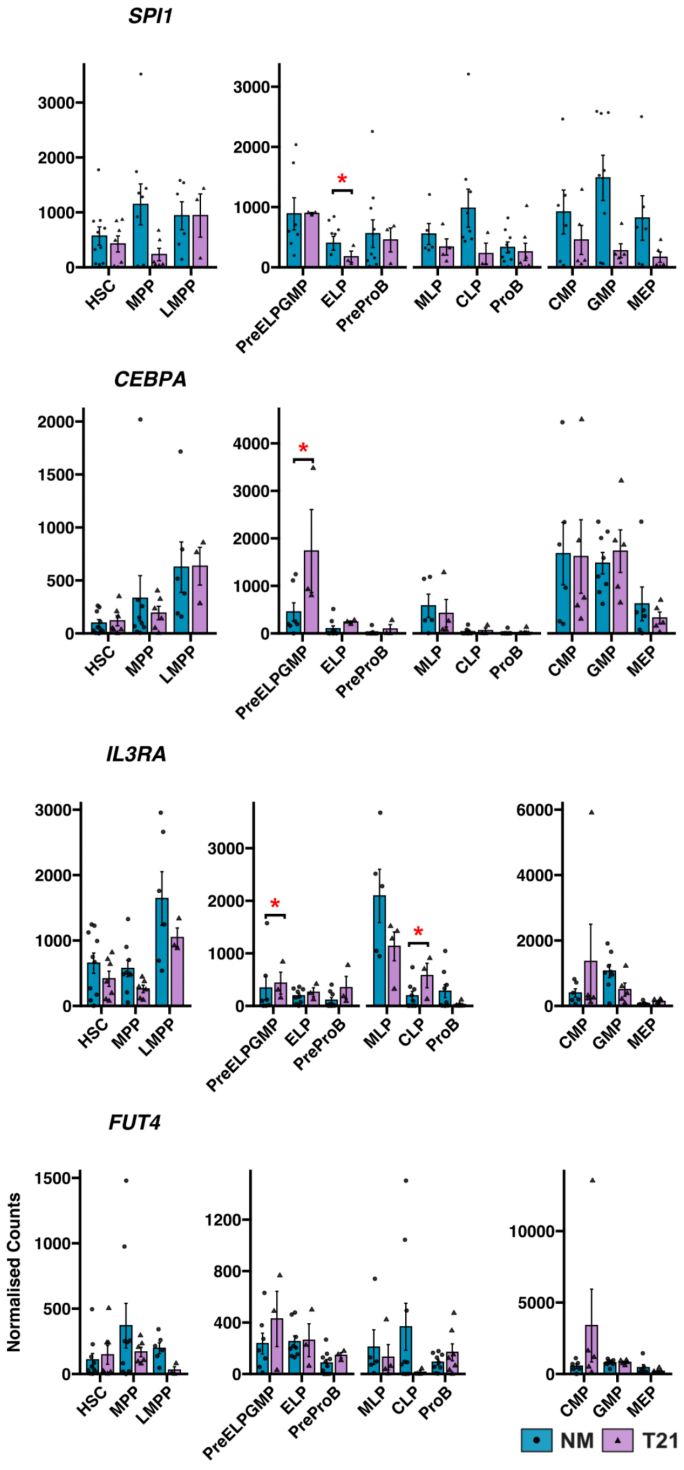

Figure 3.12: Expression of genes with a known role in myeloid specification in NM and T21 HSPC by RNA-Seq (50-100 cells). For each gene, graphs are grouped (from left to right) for primitive HSPC, fetal specific lymphoid progenitors, adult type lymphoid progenitors, and myeloid progenitors. Gene expression data shown as mean normalised counts ± SEM, * denotes significance by DESeq2 (p-adj<0.1). NM (normal, blue bars represent mean expression, dots represent biological samples, n=5-10); T21 (Trisomy 21, lilac bars represent mean expression, triangles represent biological samples, n=3-7).

and GMP, suggesting that in T21 this population are poised to differentiate into GMP rather than ELP, or that PreELP/GMP which are incompletely characterised may be a mixed population, which, in T21 fetal BM are more PreGMP-like.

IL3RA and *FUT4* are hallmark genes governing myeloid differentiation and are used as cell surface markers to immunophenotypically define early myeloid progenitors. While IL3 signalling itself appears not to be required for myeloid differentiation, since *Il3*-/- mice have normal monocyte and granulocyte profiles, IL3 promotes myeloid expansion from HSPC *in vitro*[573]. In T21 fetal BM, expression of *IL3RA* was significantly increased in PreELP/GMP and CLP. PreELP/GMP are incompletely characterised, and may represent a mixed population, in which case this would suggest T21 fetal BM PreELP/GMP may be poised to differentiate into GMP, perhaps representing a more PreGMP than PreELP population. The increase in *IL3RA* expression in CLP may represent impaired silencing of myeloid programmes in T21 fetal BM lymphoid progenitors.

Expression of monocyte genes

I next considered genes involved in monocyte development. Key genes in monocyte differentiation include: *IRF8*, *CSF1R*, *LYZ* and *CST7*[574].

Interferon Regulatory Factor 8, (*IRF8*) is essential for the survival and development of monocytes, macrophages and dendritic cells, and suppresses granulocytic differentiation[220, 575, 576]. *IRF8* is expressed in all HSPC but increases in response to IFNγ stimulation[577]. There were no significant differences in *IRF8* expression between NM and T21 fetal BM HSPC, although there was a trend towards higher *IRF8* in T21 compared to NM LMPP (Figure 3.13).

CSF1R/*Csf1r*, which encodes the receptor for M-CSF, instructs murine GMP towards a monocytic fate *in vitro* and is central to monocyte survival and differentiation[578, 579]. There were no clear and significant differences in *CSF1R* expression between T21 and NM fetal BM HSPC.

Expression of the monocyte effector protein genes *LYZ* and *CST7* was increased in some T21 fetal BM HSPC populations, most notably in HSC, MPP and CMP (Figure 3.13).

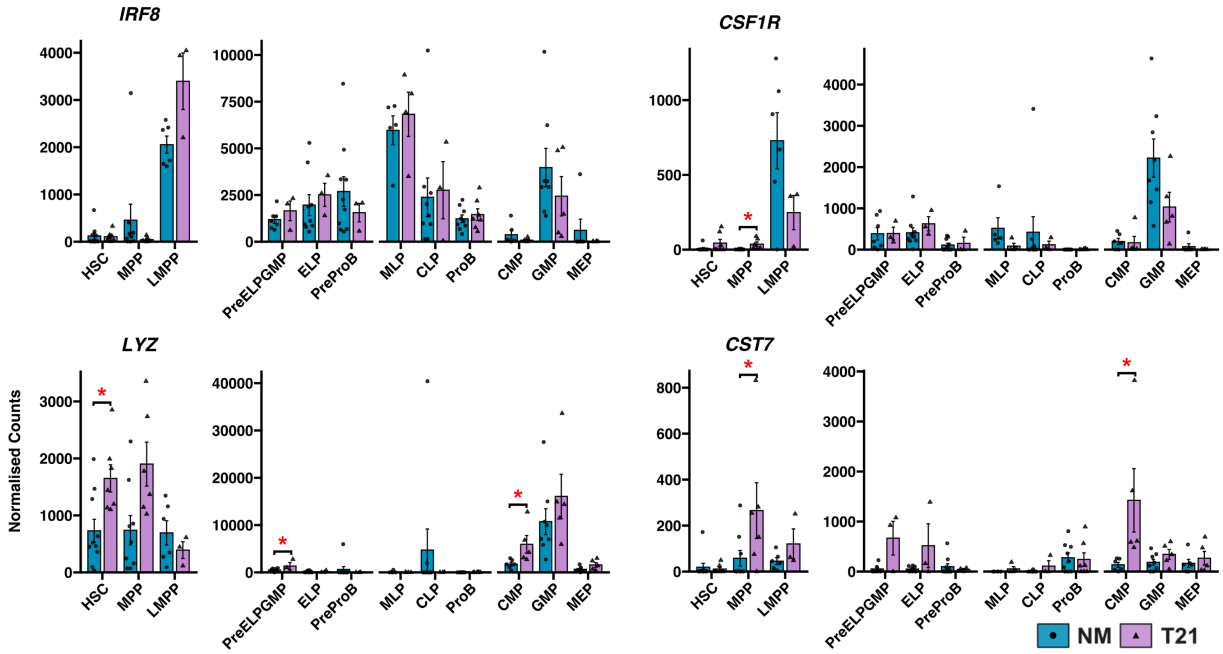

Figure 3.13: Expression of genes with a known role in monopoiesis in NM and T21 HSPC. Gene expression was measured by RNA-Seq (50-100 cells). For each gene, graphs are grouped (from left to right) for primitive HSPC, fetal specific lymphoid progenitors, adult type lymphoid progenitors, and myeloid progenitors. Gene expression data shown as mean normalised counts ± SEM, * denotes significance by DESeq2 (p-adj<0.1). NM (normal, blue bars represent mean expression, dots represent biological samples, n=5-10).

Taken together, these data suggest there may be increased monocytic specification in populations with monocytic potential in T21 fetal BM but further studies would be needed to confirm this.

Expression of granulocytic genes

I next considered the expression of key genes associated with granulocyte development: *CSF3R*, *GFI1*, *CTSG*, *AZU1*, *MPO* and *PRTN3*[580] (Figure 3.14).

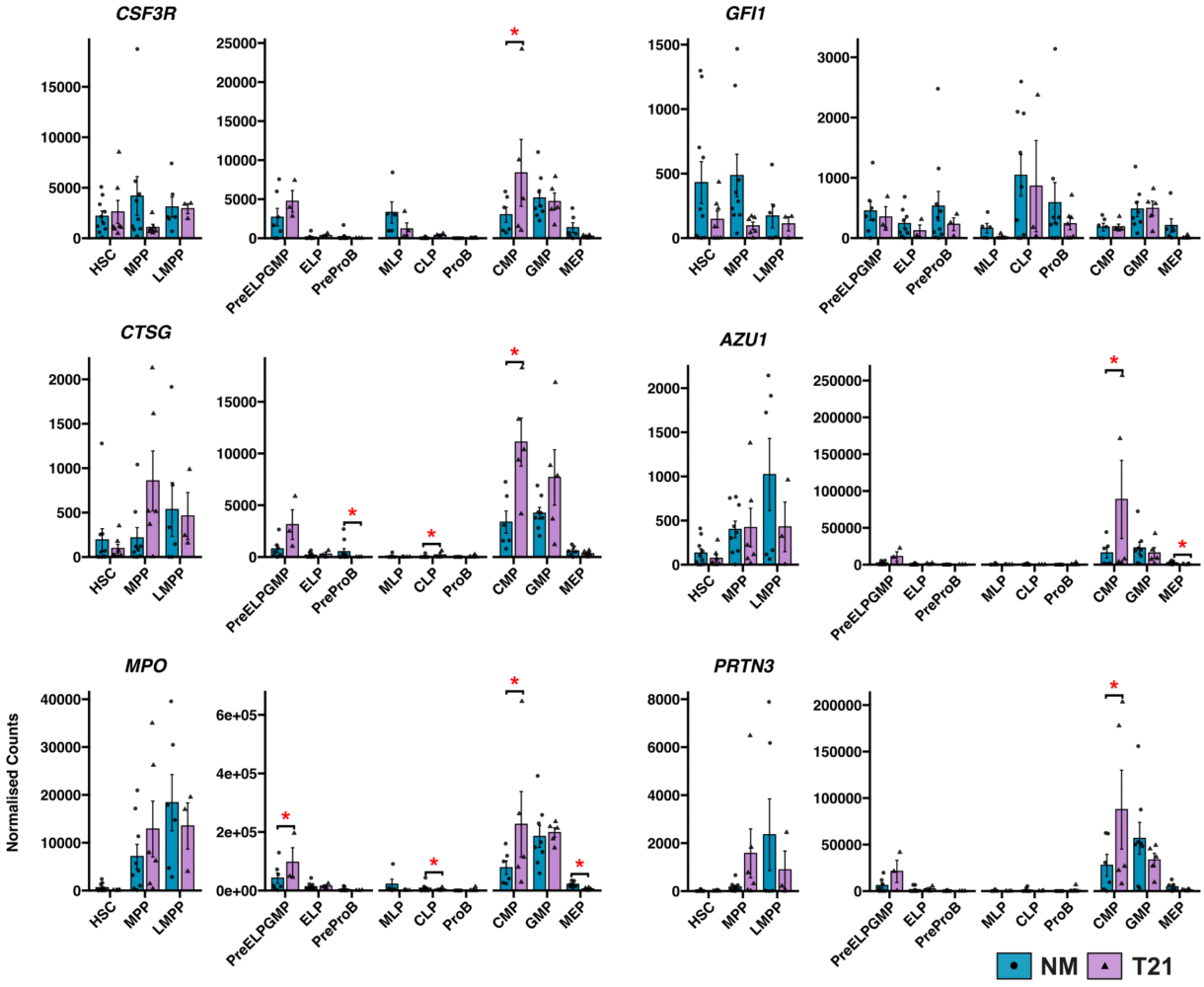

Figure 3.14: Expression of genes with a known role in granulopoiesis in NM and T21 HSPC. Gene expression was measured by RNA-Seq (50-100 cells). For each gene, graphs are grouped (from left to right) for primitive HSPC, fetal specific lymphoid progenitors, adult type lymphoid progenitors, and myeloid progenitors. Gene expression data shown as mean normalised counts ± SEM, * denotes significance by DESeq2 (p-adj<0.1). NM (normal, blue bars represent mean expression, dots represent biological samples, n=5-10); T21 (Trisomy 21, lilac bars represent mean expression, triangles represent biological samples, n=3-7).

CSF3R encodes the receptor to the cytokine G-CSF, and plays a role in commitment towards granulocytic differentiation[581]. Mutations in *CSF3R* are responsible for some forms of Severe Congenital Neutropenia (SCN)[582]. However, there were no significant differences in *CSF3R* expression in T21 fetal BM HSPC compared to NM HSPC, apart from an increase in *CSF3R* expression in T21 CMP, which was driven by a high level of expression in a single sample (Figure 3.14).

GFI1 encodes a transcription factor with a role in granulocytic specification, amongst other roles in haematopoiesis. In humans, rare mutations in *GFI1* result in SCN [583], reflecting the phenotype observed in *Gfi1*-/- mice[584]. However, GFI1 also has wider functions in haematopoiesis including HSC self-renewal[585, 586] and lymphopoiesis, specifically in CLP expansion and in the differentiation into and expansion of CD4+ and CD8+ T cells[583, 584, 587, 588]. There were no significant differences between *GFI1* expression in NM and T21 fetal BM HSPC, although there was a modest, non-significant reduction in *GFI1* expression in T21 fetal BM HSC and MPP (Figure 3.14).

Similarly, expression of genes encoding key components of neutrophilic granules, *CTSG*, *AZU1*, *MPO* and *PRTN3*, peaks in NM fetal BM GMP (Appendix Figure 8, page 202), but these genes were most highly expressed in T21 CMP, and had a significantly increased expression compared to NM fetal BM CMP. This premature expression of granulocytic programmes, and granulocytic effector genes, may reflect increased granulocytic priming in T21 CMP.

Taken together, these data found no evidence of increased myeloid gene expression in LMPP as a cause of the block in B lineage development in T21 fetal BM. However, the genes studied in this initial analysis represent just a fraction of the genes involved in haematopoiesis, and identifying differences in gene expression at the LMPP stage is likely to require a broader, unbiased analysis.

3.4.5 Differential gene expression and chromatin accessibility

Since the differences in the frequency of immunophenotypic HSPC suggest that a block in lymphoid commitment is likely to occur at, or immediately downstream of LMPP, I focused my analysis on differences in gene expression and chromatin accessibility in T21 compared to NM fetal BM HSC, MPP and LMPP. I was also keen to look for differences between PreELP/GMP, ELP, MLP and CLP but unfortunately their scarcity in T21 fetal BM meant that it was only possible to FAC-sort the numbers of cells required for ATAC-Seq (900-2000) from one or two T21 samples from each of these populations in sufficient numbers for ATAC-Seq. Table 3.1 and Table 3.2 summarise the datasets of bulk RNA- and ATAC-Seq generated from FAC-sorted fetal BM HSPC.

Population	**n NM**	**n T21**	**n DEG**	**n up in T21**	**n down in T21**
HSC	10	7	890	673	217
MPP	9	6	1063	758	305
LMPP	6	3	452	217	235
MLP	5	4	532	295	237
PreELP/GMP	7	3	1904	1054	850
ELP	9	3	1702	548	1154
CLP	9	3	1146	664	482
PreProB	10	3	292	231	61
ProB	9	7	746	601	145
CMP	6	5	776	598	178
GMP	8	5	551	297	254
MEP	6	5	636	289	347

Table 3.1: Summary of number of libraries sequenced by fetal BM HSPC population from different biological donors for RNA-Seq, and the number of differentially expressed genes (DEG) calculated by DESeq2 (P-adj<0.1).

Population	n NM	n T21	n DAP	n DAP up in T21	n DAP down in T21
HSC	3	4	117	109	8
MPP	4	3	231	112	119
LMPP	5	4	323	223	100
PreELP/GMP	4	1	-	-	-
ELP	2	0	-	-	-
CLP	4	2	-	-	-
PreProB	5	1	-	-	-
ProB	5	3	684	590	94

Table 3.2: Summary of number of libraries sequenced by fetal BM HSPC population from different biological donors for ATAC-Seq, and the number of differentially accessible peaks (DAP) calculated by DESeq2 (P-adj<0.1). Differential accessibility analysis was not conducted in HSPC populations in which n was less than two.

PCA of the top 1000 variably expressed genes showed that both T21 and NM fetal BM samples cluster by HSPC type (Figure 3.15), with lymphoid progenitors separating from HSC/MPP in PC1. When plotted together, HSPC from NM and T21 fetal BM followed a similar clustering pattern.

This was also the case by ATAC-Seq, with HSPC from NM and T21 fetal BM showing separation of HSC, MPP and LMPP from lymphoid progenitors in PC1, and B cells separating from HSPC in PC2 (Figure 3.16). Similarly, when plotted together, HSPC derived from NM and T21 fetal BM clustered together.

Interestingly, T21 fetal BM PreELP/GMP clustered closer to LMPP, compared to NM fetal BM PreELP/GMP, which cluster closer to ELP and PreProB by both ATAC and RNA-Seq (Figures 3.15 and 3.16). This suggests T21 fetal BM PreELP/GMP are less poised to differentiate into ELP, in line with some of the observed differences in lineage-specific gene expression, and, as mentioned, PreELP/GMP may represent a mixed population which in T21 fetal BM are more PreGMP than PreELP.

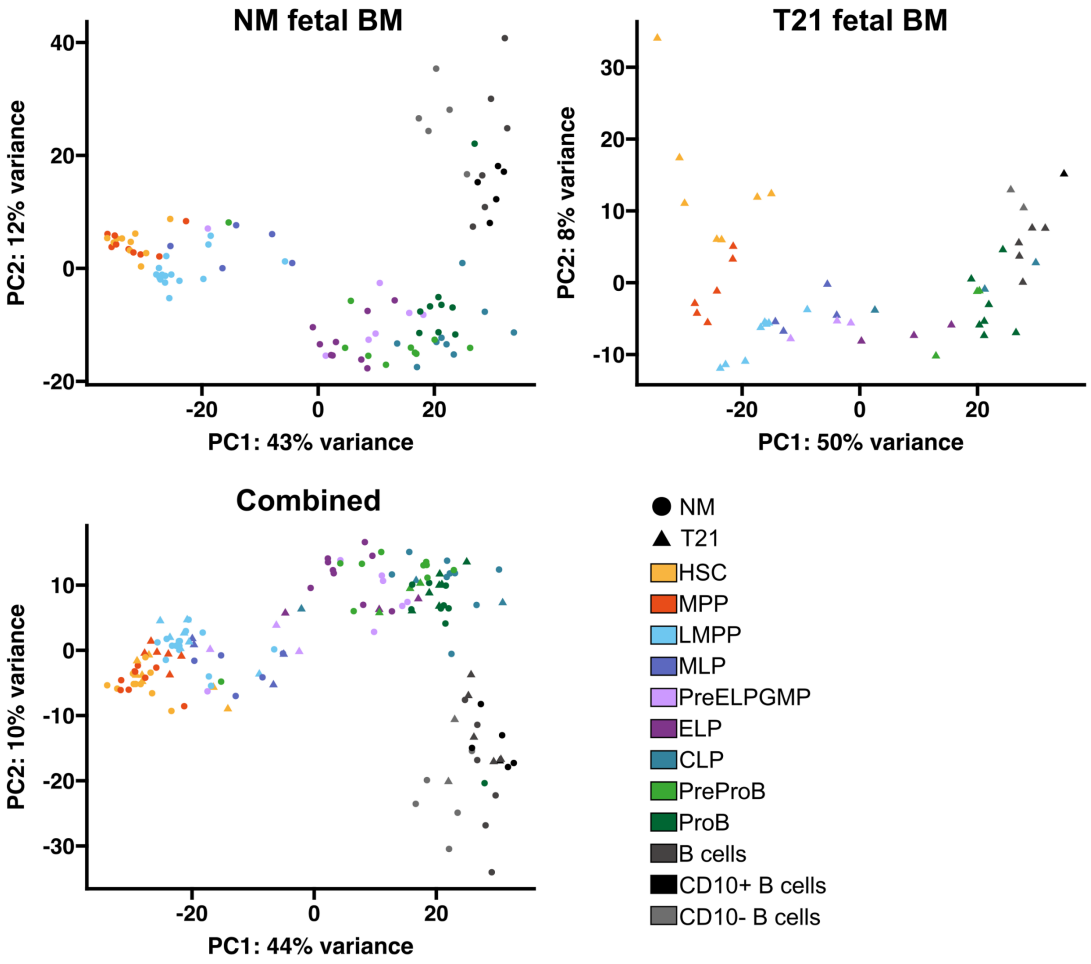

Figure 3.15: PCA of the top 1000 most variably expressed genes by RNA-Seq in NM and T21 fetal BM. NM, normal, circles, n=5-10, top left panel; T21 trisomy 21, triangles, n=3-7, top right panel. Gene expression was measured by RNA-Seq (50-100 cells).

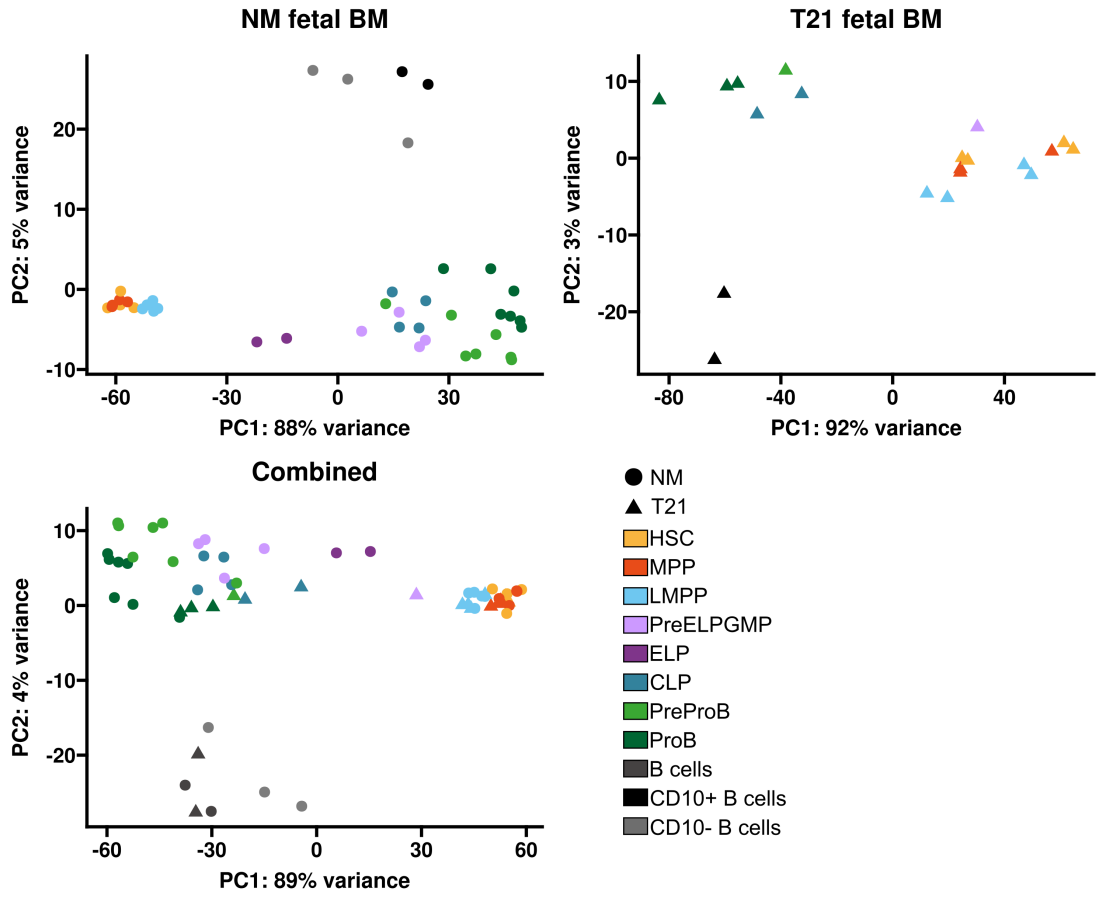

Figure 3.16: PCA of the top 1000 most variably accessible peaks in NM and T21 fetal BM. NM, normal, triangles, n=2-5, top left panel; and T21, trisomy 21, n=1-4, top right panel. Chromatin accessibility was measured by ATAC-Seq (900-2000 cells).

3. Results I: the impact of T21 on the gene expression and chromatin accessibility of fetal BM progenitors

To gain further insight into the impact of T21, I next compared the differences in gene expression and chromatin accessibility between T21 and NM samples by chromosome as well as by HSPC type (Figure 3.17), which showed several interesting findings.

First, that the proportion of differentially upregulated genes per chromosome was greatest in chromosome 21 and majority of HSPC populations had a high proportion of differentially expressed genes on chromosome 21 with the notable exceptions of MLP and PreProB. This confirms previous conclusions that although there is upregulation of chromosome 21 genes in T21 HSPC, the extent of these changes is cell context-dependent.

A second important finding was that, particularly in PreELP/GMP, ELP and CLP, there were large numbers of differentially expressed genes between T21 and NM fetal samples on every chromosome indicating that T21 caused global perturbation of gene expression and that this may be particularly disruptive in these early lymphoid populations.

The small number of T21 samples with available ATAC-Seq data limited the reliability of the conclusions that could be drawn about differential chromatin accessibility by chromosome although it is potentially interesting that the largest number of differentially accessible peaks was on chromosome 21 and that the HSPC population where this was most apparent was LMPP. However, more data would be needed to test the reliability of these findings and also to determine whether differences would also be apparent in other HSPC populations.

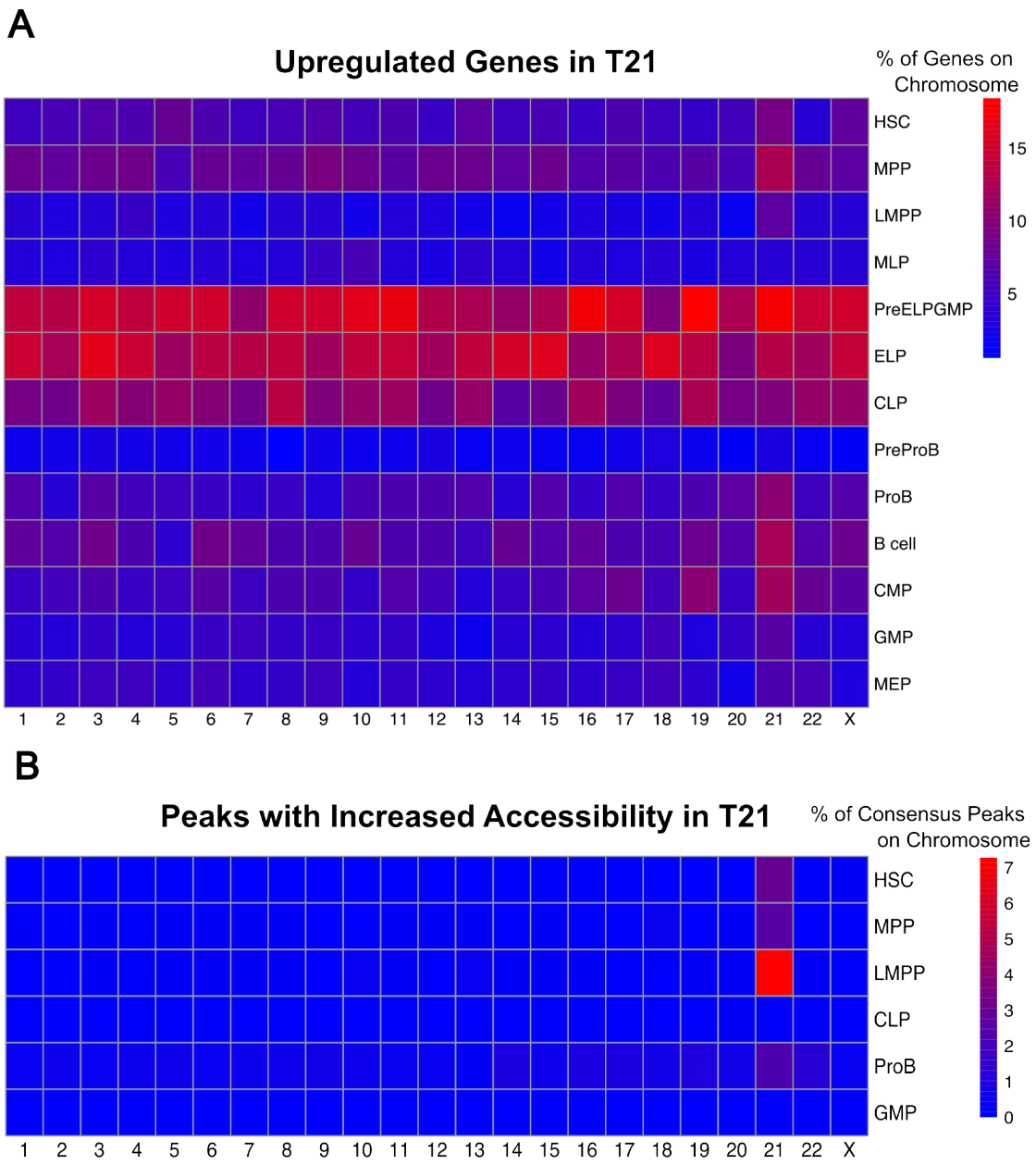

Figure 3.17: T21 results in genome wide changes in gene expression and chromatin accessibility. Heatmap of percentage of genes per chromosome that are upregulated in T21 fetal BM HSPC populations by RNA-Seq (50-100 cells, n NM=5-10, n T21=5-7)(A) and peaks on a given chromosome that are more accessible in T21 by ATAC-Seq (900-2000 cells, n NM =3-5, n T21 = 2-4) (B).

On chromosome 21 itself, differences in chromatin accessibility and gene expression appeared in a similar region, on the long arm of chromosome 21 (q22.11 to q22.3). Although this includes the so called Down Syndrome Critical Region (DSCR) the precise relationship of differential expression of the number of genes in this region with specific phenotypes is not yet clear [366, 369, 370]. Interestingly in my analysis, there were only a small number of differentially expressed genes on chromosome 21 in T21 HSPC (Figure 3.18); these have been listed in Tables 8-14, pages 215-219 in the appendices.

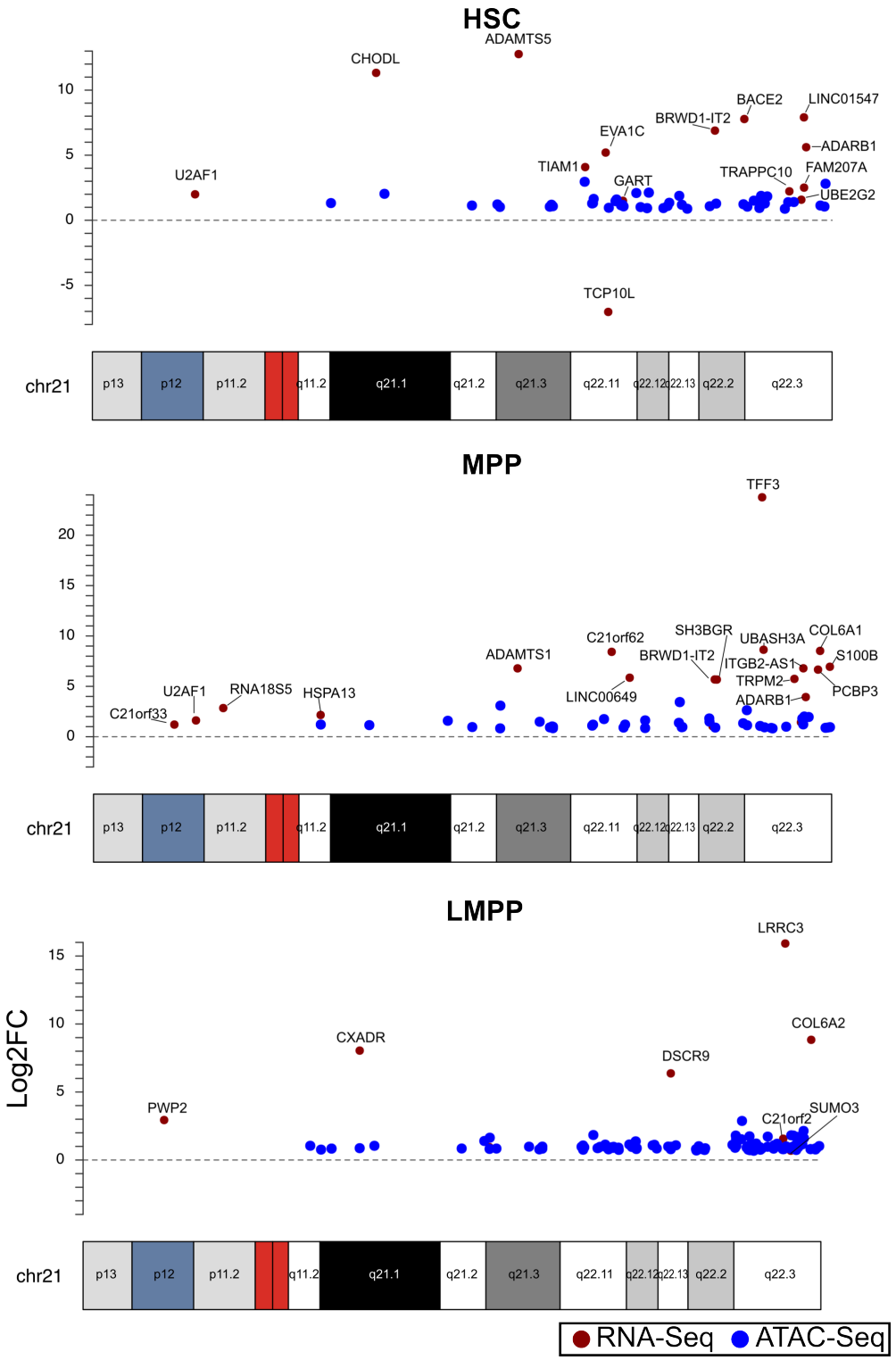

Figure 3.18: Differential chromatin accessibility and gene expression on chromosome 21 in T21 HSC, MPP and LMPP. A Giemsa banding ideogram summarising the genomic location of differentially accessible peaks (blue) and differentially expressed genes (maroon) by DESeq2 (p-adj<0.1). Black and grey bands represent regions positively stained by Giemsa banding, which tend to be AT-rich; white regions are negative for Giemsa banding staining and tend to be CG-rich. The centromere is marked by red bands, and the blue band marks the satellite stalk. The most recent definition of the Down Syndrome Critical Region is associated with 21q22.13[360, 366, 589].

Gene	**Function in Haematopoiesis**
BACH1	BACH1 and BACH2 repress myeloid programmes, promoting commitment to the B lineage [590]
DYRK1A	A kinase involved in regulating cell cycle; plays a role in inhibiting B cell proliferation in germinal centres [591]. Also involved in promoting autoimmunity through non-canonical NFκB activation[592] and B-ALL by non-canonical NFκB activation and by activating FOXO1 and STAT3[592, 593]. Reviewed recently in [594].
ERG	Plays a role in activating B lineage activating genes *Ebf1* and *Pax5*[124]. Also promotes megakaryopoiesis; known oncogene in ML-DS [595]. Implicated in the fetal to adult transition in haematopoiesis [125]
ETS2	Promotes megakaryopoiesis, known oncogene in ML-DS [595]. Also plays a role in promoting inflammatory macrophage-mediated inflammation [596]
GABPA	Plays a role in myelopoiesis and B lymphopoiesis [597, 598]
HMGN1	Plays a role in chromatin remodelling. Overexpression recapitulates B lymphoid phenotype in T21 models[380, 532]
IFNAR1, *IFNAR2*, *IFNGR2*	Interferon receptors. Increased expression of *IFNAR1* and *IFNAR2* was sufficient to recapitulate hypersensitivity to interferon signalling in immortalised fibroblasts [431]. IFNα and IFNγ promote myelopoiesis [599, 600]
IL10RB	Encodes the receptor for IL10, an anti-inflammatory cytokine. *Il10rb* knockout mice show a reduction in B cells, and increased GMP and monocytes [601]
MX1	Involved in the type I interferon response [602], which plays a role in promoting emergency myelopoiesis [600]
RCAN1	A negative regulator of the calcineurin–NFAT pathway, which inhibits megakaryopoiesis [603]. Overexpression of *RCAN1* in transgenic mice recapitulates aspects of the T-cell defect in T21; reduced frequency, proliferation, and aberrant cytokine production[604]
RUNX1	Master haematopoietic transcription factor; involved in differentiation of multiple haematopoietic lineages, including B lineage specification [605, 606]. Implicated in ML-DS pathogenesis [607]

Table 3.3: Genes encoded on Chromosome 21 with known roles in haematopoiesis.

3.4.6 Differences in chromatin landscape in T21 fetal BM HSPC

I first conducted pairwise differential chromatin accessibility analysis for a given population in NM and T21 fetal BM HSPC. The results from this analysis are summarised in Table 3.2; all differentially accessible peaks associated with genes are provided in the appendices (Tables 17, 18, 19, pages 224, 227, 232).

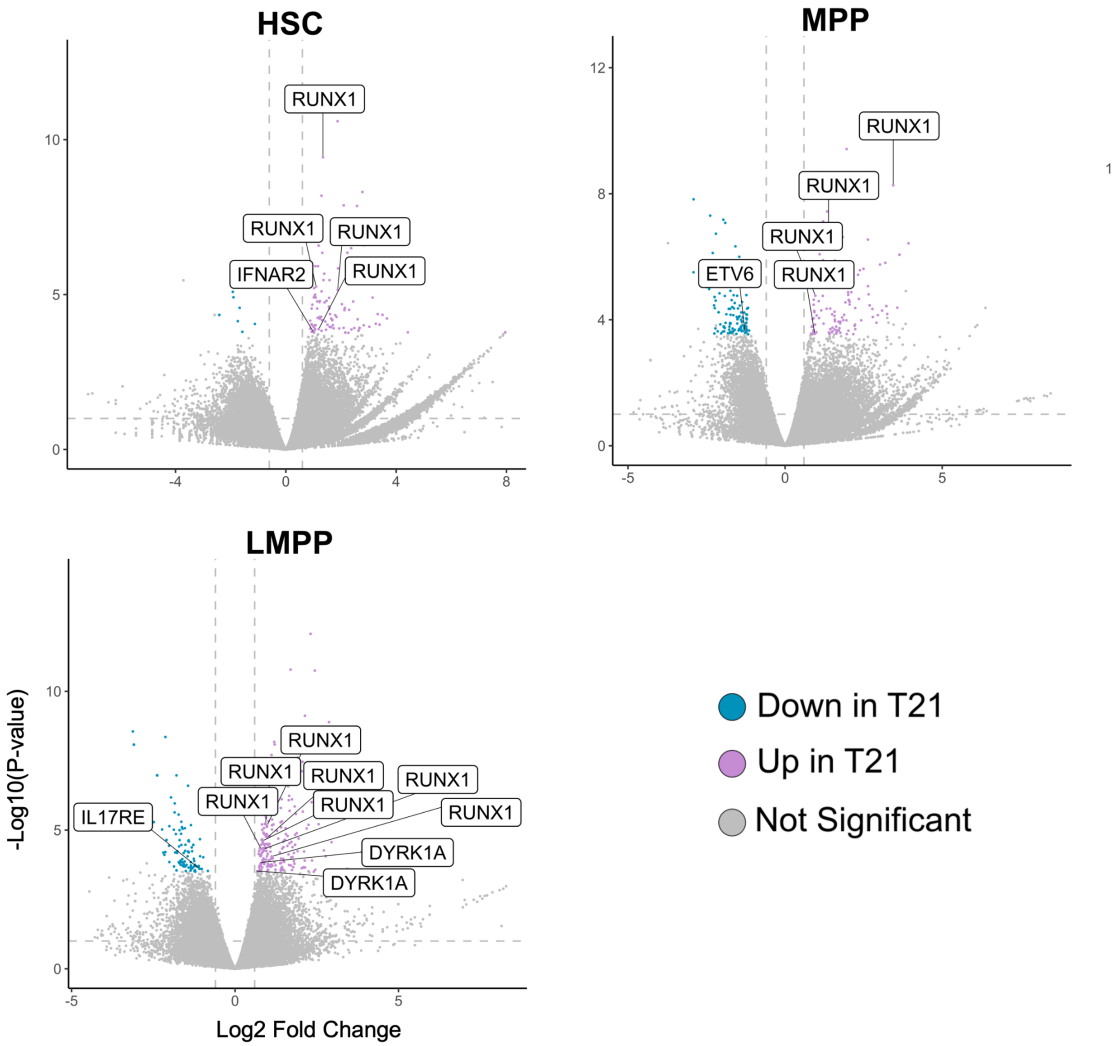

Figure 3.19: Differentially accessible peaks in T21 HSC, MPP and LMPP. Volcano plots showing differentially accessible peaks between NM (n=3-5) and T21 (n=3-4) HSPC by DESeq2 (p-adj <0.1). Dashed lines are at p=0.05 and log2FoldChange=±0.6.

T21 HSPC showed an overall increase in chromatin accessibility (Table 3.2, Figure 3.19), of which peaks on chromosome 21 were overrepresented (Figure 3.17) as would be expected in T21 HSPC, which have an extra copy of chromosome 21.

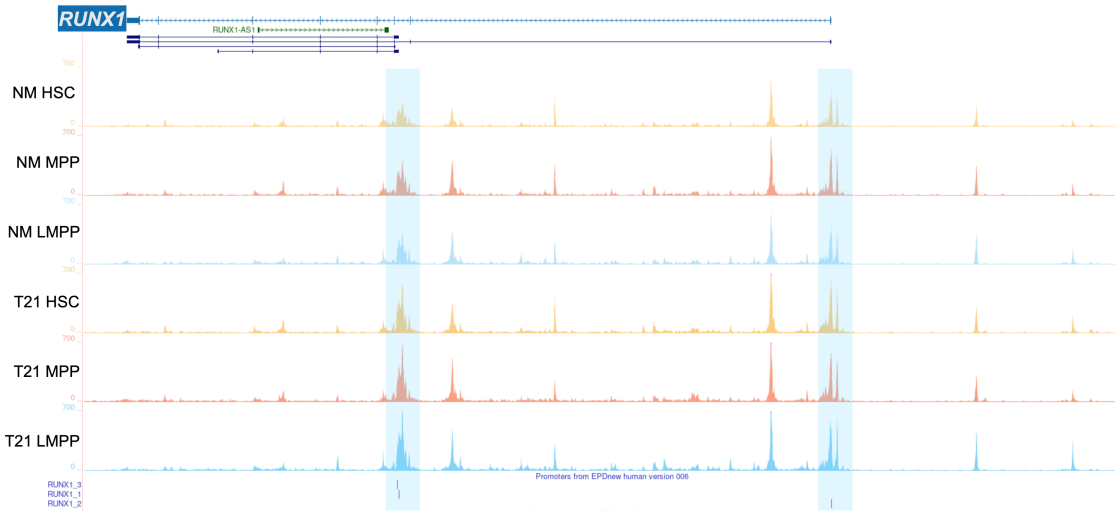

Figure 3.20: RUNX1 chromatin in T21 HSC, MPP and LMPP. Peak traces of the averaged chromatin accessibility of *RUNX1* across NM (n=3-5) and T21(n=3-4) HSC, MPP and LMPP. *RUNX1* promoters according to the European Promoter Database are highlighted.

Of the DAPs associated with (less than 1000bp upstream of or within) protein-coding genes, peaks associated with the chromosome 21 gene *RUNX1* were significantly more accessible in T21 HSC, MPP, and LMPP (Figure 3.19), though these did not include the *RUNX1* promoters P1/ P2 (Figure 3.20). Additionally, RUNX1-binding motifs were significantly more accessible in T21 HSC and LMPP, and while they did not reach statistical significance in MPP, RUNX1 binding motifs were among the top five overrepresented motifs in T21 MPP and LMPP (Figure 3.21). Increased RUNX1 motif accessibility has also been described recently by scATAC-Seq analysis in T21 fetal liver HSC[388].

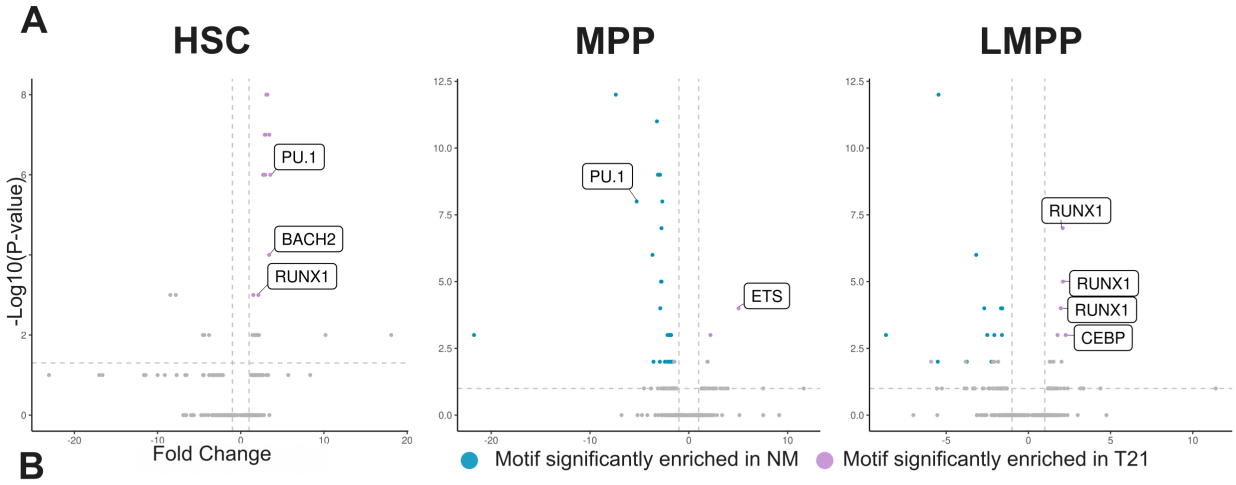

Figure 3.21: Differentially accessible transcription factor motifs in T21 HSC, MPP and LMPP. (A) Volcano plots showing significantly differentially accessible transcription factor binding motifs between NM (n=3-5) and T21 (n=3-4) HSC, MPP and LMPP by Homer (FDR <0.1). Dashed lines are at p=0.05 and log2FoldChange=±0.6.(B) Top 5 motifs enriched in T21 fetal BM HSC, MPP and LMPP. Not all motifs shown in tables are statistically significant; Benjamini–Hochberg adjusted q-values are provided.

This is potentially a very important finding because RUNX1 is one of the most important haematopoietic transcription factors and plays key roles both in haematopoiesis and leukaemia in humans and in mice. Studies in mice show that RUNX1 is essential for the emergence of definitive haematopoiesis in embryonic development[17, 608–610] (reviewed in [611, 612]). RUNX1 is also essential for normal megakaryopoiesis and lymphopoiesis: conditional knockouts of *Runx1* in mice show an early B lymphoid arrest and a marked decrease in megakaryocytes [605, 613]. In humans, inherited mutations in *RUNX1* cause familial platelet disorder, a condition marked by thrombocytopenia[614].

The *RUNX1* gene in humans is encoded on the antisense strand, and contains two alternative promoters, P1 (distal) and P2 (proximal). Alternative promoter usage, alongside alternative splicing gives rise to different isoforms of RUNX1, amongst which isoforms *RUNX1A*, *RUNX1B* and *RUNX1C* are best studied. *RUNX1A* and *RUNX1B* transcription is controlled by the P2 promoter, while the P1 promoter governs *RUNX1C* transcription[615]. Both P1 and P2 promoters are hypermethylated in newborns with T21, with the P2 promoter being significantly hypermethylated[379].

An imbalance in RUNX1 isoform ratios has been shown to contribute to the pathology of ML-DS, specifically, with an increased *RUNX1A*:*RUNX1C* ratio, which cooperates with the preleukaemic *GATA1s* mutations acquired at the TAM stage of the disease[607]. Additionally, *RUNX1A*:*RUNX1B*/*RUNX1C* ratio has been reported to be higher in T21 fetal HSPC as a whole[607]. Though the different roles of human RUNX1 isoforms in B lymphopoiesis have not been characterised to date, RUNX1 plays an important role in B lymphoid specification in mice, by regulating expression of *Ebf1*[605].

Given the potential implications of an imbalance in *RUNX1* transcripts, and the existing literature about RUNX1 isoform imbalance in T21, I carried out differential exon usage analysis with DEXSeq[516], to infer differences in *RUNX1* isoform balance in T21 fetal BM HSC, MPP and LMPP using the RNA-Seq dataset (Figure 3.22).

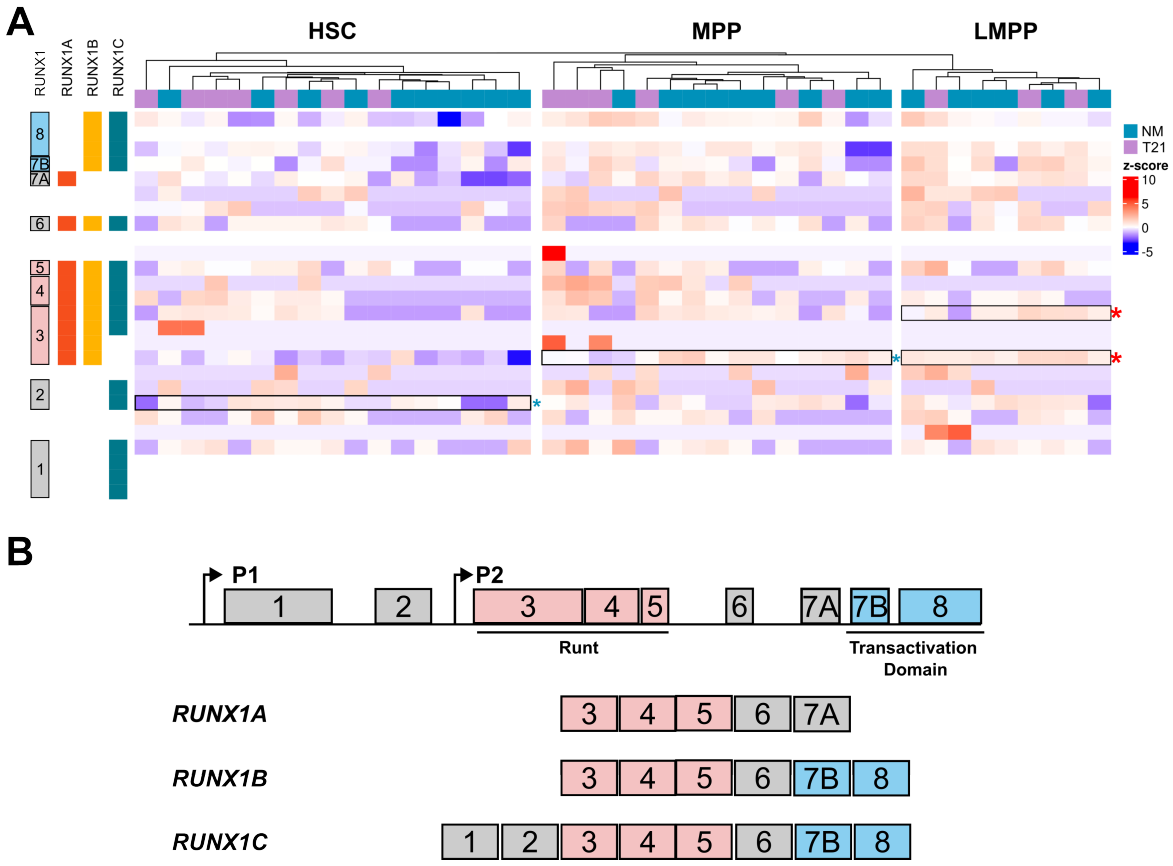

Figure 3.22: Differential *RUNX1* exon usage in T21 fetal BM HSC, MPP and LMPP. (A) Non-overlapping exonic bins of the *RUNX1* gene are plotted along the y axis, ordered by genomic position, with the panel on the left representing exon usage by isoforms *RUNX1A*, *RUNX1B* and *RUNX1C*. Differently expressed exonic regions are highlighted by a black box and marked by *, denoting FDR <0.05 by DEXSeq, with a red * representing increased expression in T21, and a blue * representing decreased expression in T21. *RUNX1* is encoded on the antisense strand, *RUNX1* transcript structure should be interpreted from the bottom upwards. (B) Schematic representing *RUNX1* exons and transcript structure of *RUNX1A*, *RUNX1B* and *RUNX1C*, with the functional exons coloured: the Runt domain (pink) binds DNA, the transactivation domain (light blue) activates gene expression. P1, promoter 1; P2, promoter 2; NM, normal, n=6-10; T21, Trisomy 21, n=3-7.

In this analysis, exonic regions associated with *RUNX1C* but not *RUNX1A* or *RUNX1B* were significantly decreased in T21 HSC. Additionally, two exonic regions associated with *RUNX1A* and *RUNX1B* were significantly upregulated in T21 LMPP. However, in T21 MPP, the converse is true, with an exonic region associated with *RUNX1A* and *RUNX1B* but not *RUNX1C* being decreased in expression. Taken together, these data suggest RUNX1 isoform balance may be altered in T21 fetal BM HSC, MPP and LMPP in a cell context specific manner. However, to properly assess the balance of *RUNX1A*, *RUNX1B* and *RUNX1C*, long-read RNA-Seq or RT-qPCR with careful primer design would be needed.

3.4.7 Differences in gene expression in T21 fetal BM HSPC

I next conducted pairwise differential gene expression analysis for a given population between NM and T21 HSPC. The results of this analysis are summarised in Table 3.1, and DEG lists of the top fifty differentially expressed genes for each population are provided in the appendices (Tables 1-7, pages 204-214).

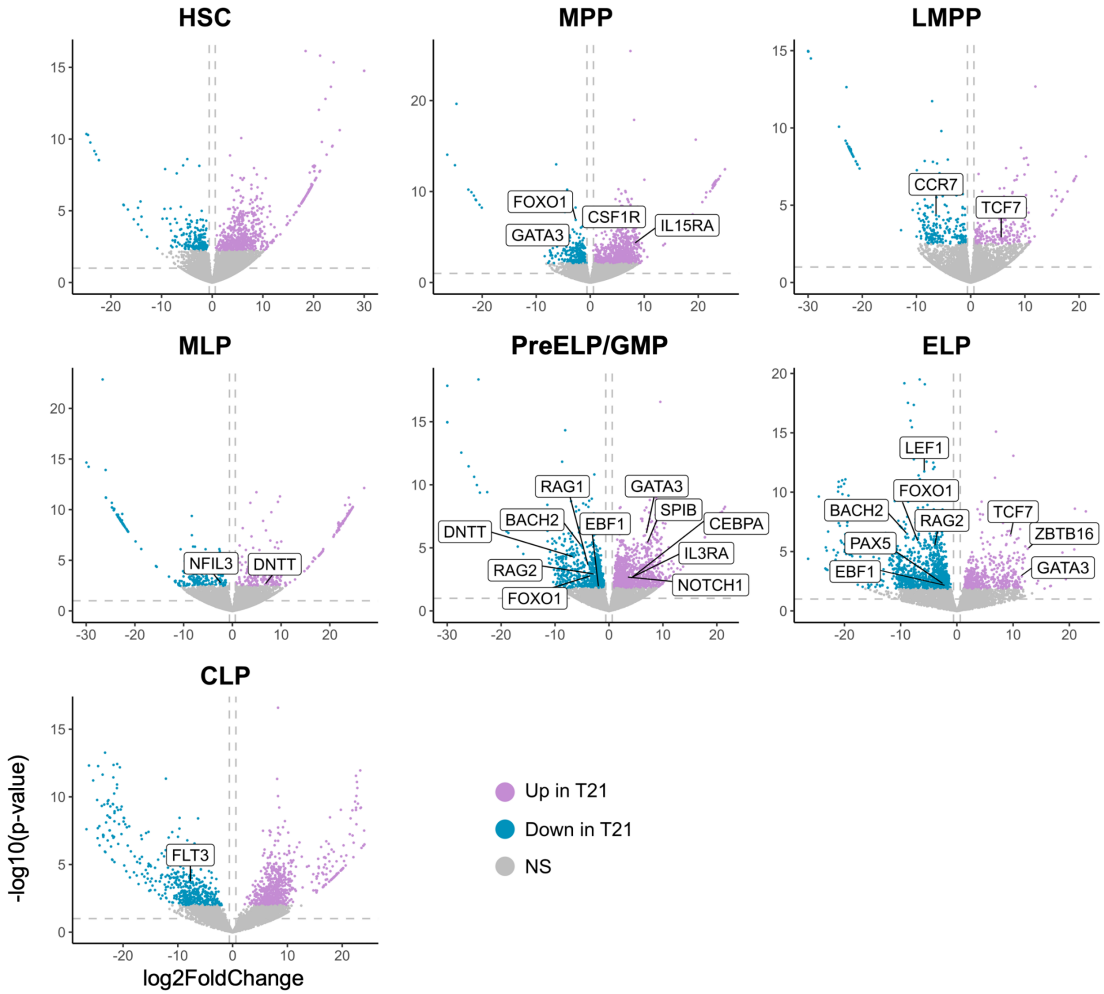

Figure 3.23: Differentially expressed genes in T21 HSPC. Volcano plots showing differentially expressed genes between in NM (n=5-10) and T21 (n=3-7) HSPC by DESeq2 (p-adj <0.1), with genes with a known role in haematopoiesis highlighted. Dashed lines are at p=0.05 and log2FoldChange=±0.6.

3. Results I: the impact of T21 on the gene expression and chromatin accessibility of fetal BM progenitors

Volcano plots showing differentially expressed genes (p-adj<0.1) showed there were a number of differentially expressed genes with known roles in haematopoietic fate decisions (Figure 3.23).

I also performed differential expression analysis between pairs of HSPC populations that are just upstream/downstream of each other in the B cell developmental pathway in NM and T21 HSPC (Figure 3.24).

The number of differentially expressed genes at each transition was similar in NM and T21 HSPC, except for the PreELP/GMP to ELP transition (Figure 3.24A). In addition, the most striking changes in expression of B lymphopoietic genes were seen in PreELP/GMP and ELP, with T21 PreELP/GMP having significantly lower expression of these genes (e.g. *FOXO1*, *BACH2*, *EBF1*, *PAX5*, *RAG1*, *RAG2* and *DNTT*), suggesting an impaired ability to properly activate the B lymphoid programme in these progenitors T21 fetal BM. There was also a concurrent increased expression of genes associated with suppressing B lymphoid programmes in T21 PreELP/GMP and ELP: *NOTCH1*[544],*GATA3*[142], *SPIB*[616], *CEBPA*[617], and *IL3RA*[618].

However, upstream of this, in LMPP, there were fewer differences. There was an increased expression of T/NK lineage transcription factor *TCF7*[550, 619] and reduced expression of the chemokine receptor *CCR7*, which is important for normal B cell development in mice and in the chick embryo[620, 621] although its role in human B lymphopoiesis is not clear.

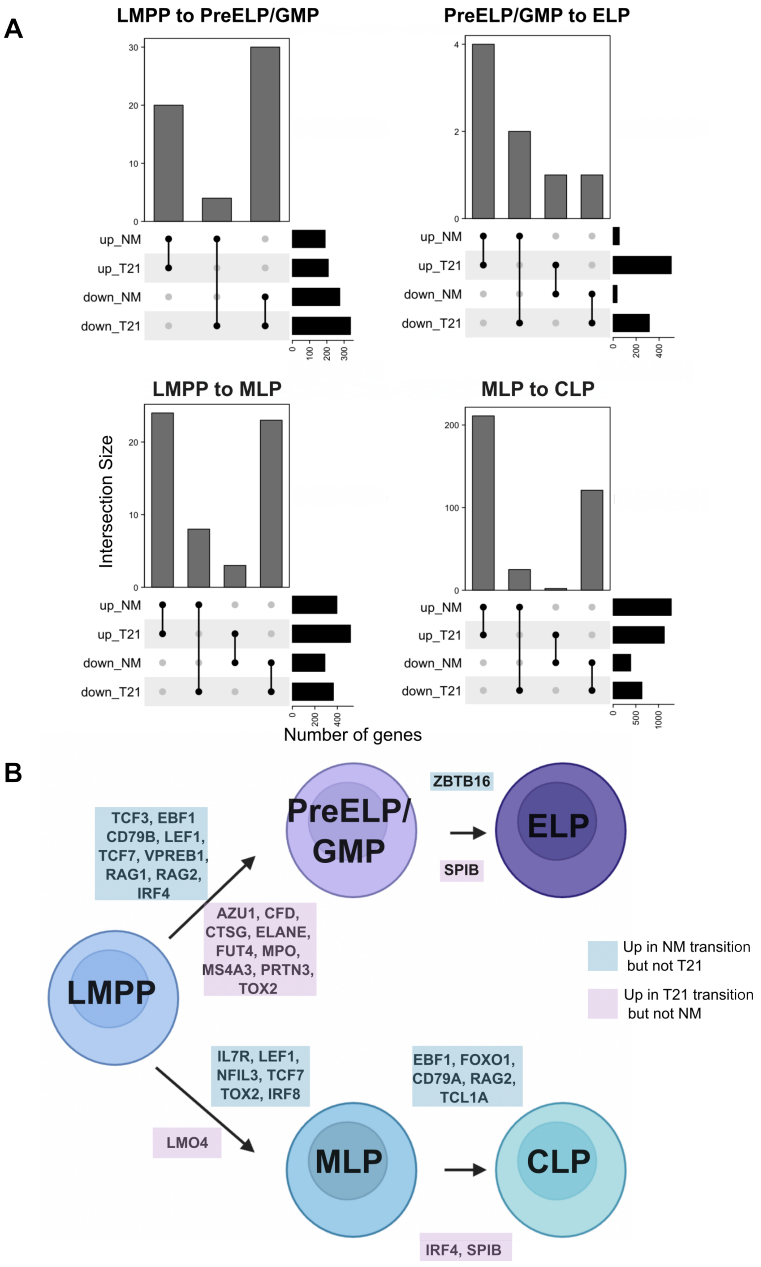

Figure 3.24: Changes in gene expression along the lymphoid differentiation trajectory in NM and T21 fetal BM. Differential gene expression between pairwise populations (LMPP and PreELP/GMP, PreELP/GMP and ELP, LMPP and MLP, and MLP and CLP) were computed by DESeq2 (p-adj <0.1) in NM (n=5-9) and T21 (n=3-4) fetal BM separately. Differentially expressed gene lists were overlapped to assess commonalities in changes in gene expression through differentiation between NM and T21 lymphoid progenitors. (A) Upset plots for a given transition. Dots with lines connected represent the intersection, with "up" indicating genes upregulated during the transition and "down" indicating genes downregulated during a given transition. Y axis represents intersection size, while the size of the individual gene lists are shown on the x axis. (B) Genes with a known role in haematopoiesis significantly upregulated in a given transition that are present in NM but not T21 (blue) or vice versa (lilac).

However, while the number of genes up or down regulated at each transition were comparable, there was very little overlap between the actual genes that were being up/down regulated at each transition between NM and T21 fetal BM HSPC. To quantify how conserved sets of differentiation-associated genes were between T21 fetal BM HSPC and NM fetal BM HSPC, I determined the number of genes that were upregulated in both NM and T21 as well as those that were downregulated; these overlapping genes were considered conserved. This number was then divided by the number of differentially expressed genes in a NM fetal BM differentiation step, to provide a measure of the percentage of gene changes for a given differentiation step between populations in T21.

This demonstrated poor concordance with only 8.2% of NM fetal BM gene changes conserved during transition from LMPP to PreELP/GMP; 4.1% for PreELP/GMP to ELP; 6.9% for LMPP to MLP; and 20% for MLP to CLP. This is suggestive of severely impaired lymphoid commitment in T21 fetal BM, with the adult-like pathway MLP to CLP transition being most conserved.

I next considered which genes were upregulated for a given transition in NM fetal BM and not in T21 fetal BM, and vice versa, and highlighted genes with a known role in haematopoiesis (Figure 3.24B).

T21 HSPC also failed to upregulate key lymphoid genes at the LMPP to PreELP/GMP transition, the LMPP to MLP transition, and the MLP to CLP transition. Rather, the LMPP to PreELP/GMP transition in T21 fetal BM included an upregulation of genes associated with myelopoiesis. The LMPP to MLP transition in T21 upregulated *LMO4*, which plays a role in ILC fate specification[622], while the same transition in NM fetal BM was characterised by upregulation of known lymphoid genes such as *IL7R*, *TCF7*, *LEF1* and *NFIL3*. Interestingly, the PreELP/GMP to ELP transition and the MLP to CLP transition in T21 but not NM saw the significant upregulation of *SPIB*, a gene important in plasmacytoid dendritic cell development[623] with a known role in suppression of lymphoid programmes, at least in mice[616].

To further understand when B lymphoid programmes are active in T21 fetal BM HSPC, I next carried out weighted gene correlation network analysis (WGCNA) on NM and T21 HSPC, generating separate gene regulatory networks for NM and T21 HSPC, and identified a single B lymphoid module in both networks - the top genes associated with these modules are provided in the appendices (Tables 15 and 16, pages 220 - 221). In NM HSPC, this was active from PreELP/GMP onwards, however, in T21, this module was not active in PreELP/GMP or ELP, and rather, was active from CLP, a more adult-like progenitor. This further supports a failure in the normal activation of B lymphoid programmes in fetal specific lymphoid progenitors in T21.

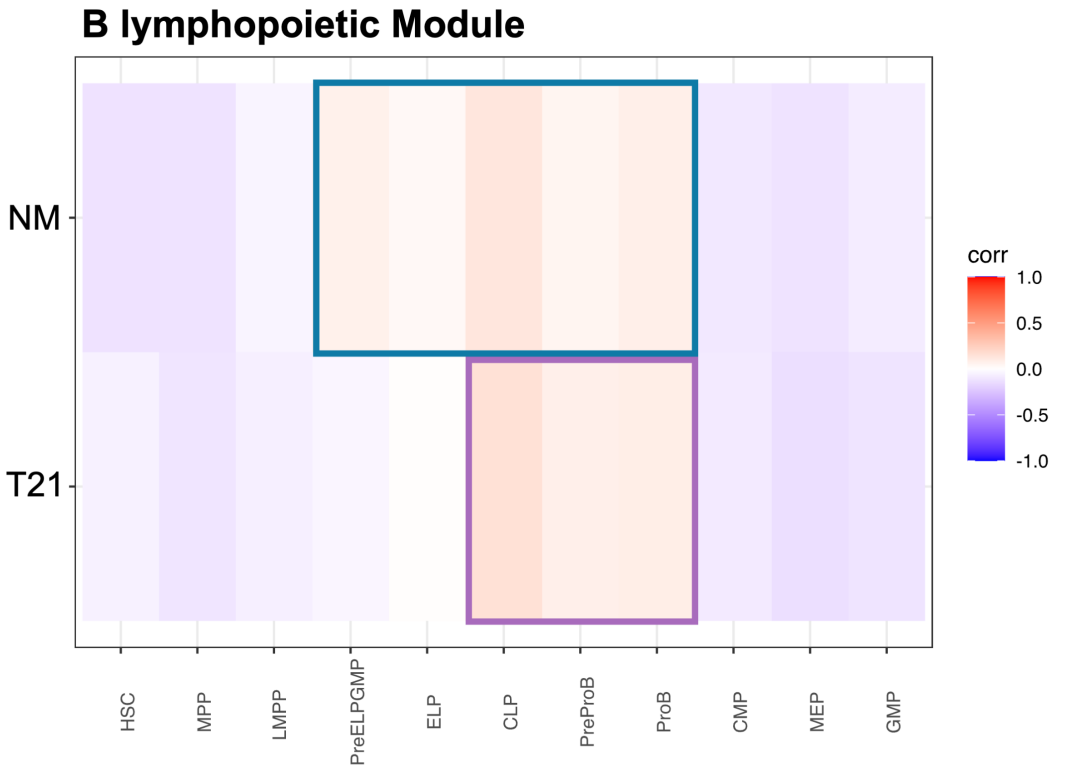

Figure 3.25: Weighted gene correlation network analysis of RNA-Seq data from NM and T21 fetal BM HSPC. B lymphoid programmes generated by WGCNA of NM and T21 HSPC gene expression by RNA-Seq (50-100 cells) show T21 B lymphoid programmes are active from CLP onwards in T21, whereas in NM fetal BM these are active from PreELP/GMP. NM, normal, n=5-10; T21, trisomy 21, n=3-7.

Inferred differences in transcription factor activity in T21 fetal BM HSPC

In addition to the bulk ATAC- and RNA-Seq datasets generated by myself or others in the lab, I also integrated and reanalysed published scRNA-Seq datasets of NM and T21 fetal BM[36, 45, 388], as described on pages 66-71 in order to investigate the transcriptomic effects of T21 at the single cell level. Reannotation, after integration, of these datasets identified an LMPP cluster and an ELP cluster (Figure 3.26), on which I focussed my analysis.

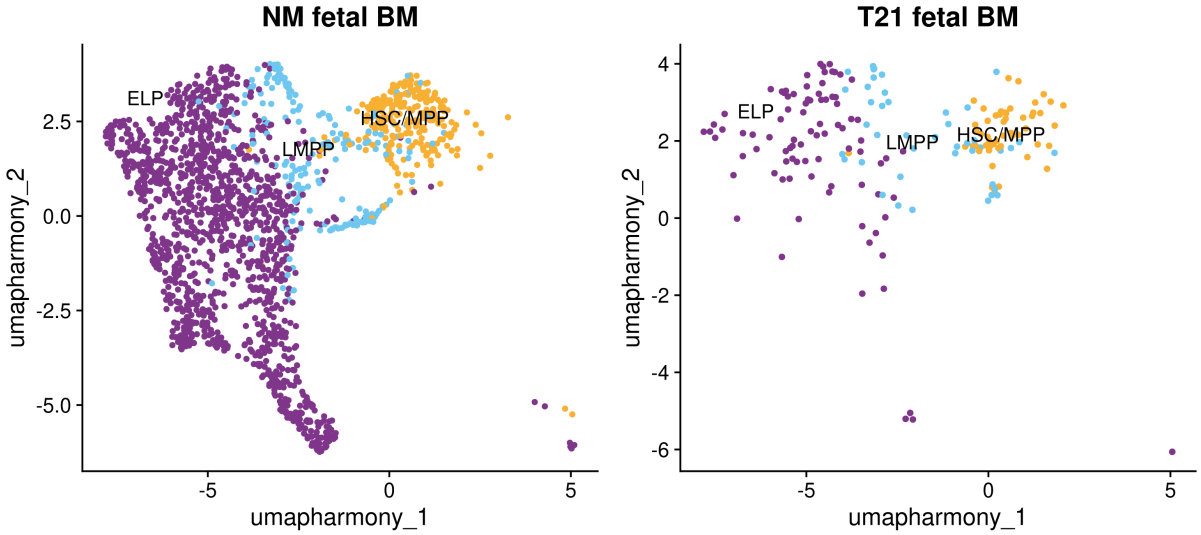

Figure 3.26: HSC, MPP, LMPP and ELP clusters by scRNA-Seq. Recently published scRNA-Seq datasets of NM and T21 fetal BM[36, 45, 388] were integrated and reanalysed, in which HSC/MPP, LMPP and ELP were transcriptomically defined based on published labels from original datasets and marker gene expression[78]. HSC/MPP (NM, k=245, n=15; T21, k=54, n=11), LMPP (NM, k=209, n=16; T21, k=42, n=10), ELP (NM, k=1309, n=15; T21, k=88, n=14).

In order to understand the regulatory mechanisms that may contribute to the impaired lymphoid specification and the failure to activate B lymphoid programmes in T21 fetal BM, I next inferred differential transcription factor activity in T21 LMPP and ELP identified by scRNA-Seq. By integrating the single cell gene expression data with curated transcription factor-target interactions from SJARACNe[530], and comparing these between NM and T21 fetal BM with NetBID2[531], I hoped to identify any key drivers of the impaired B lymphopoiesis in T21 fetal BM.

The granulocyte-monocyte transcription factor C/EBPα, a transcription factor well known for its role in myeloid lineage commitment [580], was inferred to be more active in T21 LMPP, while early lymphoid specification transcription factors IKZF1 and TCF1 were inferred to be less active. SPI1, which plays a role in restricting cell fate to a lympho-myeloid fate[624], also was inferred to be significantly less active. Together, these further support the bulk RNA-Seq findings of impaired B lymphoid specification in T21 fetal BM LMPP (Figure 3.27).

Looking downstream, in T21 ELP, there was a significant increase in inferred activity of the T/NK transcription factors NFIL3, GATA3 and ZBTB16, [625][142][626], together with reduced inferred activity of early B lymphoid transcription factors BCL11A, TCF3, LEF1, and EBF1 (Figure 3.27). This is in line with the results from differential expression analysis for the bulk RNA-Seq dataset, in which *GATA3* expression was increased in T21 fetal BM ELP, while *EBF1* expression was decreased (Figure 3.23).

Together, these provide further evidence that B lymphoid commitment is impaired in T21 fetal BM ELP.

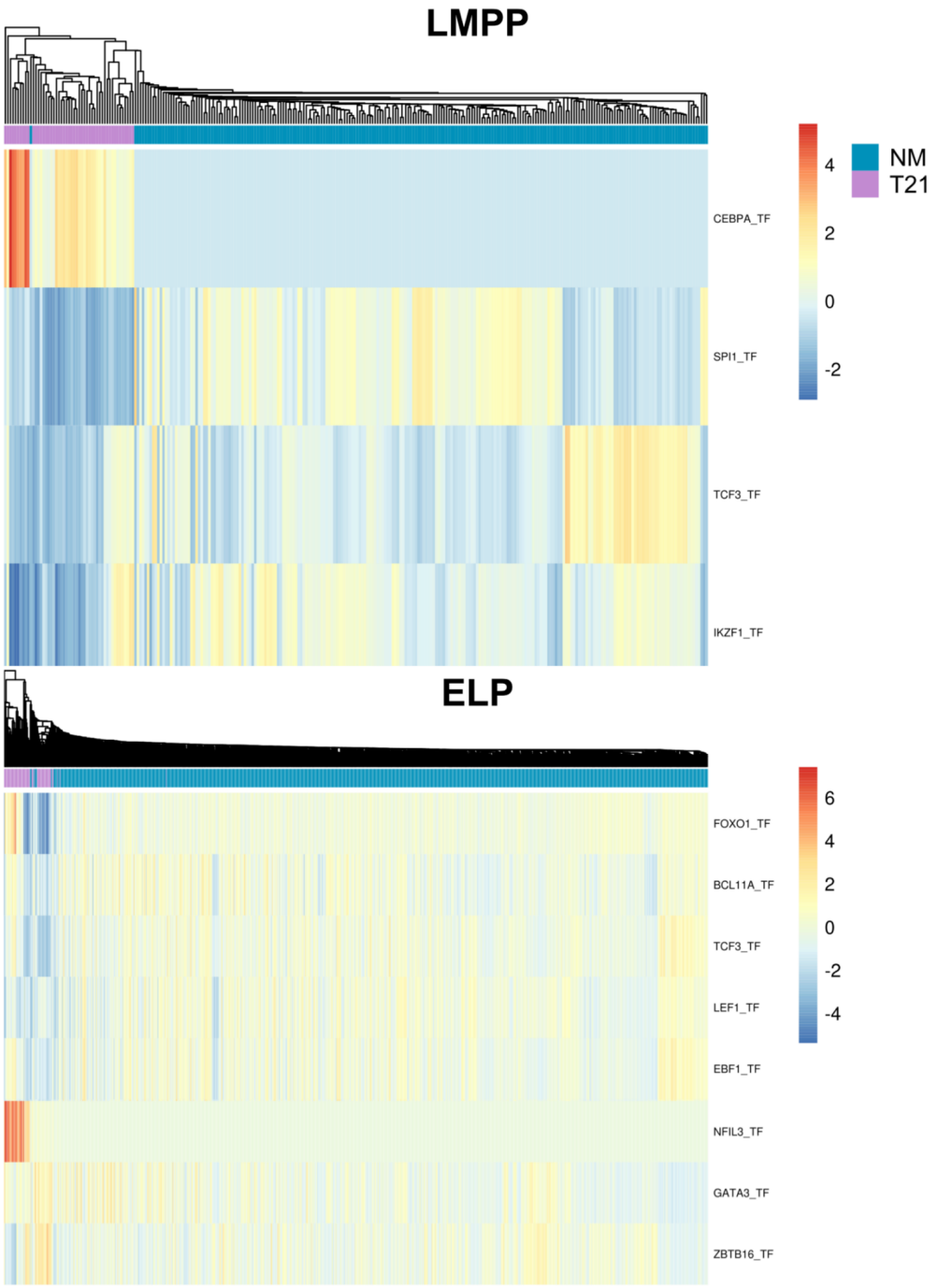

Figure 3.27: Differential inferred transcription factor activity in fetal BM LMPP and ELP. Transcription factor activity was inferred in T21 fetal BM LMPP and ELP identified by scRNA-Seq using SJARACNe. NetBID2 was used to identify differentially active transcription factors between NM and T21 LMPP and ELP (FDR <0.05), of which transcription factors with a known role in B lymphopoiesis, myelopoiesis and T/NK lymphopoiesis were selected. LMPP (NM, k=209, n=16; T21, k=42, n=10), ELP (NM, k=1309, n=15; T21, k=88, n=14).

3.4.8 Inflammatory signalling in T21 fetal BM

While majority of my analysis so far focussed on transcription factors and genes with a known role in haematopoiesis and/or lineage specification, I decided to take a more unbiased approach and carried out GSEA on lymphoid progenitors in NM and T21 fetal BM using MSigDB's Hallmark gene sets, a collection of fifty gene sets across a range of biological processes. Across these, the only significantly enriched gene sets in T21 HSPC were inflammatory response gene sets in T21 fetal BM HSPC (LMPP, PreELP/GMP, ELP, MLP and CLP), of which TNFα signalling via NFκB gene set was consistently significantly enriched in T21 (Figure 3.28).

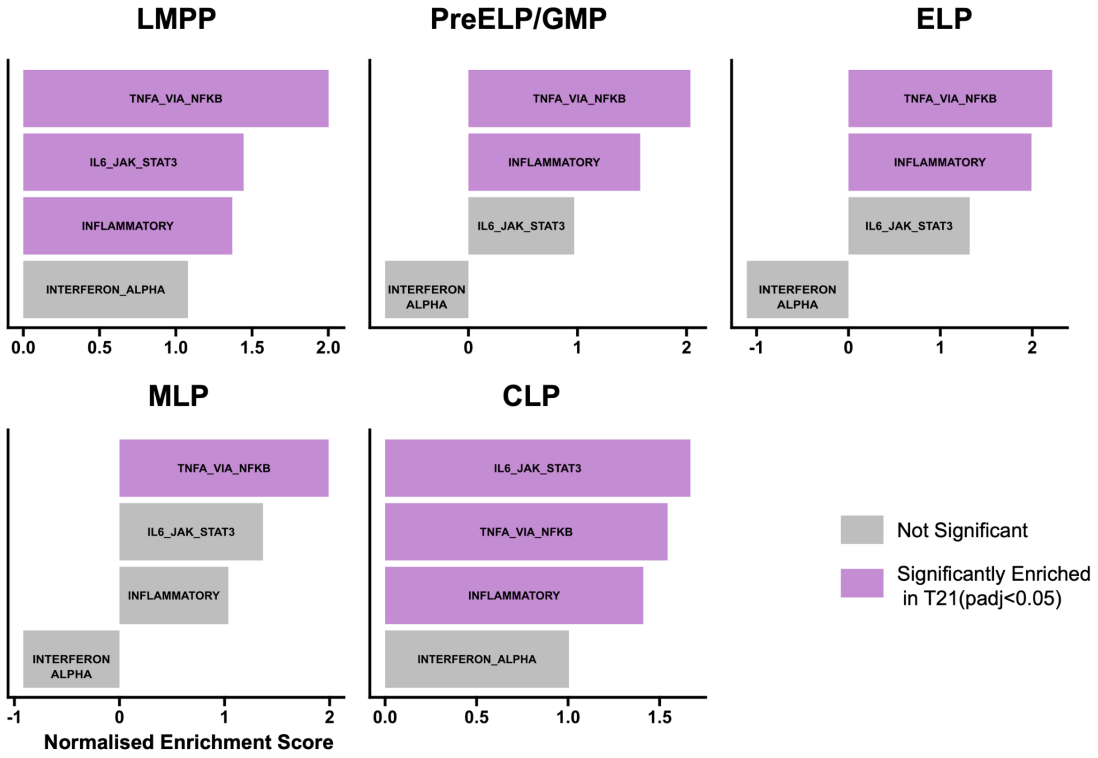

Figure 3.28: Inflammatory response gene sets are enriched in T21 HSPC. GSEA using MSigDB's Hallmark gene sets (p-adj <0.05). NM, normal, n=5-9; T21, trisomy 21, n=3-4.

To further explore this signal at the level of individual genes in these HSPC populations, I next considered the expression patterns of DEG contributing to the TNFα response pathway in T21 fetal BM lymphoid progenitors.

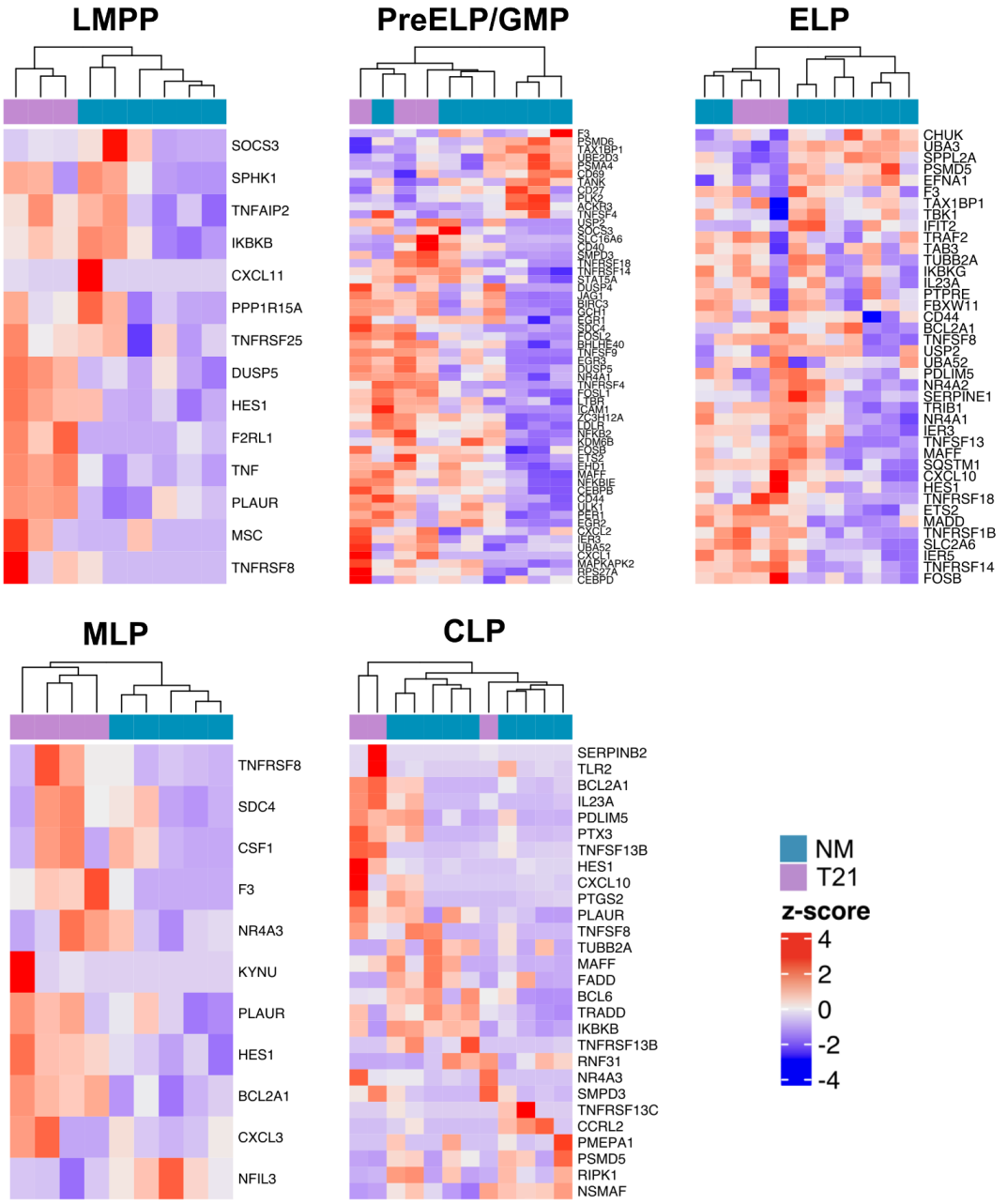

Figure 3.29: T21 lymphoid progenitors have increased expression of genes associated with TNFα signalling. Gene expression was measured by RNA-Seq (50-100 cells). TNFα signalling genes taken from MSigDB's Hallmark TNFα response or MSigDB's TNF signalling gene sets. Significance was determined by pairwise comparisons of NM and T21 HSPC by DESeq2 (p-adj <0.1). NM, normal, n=5-9; T21, trisomy 21, n=3-4.

Heatmaps of these DEG associated with TNFα response gene sets, showed that HSPC from T21 fetal BM showed a consistent upregulation of TNFα response genes in T21 fetal BM (Figure 3.29). I focussed my analysis on LMPP, the population upstream of the block in lymphoid specification in T21. In T21 fetal BM LMPP, there was a significant increase in expression of *TNF* itself, alongside some TNF superfamily receptors, (*TNFRSF25* and *TNFRSF8*, which can activate NFκB[627], the main transcription factor responsible for coordinating an inflammatory response to TNFα signalling[628]; and *IKBKB*, a protein responsible for disinhibiting NFκB[629].

Additionally, overall expression of genes in MSigDB's Hallmark and Reactome TNFα response gene sets was higher in T21 fetal BM LMPP compared to NM fetal BM LMPP (Figure 3.30).

These changes in TNFα signalling genes may be relevant to the lymphopoietic defect in T21 fetal BM HSPC either indirectly or directly. TNFα has been shown to impair B lymphopoiesis indirectly, by suppressing CXCL12 secretion from the BM niche in mice[630]. Additionally, NFκB, when constitutively activated in murine ProB progenitors, causes decreased expression of *Ebf1, Pax5, and Ikaros* transcripts, resulting in an overall decrease in B cells[631].

TNFα has been reported to be increased in other T21 contexts with higher levels of the cytokine in the circulation, both in children [423, 426] and adults [403, 425, 426, 632], as well as increased gene expression in T21 fetal BM [36] and the postnatal thymus[633]. This may point to a wider dysregulation in TNFα signalling in T21, and may be an interesting candidate pathway contributing to impaired B lymphopoiesis in T21.

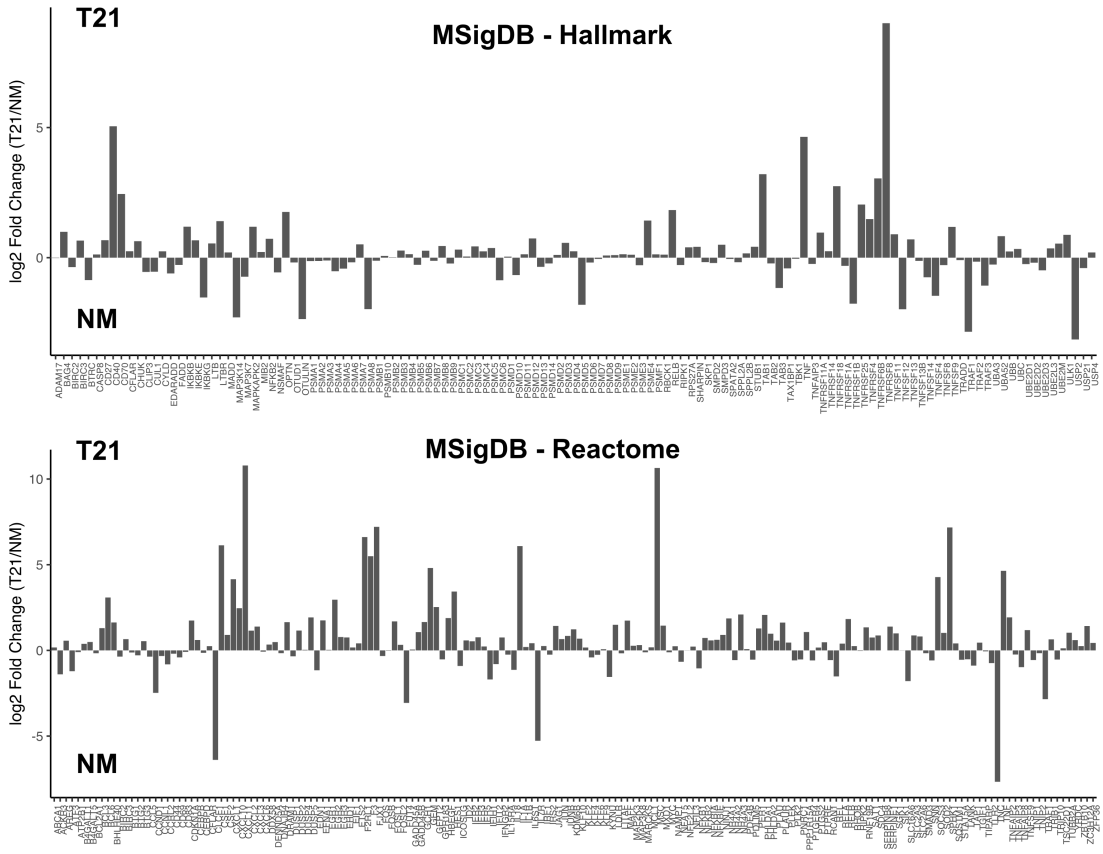

Figure 3.30: Fold change in expression of TNFα response genes in NM and T21 fetal BM LMPP. MSigDB's Hallmark and Reactome TNFα response gene sets were used. A positive fold change is indicative of an increased expression in T21 LMPP by RNA-Seq (50-100 cells), NM n=5; T21 n=3.

3.5 Summary and discussion

This chapter sought to explore whether differences in gene expression and chromatin accessibility could explain perturbed B lymphopoiesis in T21 fetal BM and the potential mechanisms involved. I first compared the frequency of HSPC between NM and T21 fetal BM. This showed a number of very marked differences consistent with previous data from our lab and others[36, 70]. One of the most notable features was a striking reduction in PreELP/GMP, ELP, CLP, PreProB and ProB progenitor frequencies, suggestive of impaired lymphoid commitment at the LMPP stage. In addition, there was an increased frequency of GMP suggesting that T21 LMPP may preferentially differentiate to GMP.

To understand this, I focussed on changes in chromatin and gene expression in T21 fetal BM lymphoid progenitors, especially LMPP. However, surprisingly, there were no striking differences in expression of known B lineage-specific genes in T21 LMPP. However, downstream, in PreELP/GMP and ELP, there appeared to be a severe impairment in switching on the necessary B cell programmes, with T21 PreELP/GMP and ELP showing a marked reduction in expression of key B lymphoid genes *EBF1*, *RAG1* and *RAG2*, and this was reflected by WGCNA, which showed a failure to activate the B lymphopoietic module in T21 PreELP/GMP and ELP. To explore what might cause this, I explored three different possibilities.

First, whether a failure to activate B lymphoid programmes was a result of preferential differentiation of T21 lympho-myeloid and lymphoid progenitors towards alternative fates, such as myeloid, or T/NK lineages, which may suppress the activation of B lymphoid programmes. T21 fetal BM LMPP expressed increased levels of key T lineage transcription factor *TCF7* and T21 fetal BM LMPP in the scRNA-Seq dataset showed a significantly increased inferred activity of C/EBPα, a key myeloid specification transcription factor[634], alongside a significantly decreased inferred activity of lymphoid specification transcription factors PU.1, TCF3 and IKZF1[56].

Downstream, T21 fetal BM PreELP/GMP expressed increased levels of key myeloid specification transcription factor genes, such as *CEBPA*. In T21 fetal BM

ELP, there was an increase in expression of T/NK specification genes, *GATA3*, *TCF7* and *ZBTB16*; and *NFIL3*, a transcription factor with an essential role in NK cell development[635] had a strikingly increased inferred activity in T21 fetal BM ELP in the scRNA-Seq dataset. While it is tempting to speculate the failure to activate B lymphoid programmes is secondary to a failure to silence alternative fates, it is difficult to definitively demonstrate this. I next considered genes encoded on chromosome 21, to link these changes in to T21.

Second, whether changes in expression of genes encoded on chromosome 21 may directly contribute to the failure to activate B lymphoid programmes, or a failure to silence alternative differentiation programmes. Analysis of the ATAC-Seq dataset pointed to a role for *RUNX1*, with chromatin upstream of its locus and its binding motifs across all chromosomes being significantly more accessible. Additionally, differential exon usage analysis provided preliminary evidence for altered *RUNX1* isoform balance in T21 fetal BM HSC, MPP and LMPP, which may be interesting[379, 607], but currently very little is known about how this would affect B lymphopoiesis.

Thirdly, whether inflammatory signalling is increased in T21 fetal BM, given the wider evidence of inflammatory dysregulation in individuals with Down syndrome[36, 403, 420–425]. GSEA following differential expression analysis in T21 lymphoid progenitors identified an enrichment in inflammatory response gene sets, of which TNFα response was consistently elevated across lymphoid progenitors. TNFα expression been previously described to be elevated in T21 fetal BM[36] by scRNA-Seq, this TNFα signalling may bias multilineage T21 fetal BM HSPC haematopoiesis towards myeloid fates at the expense of lymphoid fates by upregulating emergency myelopoietic pathways[344, 636], suppressing B lymphoid gene expression programmes[631], and impairing niche support for B lymphopoiesis[630]. These mechanisms were delineated in murine models and so further experiments would be needed in a fetal BM context to assess the impact of this on B lymphopoiesis.

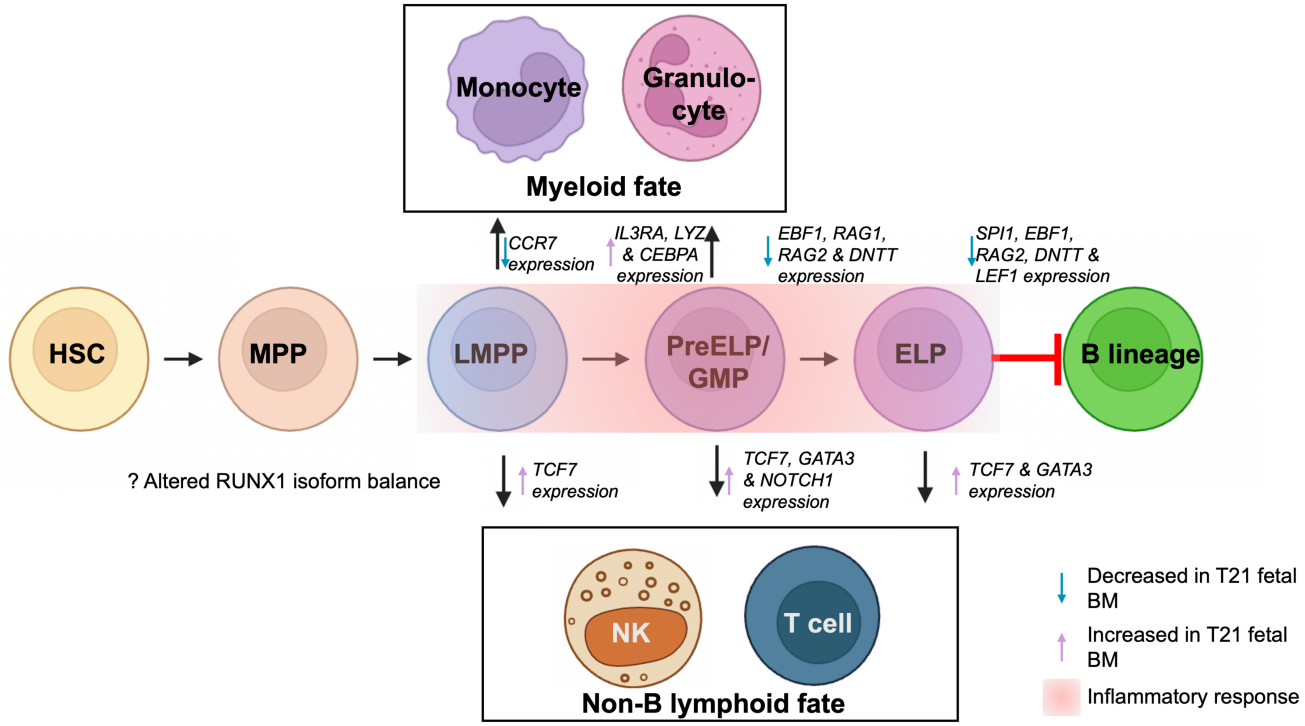

Figure 3.31: Potential mechanisms of impaired B lineage commitment in T21 fetal BM. Significantly decreased expression of B lymphoid commitment genes in lymphoid progenitors, accompanied by significantly increased gene expression of myeloid/T/NK lineage genes may point to a role for a failure to silence alternative lineage fates in impairing B lineage commitment. Additionally, inflammatory signalling in T21 fetal BM lymphoid progenitors may compound this. The contribution of *RUNX1* isoform imbalance, if present, is unclear in T21 HSC, MPP and LMPP.

3.5.1 Future work

Together, these data provided preliminary evidence of a failure to activate B lymphoid programmes in T21 fetal BM compared to NM fetal BM. I hypothesised that this failure to activate B lymphoid programmes occurs secondary to impaired lymphoid commitment in T21 fetal BM LMPP, as suggested by the marked decrease in fetal specific lymphoid progenitors in T21 fetal BM. My data have suggested three main avenues for future work:

1. Disruption of normal B lymphoid gene regulatory networks by failure to silence other non-B lineage affiliated genes. This hypothesis could be tested by assessing whether knockdown of myeloid transcription factors, such as *CEBPA* or T/NK transcription factors *GATA3* or *TCF7* can preferentially rescue B lymphopoiesis in T21 fetal BM lymphoid progenitors.

2. Disruption to the balance of isoform expression of the chromosome 21 gene *RUNX1*. This would need validating by directly quantifying *RUNX1* isoform transcript frequency in T21 fetal BM HSPC, followed by functional testing how an imbalance in *RUNX1* isoform expression may affect B lymphopoiesis.

3. The impact of increased inflammatory signalling, either intrinsic or niche-mediated, on fetal lymphopoiesis in T21 fetal BM. I investigate this further in the following chapters.

4

Results II: Characterising the haematopoietic support provided by T21 fetal BM MSC

4.1 Background and aims

Gene expression analysis of T21 HSPC has implicated inflammatory signalling from the bone marrow (BM) niche as a potential driver of haematopoietic skewing in T21 (Chapter 3). In individuals with Down syndrome, the cells comprising the BM niche also carry a supernumerary copy of chromosome 21; however, the extent to which this alters their ability to support or disrupt haematopoiesis through inflammatory cues is poorly understood.

The BM niche consists of a heterogeneous network of stromal cells, endothelial cells, and haematopoietic-derived elements such as megakaryocytes and macrophages. Within the stromal compartment, mesenchymal stromal cells (MSC) are particularly important. These include MSC subsets, such as LEPR+ MSC and CAR cells that can further differentiate into osteogenic or adipogenic lineages and are well-established as key players in supporting haematopoiesis [637–639]. MSC secrete cytokines such as IL7, SCF, IGF1 and CXCL12 that support HSPC survival and B lymphopoietic commitment[253].

An inflammatory BM niche is a key contributor to haematopoietic dysfunction in a number of diseases. For example, in myelodysplastic syndromes, mouse models have shown that changes in MSC in are sufficient to result in neoplastic disease[640]. Similar inflammatory remodelling of the niche is observed in ageing, where MSC display an inflammatory signature[641], and inflammatory cytokine production from stromal cells can drive a myeloid skew to haematopoiesis[642].

The aim of the experiments presented in this chapter was to investigate whether T21 fetal BM MSC contribute to the haematopoietic abnormalities observed in T21, with a particular focus on their role in contributing to an inflammatory niche for haematopoiesis.

4.2 Haematopoietic support of fetal BM MSC *in vitro*

4.2.1 Optimising an *in vitro* MSC co-culture system

To assess the capacity of MSC to support haematopoiesis, I conducted a pilot experiment co-culturing NM fetal BM CD34+ (n=1) haematopoietic cells on NM (n=1) or T21 (n=1) fetal BM MSC at low passage number (passage 2-6). This showed that while fetal BM MSC were able to maintain and differentiate CD34+ HSPC in the absence of additional cytokines (Figure 4.1B), the majority of the cells were Lin+ (largely myeloid) (data not shown), making it difficult to assess the effect on B cell and NK cell lymphopoietic support without further optimisation.

In the native BM, a number of cell types other than MSC secrete cytokines necessary for lymphopoiesis[253] (Table 4.2) and to better characterise haematopoietic support by fetal BM microenvironment, this co-culture system required optimisation.

Historically, differentiating B cells *in vitro* has been reported to be difficult[643–646], given the number of stage-specific microenvironmental cues required for B lymphopoiesis[253]. I used these early reports to guide the development of an optimised fetal BM MSC co-culture system, as summarised in Table 4.1.

HSPC Source	**Stromal Cell**	**Added Cytokines**	**Citation**
Cord Blood CD34+	Human BM MSC	SCF(10 ng/mL), FLT3L(5 ng/mL)	[646]
Cord Blood CD34+	Human BM MSC	IL3(1ng/mL), FLT3L(1-50ng/mL), IL7(5ng/mL), SCF(25ng/mL)	[98]
Mouse LSK (Lin-Sca-1+c-Kit+)	Mouse BM MSC	SCF, FLT3L, IL7	[647]
B cells	Human BM MSC	IL4	[648]
PreB cells	Mouse BM MSC	IL7(0.5ng/mL)	[649]
Human ProB	AFT024 (murine FL stroma)	Initially FLT3L, SCF, IL7, IGF1, IL2 IL3 Then IL4, IL5, IL6 and IL10	[650]
Sorted BM CD34+CD38-Lin-	AFT024	IL2 (100U/mL), FLT3L (10ng/mL), SCF (20ng/mL), IL7 (20ng/mL), IL3 (5ng/mL)	[651]
Cord Blood CD34+	S17 (murine BM stromal cell line)	IL4(100ng/mL), IL10 (100ng/mL)	[652]
Cord Blood CD34+	S17	IL7 (5-50ng/mL), SCF (10-100 ng/mL)	[653]
Sorted FL HSC	OP9 (murine BM stromal cell line)	IL7 (50ng/mL) or TSLP (50ng/mL)	[132]
Mouse LSK	OP9	IL7 (2ng/mL), SCF(5ng/mL), FLT3L(5ng/mL)	[654]
Cord Blood CD34+	MS5 (murine BM stromal cell line)	SCF (10ng/mL), G-CSF (10ng/mL)	[655]
FAC-sorted fetal BM lymphoid progenitors	MS5	IL2(10ng/mL), FLT3L(10ng/mL), SCF(20ng/mL), IL7(5ng/mL)	[20]
Cord Blood CD34+	MS5, OP9	IL3(10ngl/mL), IL7(20ng/mL), FLT3L(50ng/mL), SCF(50ng/mL)	[656]

Table 4.1: Summary of published stromal co-culture systems

Cytokine	**Source in BM**	**Role in lymphopoiesis**	**Citation**
IL7	MSC, osteoMSC, osteoblasts	B lineage specification and commitment, B progenitor survival and proliferation, B cell maturation	Human:[98, 657]; Murine:[658, 659]
FLT3L	MSC, endothelial cells, NK cells, T cells	Lymphoid specification and commitment	Human:[320, 660]; Murine:[128, 321, 535]
SCF	Endothelial cells, MSC	HSC survival and expansion	Human:[661–663]; Murine:[664]
IL2	T cells	T lymphopoiesis, NK lymphopoiesis, proliferation and activation, B cell maturation	Human:[665, 666]; Murine:[667]

Table 4.2: Cytokines used to supplement MSC co-cultures of fetal BM HSPC and their role in lymphopoiesis.

SCF, IL7 and FLT3L are often added to MSC co-cultures to improve B lymphoid output, and I used this as a starting point for optimising my own co-culture system. I also added IL2, to allow support for NK lymphopoiesis by fetal BM MSC to be evaluated. I have summarised the roles of these lymphopoietic cytokines in Table 4.2.

Supplementation of lymphopoietic cytokines at standard concentrations to the co-culture system improved output of CD45+ cells over the course of the experiment (Figure 4.1B). However, the output of MSC co-cultures remained largely myeloid, with little B or NK lymphoid output (Figure 4.1C). Though very few B cells were produced in this system, there was a reduction in total B cells produced when NM fetal BM CD34 cells were grown on T21 fetal BM MSC, although not reaching statistical significance (Figure 4.1D).

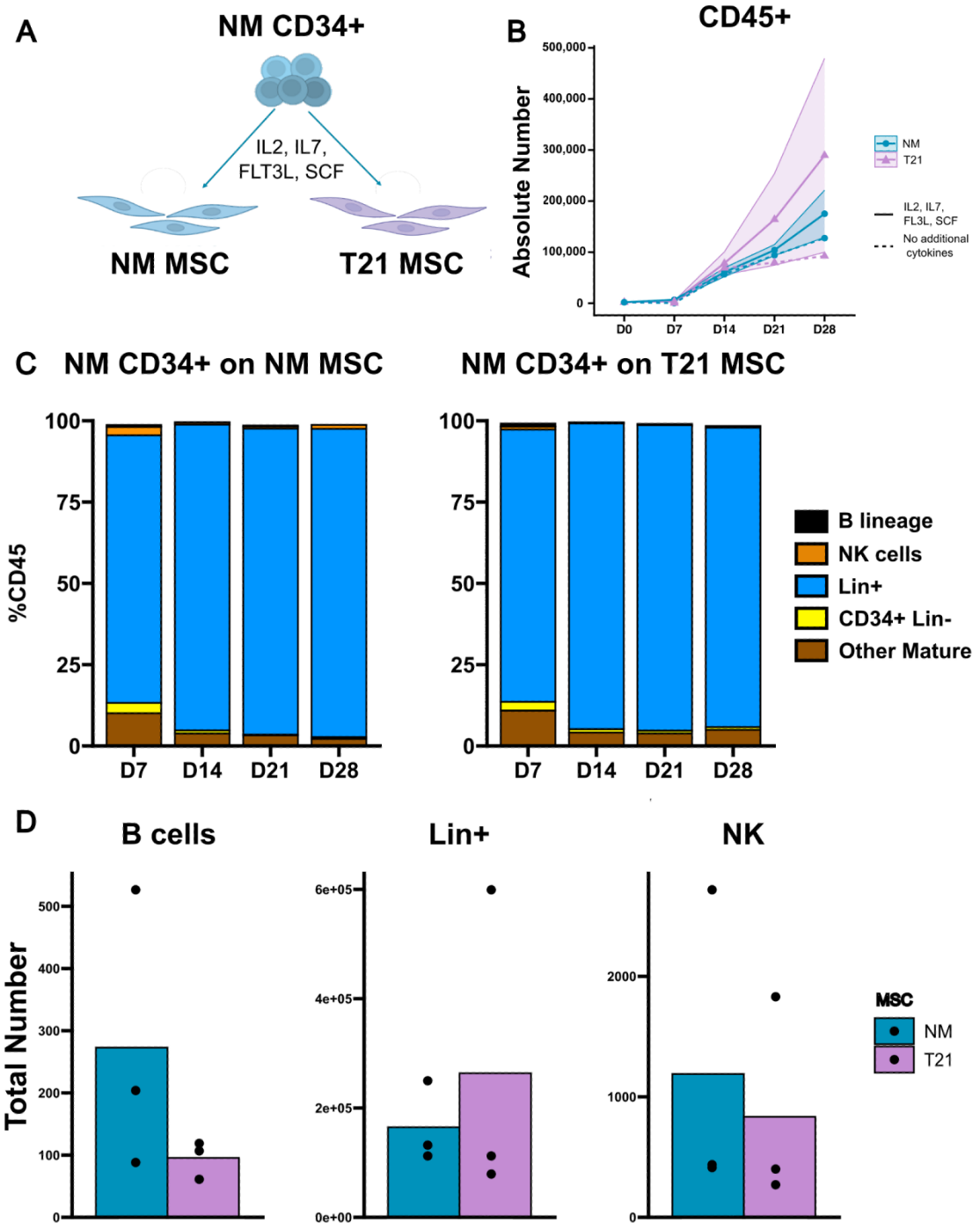

Figure 4.1: Fetal BM MSC co-cultures support a mostly myeloid cell output. (A) 2000 bead-selected NM fetal BM CD34+ cells (n=1) were co-cultured on NM (n=3) or T21 (n=3) fetal BM MSC, supplemented with IL2 (10ng/ml), IL7 (5ng/ml), FLT3L (10ng/ml) and SCF (20ng/ml). Output of HSPC as (B) absolute number of CD45+ cells (mean ± SEM), with added IL2, IL7, FLT3L and SCF (full lines), or without any added cytokines (dashed lines). (C) Proportional cellular output of all CD45+ cells from the same NM fetal BM HSPC sample cultured on NM or T21 fetal BM MSC with added IL2, IL7, FLT3L and SCF by immunophenotype; and (D) total number of B cells (left), Lin+ cells (middle) and NK cells (right) produced by the same NM fetal BM HSPC sample cultured on NM (blue bars) or T21 (lilac bars) fetal BM MSC over the 4-week course of this experiment. NM: normal; T21 Trisomy 21; D: day. Lin: CD3/11b/14/33.

I next considered the concentration of cytokines used in this system, testing different concentrations of the aforementioned cytokine cocktail to optimise the system (Figure 4.2). Additionally, I tested the ability of SFEMII medium supplemented with FBS, and 5ng/ml of IL3 and IL7 to support B lymphopoiesis - this medium is routinely used in our research group to sustain B lymphoid blasts *in vitro*. I also used MS5, a murine BM stromal cell line[504] that is regularly used to support B lymphopoiesis *in vitro*[20, 645, 656].

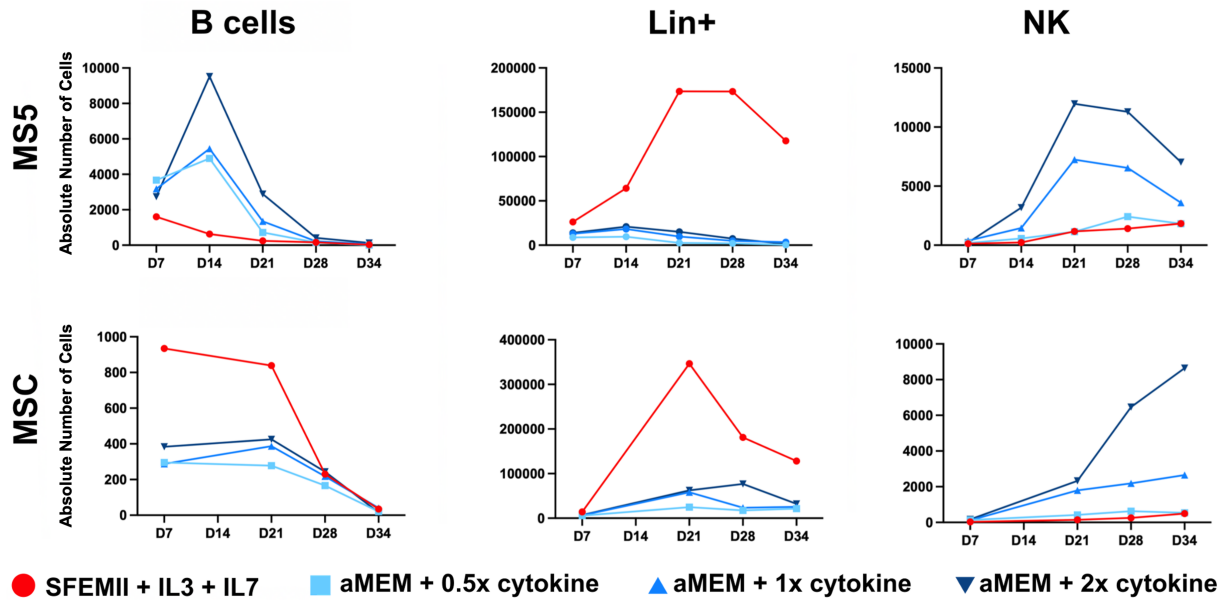

Figure 4.2: Optimisation of the MSC co-culture system. Bead-selected NM fetal BM CD34+ cells (n=1) were co-cultured on MS5 stromal cells or NM fetal BM MSC (n=1) with different cytokine "cocktail" conditions. IL3 was used at a concentration of 5ng/ml. 1x cytokine cocktail includes IL2 (10ng/ml), IL7 (5ng/ml), FLT3L (10ng/ml) and SCF (20ng/ml). MS5 murine BM stromal cells were used as a positive control (top panels). D: day. Lin: CD3/11b/14/33.

Interestingly, NM fetal BM CD34+ cells co-cultured on MSC in SFEMII supplemented with FBS, IL3 and IL7 produced the greatest number of B cells (Figure 4.2). To understand whether this was due to a different base medium, as SFEMII contains human insulin and transferrin, unlike αMEM, I tested different combinations of cytokines in SFEMII (Figure 4.3). Compared to αMEM, output from co-cultures grown in SFEMII produced many more B cells and B progenitors, and Lin+ cells, at the expense of NK cells. The cytokine condition IL2, IL7 and

FLT3L, with or without SCF performed best at supporting B lymphopoiesis, and co-cultures supplemented with SCF produced more Lin+ cells overall.

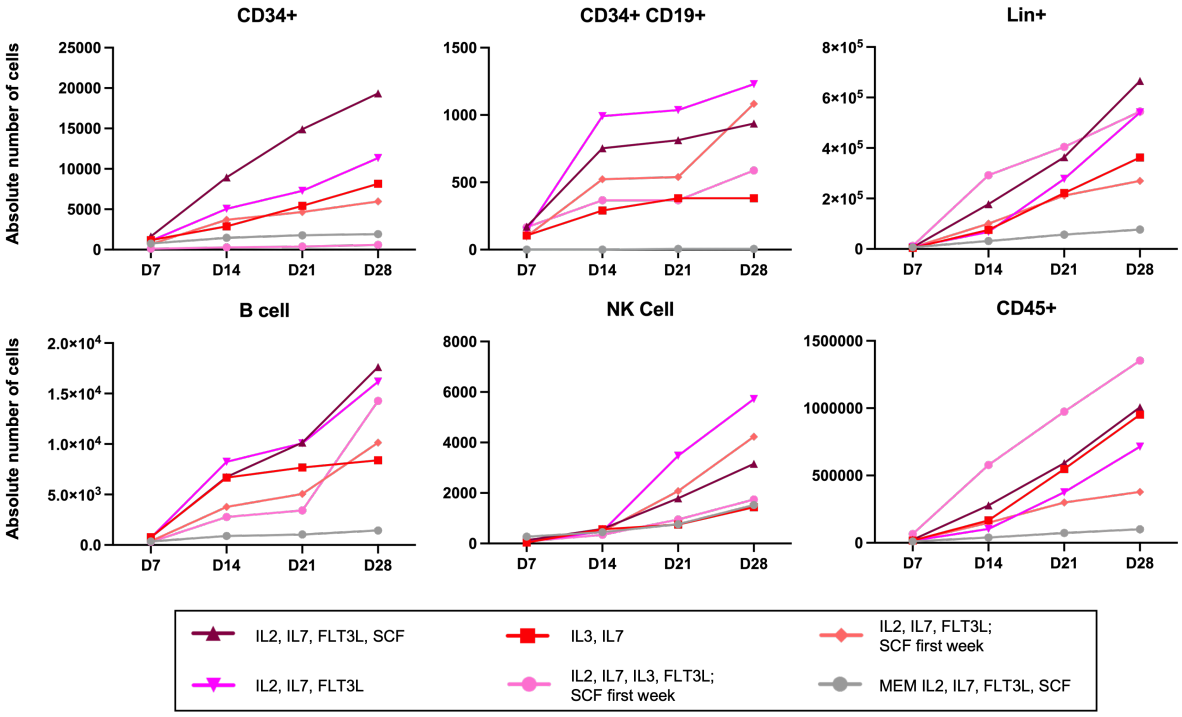

Figure 4.3: Optimisation of the MSC co-culture cytokines. Bead-selected CD34+ cells (n=1) were cultured on fetal BM MSC in SFEMII media with different cytokine combinations. Cytokines were used at the following concentrations: IL2 (10ng/ml), IL3 (5ng/ml), IL7 (5ng/ml), FLT3L (10ng/ml) and SCF (20ng/ml). D: day. Lin: CD3/11b/14/33.

To test which conditions were optimal for supporting B lymphopoiesis from HSC, MPP and LMPP, the populations upstream of the block in lymphoid development in T21 fetal BM, I co-cultured 100 FAC-sorted HSC, MPP and LMPP on NM fetal BM MSC supplemented with IL2, IL7 and FLT3L, with or without additional SCF (Figure 4.4). I decided to test SCF in the co-culture system because of its well-recognised role in HSC survival and expansion *in vitro*[297, 668]. Consistent with this, for HSC, MPP and LMPP, the addition of SCF improved B cell output (albeit for a single experiment) (Figure 4.4), perhaps by supporting HSPC survival long enough to permit NK or B cell differentiation.

Taken together, the results from this series of optimisation experiments suggested that using SFEMII as a base medium, supplemented with FBS, IL2 (10ng/ml), IL7

(5ng/ml), FLT3L (10ng/ml) and SCF (20ng/ml) was optimal for the support of B lymphopoiesis in *in vitro* MSC co-culture assays. These conditions were used in subsequent experiments in this chapter.

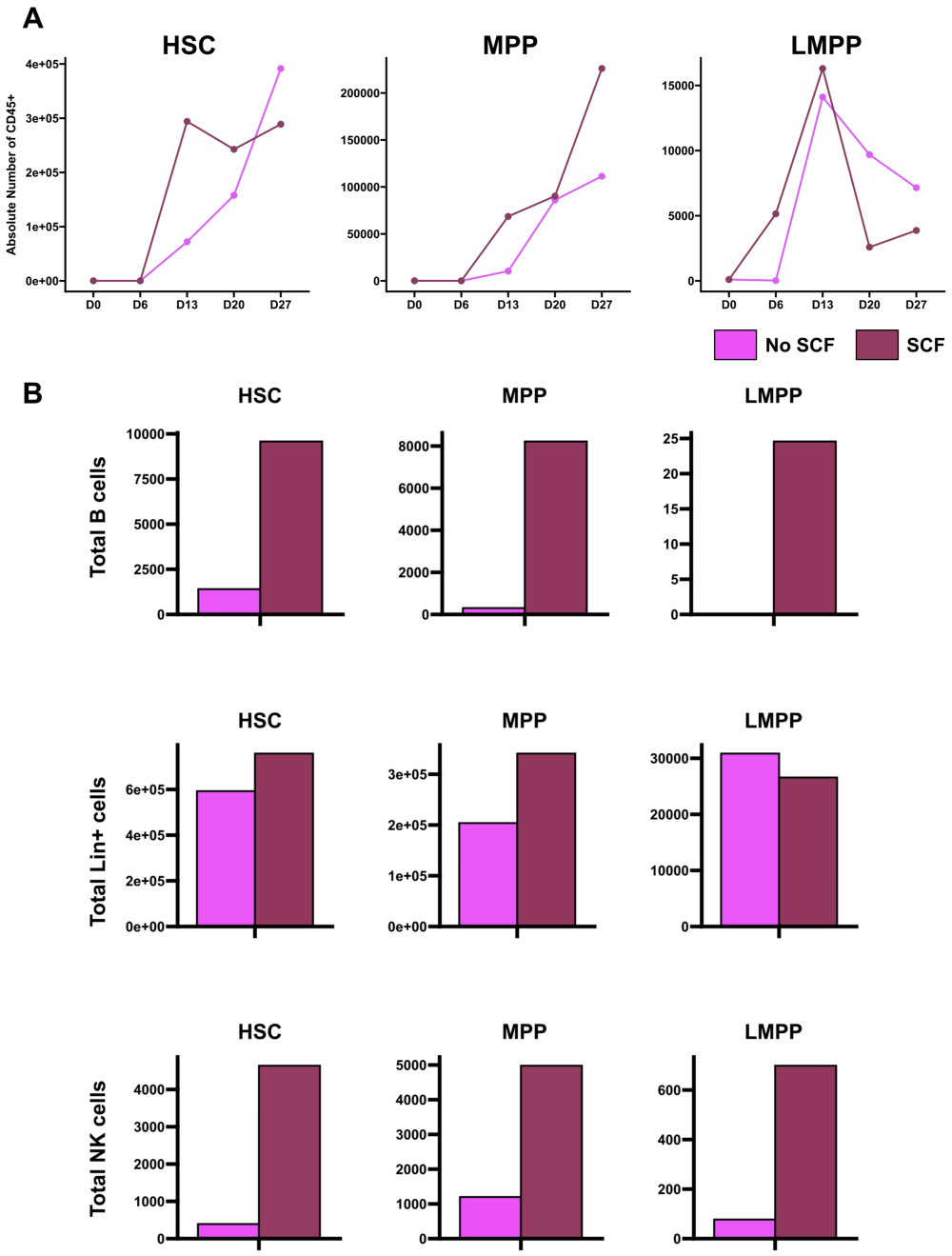

Figure 4.4: Supplementation of MSC co-cultures with SCF improves B cell output from HSC, MPP and LMPP. FAC-sorted HSC, MPP and LMPP from NM fetal BM (n=1) were co-cultured with fetal BM MSC with IL2 (10ng/ml), IL7 (5ng/ml), FLT3L (10ng/ml), and either with or without SCF (20ng/ml). (A) Absolute values of CD45+ (B) total B/ NK/ Lin+ cells produced over the experiment. D: day. Lin: CD3/11b/14/33.

4.2.2 The impact of T21 fetal BM MSC on normal B lymphopoiesis

Having optimised the MSC co-culture assay to support B lymphopoiesis, I compared the support of B lymphopoiesis between NM and T21 fetal BM MSC. Though my initial experiments used bead-selected CD34+ cells, a large proportion of NM fetal BM CD34+ is comprised of B lineage committed progenitors[20], which may mask any differences in B lymphoid differentiation from the most upstream progenitors. Therefore, I sorted NM fetal BM HSC, MPP and LMPP for co-culture experiments, as these progenitor populations lie upstream of the block in B lymphopoiesis in T21 fetal BM (Chapter 3), and assessed their differentiation on NM or T21 fetal BM MSC.

While there were no differences in overall CD45+ numbers from NM HSC, MPP or LMPP when co-cultured on NM or T21 fetal BM MSC (Figure 4.5B), as a proportion of total CD45+ cells, T21 fetal BM MSC supported NK cell output preferentially (Figure 4.5C). There was also decreased B lymphoid output from NM HSC/MPP/LMPP when co-cultured with T21 fetal BM MSC (Figure 4.6), although this did not reach statistical significance, perhaps due to the variability between MSC samples. However, this, alongside the lower B lymphoid output from NM fetal BM CD34+ cells on T21 fetal BM MSC (Figure 4.1) suggests that T21 fetal BM MSC may contribute to the T21 defect in B lymphopoiesis. To understand the molecular mechanisms that may drive these functional differences, I performed RNA-Seq on MSC derived from NM and T21 fetal BM.

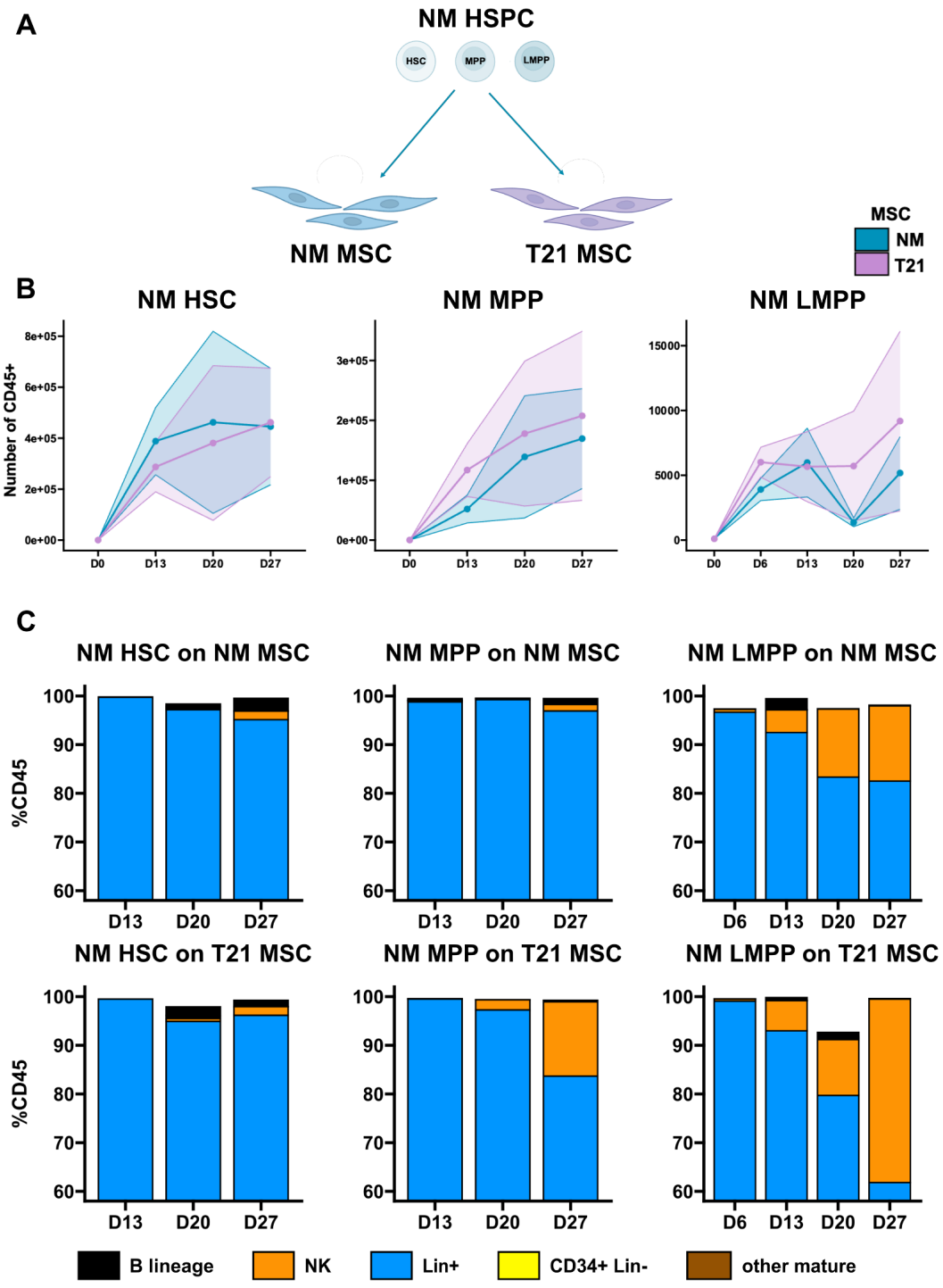

Figure 4.5: Haematopoietic cell output of NM fetal BM HSC, MPP and LMPP on NM and T21 fetal BM MSC. (A) 100 FAC-sorted NM fetal BM HSC, MPP and LMPP from 4 donors were co-cultured with NM (n=3-4) or T21 (n=3-5) fetal BM MSC over 28 days under optimised co-culture conditions. (B) Fetal BM MSC support expansion of the HSC, MPP and LMPP. Data is presented as mean absolute CD45+ (line) ± SEM (shaded area). (C) The relative output of HSPC when cultured on NM or T21 fetal BM MSC, as a percentage of CD45+ cells. NM: normal; T21 Trisomy 21; D: day; Lin: CD3/11b/14/33.

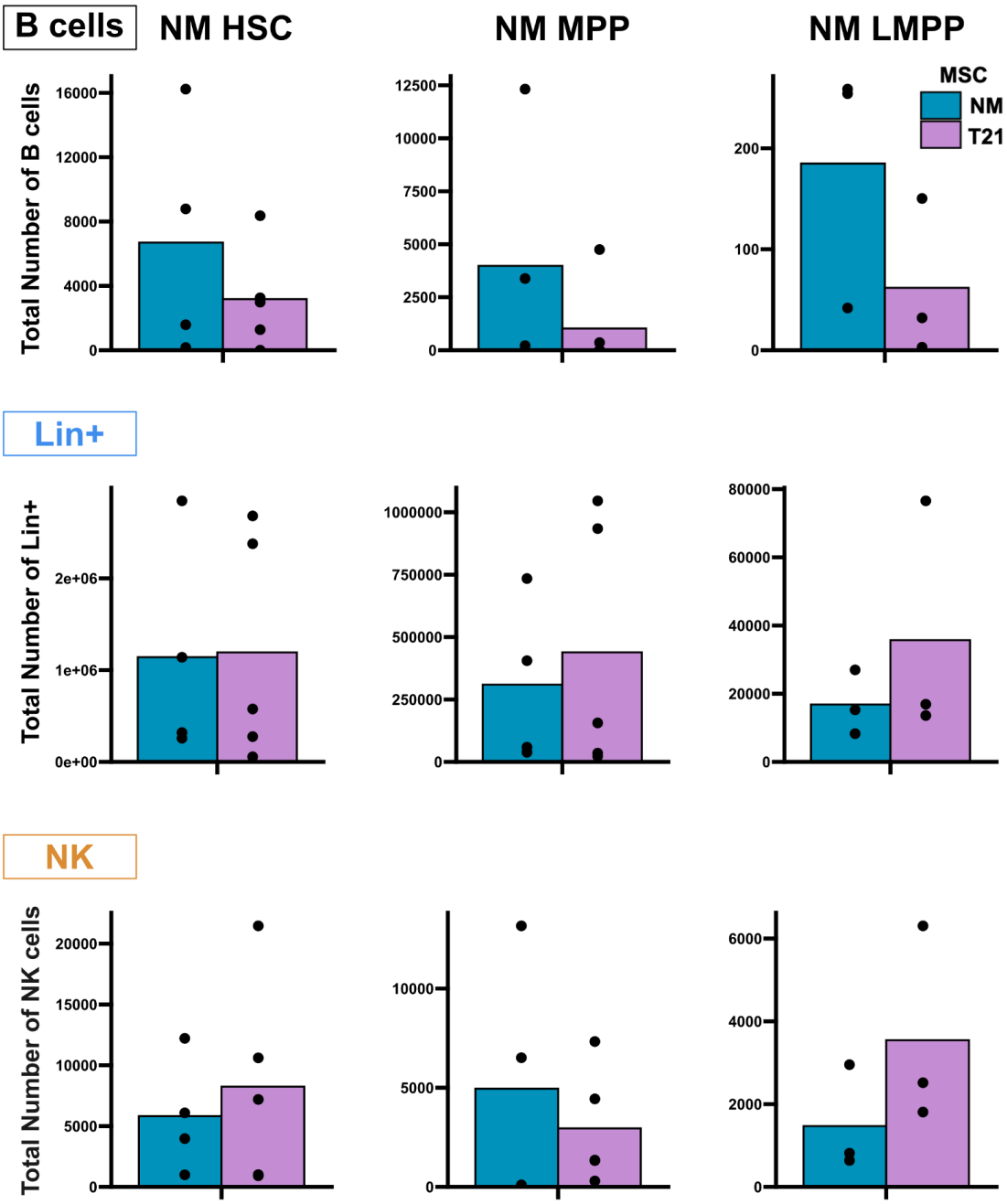

Figure 4.6: Absolute numbers of B cells, Lin+ myeloid cells and NK cells produced by NM fetal BM HSC, MPP and LMPP co-cultured with either NM or T21 fetal BM MSC. Cumulative output when 100 NM fetal BM HSC, MPP and LMPP from 4 donors were co-cultured with NM (n=3-4) or T21 (n=3-5) fetal BM MSC. Each dot represents one biological MSC sample. NM: normal; T21 Trisomy 21; Lin: CD3/11b/14/33.

4.2.3 Molecular profiling of NM and T21 fetal BM MSC

RNA from 500,000 MSC at low passage number (2-9) derived from NM and T21 fetal BM was extracted and used to prepare libraries which were sequenced to characterise molecular differences between T21 and NM fetal BM MSC.

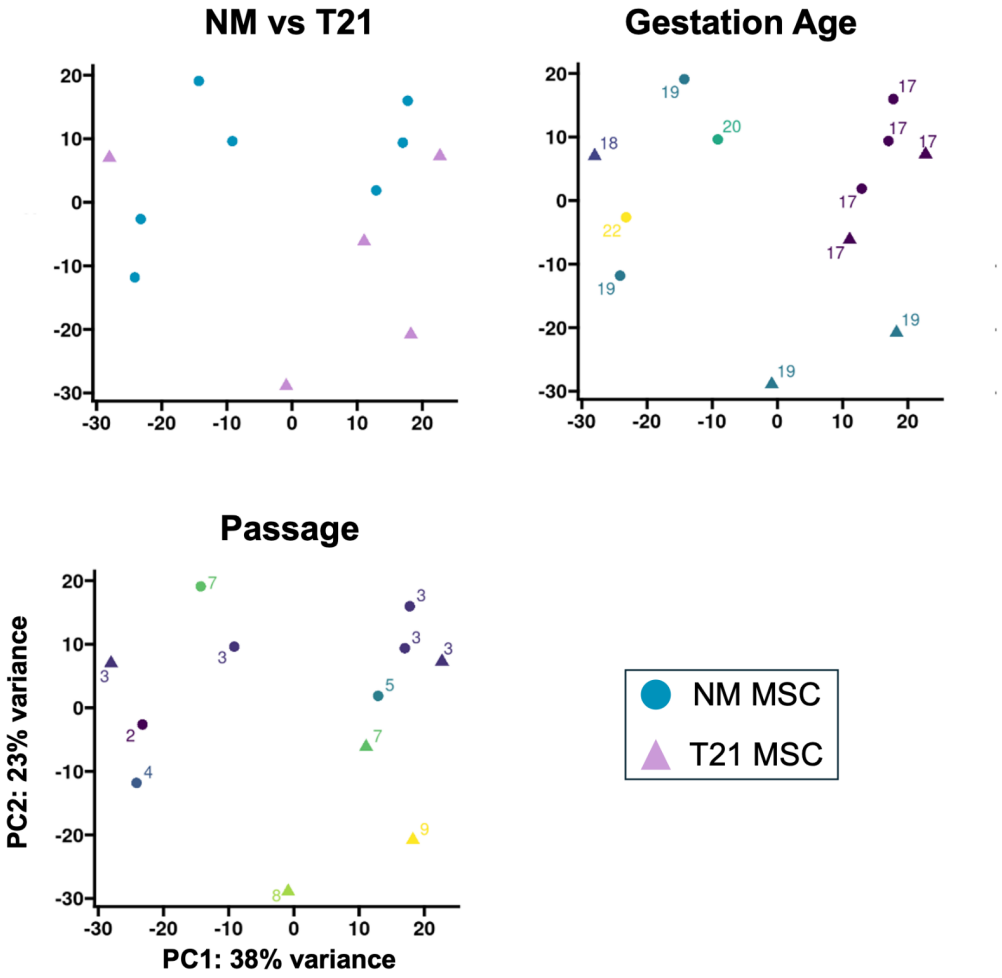

Figure 4.7: PCA of the top 500 most variably expressed genes in derived fetal BM MSC. NM fetal BM MSC are represented as circles (n=7) and T21 fetal BM MSC (n=5) as triangles, colour of dots reflects title of graph. NM: normal; T21 Trisomy 21.

PCA of the top 500 most variably expressed genes showed a modest separation by T21 in PC1 (Figure 4.7). Differential gene expression analysis between NM and T21 fetal BM MSC by DESeq2 identified 95 differentially expressed genes (p-adj <0.1), almost half of which (42/95; 44%) were on chromosome 21 indicating the strong effect of T21 on the transcriptome of these cells (Figure 4.8) (Appendix

Table 20, page 237). Triplication of genes on chromosome 21 appeared to have a much greater effect on gene expression of chromosome 21 genes in T21 fetal BM MSC compared to HSPC (Figure 3.17), which was also found by scRNA-Seq of T21 fetal BM[36] - perhaps as gene dosage may need to be more tightly controlled in HSPC compared to MSC.

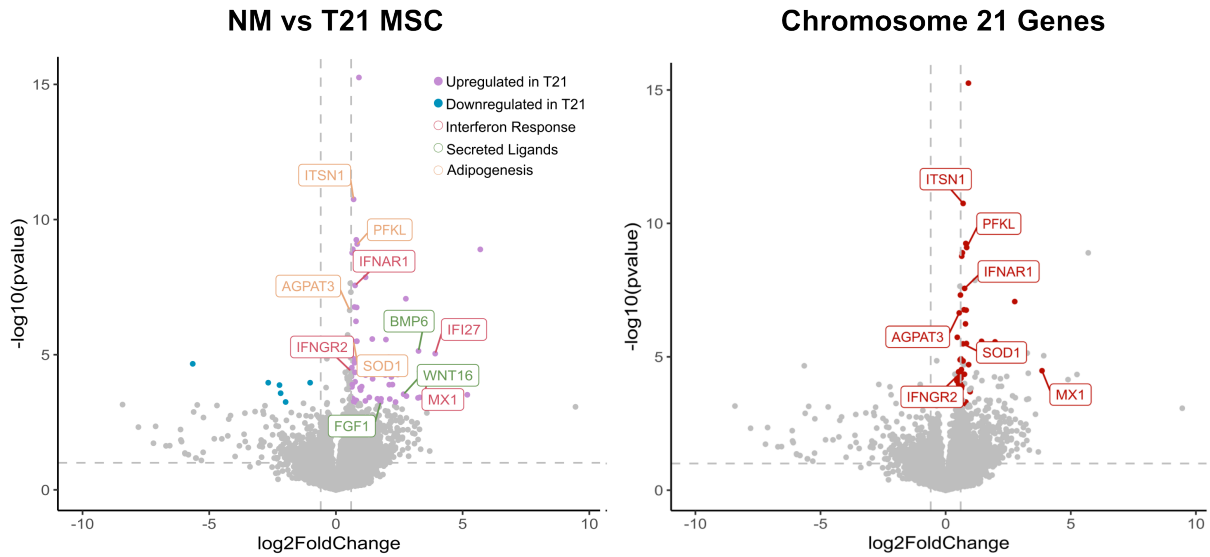

Figure 4.8: The impact of T21 on fetal BM MSC gene expression. (A) Differential expression analysis with DESeq2 finds 95 differentially expressed genes (p-adj <0.1), (B) of which 42 are on chromosome 21 (red). NM: normal; T21 Trisomy 21.

The fold change increase in most of the chromosome 21 genes was around 1.5 times higher, as would be predicted by the presence of one additional copy of chromosome 21. Among these genes, T21 fetal BM MSC overexpressed genes involved in the interferon response *IFNAR1*, *IFNGR2*, *MX1* and *IFI27*; all of which, except *IFI27*, are on chromosome 21. Additionally, there was a significant enrichment by GSEA for IFNα, IFNγ and TNFα responses in T21 fetal BM MSC compared to their normal counterparts (Figure 4.9). Interestingly, though cultured T21 fetal BM MSC upregulated inflammatory response genes compared to their normal counterparts, when their supernatants were tested by a Luminex cytokine assay, there was no detectable expression of IFNα, IFNγ or TNFα (data not shown).

Additionally, genes part of the MSigDB Hallmark Adipogenesis gene set were significantly upregulated in T21 fetal BM MSC compared to NM fetal BM MSC

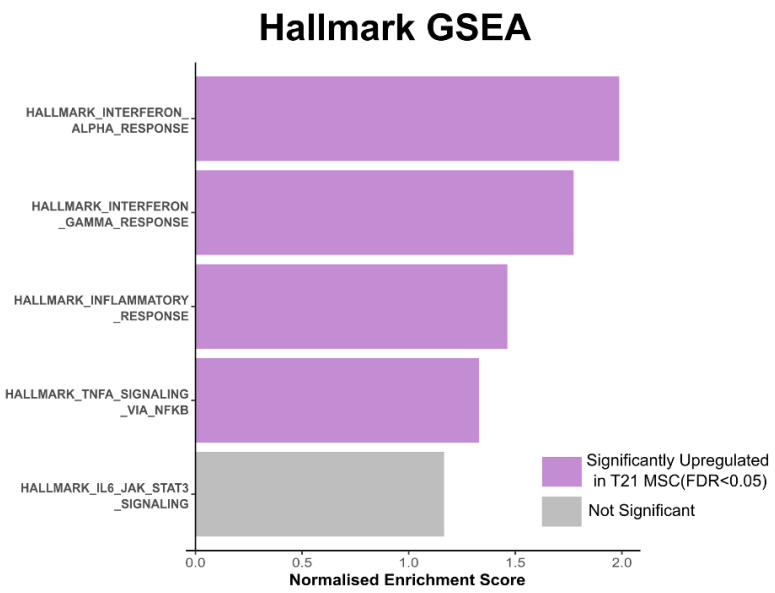

Figure 4.9: T21 fetal BM MSC show a significant enrichment for inflammatory response gene sets by GSEA. FDR = 0.05. T21 fetal BM MSC (n=5), NM fetal BM MSC (n=5).

(Figure 4.8), all of which were encoded on chromosome 21. Selective differentiation of MSC to one lineage has been reported to occur at the expense of other lineages, with osteogenic differentiation inhibiting adipogenic differentiation, and vice versa, as reviewed in [669]. Together, these raise the possibility of an altered balance of osteoblastic versus adipogenic differentiation in T21 fetal BM MSC. Given the role of osteolineage cells in supporting early lymphoid progenitors [248, 252, 253], a decrease in BM osteolineage cells in T21 fetal BM might contribute to impaired B lymphopoiesis in T21, and I will explore this further in the following chapter.

To better understand how T21 fetal BM MSC might provide impaired B lymphopoietic support, I interrogated all the differentially expressed genes (Figure 4.8) with the CellChat database[529]. T21 fetal BM MSC significantly overexpressed genes encoding three secreted proteins compared to NM fetal BM MSC: *BMP6*, *WNT16* and *FGF1*. FGF1 and WNT16 have been reported to negatively regulate osteoblastic differentiation by acting on the BMP family members BMP2 and BMP4 [670–672]. The BMP family play a key role in osteoblast differentiation [673], with BMP2 and BMP4 being well characterised as potently osteogenic [674]. Though less

well studied, BMP6 is reported to promote bone formation, with the administration of BMP6 to ovariectomised rats improving bone volume and structure[675], though the importance of BMP6 alone is unclear, as *Bmp6*-/- mice have no major defects in bone formation, except for delayed ossification of the sternum during fetal life[676], suggesting other BMPs may compensate. BMP6 has also been reported to impair B lymphopoiesis *in vitro*[677]. However, the concentration of BMP6 used in this study (62.5–1000ng/mL) markedly exceeds the concentration that I detected (0-362pg/ml) in culture supernatants by ELISA *in vitro* (discussed later). Further experiments would be required to assess whether increased BMP6 contributes to impaired B lymphopoiesis in T21 fetal BM.

As analysis of the RNA-Seq data showed increased *JAG1* gene expression, albeit not significantly, (p-adj value just above significance cut-off of <0.1 at 0.11) (Figure 4.10), I decided to explore this further as JAG1 has been reported to play a role in preferentially promoting NK lymphopoiesis at the expense of B lymphopoiesis *in vitro*[544], consistent with the observations in our functional assays (Figure 4.5). Notch signalling plays a key role in directing early lymphoid fate towards NK/T lineages at the expense of the B lineage[545, 547], and JAG1 alone is sufficient to inhibit B lymphopoiesis [544]. Additionally, TNFα signalling has been reported to upregulate *JAG1* expression[678, 679], and my data has shown that the TNFα response was significantly upregulated in T21 fetal BM MSC (Figure 4.9).

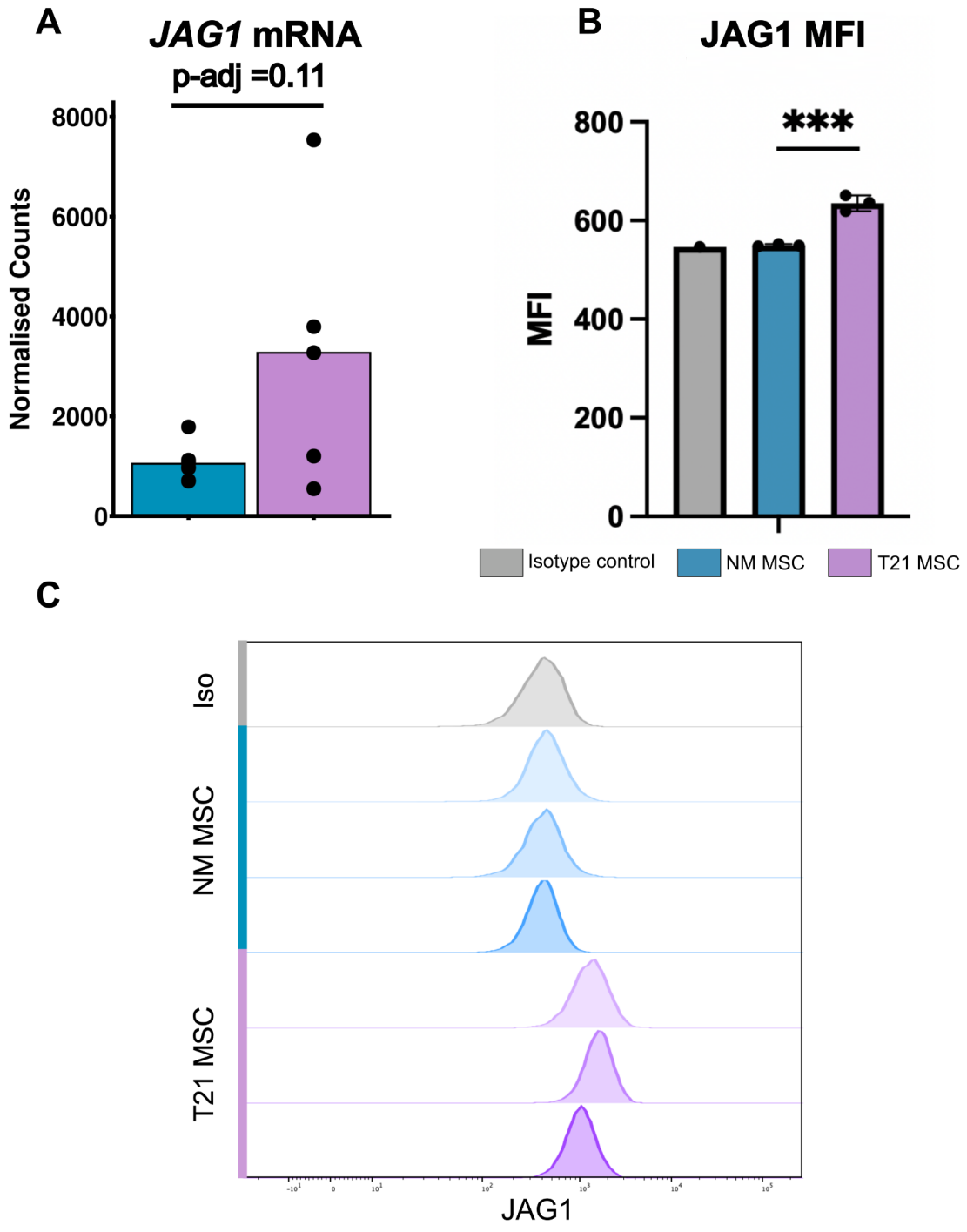

Figure 4.10: T21 fetal BM MSC overexpress the Notch ligand JAG1. (A) *JAG1* mRNA, measured by RNA-Seq of NM (n=7) T21 (n=5) fetal BM MSC and (B) on the cell surface, measured by flow cytometry as unscaled, compensated mean MFI per sample. (C) A histogram of JAG1 MFI. T21 fetal BM MSC (n=3), NM fetal BM MSC (n=3). Iso, isotype control. NM: normal; T21 Trisomy 21. T-test, *** p-adj <0.001.

Differences in protein expression in T21 fetal BM MSC

I next interrogated the differences in expression of key cytokines/secreted proteins in NM vs. T21 fetal BM MSC using flow cytometry, Luminex assays and ELISA.

To confirm the significance of the increased expression of *JAG1* gene in T21 fetal BM MSC, I also assessed protein expression of JAG1 on NM and T21 fetal BM MSC by flow cytometry. T21 fetal BM MSC appeared to have an increased expression of the Notch ligand JAG1 when measured by flow cytometry (Figure 4.10B, C), which may contribute to the skew in output towards the NK lineage when NM fetal BM HSPC are cultured on these MSC compared to NM fetal BM MSC.

Supernatants of cultured NM and T21 fetal BM MSC were collected after 48 hours and tested for cytokine concentrations by a custom Luminex assay for 22 cytokines (detailed in Table 2.4, page 58), or by ELISA for BMP6. MSC derived from NM and T21 fetal BM did not secrete detectable levels of TNFα, IFNα or IFNγ (data not shown), although, the significance of this is unclear, as these assays were conducted without positive controls.

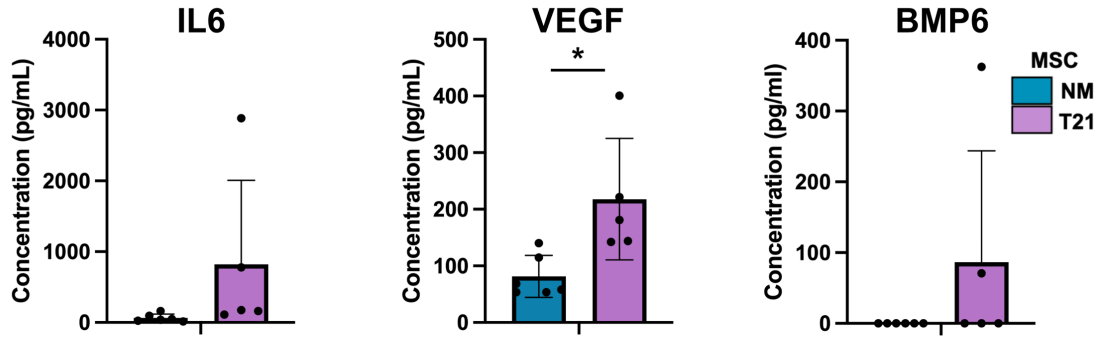

Figure 4.11: Differences in cytokine secretion in T21 fetal BM MSC compared to NM fetal BM MSC. 500,000 NM and T21 fetal BM MSC (passage 2-9) were cultured in αMEM supplemented with 100U/mL Penicillin, 100μg/mL Streptomycin, 2mM L-glutamine, 50μM 2-Mercaptoethanol, 10mM HEPES for 48 hours, before supernatants were collected. IL6 and VEGF were measured by Luminex assay, and BMP6 by ELISA. N NM fetal BM MSC = 6, N T21 fetal BM MSC = 5, each dot represents one biological MSC replicate. NM: normal; T21 Trisomy 21.

However, compared to NM fetal BM MSC, T21 fetal BM MSC did produce significantly more VEGF (Figure 4.11), a factor reported to impair B lymphoid commitment[680]. In addition, TNFα signalling in human adult and neonatal BM MSC has been reported to increase their secretion of IL6 and VEGF *in vitro*[681], so it may be that these differences in T21 fetal BM MSC compared to NM fetal BM MSC are secondary to the increased TNFα response.

Together, these gene and protein expression data suggest that there is an elevated inflammatory response in T21 fetal BM MSC, perhaps due to a combination of constitutive interferon signalling and a response to endogenous secreted TNFα originating in the native T21 BM; I will explore this further in Chapter 5.

4.2.4 Crossover fetal BM MSC co-culture assays

I next co-cultured T21 fetal BM HSC, MPP and LMPP from 3 biological donors with NM (n=3) or T21 fetal BM MSC (n=3), to test whether NM fetal BM MSC were able to rescue abnormal haematopoietic differentiation of T21 fetal BM HSPC. Briefly, ∼100 T21 fetal BM HSC, MPP and LMPP were plated on either NM or T21 fetal BM MSC as described in Chapter 2 and the output measured with weekly flow cytometry.

NM and T21 fetal BM MSC both showed a similar ability to support expansion of T21 HSC, MPP and LMPP (Figure 4.12B). The *in vitro* output of these co-culture experiments with T21 HSC, MPP and LMPP was largely myeloid, with some NK output, and very little B lymphoid output (Figure 4.12C). There appeared to be no difference in proportional lineage output from T21 fetal BM HSPC when cultured on NM or T21 fetal BM MSC. This was also the case when total absolute number of B, myeloid, and NK cells produced in the experiment from T21 HSC, MPP and LMPP on NM and T21 fetal BM MSC was compared (Figure 4.13).

When considered across experimental conditions, T21 fetal BM MSC were not significantly different in supporting B or NK lymphopoiesis or myelopoiesis by 2 way ANOVA, and there was no significant interaction between the source of HSPC and MSC. Rather, the only significant effect by 2 way ANOVA was HSPC source, with T21 fetal BM HSC, MPP and LMPP producing very few or no B cells compared to their normal counterparts, regardless of support from NM or T21 fetal BM MSC. This highlights the extent of the changes in HSPC-intrinsic behaviour caused by T21, and though T21 fetal BM MSC appeared to provide reduced support for B lymphopoiesis from NM fetal BM HSC, MPP and LMPP (Figure 4.6), NM fetal BM MSC failed to rescue the T21 defect in B lymphopoiesis.

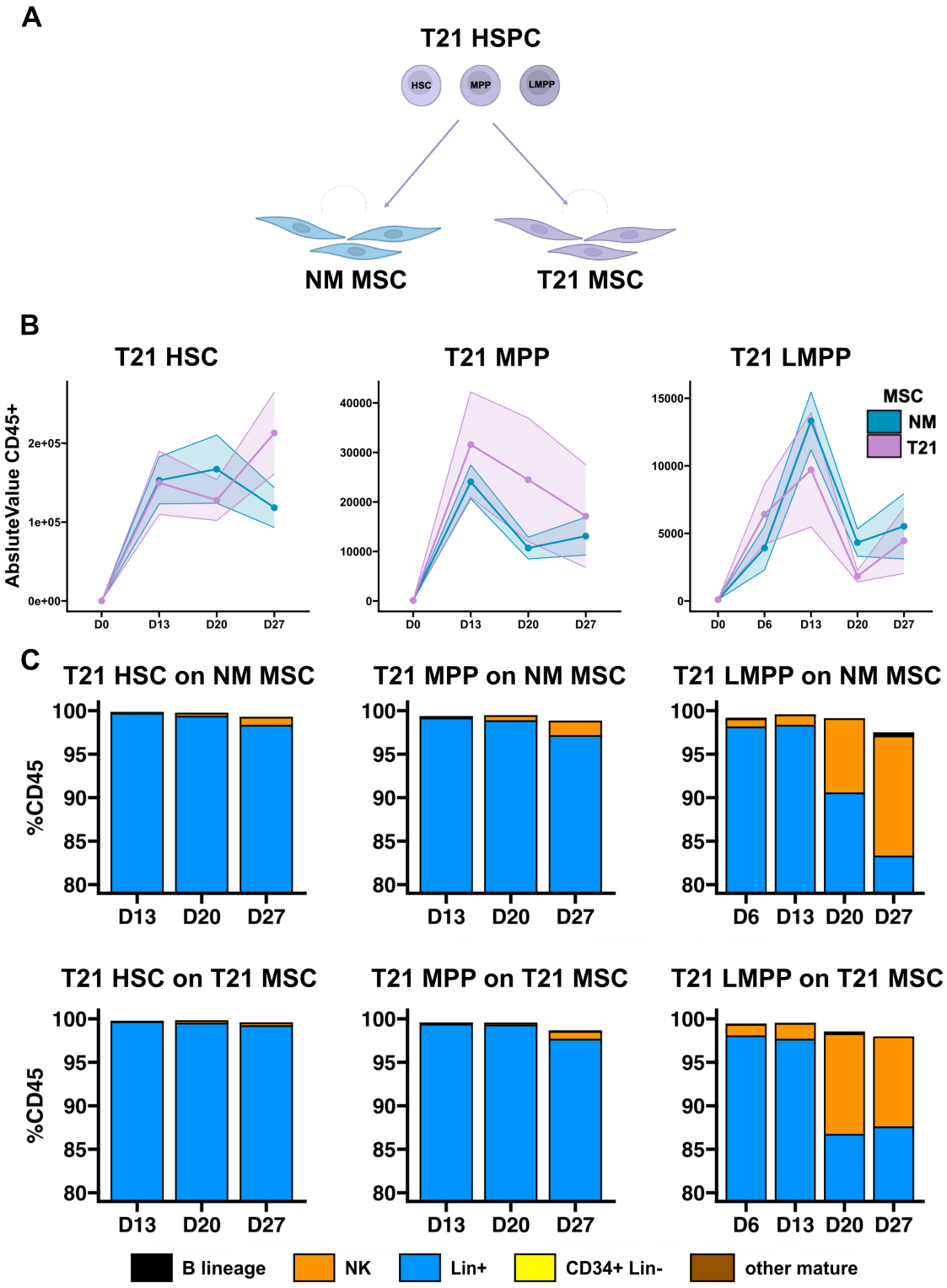

Figure 4.12: NM fetal BM MSC are unable to rescue T21 haematopoiesis. (A) 89-100 FAC-sorted T21 fetal BM HSC, MPP and LMPP (n=3) were co-cultured on NM (n=3) or T21 fetal BM MSC (n=3) for 28 days. (B) Fetal BM MSC support T21 haematopoiesis. Data is presented as mean absolute CD45+ ± SEM. (C) The relative output of T21 HSPC when cultured on NM or T21 fetal BM MSC, as a percentage of CD45+ cells. NM: normal; T21 Trisomy 21; D: day. Lin: CD3/11b/14/33.

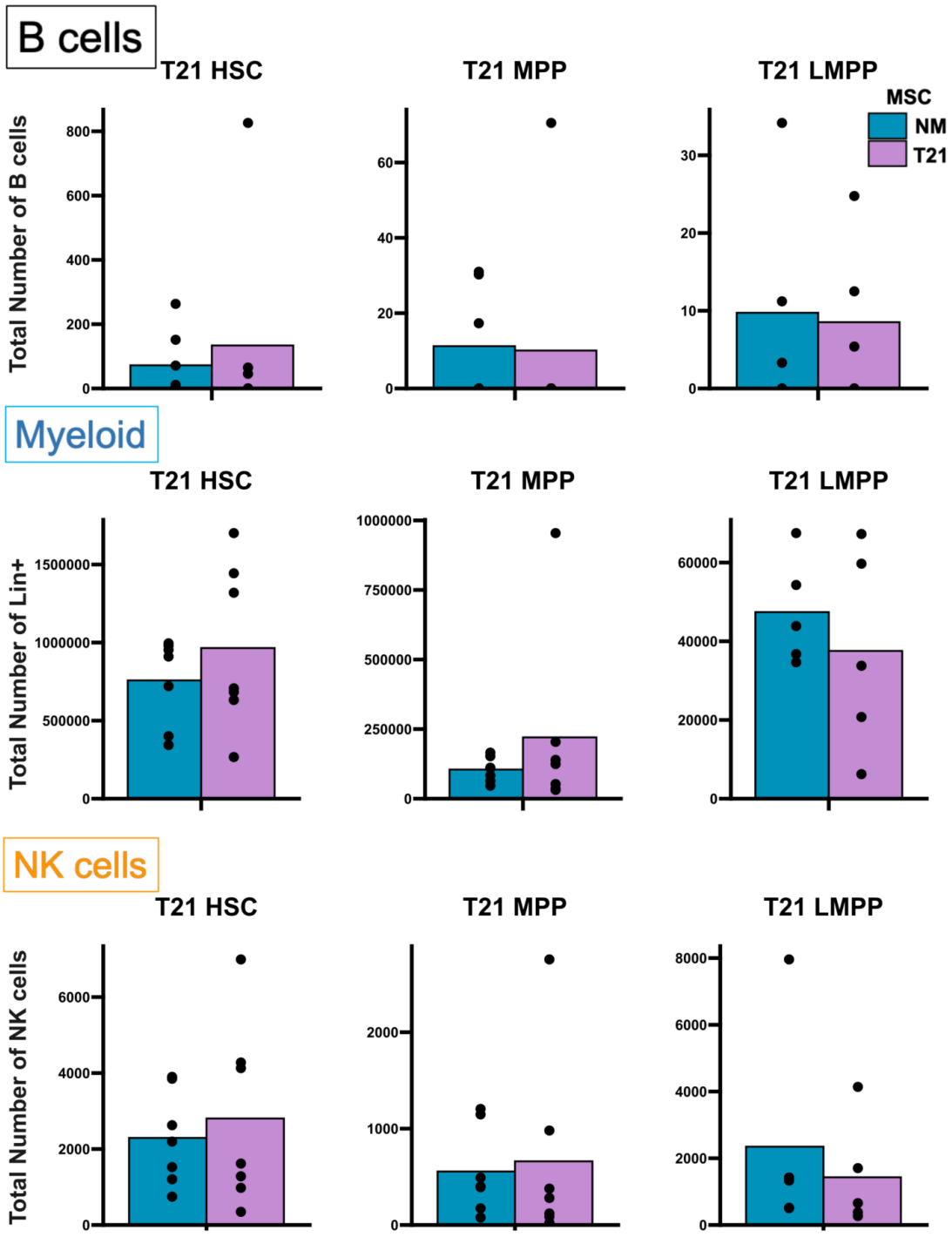

Figure 4.13: NM fetal BM MSC are unable to rescue T21 haematopoiesis. Total output of B cells, Lin+ cells and NK cells produced by FAC-sorted T21 fetal BM HSPC (n=3, 89-100 cells) when differentiated on NM (n=3) or T21 (n=3) fetal BM MSC. Each dot represents one combination of MSC and HSPC. NM: normal; T21 Trisomy 21. Lin: CD3/11b/14/33.

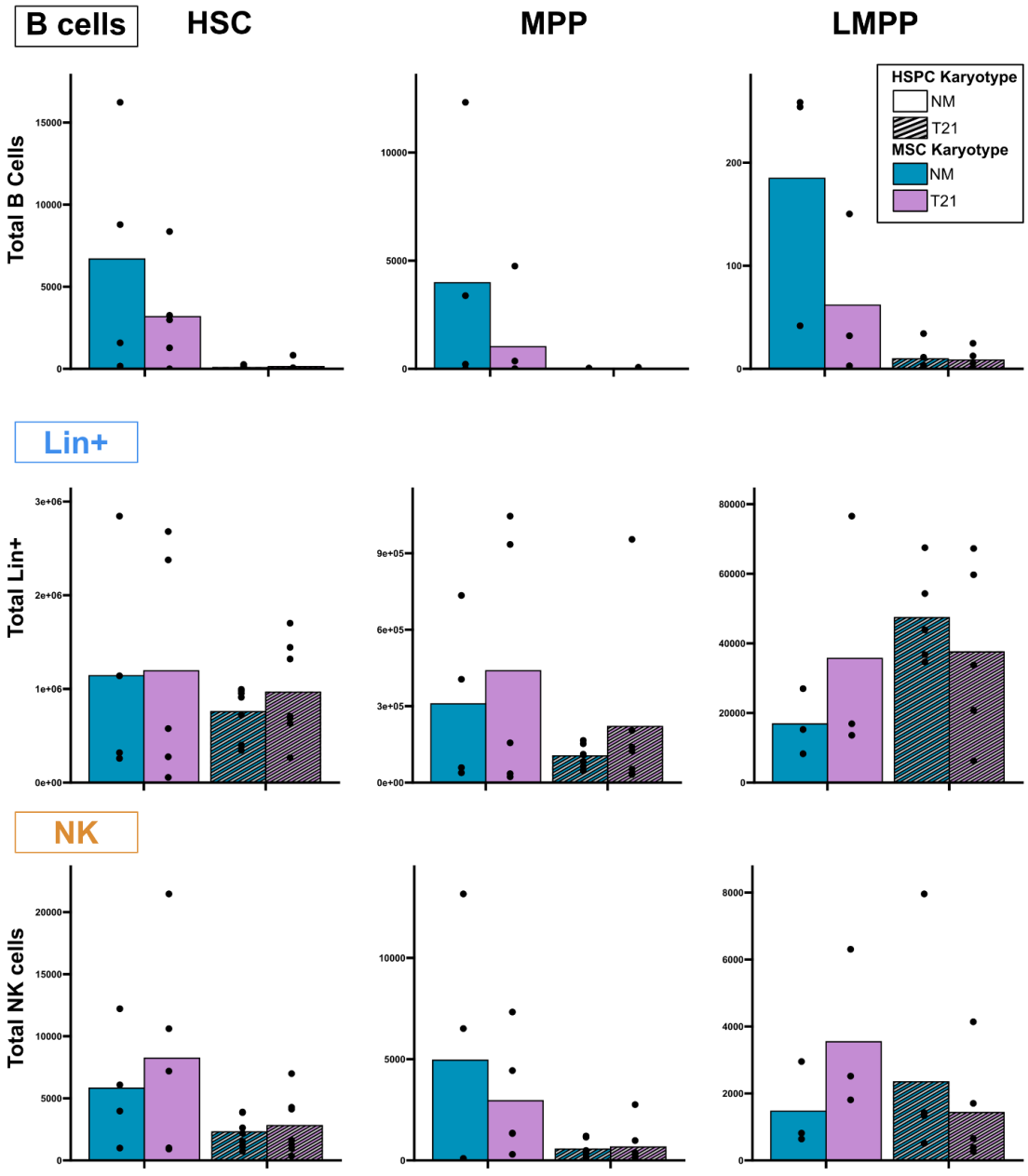

Figure 4.14: T21 cell-intrinsic differences in lymphoid potential of fetal BM HSC, MPP and LMPP predominate over extrinsic effects mediated by T21 fetal BM MSC. Total output of B cells, Lin+ cells and NK cells produced by NM (n=4, clear bars) or T21 fetal BM HSPC(n=3, hashed bars) when differentiated on NM (n=3-4, blue) or T21 (n=3-5, lilac) fetal BM MSC. Each dot represents one combination of MSC and HSPC. NM: normal; T21 Trisomy 21. Lin: CD3/11b/14/33.

4.3 Summary and discussion

The experiments in this chapter aimed to delineate the relative contributions of HSPC and MSC to the haematopoietic lineage skew observed in T21 fetal BM. While previous work assessing differentiation of sorted T21 HSPC populations was carried out on MS5 stroma, it is worth noting, however, that there are important differences between MS5 and primary fetal BM MSC. Notably MS5 produce 40-fold more IL7 compared to adult human primary MSC *in vitro*[98]. Developing a fully human fetal co-culture system allows us to more faithfully recapitulate B cell development in the native fetal bone marrow *in vitro*.

Initial co-culture experiments with NM HSPC on T21 or NM fetal BM MSC suggested that T21 fetal BM MSC provided less support for B lymphopoiesis and instead provided increased support for NK lymphopoiesis. Studying differences in gene and protein expression between NM and T21 fetal BM MSC suggested that T21 fetal BM MSC displayed an inflammatory response phenotype, specifically to TNFα and type I interferon signalling, suggesting a pro-inflammatory T21 fetal BM environment.

However, my cytokine assays show that NM and T21 fetal BM MSC do not secrete TNFα or type I interferons *in vitro*. This suggests two possibilities:

1. There may be a constitutive activation of the inflammatory response in T21 fetal BM MSC. Recent work shows that triplication of the type 1 interferon receptors *IFNAR1* and *IFNAR2* in T21 immortalised fibroblasts leads to an overactive type-1 interferon response *in vitro*[431].

2. Alternatively, TNFα might be secreted by other stromal or haematopoietic cells in T21 fetal BM. There are a number of reports showing that circulating TNFα is increased in individuals with Down syndrome[425, 426, 431, 682, 683], suggesting that there may be dysregulated TNFα production beyond fetal life. It is plausible that either, or both the mechanisms might be at play in fetal BM.

The fact that NM fetal BM MSC failed to rescue abnormal haematopoiesis when T21 fetal BM HSPC were co-cultured with them, also suggests that BM MSC alone are unlikely to be responsible for the skewed lineage output of T21 fetal BM HSPC . Although, it is possible that T21 fetal BM HSPC, having been exposed to a proinflammatory niche, retain this phenotype *in vitro*. Additional factors beyond MSC-HSPC interactions may also influence haematopoietic output and inflammatory signals. For example, secreted signals from mature haematopoietic cells generated in these co-cultures could contribute to the observed defects in B lymphopoiesis.

MSC, *in vivo*, are a highly heterogenous group of cells with different roles in supporting haematopoiesis[248, 252, 684], however, when cultured *ex vivo* and passaged, they appear relatively homogenous. In addition to losing the cellular complexity seen in the native BM, it is possible that gene expression patterns among MSC change when MSC are cultured [685, 686]. To understand these differences, it would be important to study MSC freshly isolated from NM and T21 fetal BM, which I explore in the next chapter.

4.3.1 Future work

These data provide preliminary evidence of inflammatory signalling affecting T21 haematopoiesis by acting on both the haematopoietic niche and HSPC. To delineate this, a series of experiments exposing NM fetal BM MSC to TNFα and IFNα, and comparing their phenotype and capacity to support B lymphopoiesis would be required.

Recent advances in iPSC-derived BM organoid systems have demonstrated that they can recapitulate stromal subtype complexity and support B lymphopoiesis in vitro [687]. These organoids may be a useful platform to investigate the role of the haematopoietic niche in the T21-associated haematopoietic abnormalities seen in fetal BM. T21 and NM iPSC could be used to generate matched stromal organoids, into which NM or T21 fetal HSPC could be engrafted. This system would allow controlled interrogation of the niche's contribution to lymphoid development, and targeted disruption of specific signalling pathways, such as TNFα, could help define their roles in the impaired B cell output observed in T21.

5

Results III: The T21 fetal BM microenvironment

5.1 Background and aims

Data presented in Chapters 3 and 4 has implicated the BM microenvironment as a contributor to impaired B lymphopoiesis in T21 fetal BM. Niche-derived proinflammatory signals may directly and indirectly contribute to abnormal haematopoiesis in T21 by acting on HSPC and MSC. Additionally, preliminary gene expression data presented in Chapter 4 have suggested a potential imbalance in osteolineage and adipolineage differentiation of T21 fetal BM MSC.

Skewed MSC lineage commitment may be particularly relevant to B lymphopoiesis, as osteolineage cells provide a niche for B lymphopoiesis, and are sources of B lymphopoietic support factors such as IL7 and CXCL12[274, 276, 304, 307, 688]. Conversely, human adipocytes have been shown to impair B lineage commitment through the secretion of inhibitory cytokines and lipid mediators, including adiponectin[689], that negatively affect B lymphoid commitment directly at a CLP stage[316], as well as indirectly, through promoting the development of a CD11b+ population that inhibits B lymphopoiesis in murine BM[317, 318]. Thus, an imbalance in MSC differentiation in T21 may contribute, at least in part, to impaired B lineage commitment in T21 fetal BM.

A key limitation of the gene expression data presented in Chapter 4 is their reliance on derived MSC expanded *in vitro*, which may not fully recapitulate the cellular diversity and spatial complexity of the native fetal BM niche. In recent years, there have been a number of single cell transcriptome atlases of fetal BM published, some of which include T21 fetal BM samples[36, 45, 388]. These datasets provide an opportunity to investigate the composition and transcriptome of a wider stromal landscape in fetal BM.

The aim of this chapter is to integrate and analyse these datasets to investigate changes in niche composition and signalling in T21 fetal BM, and how these may contribute to impaired B lymphopoiesis.

5.2 Comparative single cell transcriptome profiling of NM and T21 fetal BM cells

I integrated three recently published scRNA-Seq datasets from fetal BM [36, 45, 388] (Figure 2.10, page 67) and performed manual reannotation of cell types based on expression of canonical marker genes (Figure 2.11, page 68). Integration of these datasets revealed 14 broad lineage groups (Figure 5.1A), which aligned well with conventional haematopoietic and stromal lineage definitions[21, 281, 288](Figure 5.1B).

As shown in Figures 5.1 and 5.2, this integrated dataset captures the major stromal and haematopoietic cell types present in BM[21, 247, 281, 288, 690]. Figure 5.1B illustrates the relative composition of this integrated dataset.

It is important to note that the data may be influenced by the use of different approaches to preparing samples for scRNA-Seq: Jardine et al. crushed and digested long bones, followed by lysing red blood cells[36]. Marderstein et al. flushed, then crushed, then digested fetal long bones. Samples were then subject to three different sorting strategies: CD45+CD34+, CD45+ and CD235a-[388]. Zheng et al. also crushed and digested fetal long bones, and sorted Lin-(CD3/CD33/CD41a/CD235a/CD11b/CD19/CD14)- CD45- cells, and Lin- CD45+CD34+ cells, subdivided into CD38± cells for samples older than 11

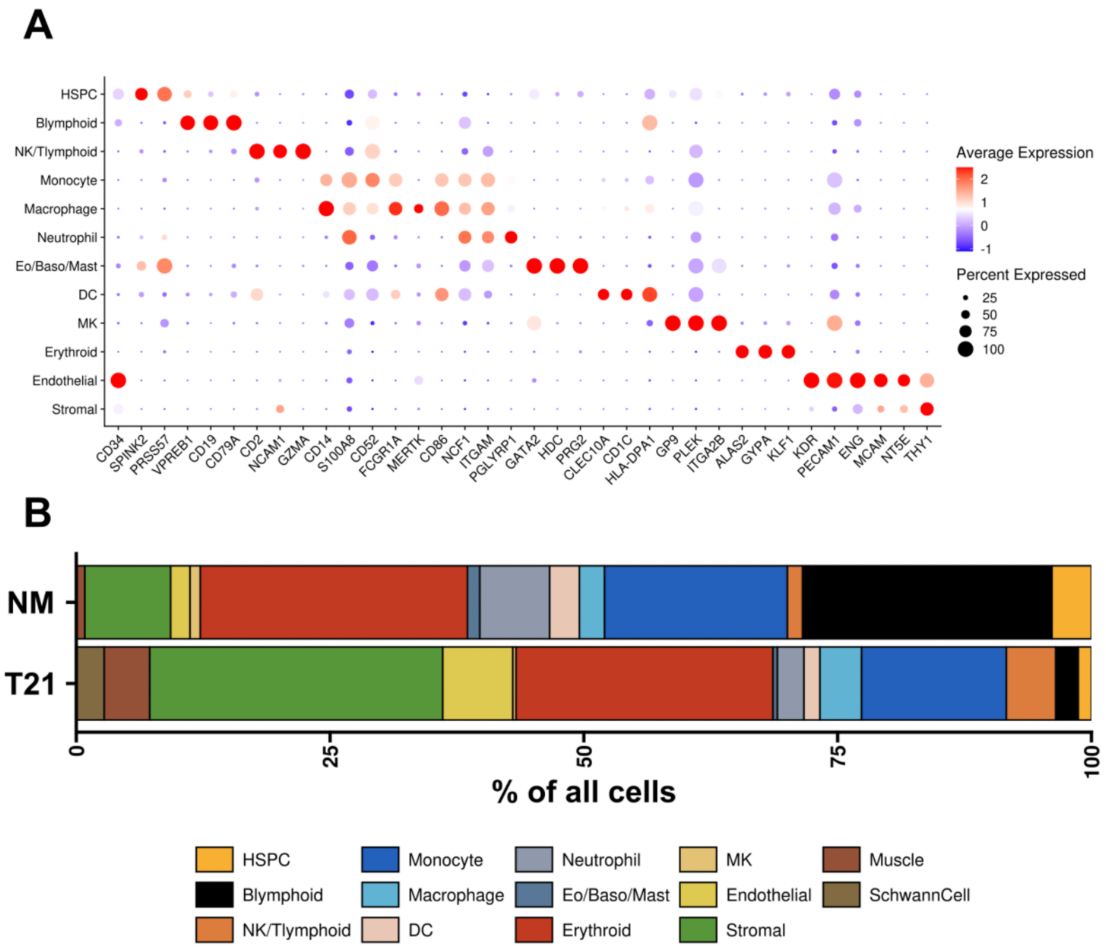

Figure 5.1: scRNA-Seq analysis of NM and T21 fetal BM. Integration and re-annotation of published scRNA-Seq datasets of NM and T21 fetal BM[36, 45, 388]. (A) Gene expression dot plot of lineage-defining genes for broad categories in fetal BM scRNA-Seq data. (B) Composition of merged datasets by broad category. Eo, eosinophil; Baso, Basophil; NM, normal (n=21, k=129040, gestation age=10-19 PCW); T21, Trisomy 21 (n=16, k=67428, gestation age=12-20 PCW).

PCW[45]. Details of individual samples' contribution to each dataset is detailed in Figure 2.12, page 69. Given these different strategies, comparisons in overall long bone haematopoietic and stromal composition are difficult to make. However, integrating these datasets allows us to overcome the limitations of each dataset, especially regarding sample and cell number. Marderstein et al. only studied three NM samples, which had very few haematopoietic cells, but sequenced single cells across twelve T21 samples. On the other hand, Jardine et al. had a very poor representation of stromal cells from T21 fetal BM, and the gestational age of these

samples was limited to 12-13 weeks. Samples from Zheng et al. also covered an earlier gestational age, allowing for better gestation matching of NM fetal BM samples across datasets (Figure 2.12, page 69). Together, this integrated dataset provides a more complete view of T21 fetal BM than any single dataset alone, allowing for more robust downstream analysis.

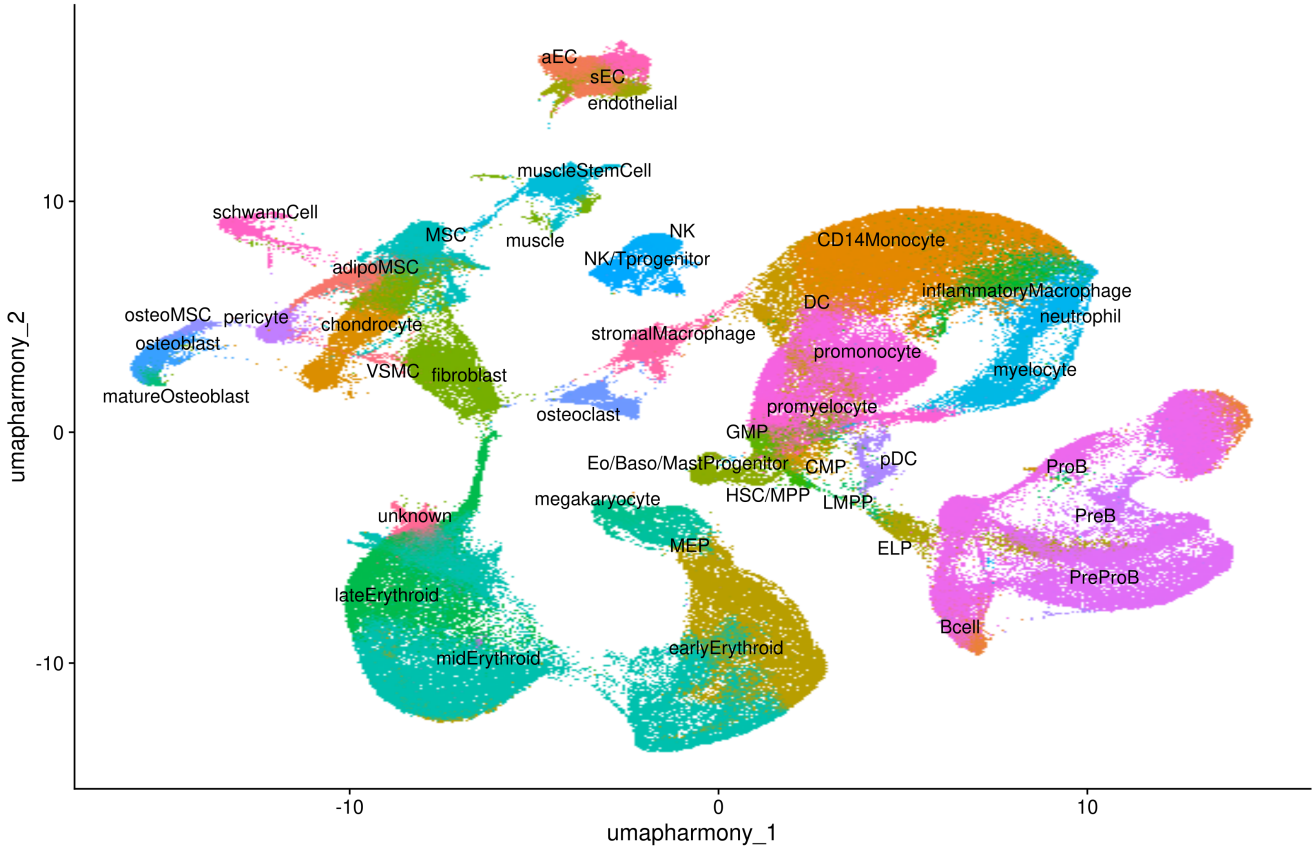

Figure 5.2: UMAP of NM and T21 fetal BM by refined clusters. Annotation of published scRNA-Seq datasets of NM and T21 fetal BM[36, 45, 388] showed representation of key populations of fetal BM. Eo, eosinophil; Baso, Basophil; NM, normal (n=21, k=129040, gestation age=10-19 PCW); T21, Trisomy 21 (n=16, k=67428, gestation age=12-20 PCW).

5.3 Differences in niche composition between NM and T21 fetal BM

To investigate whether there were any differences in BM niche composition between NM and T21 fetal BM, I compared the frequency of non-haematopoietic cells from

samples prepared for scRNA-Seq in the same way[388]. There were no significant differences in niche composition except that the frequency of transcriptomically-defined chondrocytes was increased in T21 fetal BM (p-value = 0.002, T-test) (Figure 5.3). However, a major drawback to the comparison of NM and T21 fetal BM samples, was that 3988 stromal cells were analysed from the three NM samples, compared to 26855 cells from eight T21 samples, with a single NM 12 PCW sample contributing 68% of all NM fetal BM stromal cells (see Figure 2.12, page 69).

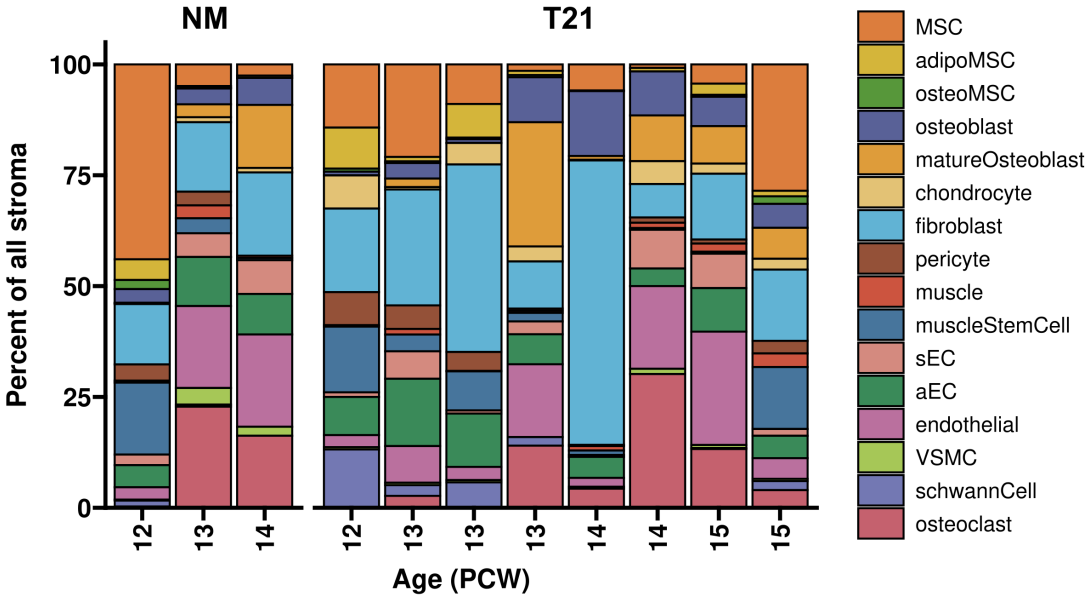

Figure 5.3: Frequency of stromal and endothelial cells in NM and T21 fetal BM. Data from Marderstein et al. [388], processed by crushing and digestion, followed by FAC-sorting CD235a negative cells, a single bar represents one biological sample. NM, normal (n=3, k=3988, gestation age=12-14 PCW); T21, Trisomy 21 (n=8, k=26855, gestation age=12-15 PCW). sEC, sinusoidal endothelial cell, aEC, arteriolar endothelial cell. Only samples where there was data from at least 100 cells were included.

Given this, I next investigated the stromal cell characteristics of fetal BM using multiparameter flow cytometry on mechanically disrupted and digested fetal bones. Most of our understanding of MSC markers comes from imaging studies in murine models, and far less is understood about human fetal BM MSC[294]. Given the heterogeneity of the stromal compartment, I adopted a dimensionality reduction and clustering strategy to analyse these data and understand co-expression patterns of stromal markers[691].

Stromal cells were identified as live cells lacking expression of CD45, CD235a, CD71 and CD31[293], and unscaled, compensated mean fluorescence intensity of these cells was arcsinh transformed before dimensionality reduction and clustering was performed.

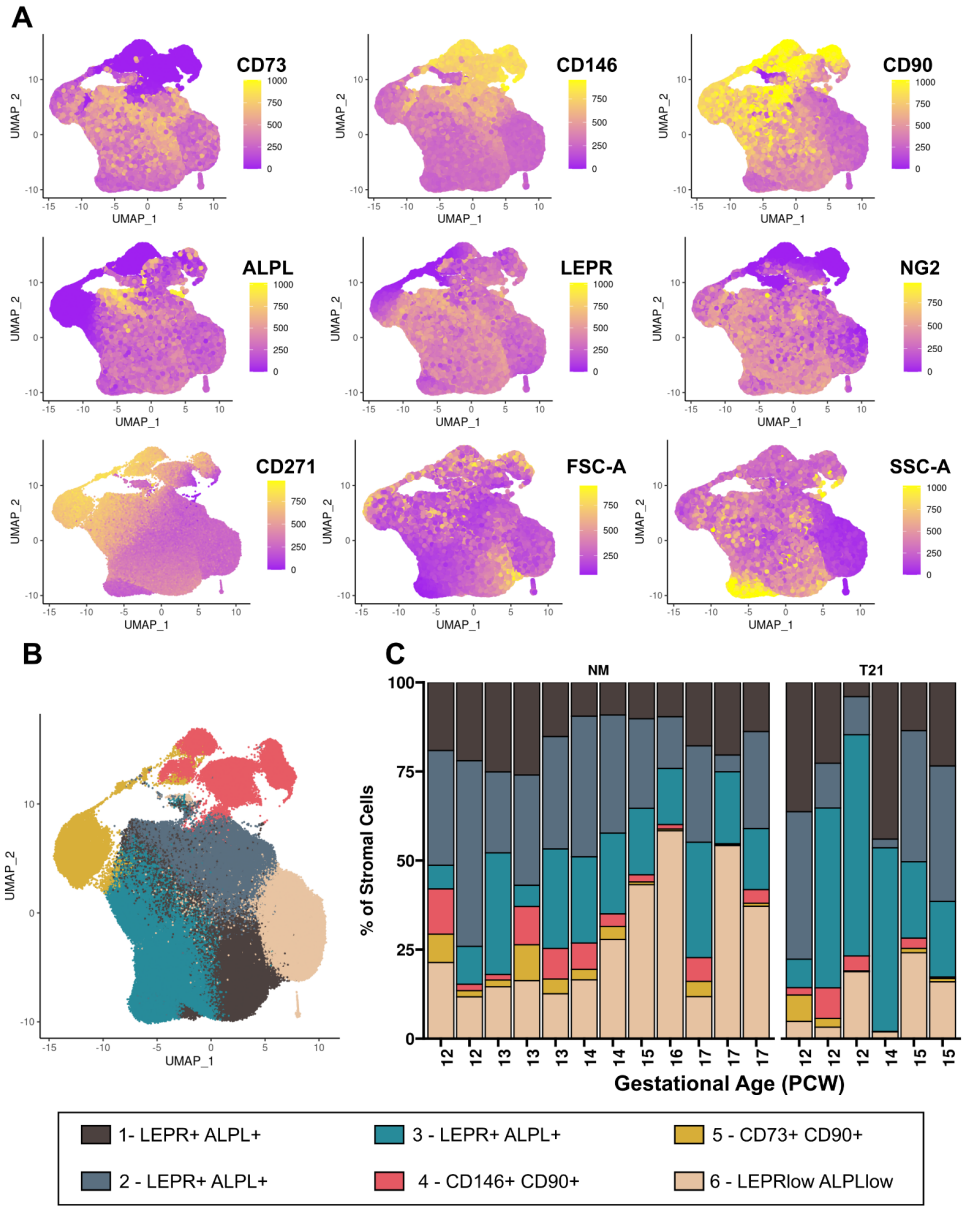

Figure 5.4: Subsets of stromal cells in native NM and T21 fetal BM. Fetal long bones were crushed and digested, and their stromal compartment was assessed by flow cytometry. Stromal were cells defined by lack of expression of CD31, CD45, CD235a and CD71. (A) MFI of each stromal marker included in the panel, (B) k-means clustering of stromal cells and (C) relative frequency of clusters in NM and T21 fetal BM through gestation. NM, normal (n=12, gestational age=12-17 PCW); T21, trisomy 21, (n=6, gestational age=12-15 PCW).

Kmeans clustering identified 6 clusters based on marker protein expression (Figure 5.4B). Clusters 1, 2, 3 and 6 appeared to co-express CD73, ALPL and LEPR, suggesting that they may be osteoMSC, with cluster 2 containing cells with the highest expression of ALPL. These clusters (1, 2, 3 and 6) appeared to make up most of the BM stromal compartment in fetal BM. Cluster 4 expressed CD90, CD146, and ALPL and CD271 at variable levels; while cluster 5 co-expressed CD90 and CD271, suggesting they may represent more primitive MSC populations[291], with cluster 4 likely to be closely associated with vasculature based on CD146 expression[292]. Across these samples, there appeared to be a gestation effect, with cluster 6, a population with low ALPL and LEPR protein expression, having an increased frequency later in gestation. Interestingly, the frequency of cluster 6 was significantly reduced in T21 fetal BM (T-test, p-adj = 0.02). Together, this characterises the patterns of stromal marker co-expression at a protein level in the NM fetal BM and the composition stromal compartment through gestation, with osteoMSC predomination in early gestation.

While this strategy is helpful in identifying patterns of co-expression, there are a number of limitations. Traditional flow cytometry analysis relies on binary true/ false decisions, while this approach uses MFI as a continuous variable. This may mean that markers which by flow cytometry have a low expression or a poor separation may lead to ambiguous clustering, and rare populations with low intensity marker expression may not separate from more abundant populations. This is especially the case with dimensionality reduction and clustering based on only nine parameters, where signal-to-noise ratio may be poorer. For instance, there was no clear osteoblast cluster by this strategy, while traditional gating identified a subset of ALPL+ LEPR- population, consistent with definitions of early osteoblasts in murine and human BM [688, 692, 693].

As there was a reduction in frequency of a cluster stromal cells that lowly expressed ALPL and LEPR in T21 fetal BM (cluster 6, Figure 5.4C), I next looked at the frequency of osteoMSC and osteoblasts using traditional gating on gestation-matched samples from NM and T21 fetal BM with gates set using FMO

controls. While dimensionality reduction and clustering is helpful for identifying patterns of co-expression, FMO-based gating allows for the precise identification of a population positive for a marker. I used ALPL as an osteolineage marker, and ALPL+LEPR+ cells to identify osteoMSC (Figure 5.5A), in line with conventional definitions[688]. While this did not reach statistical significance, T21 fetal BM had decreased osteoMSC frequency (Figure 5.5B).

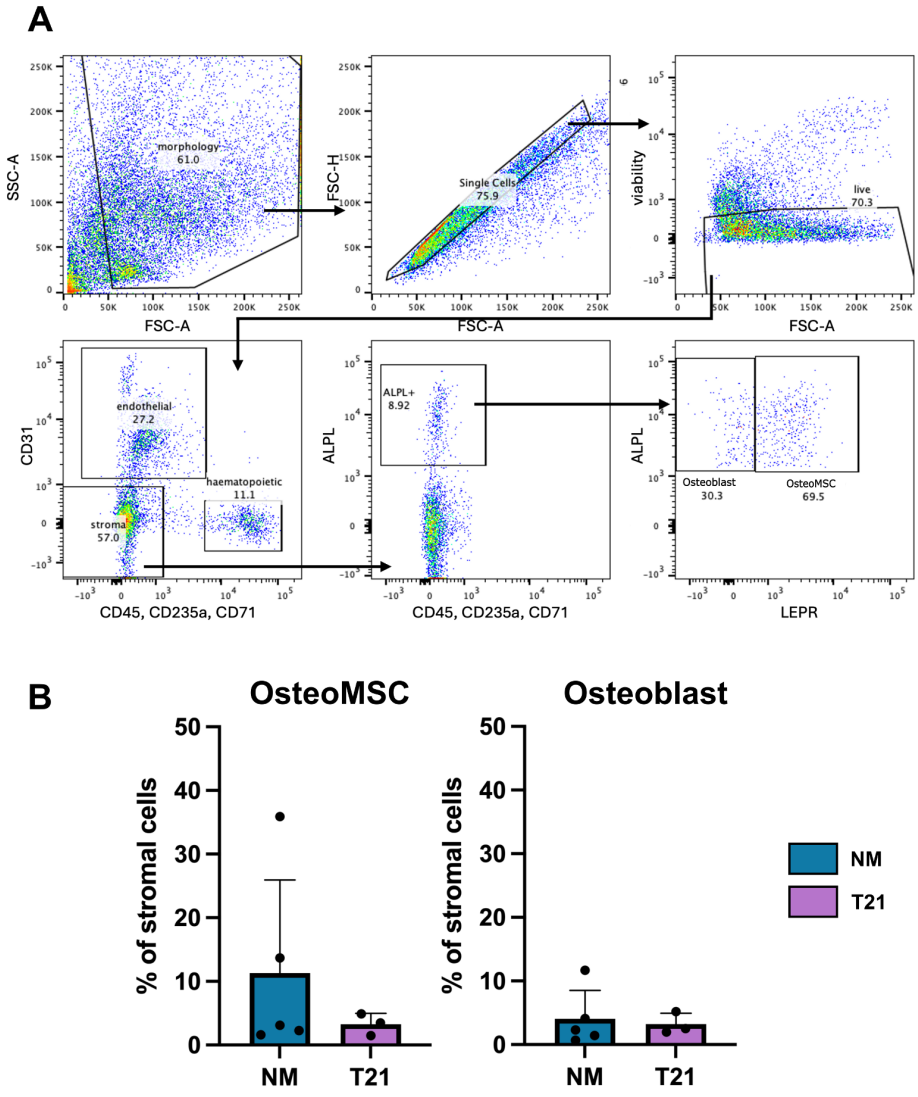

Figure 5.5: Frequency of osteoMSC and osteoblasts assessed by flow cytometry in gestation matched NM and T21 fetal BM. (A) Gating strategy characterising osteoMSC, defined by co-expression of LEPR and ALPL, osteoblasts by expression of ALPL and not LEPR. Stromal cells defined by lack of expression of CD31, CD45, CD235a and CD71. (B) Frequency of osteoMSC and osteoblasts in NM and T21 fetal BM. NM, normal (n=5, gestation age=12-13 PCW); T21, Trisomy 21 (n=3, gestation age=12-13 PCW).

5.3.1 Differences in osteolineage differentiation in T21 fetal BM

To explore whether the observed trend toward reduced osteoMSC frequency in T21 fetal BM reflects broader alterations in MSC differentiation trajectories, I next conducted trajectory inference analysis using Monocle3[528] on fetal BM MSC, and their differentiated subsets adipoMSC and osteoMSC[281, 694]. Unsupervised trajectory inference showed a branch at MSC towards osteo- or adipo- fates (Figure 5.6A) and (Figure 5.6B) by pseudotime, with the root being set at undifferentiated MSC. There also appeared to be a third branch of differentiation from MSC, which may reflect fibroblastic/chondrocytic primed MSC. When the frequencies of MSC, osteoMSC, and adipoMSC across all datasets[36, 45, 695] and all samples were considered together, there was an apparent increased proportion of adipoMSC and decreased proportion of osteoMSC in T21 fetal BM compared to NM fetal BM (Figure 5.6C).

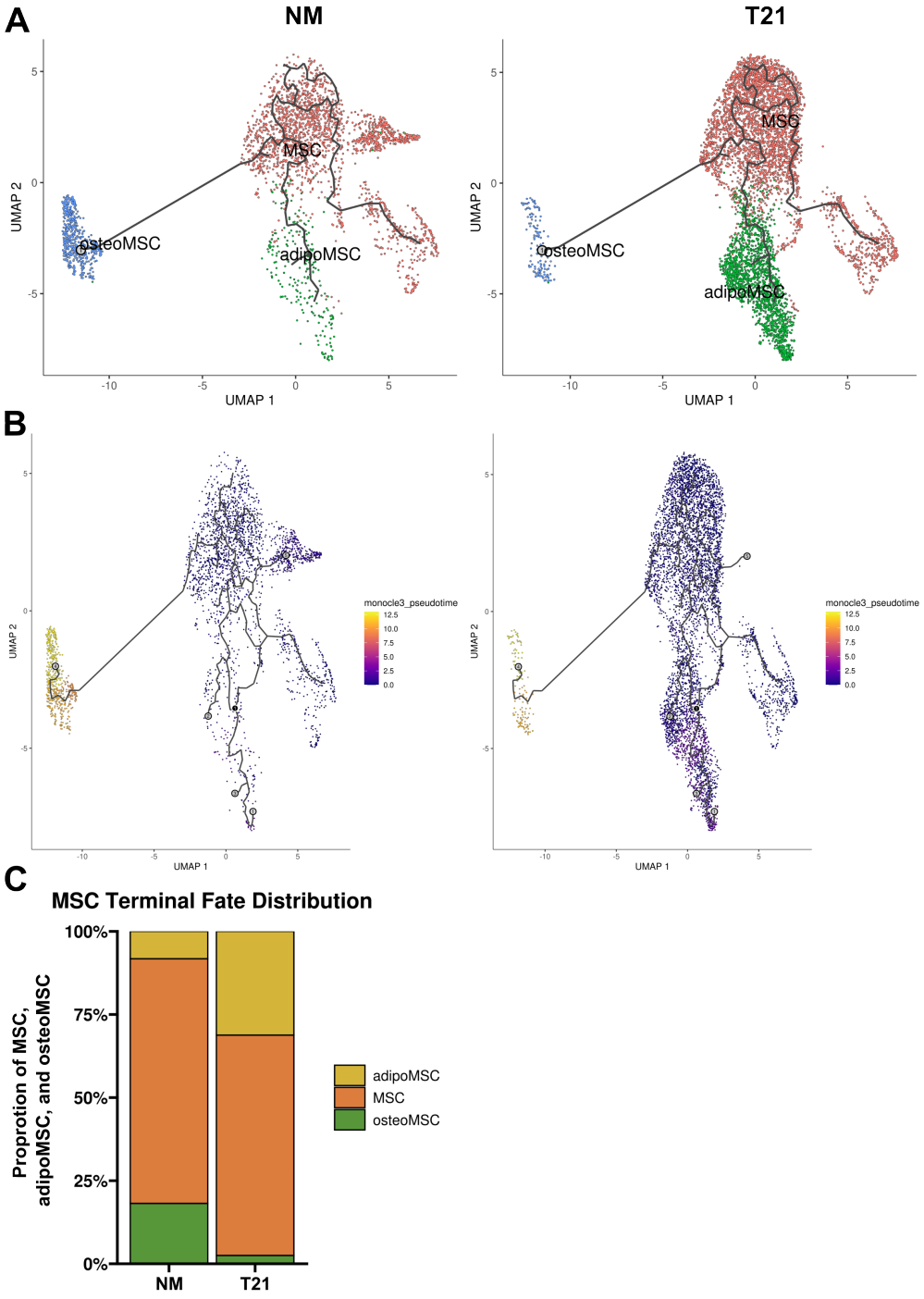

Figure 5.6: scRNA-Seq trajectory inference analysis for fetal BM MSC towards osteogenic and adipogenic fates. (A) Monocle3-inferred differentiation trajectories of MSC into osteoMSC and adipoMSC displayed by UMAP and (B) coloured by pseudotime, with purple representing stages earlier in differentiation and yellow representing later stages. (C) Distribution of MSC fate in NM and T21 fetal BM across all samples. NM, normal (n=21, k=2982, gestation age=12-17 PCW); T21, Trisomy 21 (n=16, k=5829, gestation age=12-20 PCW)[36, 45, 695].

I next considered differences in inferred transcription factor activity that may underpin altered cell fate decisions in T21 fetal BM MSC, using SJARACNe in tandem with NetBID2[530, 531] in the undifferentiated MSC population identified by scRNA-Seq ("MSC" in Figures 5.3 and 5.6).

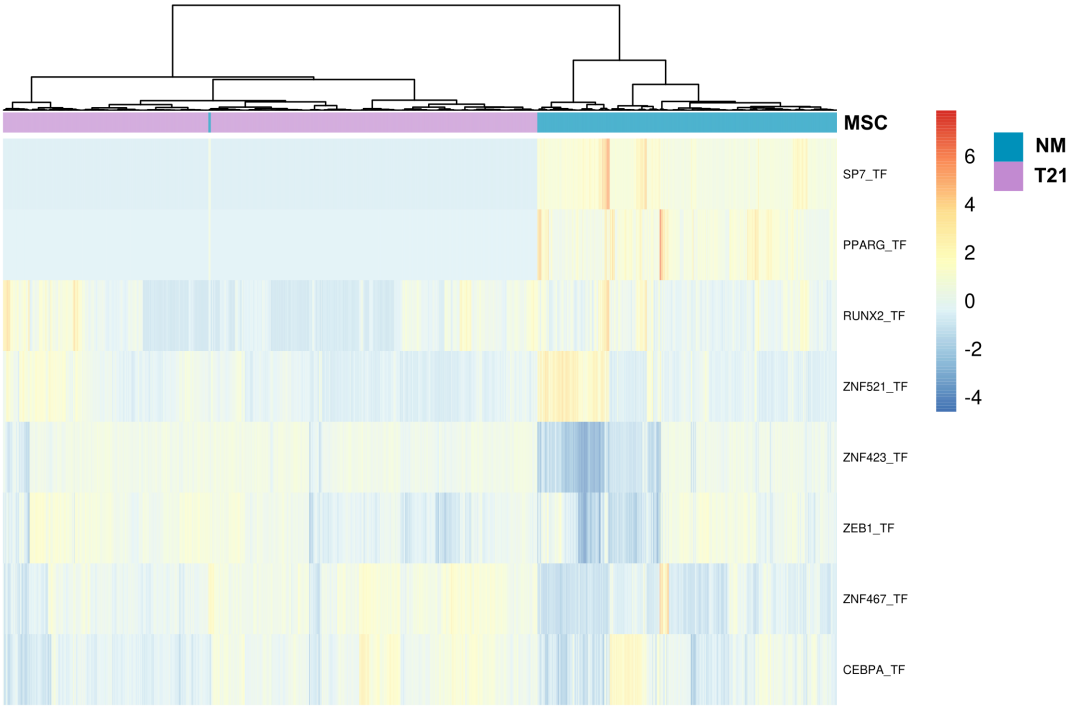

Figure 5.7: Inference of transcription factor activity governing osteogenic or adipogenic fate from gene regulatory networks in fetal BM MSC. Transcription factor regulon activity analysis with SJARACNe and NetBID2 was used to identify differentially active (FDR <0.05) transcription factors in NM and T21 fetal BM MSC with a known role in osteolineage or adipolineage fate. NM, normal (n=21, k=2195, gestation age=12-17 PCW); T21, Trisomy 21 (n=16, k=3864, gestation age=12-20 PCW).

This revealed several differences in inferred transcription factor activity in osteogenesis and adipogenesis between NM and T21 fetal BM MSC (Figure 5.7). The inferred activity of master osteogenic transcription factors RUNX2 and SP7 was significantly decreased in T21 fetal BM MSC. RUNX2 and SP7 are both essential for osteoblast formation, as demonstrated by studies in knockout mice. *Runx2* homozygous knockout mice are born without ossified bones, lack mature osteoblasts, and die soon after birth[696, 697], and a similar phenotype is observed in *Sp7*-null mice, which also lack ossified bones, mature osteoblasts, and die soon after

birth[698]. Additionally, heterozygous mutations *SP7* in humans are responsible for a rare form of osteogenesis imperfecta[699].

Consistent with this, ZEB1, a transcription factor reported to bind and negatively regulate *RUNX2* and inhibit osteolineage commitment in human MSC *in vitro* and in murine MSC[700, 701] had an increased inferred activity in T21 fetal BM MSC.

Additionally, transcription factors associated with adipolineage commitment, ZNF423 and ZNF467, which activate transcription of master adipogenic transcription factor *Pparg*/*PPARG* in mice [702, 703] and human MSC *in vitro*[704] had an increased inferred activity by NetBID2. Consistent with this, ZNF521, a negative regulator of pro-adipogenic transcription factor ZNF423 in mice[705, 706] and humans[707], had significantly decreased inferred activity in T21 fetal BM MSC. C/EBPα, another transcription factor involved in adipocyte development[708] in concert with PPARγ [709–712] was also inferred to have higher activity in T21 fetal BM MSC. Conversely, PPARγ, a master adipogenic transcription factor[713], had a significantly decreased inferred activity in T21 fetal BM MSC. However, PPARγ plays a role in differentiation of preadipocytes to adipocytes[713], and so may be less important in undifferentiated MSC.

Taken together, inferred transcription factor activity suggest that T21 fetal BM MSC appear to be primed for adipogenesis at the expense of osteogenesis. Given the role of osteolineage cells in supporting B lymphopoiesis[304], these data suggest that impaired osteolineage differentiation in T21 may contribute to impaired B lymphopoiesis.

In order to infer the impact a skew in MSC differentiation may have on support for B lymphopoiesis, I considered gene expression of MSC, adipoMSC, osteoMSC and osteoblasts in NM and T21 fetal BM, and conducted pairwise differential receptor/ligand expression analysis comparisons for a given population between NM and T21 using CellChat[529] (Figure 5.8). While T21 fetal BM MSC expressed known lymphopoietic support cytokines to a similar extent to their normal counterparts, there were also a number of differences in differentiated MSC subsets (Figure 5.8).

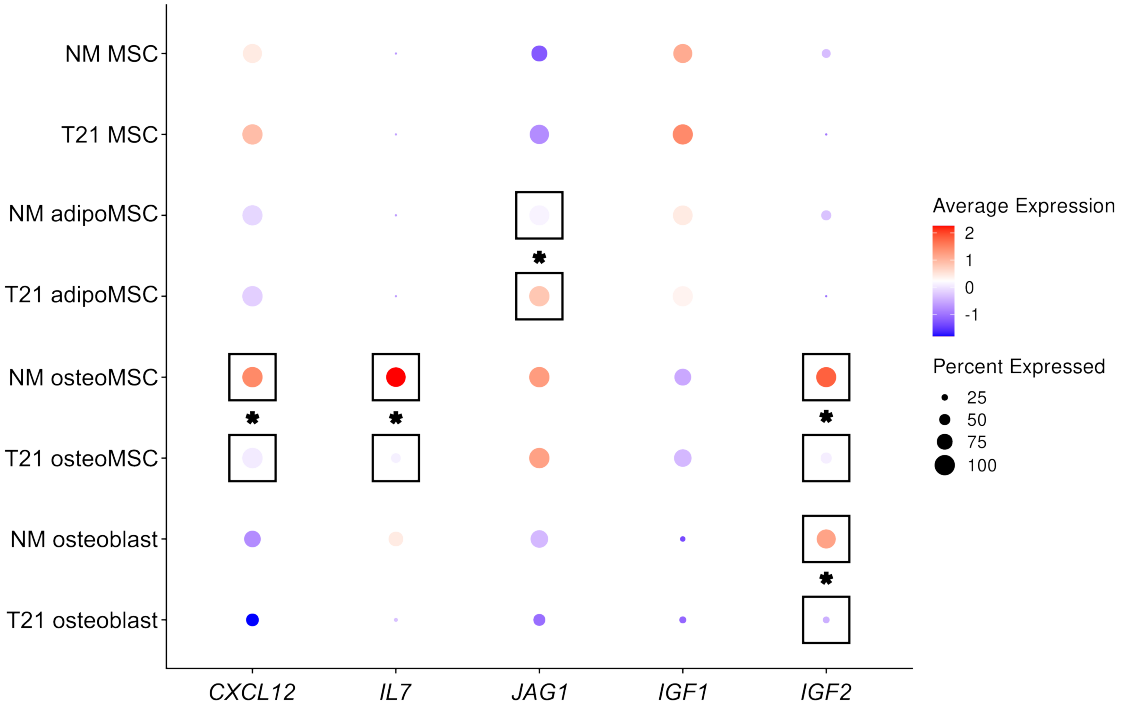

Figure 5.8: Gene expression of lymphopoietic cytokines by fetal BM stromal cells. Genes highlighted in a black box are statistically significantly differentially expressed between NM and T21 for a given population by CellChat (* denotes FDR <0.05). Dot size reflects % expression, while colour denotes scaled expression per gene. NM, normal (n=21, k=2982, gestation age=12-17 PCW); T21, Trisomy 21 (n=16, k=5829, gestation age=12-20 PCW).

As reviewed in Chapter 1, studies in both mice and humans have shown that IL7 is important in supporting B lymphopoiesis[98, 299, 300, 658]. CXCL12 is essential for guiding lymphoid progenitors to their niche in mice: conditional ablation of *Cxcl12* expressing MSC reduces CLP and ProB numbers[289]; while deletion of *Cxcl12* in LEPR+ MSC, CAR cells and osteoblasts result in a reduction in B progenitors[248, 298]. In human cord blood HSPC, CXCL12 has been shown to promote B lymphopoiesis *in vitro*, with blocking the CXCL12 receptor CXCR4 resulting in a suppression of B lymphopoiesis[714].

Both T21 and NM fetal BM MSC also expressed *IGF1*, which has been shown to support B lymphopoiesis from human HSPC *in vitro*[311, 715] and in murine models[309, 716, 717], but there was no significant difference between them.

On the other hand expression of the related gene, *IGF2*, was significantly lower in T21 compared to NM fetal BM osteoMSC and in T21 fetal BM osteoblasts compared to their NM counterparts (Figure 5.8). IGF2 promotes osteogenic differentiation from MSC in humans[718] and in mice [719, 720], suggesting this may contribute in part to the preliminary defect in osteolineage differentiation in T21 fetal BM. The effects of IGF2 on human fetal B lymphopoiesis have not been studied although experiments in our lab have shown IGF2 regulates the balance in megakaryocytic versus erythroid differentiation in human fetal liver[489]. In mice, IGF2 also supports HSC maintenance and expansion[232, 721, 722], and homozygous *Igf2*-null mice have a reduction in splenic B cells[723].

Finally, *JAG1*, a notch ligand that promotes NK/T lymphoid commitment at the expense of the B lineage [544] was increased in expression in T21 compared to NM fetal BM adipoMSC (Figure 5.8). These data suggest there is impaired commitment to osteogenic fate - alongside decreased expression of B lymphopoietic support cytokines from osteoMSC in T21 fetal BM. Concomitantly there may be skewing of T21 fetal BM MSC differentiation towards adipoMSC, which express higher levels of *JAG1*. Together, these factors may contribute to impaired B lymphopoiesis and promote NK/T lymphopoiesis in T21 fetal BM.

5.3.2 Functional validation of transcriptomic findings

To test the hypothesis that osteoblastic differentiation is impaired in T21 fetal BM MSC, I cultured T21 fetal BM MSC either with or without osteogenic culture medium. Culture-derived NM and T21 fetal BM MSC at a low passage number (4-5 passages) were grown in control (αMEM-C10 medium) or osteogenic (αMEM-C10 medium supplemented with 50μM ascorbic acid, 10mM β-glycerophosphate and 100nM dexamethasone) conditions and differentiation of MSC into osteoMSC (defined as LEPR+ALPL+) was measured after 14 days by flow cytometry.

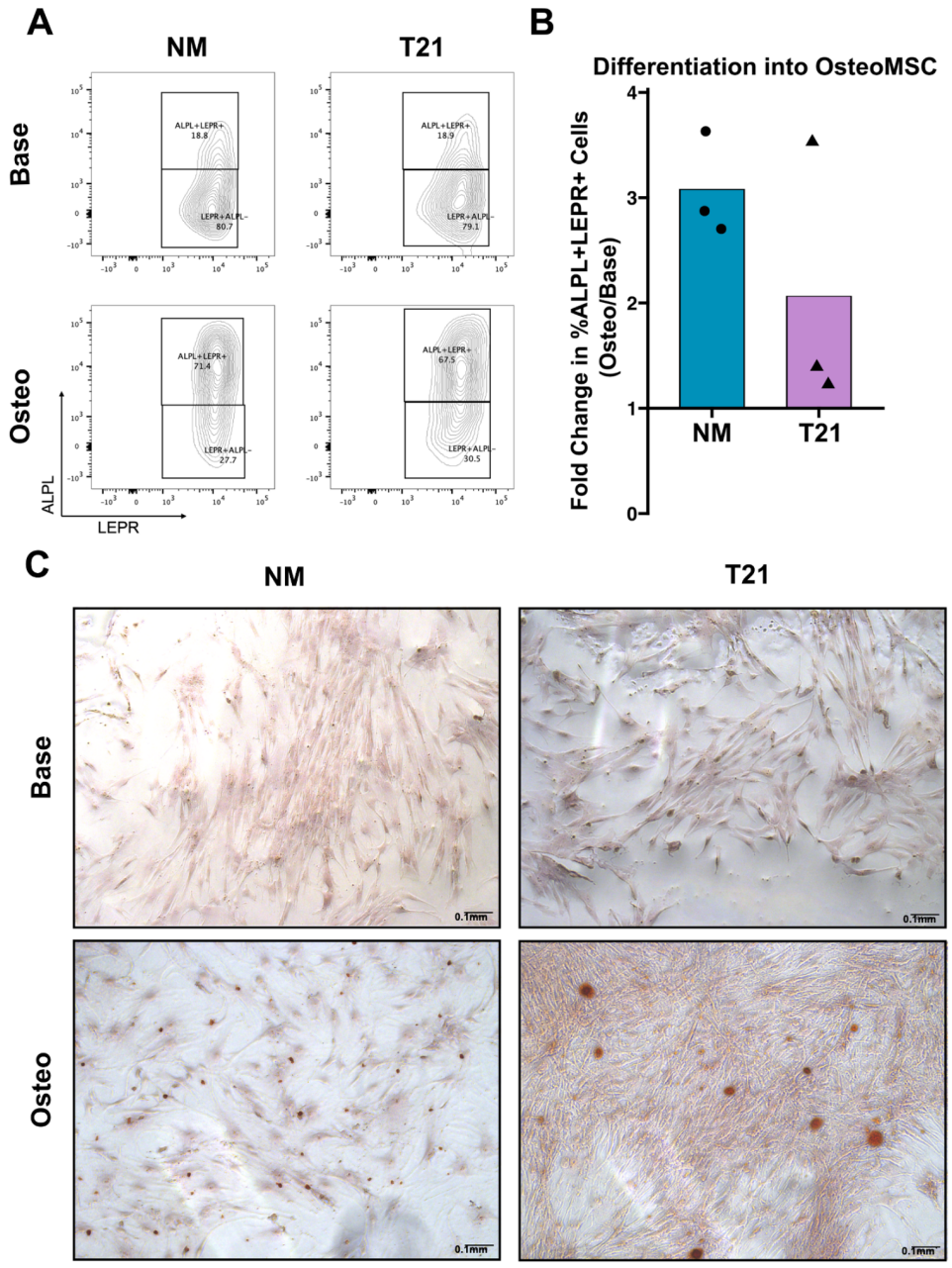

Figure 5.9: Osteo-lineage differentiation of NM and T21 fetal BM MSC *in vitro*. NM and T21 fetal BM MSC were cultured over two weeks *in vitro* under basal (αMEM-C10 medium) or osteogenic (osteo) (αMEM-C10 medium supplemented with 50μM ascorbic acid, 10mM β-glycerophosphate and 100nM dexamethasone) conditions. (A) Representative plots of live MSC under basal and osteogenic conditions (B) Fold change of the proportion of live cells co-expressing ALPL and LEPR under osteogenic conditions compared to basal conditions at day 14 of culture and (C) Alizarin Red staining at D14 of MSC under basal or osteogenic conditions. Scale bar = 100μm. NM, normal (n=3, passage=4-5, gestation age=17-18 PCW); T21, Trisomy 21 (n=3, passage=4-5, gestation age=17-18 PCW).

As shown in Figure 5.9, MSC from all NM but only one of three T21 fetal BM MSC samples underwent osteogenic differentiation *in vitro*, as assessed by fold change of percentage of ALPL+LEPR+ cells. To test differentiation of fetal BM MSC into osteoblasts, I carried out Alizarin Red staining to qualitatively assess matrix mineralisation. When cultured under osteogenic conditions, both NM and T21 fetal BM MSC showed calcium deposition *in vitro* after 14 days, with no clear differences in matrix mineralisation between NM and T21 fetal BM MSC. Though qualitative, Alizarin Red staining can be quantified, by extracting Alizarin Red dye using cetylperidinium chloride and performing spectrophotometry to quantify absorbance[724–726] - however, I did not perform this for this experiment.

However, matrix mineralisation at day 14 is only modest, and by flow cytometry, there are no ALPL+LEPR- osteoblasts at this time point. As such, longer *in vitro* MSC differentiation assays, coupled with quantitative Alizarin Red staining, would be required to more rigorously assess differences in osteoblastic differentiation and function *in vitro* between NM and T21 fetal BM MSC.

5.4 Understanding the role of haematopoietic cells that form part of the fetal BM microenvironment

I next considered differences in composition of the fetal BM haematopoietic compartment from published datasets[36, 45, 388], again only including in the analysis samples that were prepared for scRNA-Seq in the same way, by sorting CD45+ cells in Jardine et al. and Marderstein et al.[36, 388]. In contrast to the data in Chapter 3 which focused on HSPC, the scRNA-Seq datasets included all haematopoietic cells, both HSPC and mature cells which might form part of the BM microenvironment.

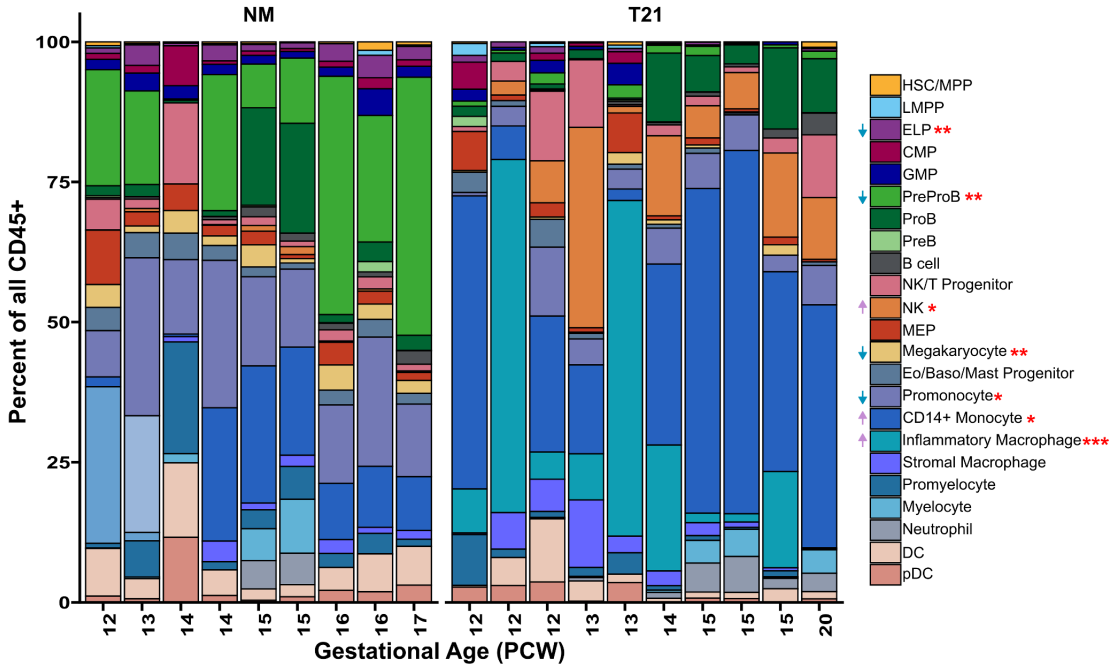

Figure 5.10: Frequency of haematopoietic cells in NM and T21 fetal BM by scRNA-Seq. Only samples processed similarly, by crushing and digestion, and sorting CD45+ cells[36, 695] are shown. T-test, * $p<0.05$, ** $p<0.01$, *** $p<0.001$; blue arrows pointing down show a population is depleted in T21 fetal BM, lilac arrows pointing up show an overrepresented population in T21 fetal BM. All statistically significant populations marked on key. NM, normal (n=9, k=57605, gestation age=12-17 PCW); T21, Trisomy 21 (n=10, k=12183, gestation age=12-20 PCW). Eo, eosinophil; Baso, Basophil; DC, dendritic cell; pDC, plasmacytoid dendritic cell. Only samples with more than 200 cells were included in this analysis.

T21 fetal BM samples showed a reduction in fetal-specific B progenitors, ELP and PreProB (Figure 5.11), as previously described by flow cytometry (Figure 3.1, page 75). Additionally, there was a significantly increased frequency of NK cells, monocytes and inflammatory macrophages in T21 fetal BM. These findings are consistent with the results from my own and previously conducted *in vitro* differentiation assays, which showed an increased myeloid output from T21 HSC, MPP and LMPP, and an increased NK output from lymphoid progenitors from T21 fetal BM HSPC (Figure 3.6, page 79, and Kate Murnane DPhil thesis).

Interestingly, megakaryocyte frequency was decreased in T21 fetal BM, as reported in Jardine et al.'s original paper[36], in contrast to T21 fetal liver[69, 387], and may reflect the technical difficulty of FAC-sorting megakaryocytes and/or capturing them for 10X scRNA-Seq.

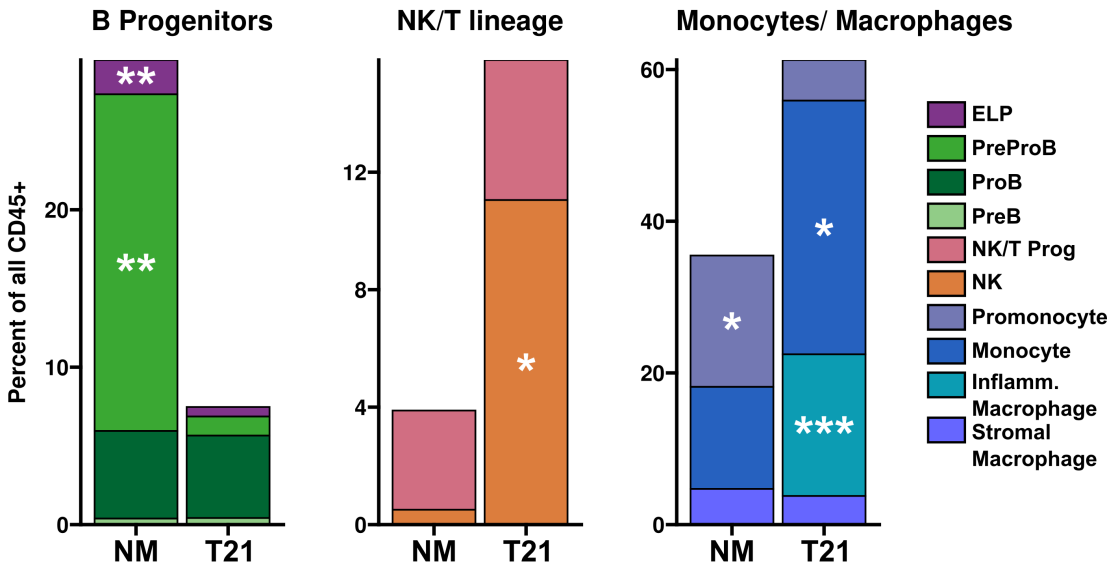

Figure 5.11: Differences in composition of haematopoietic cells in T21 fetal BM by scRNA-Seq. Only samples processed in the same way with over 200 cells were included in this analysis [36, 695]. NM, normal (n=9, k=42190, gestational age=12-17 PCW); T21, Trisomy 21 (n=10, k=9974, gestational age=12-20 PCW). T-test, * p<0.05, ** p <0.01, *** p <0.001.

To confirm the changes in the frequency of NK cells and monocyte/macrophages, I isolated fetal BM mononuclear cells and assessed the frequency of these cell types by flow cytometry. This showed a significant increase in NK cells in T21 compared to NM fetal BM (Figure 5.12). Total monocyte numbers (as assessed by the % of CD45+ cells that were CD14+) were not significantly different (Figure 5.12); however, the numbers of macrophages were not specifically determined as these BM samples were derived from flushed rather than crushed and digested bone.

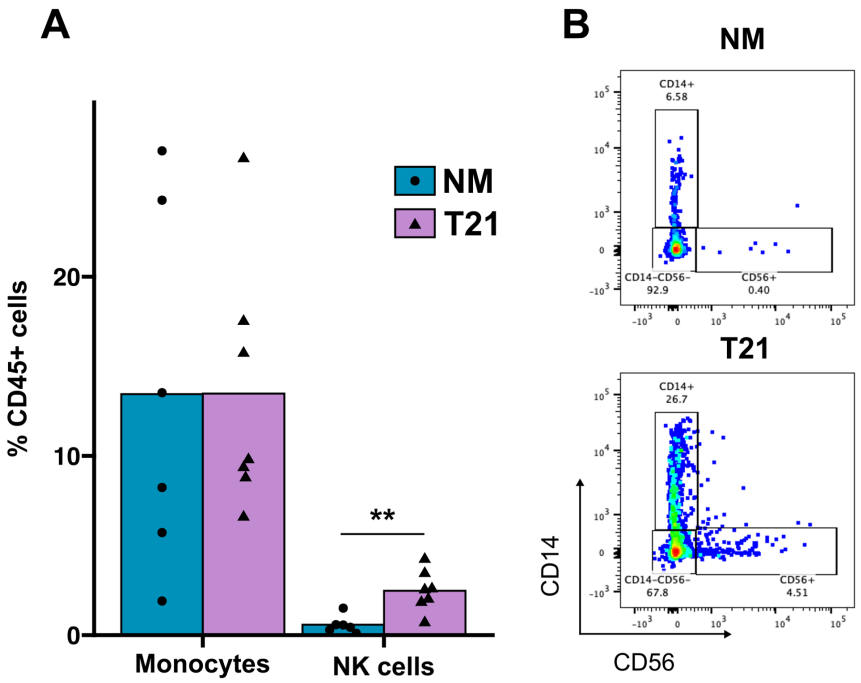

Figure 5.12: Frequency of NK cells and monocytes in NM and T21 fetal BM mononuclear cells. Mononuclear cells were isolated from the Ficoll-separated mononuclear layer and assessed by flow cytometry, summarised in (A). (B) Representative plots from NM and T21 fetal BM MNC, gated on live CD45+ cells. Monocytes defined by CD14 expression, NK cells by CD56 expression. NM, normal (n=6, gestation age=12-14 PCW, individual values represented by circles); T21, Trisomy 21 (n=7, gestation age=12-14 PCW, individual values represented by triangles).T-test,** p <0.01.

5.4.1 Inflammatory TNFα signalling in T21 fetal BM

The data in Chapters 3 and 4 identified a significant increase in TNFα response in T21 lymphoid progenitors and MSC by GSEA (Figures 3.28, 3.29 3.30, and 4.9, pages 120-123 and 143). Therefore, I next interrogated the scRNA-Seq dataset to identify the sources of TNFα in T21 fetal BM.

TNF expression in inflammatory macrophages was significantly increased in T21 fetal BM, while *TNFSF14* (LIGHT) expression was increased in T21 NK cells (Figure 5.13). Both of these populations had an increased frequency in T21 fetal BM (Figure 5.11). Expression of the receptors for TNFα TNFR1 (encoded by *TNFRSF1A*), and TNFR2 (encoded by *TNFRSF1B*); and TNFSF14 (*LTBR*) were also significantly increased in T21 LMPP (Figure 5.13). Analysis of the data using CellChat showed an increased inferred communication probability for both TNFα and LIGHT between T21 inflammatory macrophages and LMPP, and T21 NK cells and LMPP, respectively (Figure 5.13 panels B and C).

While inflammatory macrophages appeared to be the primary source of TNFα in NM fetal BM, B lineage cells also contributed to TNFα signalling. In T21 fetal BM, inflammatory macrophages remained the primary source of TNFα, but other haematopoietic cells also expressed *TNF* (dendritic cells, neutrophils, promonocytes and stromal macrophages, alongside NK/T progenitors)(Figure 5.14).

These data suggest aberrant TNFα production from increased numbers of T21 fetal BM macrophages, and other haematopoietic cells, may be responsible for the higher TNFα signalling in T21 fetal BM LMPP.

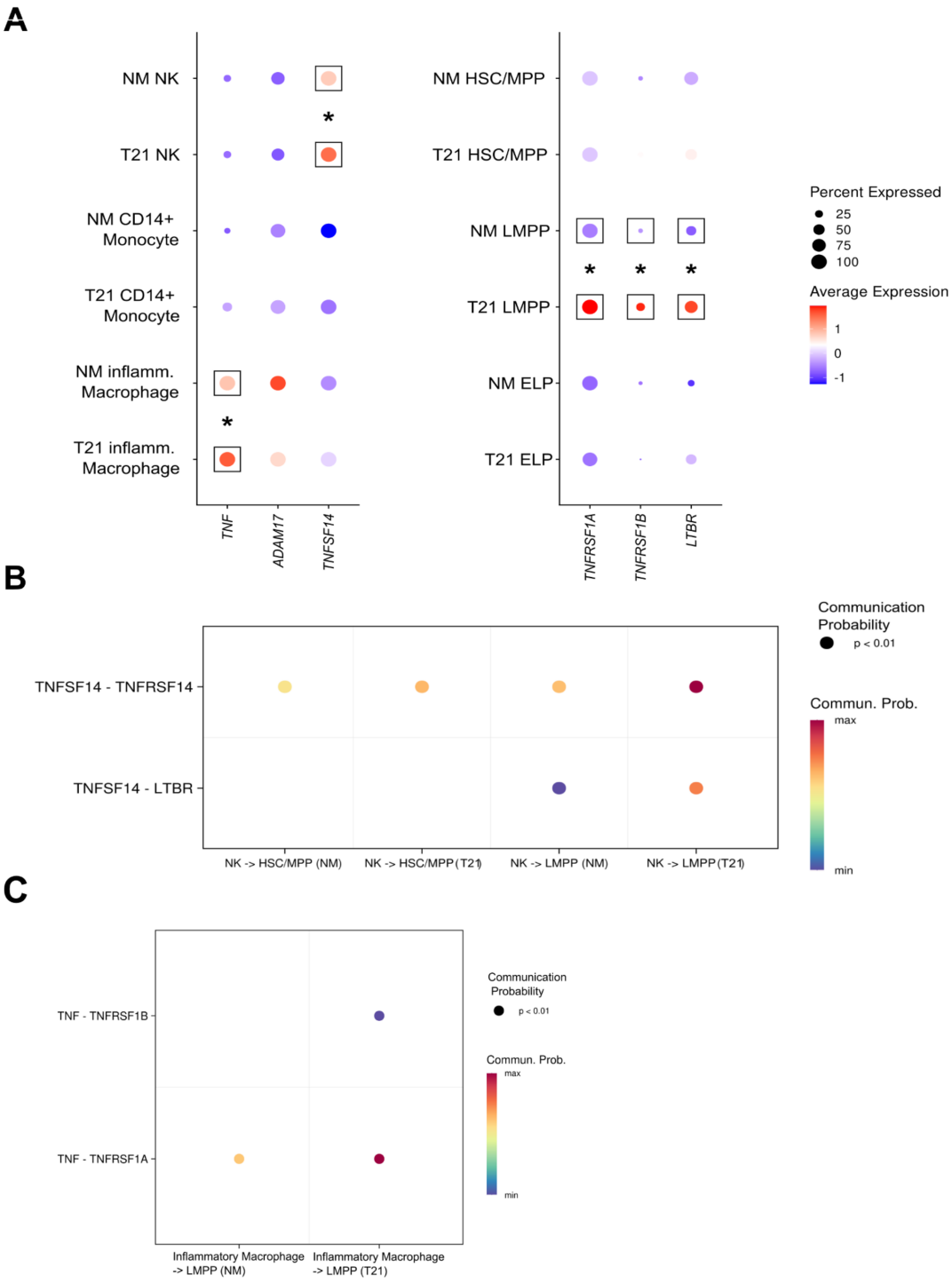

Figure 5.13: TNF signalling in fetal BM as inferred by gene expression. (A) Gene expression of TNF ligands and TNF receptors. Genes highlighted in a black box are statistically significantly differentially expressed between NM and T21 for a given population by CellChat (* denotes FDR <0.05). Communication probability by CellChat between (B) NK cells and HSC/MPP and LMPP for LIGHT signalling, and (C) TNFα signalling between inflammatory macrophages and LMPP. NM, normal (n=21, gestation age=12-17 PCW); T21, Trisomy 21 (n=16, gestation age=12-20 PCW)[36, 45, 695].

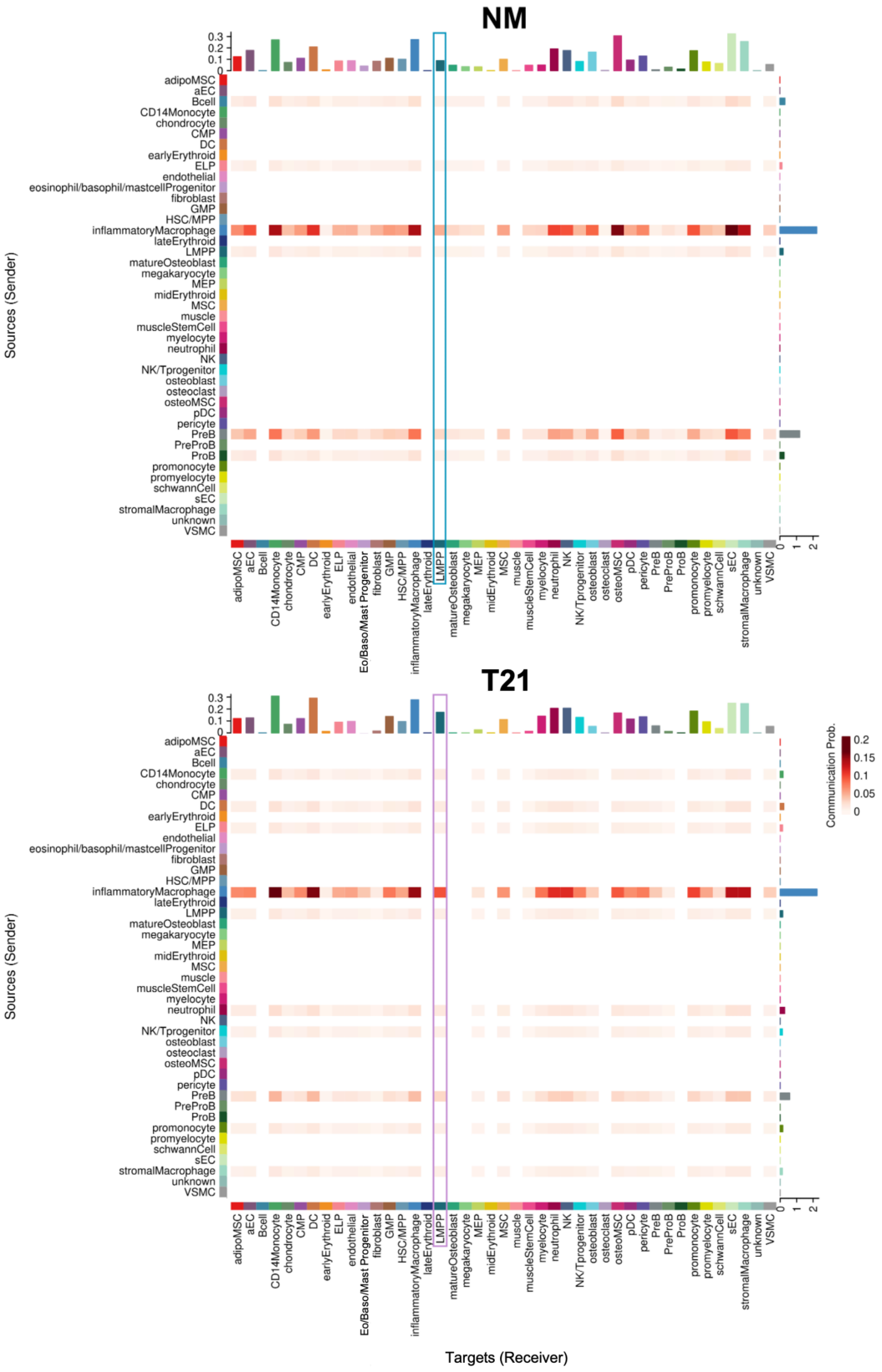

Figure 5.14: Sources and targets of TNFα in fetal BM inferred by CellChat. Key targets (x axis) and sources (y axis) in NM (top) and T21 (bottom) fetal BM. LMPP are highlighted. NM, normal (n=21, k=129040, gestation age=10-19PCW); T21, Trisomy 21 (n=16, k=67428, gestation age=12-20PCW)[36, 45, 695].

To test whether TNFα protein was increased in T21 fetal BM, I carried out intracellular flow cytometry staining for TNFα in fetal long bone samples that were processed by crushing and digestion. To detect TNFα, samples were stimulated with a low concentration of LPS (10ng/ml) and treated with a protein transport inhibitor (GolgiPlug, BD Biosciences) for five hours (Figure 5.15).

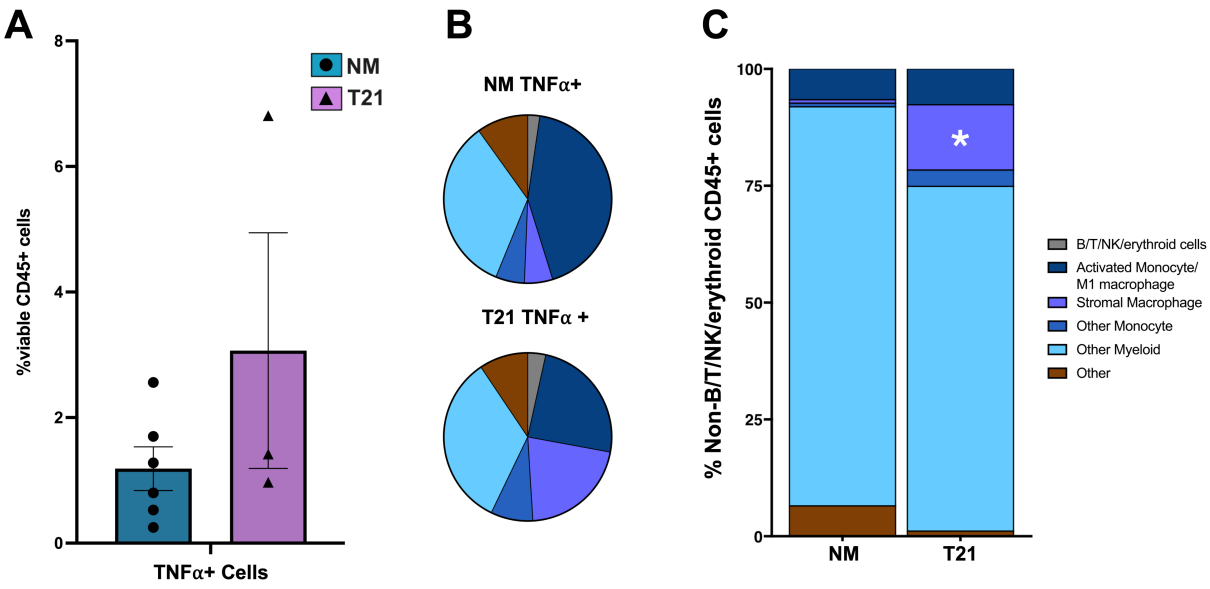

Figure 5.15: TNFα production in fetal BM. TNFα was measured by intracellular flow cytometry in NM and T21 fetal BM samples treated with a 10ng/ml LPS and a protein transport inhibitor. (A) Percentage of CD45+ cells expressing TNFα in NM and T21 fetal BM and (B) the identity of of TNFα expressing cells in NM and T21 fetal BM. (C) Composition of myeloid compartment of NM and T21 fetal BM. NM, n=6, gestational age= 12-17 PCW, circles represent individual data points in (A). T21, n=3, gestational age= 12-15 PCW, triangles represent individual data points in (A). B/T/NK/erythroid cells defined by expression of CD2/3/19/56/71/235a; activated monocytes/M1 macrophages (CD11b+CD14+TLR4+CD86+) other monocytes (CD11b+CD14+TLR4-CD86-); stromal macrophage (CD163+TLR4-CD86-CD11b-); and other myeloid (CD11b+CD14-) - see Figure 2.12, page 69 for gating strategy. *, T-test, $p<0.05$.

While less striking than the gene expression data, there appeared to be increased TNFα protein production in T21 fetal BM, however, more T21 fetal BM samples would need to be tested to assess whether this is significant (Figure 5.15A). The identity of cells producing TNFα in NM and T21 fetal BM differed, with the main TNFα-producing cells in NM fetal BM being mostly activated monocytes/inflammatory (M1) macrophages, while in T21, stromal macrophages

(defined by CD163 expression) were a larger proportion of TNFα-producing cells than in NM fetal BM (Figure 5.15B). This may reflect differences in overall myeloid compartment composition in T21 fetal BM, in which CD163+ stromal macrophages were more abundant by flow cytometry (Figure 5.15C).

Increased TNFα signalling at the LMPP stage (Figures 3.28, 3.29, and 3.30, pages 120 to 123) may impair lymphoid commitment, given its role in murine monocyte development[727] and murine emergency myelopoiesis[344]. In addition, previous work on human CD34+ cells *in vitro* suggested that TNFα potentiates IL3 and GM-CSF signalling, enhancing the early stages of myelopoiesis[728]. Other reports from *in vitro* experiments on human adult BM mononuclear cells suggest that TNFα suppresses overall colony-forming ability[729].

Indirect evidence for the role of TNFα in human B lymphopoiesis comes from autoimmune/inflammatory diseases where TNFα inhibitors are a third line treatment[730]. Patients with rheumatoid arthritis were reported to have fewer B cells than healthy controls[731, 732], while treatment with etanercept, a TNFα inhibitor, restored B cell frequency in rheumatoid arthritis patients[732]. A similar phenomenon is reported in patients with inflammatory bowel disease[733, 734].

There is also evidence that TNFα can indirectly impair B lymphopoiesis, by impairing CXCL12 production from murine BM niche[630] or by attenuating IGF1 signalling in the BM, by upregulating liver IGFBP1 production, as tested in murine models and supported by observations in human patients receiving anti-TNFα therapy for inflammatory joint disease[715].

Given that circulating TNFα is reported to be higher in individuals with Down syndrome[403, 425, 426, 683], TNFα signalling is a potentially attractive candidate mechanism contributing to the B lymphoid defect and myeloid skew in T21 fetal BM.

5.4.2 Functional validation of the role of TNFα in human fetal B lymphopoiesis

To directly test the impact of TNFα on differentiation of fetal BM HSC, MPP and LMPP, populations upstream of the hypothesised block in B lymphoid differentiation in T21, I cultured FAC-sorted NM fetal BM HSC, MPP and LMPP on MS5 stroma as before (Figure 3.6, page 79) but with increasing concentrations of TNFα and assessed their cellular output.

Addition of TNFα to NM fetal BM HSC, MPP and LMPP resulted in an overall reduction in the number of total CD45+ cells in a dose-dependent manner (Figure 5.16A). This is consistent with what has been described previously in murine HSPC[344] and adult BM MNC[729] (Figure 5.16A). In addition to reduced overall cell numbers, TNFα altered the proportional lineage output of HSC, MPP and LMPP, with a striking reduction in B cell and NK cell frequency, even at the lowest concentrations of TNFα. This was also accompanied by a concurrent increase monocyte output from HSC and MPP *in vitro* at the lowest concentrations of TNFα (0.1 and 1ng/ml), while higher concentrations of TNFα appeared to favour differentiation into other myeloid cells from HSC, MPP and LMPP (Figure 5.16B).

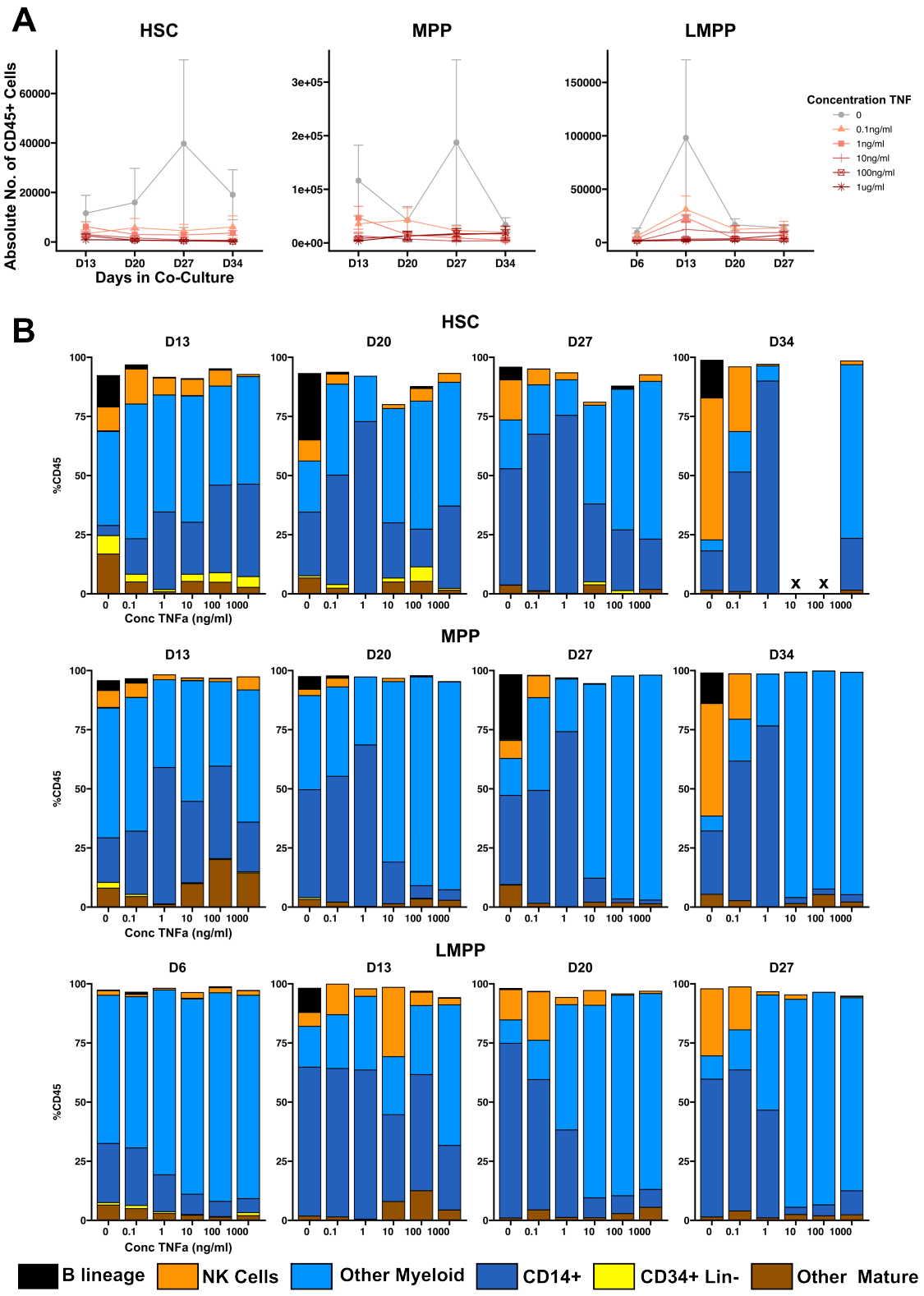

Figure 5.16: Co-cultures of NM fetal BM HSC, MPP and LMPP in the presence of TNFα. 100 FAC-sorted HSC, MPP and LMPP were plated on MS5 stromal cells and their differentiation was assessed over 4-5 weeks (D, day) (A) as mean absolute number of CD45+ cells ± SEM and (B) by mean proportional output. Samples with fewer than 50 CD45+ cells were excluded for panel B (marked by X), n=3. Other Myeloid: CD11b/CD15/CD33+ CD14-.

I also collected the supernatants from these co-culture assays, and tested media collected at day 13 of co-culture from NM and T21 LMPP for secreted TNFα by ELISA. I used THP1 cells treated with PMA to induce macrophage differentiation, and subsequently stimulated with 10ng/ml LPS as a positive control. This showed comparable levels of secreted TNFα in co-culture supernatants from NM and T21 LMPP at day 13 in culture, the time point at which the most B cells are produced (Figure 5.17A).

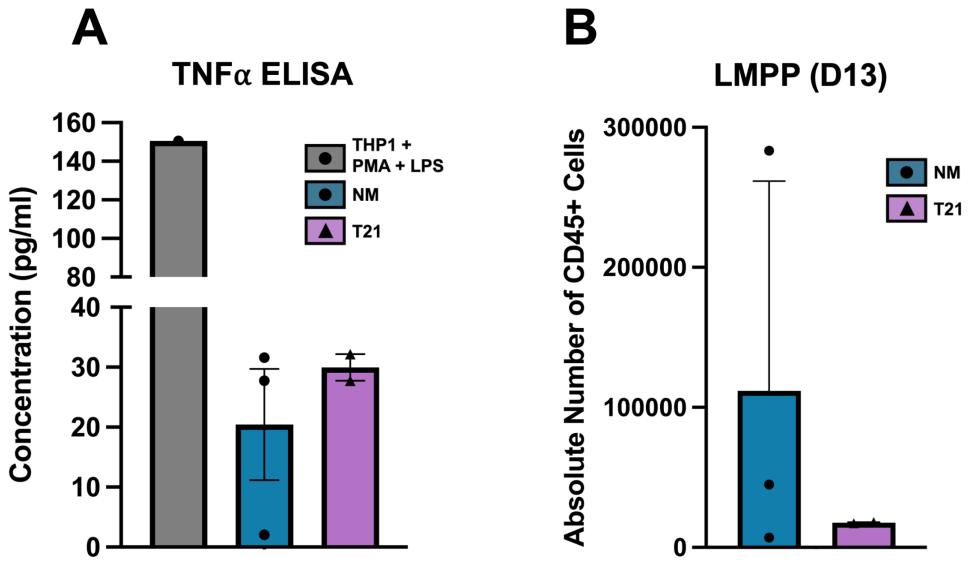

Figure 5.17: Secreted TNFα in NM and T21 fetal BM LMPP co-culture supernatants. (A) Concentration of TNFα as detected by ELISA at day 13 of co-culture. (B) Absolute number of CD45+ cells at day 13 (D13) of co-culture, as measured by flow cytometry, from cultures initiated with 100 NM or T21 fetal BM LMPP, NM, n=3; T21, n=2.

Although equal levels of TNFα in NM and T21 LMPP co-cultures may appear inconsistent with the hypothesis that TNFα is elevated in T21 fetal haematopoiesis, this result could be interpreted in the context of cellular output. T21 fetal BM LMPP generated fewer CD45+ cells in culture than NM fetal BM LMPP (Figure 5.17B), in line with what has been previously described (Kate Murnane DPhil Thesis). Therefore, for total TNFα to be equivalent, TNFα production per cell must be higher in T21 LMPP co-cultures. While in these *in vitro* assays all cells

share the same concentration of cytokines, this may not be the case in native BM within specialised niches.

TNFα is first synthesised as a transmembrane protein, and is only secreted once it is cleaved by the enzyme TACE (encoded by *ADAM17*)[735, 736]. Interestingly, *ADAM17* expression in T21 inflammatory macrophages by scRNA-Seq appeared to be lower than their normal counterparts, though this did not reach significance (Figure 5.13). While secreted TNFα is well studied as an inflammatory mediator (as reviewed in [737]), transmembrane TNFα is also an important mediator of local inflammation[738–740]. It is possible that transmembrane TNFα signalling plays a greater role in mediating the T21 TNFα response in T21 fetal lymphoid progenitors.

Experiments in human cell lines have demonstrated that both transmembrane and secreted forms forms of TNFα can bind the receptors TNFR1 (encoded by *TNFRSF1A*) and TNFR2 (encoded by *TNFRSF1B*), but TNFR2 binds, and is more strongly activated by transmembrane TNFα[741]. While signalling through both TNFα receptors activates the canonical NFκB pathway, which results in cell activation, differentiation and inflammation, TNFR1 signalling can lead to apoptosis and necroptosis, while TNFR2 signalling can also result in the activation of the alternative NFκB pathway, which also results in cell proliferation (reviewed in [742]). Taken together, these differences in TNFα signalling may be a potential explanation for the differential haematopoietic output from T21 LMPP.

5.5 Summary and discussion

This chapter aimed to explore differences in niche composition and signalling in T21 fetal BM and how these may contribute to impaired B lymphopoiesis. Integrating recently generated scRNA-Seq datasets of NM and T21 fetal BM[36, 45, 388] provided novel insights into niche composition and signalling that would have not been identified in any of the datasets in isolation, due to insufficient n numbers across gestational ages and representation of rarer cell populations. This analysis provided preliminary evidence of two potential mechanisms that may contribute to impaired B lymphopoiesis in T21 fetal BM: (1) decreased stromal support from

T21 osteoMSC for B lymphopoiesis, and (2) increased TNFα signalling originating from the T21 fetal BM haematopoietic niche.

Reduced osteolineage stromal support for B lymphopoiesis in T21 fetal BM

Individuals with Down syndrome exhibit abnormal bone development[492]; *in utero*, they have decreased long bone length[498, 499], and in postnatal life have lower bone mineral density, and an increased risk of fractures and osteoporosis[493]. This is also recapitulated in murine models of Down syndrome[494, 495].

Flow cytometry of fetal BM showed a reduced trend in osteoMSC frequency in T21, and transcriptomically, undifferentiated T21 fetal BM MSC appeared to be primed towards adipoMSC differentiation, rather than osteoMSC. Inferred activity of key osteoblastic transcription factors, SP7 and RUNX2, was reduced in T21 fetal BM MSC, and instead there was an increase in inferred activity of transcription factors with a known role in adipogenesis, suggestive of impaired osteolineage differentiation in T21.

Functional validation of impaired osteolineage differentiation from cultured T21 fetal BM MSC *in vitro* provided preliminary evidence for impaired osteoMSC differentiation from T21 fetal BM MSC, though further experiments would be needed to confirm this. In addition to reduced numbers, the osteoMSC in T21 fetal BM expressed significantly lower levels of *CXCL12*, *IL7* and *IGF2* compared to their normal counterparts, all of which are cytokines which support B lymphopoiesis [98, 290, 723, 743]. This raises the possibility that both decreased osteoMSC frequency and a reduction in cytokines supporting B lymphopoiesis may contribute to the failure to activate the B lymphoid programme in T21 lymphoid progenitors.

Inflammatory TNFα signalling in T21 fetal BM

Interrogation of the scRNA-Seq data allowed identification of several sources of TNFα, the primary source being inflammatory macrophages, which were significantly increased in frequency in T21 fetal BM. Intracellular flow cytometry also showed that there was a (non-significant) increase in TNFα-producing cells in T21 fetal

BM, primarily myeloid cells. Taken together, these observations suggest that TNFα signalling in T21 fetal BM was increased, as a result of an increased frequency of TNFα producing cells and increased *TNF* expression in these cells in T21.

Preliminary validation of the role of TNFα in fetal B lymphopoiesis found that the addition of TNFα, even at low concentrations (0.1ng/ml), reduced total haematopoietic output and B lymphoid output, favouring myelopoiesis, recapitulating some features of T21 haematopoiesis.

These findings provide interesting preliminary evidence suggesting that elevated TNFα signalling in T21 fetal BM may impair B lymphopoiesis.

5.5.1 Future work

Although analysis of the integrated scRNA-Seq dataset has been valuable for characterising the BM niche in T21 fetal BM, revealing that stromal cells may provide diminished B lymphopoietic support and that macrophages mediate inflammatory signalling through TNFα production, spatial studies of fetal BM would be interesting in order to determine whether spatially delineated niches support B lymphopoiesis within the fetal BM, and whether this is altered in T21. Additionally, adipocytes are not captured well by scRNA-Seq, but could be identified in tissue sections of fetal BM, which could test the hypothesis that T21 fetal BM MSC are primed to differentiate into adipocytes; it would also be interesting to test whether T21 fetal BM MSC show an increased adipocytic differentiation *in vitro*. Functional testing to assess whether osteolineage cells derived from T21 fetal BM provide decreased B lymphopoietic support, and whether fetal BM adipocytes inhibit B lymphopoiesis could also provide interesting new insights. Finally, further investigation of the potential role of TNFα in inhibiting T21 B lymphopoiesis would be useful including testing the effects of TNFα inhibitors and assessment of the balance between membrane bound and secreted TNFα.

6
Discussion

Previous studies in adults and children have conclusively shown that individuals with Down syndrome have a striking reduction in B cell frequency. This is clinically important because these individuals also have an increased risk of severe infection, infection-related mortality, autoimmunity [386, 398, 403, 434, 435, 439] and B cell leukaemia[354, 356, 440]. This reduction in B cell frequency can be traced back to fetal life where reduced B progenitors and reduced B cell output from upstream HSC and multipotent progenitors is found both in T21 fetal liver and BM[36, 69]. However, the molecular basis of this has been unclear.

In this thesis, I have investigated the cellular and molecular basis of impaired fetal B lymphopoiesis in T21 fetal BM, the main site of B lymphopoiesis from the second trimester onwards[20], by molecularly characterising T21 fetal BM HSPC, characterising and functionally testing the role of the T21 fetal BM niche, and specifically testing the role of niche-derived inflammatory signalling in T21 fetal BM in impairing B lymphopoiesis.

6.1 The impact of T21 on fetal BM B lymphopoiesis

In Chapter 3, I measured the frequency of lymphoid progenitors in T21 fetal BM, to try to identify the point along the haematopoietic hierarchy at which B lymphopoiesis is impaired. As well as confirming the profound reduction in the fetal-specific lymphoid progenitors ELP and PreProB in T21 fetal BM, I also found reduced numbers of their upstream progenitor PreELP/GMP alongside a more moderate reduction in CLP, the principal committed common lymphoid progenitor in adult BM. This was accompanied by an increase in the multi-lymphoid progenitor MLP which is recognised in adult BM as the progenitor upstream of CLP[67, 68]. Neither MLP nor CLP had previously been demonstrated in fetal BM and their frequency was very low both in NM and T21 fetal BM suggesting that they mainly represent an adult-type pathway. Taken together the frequency data suggest that the defect in T21 fetal BM mainly resides in the CD10-ve fetal-specific pathway of B lymphoid development.

To investigate the mechanisms underlying this defect, I especially focused on the HSPC upstream of the block in the fetal-type pathway. I first tested the haematopoietic output of T21 HSC, MPP and LMPP *in vitro*, which demonstrated a striking reduction in B lymphoid output from these early stages in differentiation and a skew towards NK cell output. The culture system used for these assays does not support T cell differentiation *in vitro* but nevertheless, these data suggest that there is already a defect specifically in B lymphoid specification upstream of PreELP/GMP, rather than lymphoid specification in general, since NK production was preserved.

Transcriptomic profiling to identify the molecular basis for these changes surprisingly, did not reveal significant differences in the level of expression of the genes I selected as indicators of B lymphoid specification and commitment in HSC, MPP and LMPP. However, this may well reflect the heterogeneity in expression levels between different samples especially in bulk RNA-Seq, and it is worth noting that overall expression of one of the major lymphoid specification genes *FLT3* was lower in T21 HSC, MPP and LMPP. In contrast, transcriptomic profiling did show that in the progenitors immediately downstream of LMPP, there

was a failure to activate B lymphoid programmes in T21 fetal BM. Thus, in the lymphoid-committed fetal-specific progenitors PreELP/GMP and ELP prior to the B lymphoid committed stage, expression of hallmark genes, such as *EBF1*, *RAG1* and *RAG2* was reduced and WGCNA showed impaired expression of the B lymphopoietic module compared to NM fetal BM controls. This would explain the severely reduced B cell output of these progenitors.

Further interrogation of the RNA-Seq and ATAC-Seq data did identify some potential clues to the mechanism of the lymphoid defects in T21 fetal BM. Given the lack of clear differences in lymphoid gene expression between T21 and NM fetal BM HSC, MPP, and LMPP when I used preselected genes, I next took an unbiased approach to see if I could identify significant differences in chromatin accessibility and gene expression. The two most striking features were first, the large number of differentially expressed genes genome-wide, particularly in PreELP/GMP, ELP and, to a lesser extent in MPP; and second, the large number of differentially expressed genes on chromosome 21, particularly in PreELP/GMP, ELP and MPP but also in HSC and LMPP. In support of this, the greatest number of differentially accessible peaks by ATAC-Seq was also, by a long way, on chromosome 21 and this was seen particularly in LMPP, HSC and MPP. The relevant genes affected were *RUNX1* (in all populations), *DYRK1A* (in LMPP) and *INFAR2* (in HSC) which play a role in B cell development and inflammation respectively.

However, overall, my analyses of bulk RNA-Seq data, ATAC-Seq data and scRNA-Seq data indicated that these changes in gene expression were complex and no single mechanism could fully explain the changes observed.

I next explored three possibilities.

First, that suppression of B lymphopoietic programmes was the result of a failure to silence alternative fates in progenitors that would normally be committed to the B lymphoid lineage. Some evidence for this was found. For example, expression of the granulocyte-monocyte transcription factor *CEBPA* was higher in T21 fetal BM PreELP/GMP, and its inferred activity was higher in LMPP compared to NM fetal

BM controls. However, these progenitors retain the ability to undergo granulocyte-monocyte differentiation and this observation may simply mean that more individual cells in what is likely to be a mixed population are undergoing commitment to the granulocyte-monocyte lineage rather than inappropriate activation of *CEBPA* in these cells. Similarly, there was increased expression of T/NK lymphoid genes in T21 fetal BM LMPP (*TCF7* overexpressed), and in T21 fetal BM ELP, in which *GATA3*, *TCF7* and *ZBTB16* were increased; and increased inferred activity of *NFIL3*, a transcription factor with an essential role in NK cell development[635]. However, as these progenitors still have the ability to produce T and NK cells this finding is consistent with the functional output of these cells rather than inappropriate activation of these genes in these cell populations. Nevertheless, ongoing expression of these lineage directing genes may be sufficient to limit the opportunities for B cell differentiation in these multilymphoid populations and further work would be needed to determine whether the ongoing expression of non-B genes directly suppresses expression key B lineage genes.

Second, as noted above, altered expression of chromosome 21 genes may contribute to impaired B lymphoid specification in T21 fetal BM HSPC. Chromatin upstream of *RUNX1*, as well as RUNX1 binding motifs were significantly more accessible in T21 fetal BM HSC, MPP and LMPP. While *RUNX1* itself was not significantly differentially expressed by RNA-Seq, there was preliminary evidence to suggest that RUNX1 isoform balance was altered in T21 fetal BM HSC, MPP and LMPP. While the direct effect of this in B lymphopoiesis has not been characterised, this has been implicated in the pathology of TAM/ML-DS[607], and RUNX1 plays an important role in B lymphopoiesis in mice, promoting B lymphoid specification, survival of B progenitors and progression through the PreB stage of B lymphopoiesis[605, 606].

Finally, a third possibility is that inflammatory signalling from the haematopoietic niche may skew T21 fetal BM HSPC fate decisions, as T21 lymphoid progenitors showed a significantly increased TNFα response compared to their normal counterparts. TNFα promotes myelopoiesis[344, 727, 728]. Additionally, there is indirect

evidence to suggest TNFα impairs B lymphopoiesis, as patients with autoimmune/ inflammatory conditions such as rheumatoid arthritis and inflammatory bowel disease have a reduced B cell frequency, which is improved upon receiving anti-TNFα treatment [731–734]. TNFα also attenuates niche-derived B lymphopoietic signals, by reducing CXCL12 secretion in murine BM[630] and resulting in increased IGFBP1 production, which attenuates IGF1 signalling in human BM[715], both of which have been linked to reducing B lymphopoiesis.

It is likely that all three of these mechanisms may contribute, at least in part, to the defect in B lymphopoiesis in T21.

6.2 The impact of T21 on stromal support for fetal BM B lymphopoiesis

In Chapter 4, I investigated the impact of the T21 fetal BM niche on fetal haematopoiesis. Overall, even though the T21 fetal BM MSC were transcriptomically distinct with a number of differentially expressed genes, functional co-culture experiments suggested that T21 MSC were likely to play a minor role in impaired B lymphopoiesis in T21 fetal BM. However, when I considered the whole stromal compartment in fetal BM in Chapter 5, rather than culture-derived MSC, there were a number of differences between T21 and NM fetal BM.

Analysis of the integrated scRNA-Seq dataset specifically identified osteoMSC, rather than undifferentiated MSC, as an especially important source of B lymphopoietic support cytokines in NM fetal BM. Furthermore, T21 fetal BM osteoMSC had significantly decreased expression of cytokines *IL7*, *CXCL12* and *IGF2*, which are important in supporting B lymphopoiesis[98, 290, 723, 743]. In addition, analysis of the scRNA-Seq dataset suggested that T21 fetal BM MSC were primed to differentiate into adipoMSC rather than osteoMSC. Defects in osteoblast function and skeletal development have been described in individuals with Down syndrome[492], which can be traced back to fetal life, with T21 fetal long bone length being decreased[498, 499]. Additionally, individuals with Down syndrome have lower bone mineral density, and an increased risk of osteoporosis and fractures[493],

and this has also been observed in T21 murine models[494, 495]. My preliminary validation of osteolineage differentiation of NM and T21 fetal BM *in vitro* suggested a decreased response to osteolineage differentiation conditions from T21 fetal BM MSC, but further experiments would be required to validate the results from bulk RNA-Seq and scRNA-Seq of NM and T21 fetal BM MSC. This would be an interesting observation because it is possible that reduction in expression of B lymphopoietic support cytokines IL7, CXCL12 and IGF2 from T21 fetal BM osteoMSC, coupled with impaired differentiation into osteoMSC, may be another mechanism contributing to impaired B lymphopoiesis in T21 fetal BM.

6.3 The impact of inflammation in T21 fetal BM on B lymphopoiesis

In Chapter 5, I explored the possible contribution of T21-mediated increased inflammation in fetal BM to the impaired B lymphopoiesis. This was prompted by the finding in scRNA-Seq analysis of increased expression of *TNF* across a broader range of cell types, suggestive of a global increase in TNFα signalling. Importantly, T21 LMPP had significantly increased expression of *TNFR1* and *TNFR2* by scRNA-Seq, suggesting they may be more responsive to TNFα. Further interrogation of the integrated scRNA-Seq datasets identified inflammatory macrophages, a population with a significantly increased frequency in T21 fetal BM by scRNA-Seq, as the primary source of TNFα in T21 fetal BM.

My preliminary experiments have supported a role for TNFα in the B lymphoid defect in T21 fetal BM, although much more work would be needed to validate these findings and to determine the precise mechanism. What I have shown is an increased trend in TNFα production in T21 fetal BM myeloid cells following LPS stimulation although this did not reach statistical significance; and that when HSC, MPP and LMPP from NM fetal BM were cultured *in vitro* with TNFα, total haematopoietic output, and particularly B cell output, was markedly reduced.

These preliminary findings suggest that increased TNFα signalling may contribute to the impairment in B lymphopoiesis in T21 fetal BM and may explain

some of the interindividual differences in the degree of impairment. The results are in line with previous studies showing increased TNFα signalling in children[423, 426] and adults[403, 425, 426, 632] with Down syndrome. However, the role of altered TNFα signalling in the postnatal defects in perturbed B cell function in infection, autoimmunity and B cell leukaemia is currently unclear.

6.4 Future work

An inherent technical limitation of working with primary fetal samples is sample size and availability, which was especially the case with T21 fetal samples. Many of my experiments required rare HSPC populations HSC, MPP and LMPP, and I occasionally had to pool samples to have adequate numbers to carry out the experiments planned. Additionally, while some of this preliminary work shows initial promise, such as TNFα signalling as a mechanism by which B lymphopoiesis is impaired in T21 fetal BM, additional work would be required in order to confirm the findings and to identify the mechanisms involved.

Several of my findings in this project that have led to some specific and tractable questions.

Firstly, it would be interesting to assess the contribution of altered *RUNX1* isoform expression, for example by using long read RNA-Seq (such as that offered by Oxford Nanopore). It would also be interesting to assess RUNX1 binding in T21 fetal BM, perhaps by CUT&RUN, as RUNX1 binding motifs were significantly more accessible in T21 fetal BM HSC, MPP and LMPP. Given the multiple roles of RUNX1 in human and murine haematopoiesis[605, 606, 744, 745], and the evidence suggesting its function may be altered in T21[379, 607], it would be interesting to better characterise RUNX1 activity in the context of T21 fetal BM HSC, MPP and LMPP, bearing in mind isoform specific differences.

Second, the integrated scRNA-Seq dataset has provided a good starting point for exploring alterations in the fetal BM niche in T21 in more detail. Spatial studies are likely to provide additional important information about the likely functional significance of cell:cell interactions inferred from computational data

and differences in frequency of specific stromal components, such as inflammatory macrophages or osteoMSC. Additionally, the observation that T21 osteoMSC express lower levels of genes such as *IL7*, *CXCL12* and *IGF2* would need to be tested and functionally validated in BM organoids. Some T21 model mice also exhibit skeletal abnormalities[494, 497, 746], and it would be interesting to study B lymphopoiesis using these models, to specifically assess altered osteoMSC support.

Finally, there remain many unanswered questions about the nature and mechanism(s) of the increased TNFα response and signalling in T21 fetal BM, including assessment of the balance between membrane bound and secreted TNFα signalling, and whether blockade of TNFα signalling can rescue T21 fetal BM B lymphopoiesis. These experiments could be done using a BM organoid model and potentially also mouse models. Given the evidence that TNFα inhibition improves B cell frequency in some inflammatory/ autoimmune disease, TNFα inhibition may be an interesting therapeutic avenue explore in T21, to improve B lymphopoiesis and temper hyperinflammation and autoimmunity in individuals with Down syndrome.

6.5 Conclusions

In this thesis, I have shown that there is a commensurate reduction in frequency of fetal-specific B lymphoid progenitors, accompanied by a striking reduction in expression of key B lymphoid genes in fetal-specific lymphoid progenitors. Collectively, these data illustrate that multiple pathways may converge to impair fetal B lymphopoiesis in T21 fetal BM, from sustained expression of non-B lymphoid genes in T21 fetal BM lymphoid progenitors, to reduced stromal support from the T21 fetal BM niche, and increased TNFα signalling from myeloid cells in T21 fetal BM. This work provides novel mechanistic insight into impaired B lymphopoiesis in T21 fetal BM and sets the scene for future work dissecting these pathways in further detail, and how they may predispose children with Down syndrome to ALL and autoimmunity.

Appendices

.1 Expression of lineage-specific genes by RNA-Seq in NM fetal BM

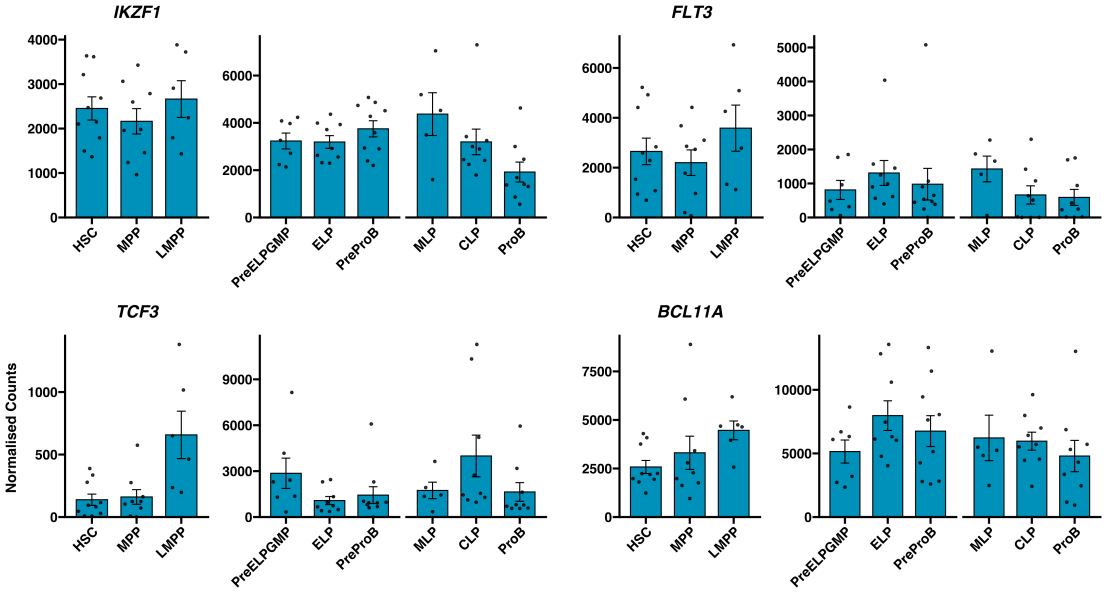

Figure 1: Expression of genes with a known role lymphoid specification in NM by RNA-Seq (50-100 cells). For each gene, graphs are grouped (from left to right) for primitive HSPC, fetal specific lymphoid progenitors, and adult type lymphoid progenitors. Mean ± SEM, * denotes significance by DESeq2 (p-adj<0.1). NM (normal, blue bars represent mean expression, dots represent biological samples, n=5-10).

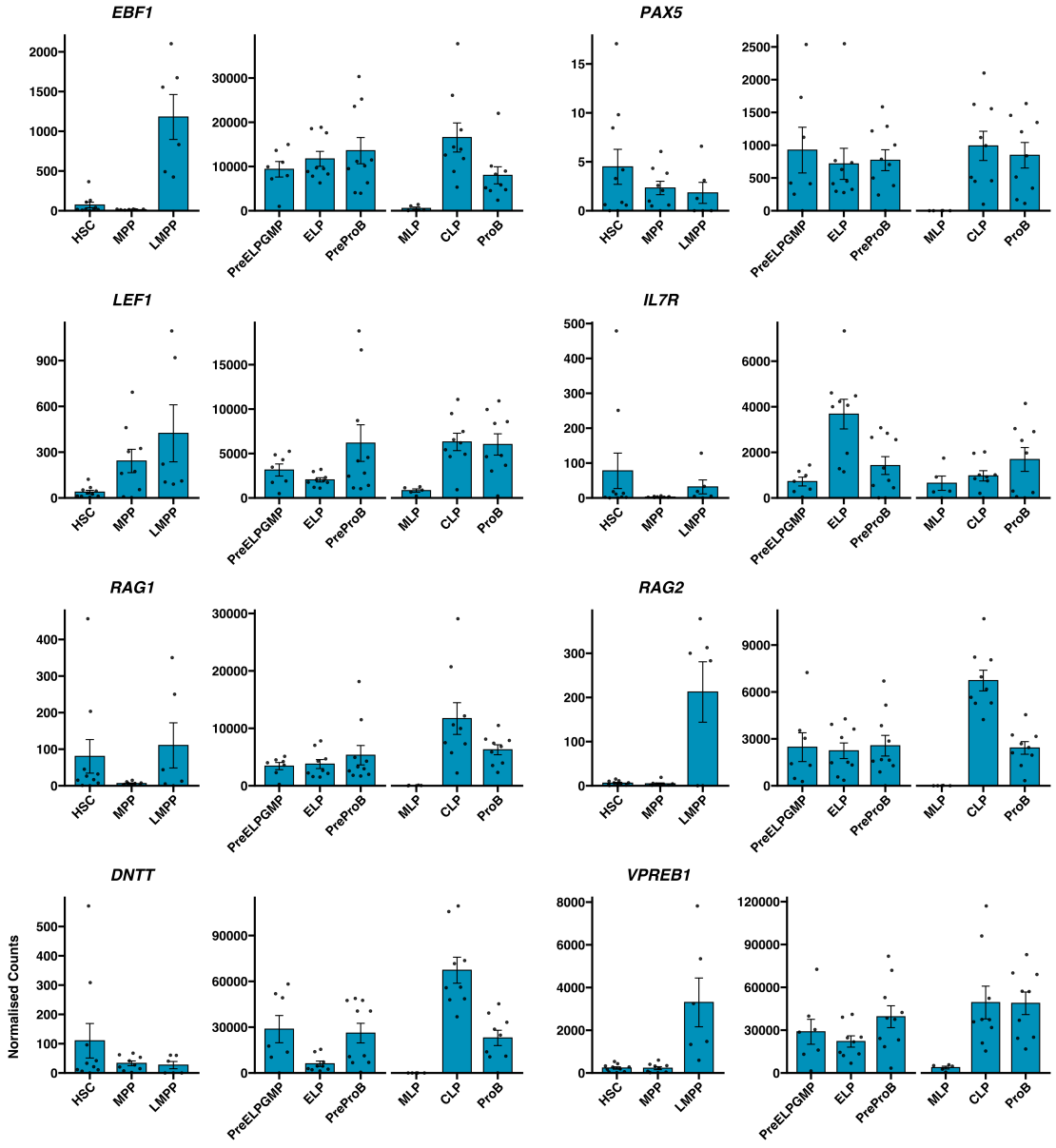

Figure 2: Expression genes with a known role in B lymphopoiesis in NM fetal BM HSPC by RNA-Seq (50-100 cells). For each gene, graphs are grouped (from left to right) for primitive HSPC, fetal specific lymphoid progenitors, and adult type lymphoid progenitors. Mean ± SEM, * denotes significance by DESeq2 (p-adj<0.1). NM (normal, blue bars represent mean expression, dots represent biological samples, n=5-10).

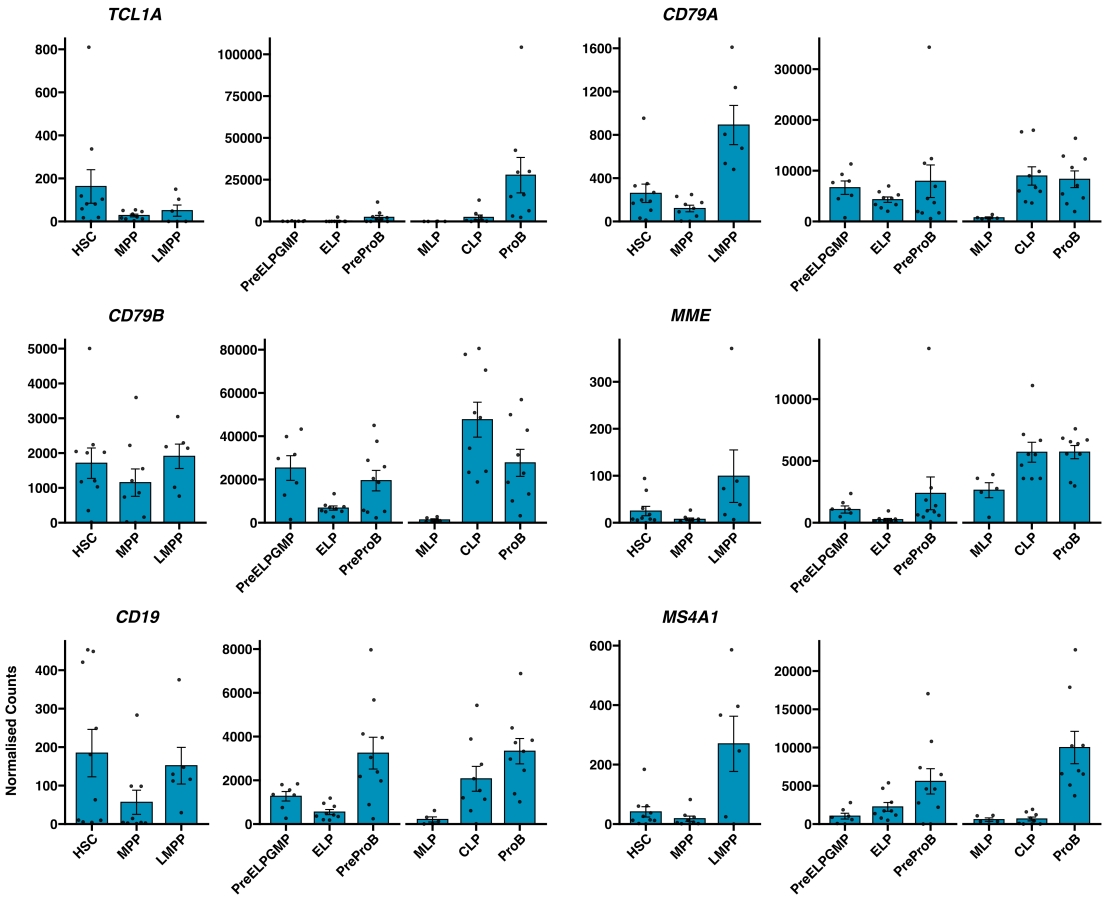

Figure 3: Expression genes with a known role in B cell development in NM fetal BM HSPC by RNA-Seq (50-100 cells). For each gene, graphs are grouped (from left to right) for primitive HSPC, fetal specific lymphoid progenitors, and adult type lymphoid progenitors. Mean ± SEM, * denotes significance by DESeq2 (p-adj<0.1). NM (normal, blue bars represent mean expression, dots represent biological samples, n=5-10).

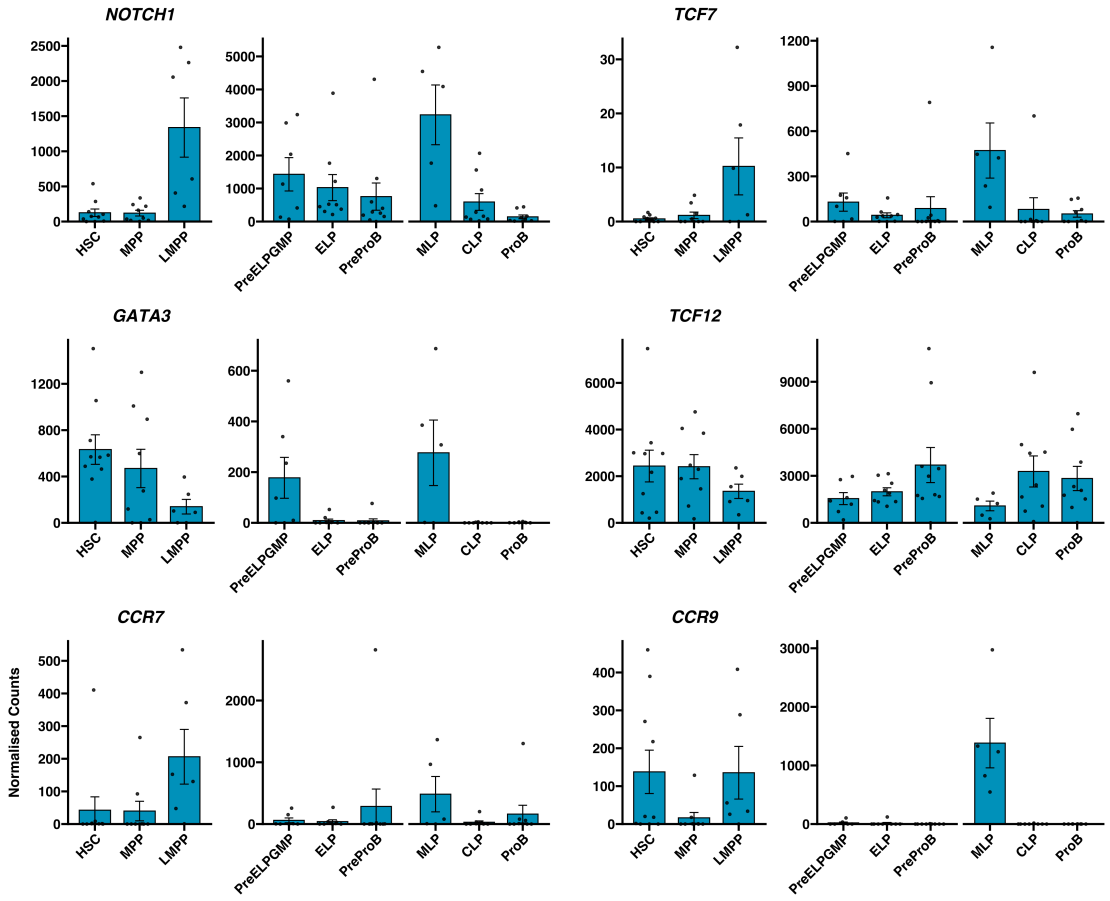

Figure 4: Expression of genes selected for their role in T lymphopoiesis in NM fetal BM HSPC by RNA-Seq (50-100 cells). For each gene, graphs are grouped (from left to right) for primitive HSPC, fetal specific lymphoid progenitors, and adult type lymphoid progenitors. Mean ± SEM, * denotes significance by DESeq2 (p-adj<0.1). NM (normal, blue bars represent mean expression, dots represent biological samples, n=5-10).

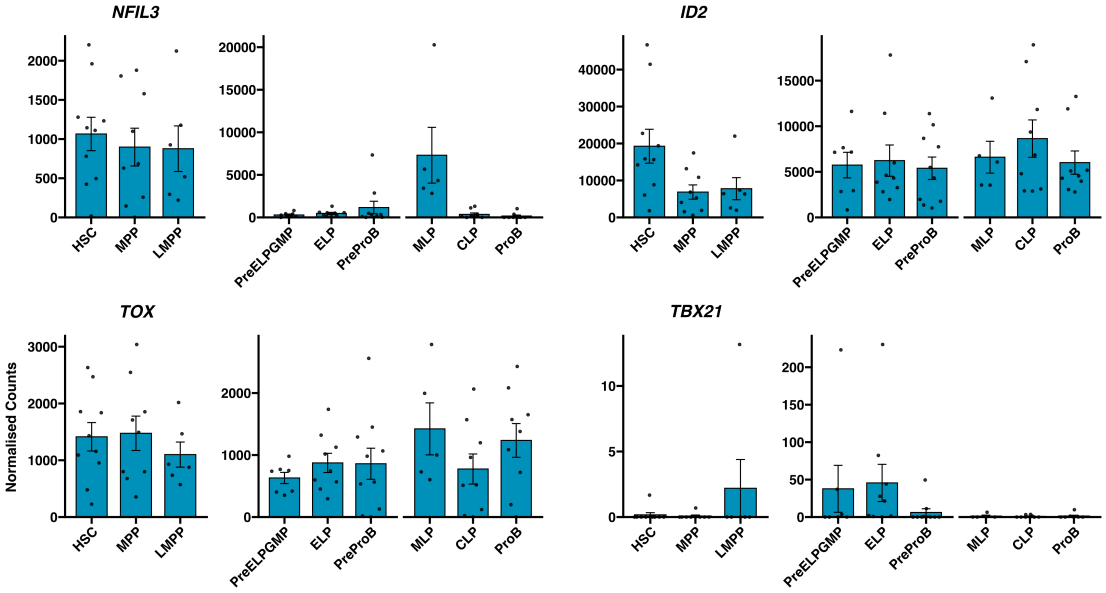

Figure 5: Expression of genes selected for their role in NK lymphopoiesis in NM fetal BM HSPC by RNA-Seq (50-100 cells). For each gene, graphs are grouped (from left to right) for primitive HSPC, fetal specific lymphoid progenitors, and adult type lymphoid progenitors. Mean ± SEM, * denotes significance by DESeq2 (p-adj<0.1). NM (normal, blue bars represent mean expression, dots represent biological samples, n=5-10).

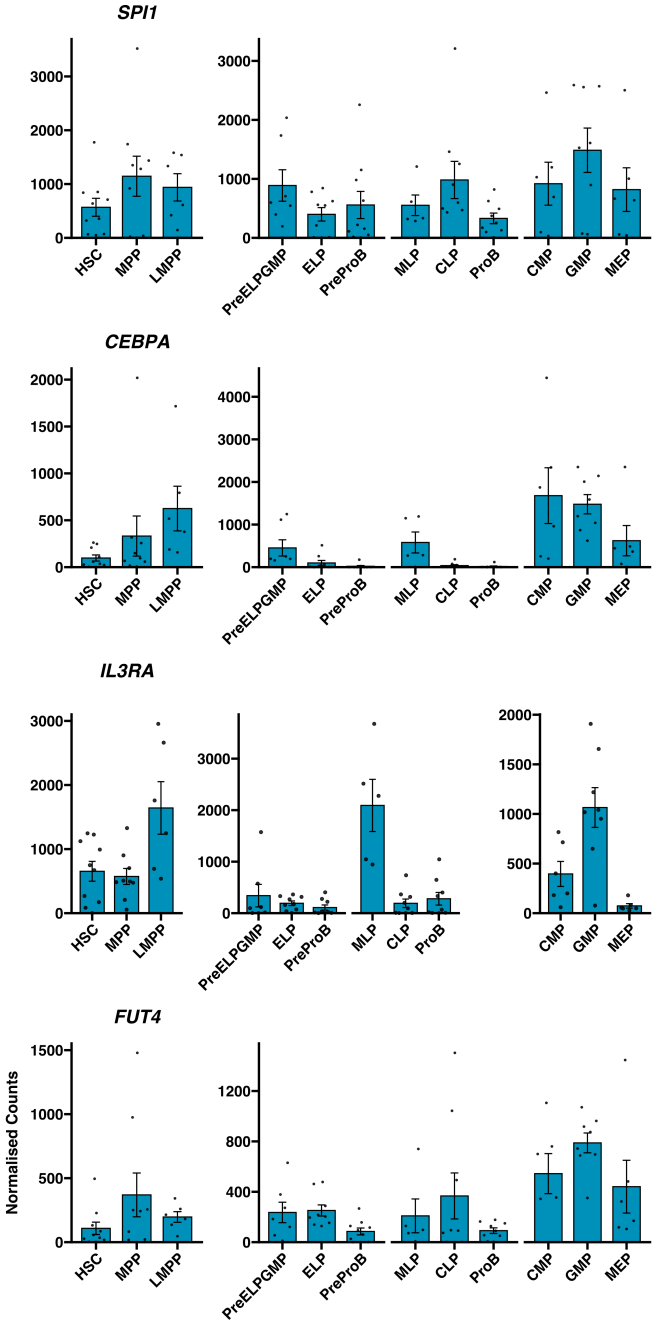

Figure 6: Expression of genes with a known role in myeloid specification in NM fetal BM HSPC by RNA-Seq (50-100 cells). For each gene, graphs are grouped (from left to right) for primitive HSPC, fetal specific lymphoid progenitors, adult type lymphoid progenitors, and myeloid progenitors. Mean ± SEM, * denotes significance by DESeq2 (p-adj<0.1). NM (normal, blue bars represent mean expression, dots represent biological samples, n=5-10).

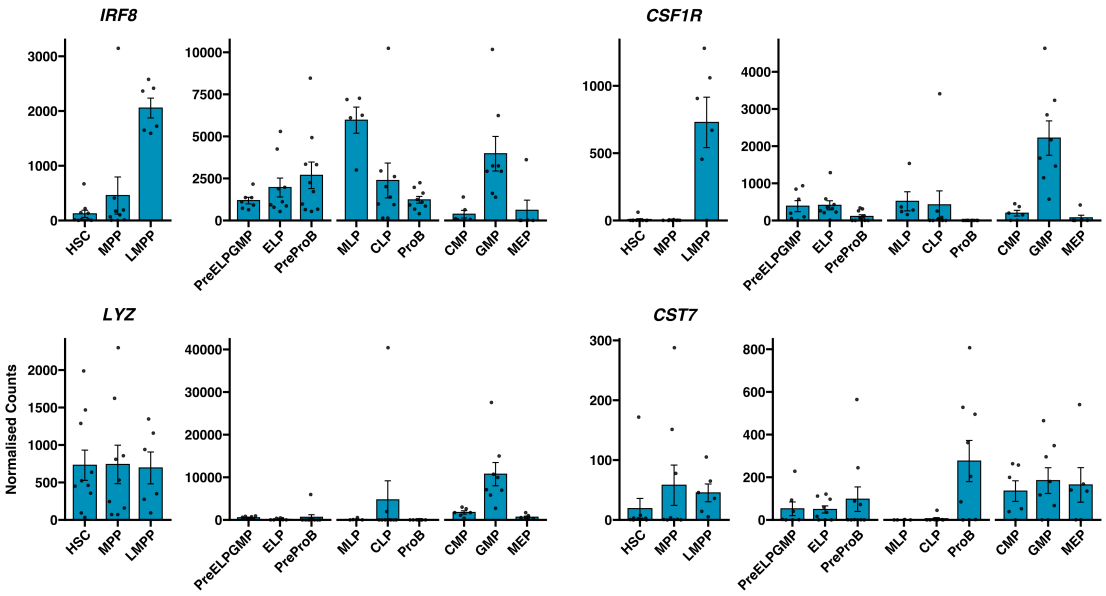

Figure 7: Expression of genes with a known role in monopoiesis in NM fetal BM HSPC by RNA-Seq (50-100 cells). For each gene, graphs are grouped (from left to right) for primitive HSPC, fetal specific lymphoid progenitors, adult type lymphoid progenitors, and myeloid progenitors. Mean ± SEM, * denotes significance by DESeq2 (p-adj<0.1). NM (normal, blue bars represent mean expression, dots represent biological samples, n=5-10).

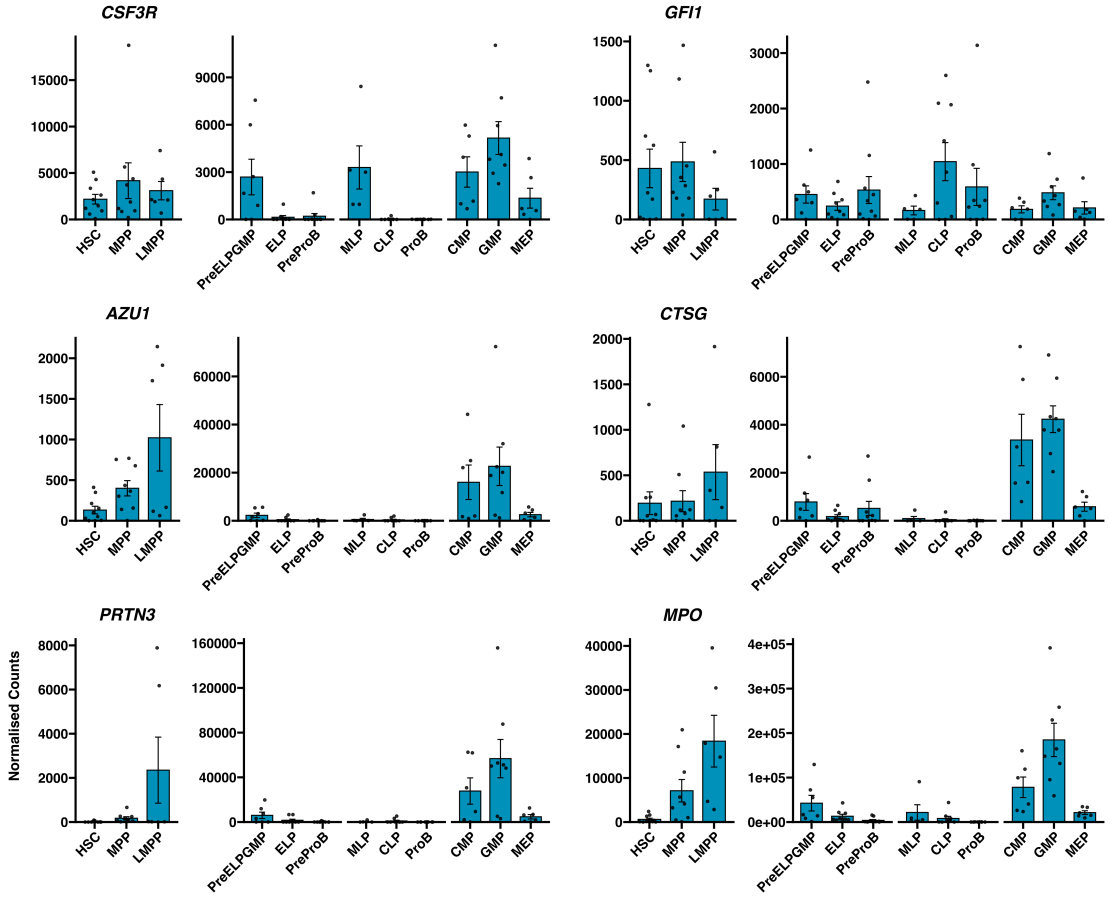

Figure 8: Expression of genes with a known role in granulopoiesis in NM fetal BM HSPC by RNA-Seq (50-100 cells). For each gene, graphs are grouped (from left to right) for primitive HSPC, fetal specific lymphoid progenitors, adult type lymphoid progenitors, and myeloid progenitors. Mean ± SEM, * denotes significance by DESeq2 (p-adj<0.1). NM (normal, blue bars represent mean expression, dots represent biological samples, n=5-10); T21 (Trisomy 21, lilac bars represent mean expression, triangles represent biological samples, n=3-7).

.2 Differential gene expression in fetal BM HSPC

.2.1 Top 50 DEG between NM and T21 fetal BM HSPC

Table 1: Top 50 differentially expressed genes between NM and T21 fetal BM HSC.

Gene	Log2FoldChange	p-adj
ADAMTS2	18.43076964	1.14479E-12
DCLK2	21.29867771	1.19805E-12
ADGRG2	23.97148007	2.34556E-12
KERA	30	5.54535E-12
OLFML1	29.98803257	5.54535E-12
EDIL3	23.42670795	5.94338E-11
GPR141	22.35685509	3.55946E-10
LOC102723704	21.06266147	1.79871E-09
ASS1	25.17476091	4.17396E-08
UBE2F-SCLY	-24.83326644	6.98482E-08
PYY2	-24.52279228	7.3883E-08
CACNB2	5.730973477	1.11495E-07
PCDHB4	21.64410621	1.91634E-07
KIF5A	-24.0605672	1.94785E-07
EDA	23.75744486	3.04146E-07
CRYAB	23.67572647	3.27903E-07
LGALS9C	-23.26053016	6.2626E-07
RASGEF1A	22.58596353	1.01094E-06
RNF182	-22.93648867	1.01094E-06
TPX2	3.514914984	1.083E-06
FAM49A	-4.918349532	1.8585E-06
CATSPER4	-22.36685835	2.01854E-06
MIR3944	-22.37482826	2.01854E-06
DNASE1L3	-5.737032916	4.35908E-06
EMILIN3	20.28880281	4.35908E-06
HERC4	-2.549518334	4.35908E-06
HS6ST2	20.12943782	4.35908E-06
SNORD70	19.86058598	4.47049E-06
PRSS35	20.10760721	5.03059E-06

Continued on next page

Gene	Log2FoldChange	p-adj
CDH2	8.253338034	5.51611E-06
EGF	-9.294589156	6.27558E-06
HAP1	21.29854881	7.93425E-06
ZNF385D	20.16980625	8.21986E-06
IL21R-AS1	21.22292754	8.28277E-06
AGTR1	21.18044951	8.5557E-06
ANKRD65	19.25148753	9.49959E-06
ARMC4	-7.00609627	1.04437E-05
SLC17A5	8.809521618	1.21266E-05
G6PD	3.911951121	1.36278E-05
BMP5	20.52367552	1.90493E-05
DUSP16	6.25905314	1.90493E-05
KCTD6	5.580207222	1.90493E-05
LOC729950	20.53634512	1.90493E-05
TMEM98	10.57449631	1.93209E-05
LINC01139	20.36734261	2.26774E-05
DEPDC1	5.981308752	2.3246E-05
LRRN3	20.32120942	2.3246E-05
CNTNAP4	20.26038814	2.48982E-05
F7	19.58357191	4.38069E-05
CCNE1	7.749283985	4.77717E-05

Table 1: Top 50 differentially expressed genes by DESeq2 between NM and T21 fetal BM HSC. NM: normal, n=10; T21, Trisomy 21, n=7

Table 2: Top 50 differentially expressed genes between NM and T21 fetal BM MPP.

Gene	Log2FoldChange	p-adj
CASC5	7.44499181	5.01463E-22
ST6GALNAC5	-24.75740788	1.60574E-16
MMACHC	8.126284941	6.24239E-15
CYP1A1	19.53612864	6.96338E-13
MIR5093	-26.46527763	2.5313E-11
CRHBP	-6.297351427	2.41163E-10
GPR141	-25.03940258	2.57363E-10

Continued on next page

Gene	Log2FoldChange	p-adj
PRR9	24.95635104	5.80991E-10
PSKH2	24.9281366	5.80991E-10
TREM2	24.0349953	2.77267E-09
TFF3	23.76720108	5.20554E-09
FKBP1B	10.02868703	5.47184E-09
LOC100128076	23.70288068	5.47184E-09
LRRIQ4	23.29625275	6.02413E-09
LOC105447645	23.40051771	6.21675E-09
AMPH	23.11601274	6.72071E-09
LOC101593348	23.30749777	6.72071E-09
CDH10	23.09062482	6.90958E-09
GPRC5A	22.96234481	7.66472E-09
HSD17B6	22.96513069	7.66472E-09
OR3A1	22.98689503	7.66472E-09
DDO	23.15329747	9.16177E-09
TSGA10IP	22.83680151	9.16177E-09
LINC00989	23.07440648	9.56276E-09
NLGN4Y	23.07141512	9.56276E-09
TOM1L1	23.08897519	9.56276E-09
SLFN14	22.67427092	1.05126E-08
CATSPERB	22.92403965	1.16928E-08
ALDH3A1	22.90491314	1.19403E-08
C20orf195	22.69349752	1.755E-08
LOC100506368	22.62176662	1.95694E-08
RAD51	5.239698516	2.42709E-08
LOC102724484	-22.56051727	2.55256E-08
TRANK1	-4.266052632	2.55256E-08
MTA3	6.496472251	3.46282E-08
LINC00892	22.21750921	3.70302E-08
GCSHP3	6.567042993	4.40786E-08
MIR924	-21.98417607	4.40786E-08
DNAI2	21.4786847	4.52788E-08
ARMC9	5.781477531	5.97793E-08
SNORD116-11	-21.53215379	9.67553E-08

Continued on next page

Gene	Log2FoldChange	p-adj
ATOH7	21.40489331	1.4818E-07
LHFP	7.674840235	2.07833E-07
LOC101927272	6.886538612	2.10751E-07
SFMBT2	4.681561949	2.12354E-07
CADM3-AS1	-21.20868585	2.34857E-07
CRIP3	-21.20868585	2.34857E-07
TTBK2	6.978563525	2.53585E-07
DCDC2C	-21.1346007	2.5771E-07
CCNF	5.460693205	3.28388E-07

Table 2: Top 50 differentially expressed genes by DESeq2 between NM and T21 fetal BM MPP. NM: normal, n=9; T21, Trisomy 21, n=6

Table 3: Top 50 differentially expressed genes between NM and T21 fetal BM LMPP.

Gene	Log2FoldChange	p-adj
DPP4	-29.97424377	2.40579E-12
FAM186A	-29.98132278	2.40579E-12
NR2F1-AS1	-29.96684438	2.40579E-12
PDZK1IP1	-29.96852646	2.40579E-12
TMEM133	-29.97719041	2.40579E-12
WNT10B	-29.96771406	2.40579E-12
ZNF396	-30	2.40579E-12
XKR9	-29.48677599	5.87118E-12
LOC100506730	-22.92256799	3.36855E-10
NPDC1	11.94553855	3.36855E-10
FYCO1	-7.120276279	2.47364E-09
LINC00472	-24.29478664	1.0216E-07
RACGAP1	-5.410004257	1.79431E-07
KU-MEL-3	-23.08684241	7.06629E-07
OR2C1	-22.85165619	9.77967E-07
FFAR2	-22.80605424	9.8887E-07
ALB	-22.14093126	1.323E-06
ANXA8	-22.30668984	1.323E-06
CASC9	-22.24847206	1.323E-06

Continued on next page

Gene	Log2FoldChange	p-adj
CIDEC	-22.09812743	1.323E-06
CTSF	9.282930323	1.323E-06
EGOT	-22.25529639	1.323E-06
GAB4	-22.58707581	1.323E-06
GRM2	-22.29155167	1.323E-06
LINC01081	-22.36074137	1.323E-06
LOC105376360	-22.43905044	1.323E-06
LY6G6D	-22.27691584	1.323E-06
OPN1SW	-22.4881198	1.323E-06
PGPEP1L	-22.38700334	1.323E-06
SVOP	-22.20628037	1.323E-06
TREML3P	-22.52632859	1.323E-06
C8orf31	-22.17925763	1.35539E-06
HIST2H2BA	-22.17871454	1.35539E-06
PRRG1	-22.12355311	1.44224E-06
FER1L6-AS2	-22.09973708	1.45328E-06
LINC00693	-21.94604587	1.816E-06
SRPK3	-21.86707125	2.00145E-06
FPR1	-21.82934808	2.07747E-06
TAS2R3	-21.69782828	2.49444E-06
OR7D2	21.24946461	2.57637E-06
PRL	-21.63875981	2.60363E-06
STRA6	10.29294965	2.99993E-06
TBC1D2	9.838024395	3.25342E-06
C2CD5	-4.221385688	3.75055E-06
ZSCAN9	-8.489038027	4.47837E-06
SLC35D3	-21.20956842	4.57283E-06
KLHL2	-6.968506533	4.872E-06
ABCG2	-6.202040295	6.0883E-06
SLC2A7	-20.9565862	6.36276E-06
CAPNS2	-20.87015613	7.04015E-06

Table 3: Top 50 differentially expressed genes by DESeq2 between NM and T21 fetal BM LMPP. NM: normal, n=6; T21, Trisomy 21, n=3

Table 4: Top 50 differentially expressed genes between NM and T21 fetal BM MLP.

Gene	Log2FoldChange	p-adj
GYPE	-26.62828307	2.22452E-19
LINC01503	-29.94920915	1.80116E-11
LOC100133669	-29.49905873	3.11868E-11
BBS12	-26.01422596	4.85197E-11
CXCL12	27.04555071	2.33545E-09
ZNF367	4.931412646	5.09958E-09
LINC00857	-25.93389067	1.07212E-08
NAP1L3	9.758842649	1.07212E-08
PP2D1	23.87577396	1.07212E-08
SFTPA1	-25.96409154	1.07212E-08
CLDN5	9.346094831	2.49928E-08
MBNL2	3.687976803	2.63535E-08
PCGEM1	-24.72984183	2.63535E-08
AGR3	24.11802326	3.63232E-08
PON1	23.13234597	3.87489E-08
CHL1	24.60547525	5.39791E-08
EDNRB	-24.72366648	5.39791E-08
IGFBP3	24.72873636	5.39791E-08
TUNAR	24.64303576	5.39791E-08
XKR9	-24.61830037	5.39791E-08
CDH11	24.49959754	5.95253E-08
HBG1	-24.22748114	5.95253E-08
C4orf36	-24.27321534	6.59278E-08
ROR2	24.40307842	6.59278E-08
B9D1	-24.34765194	7.17208E-08
RGMB	24.31728527	7.17208E-08
LOC102724691	24.00210354	7.59912E-08
PCDHB14	24.21967111	7.59912E-08
ALDH8A1	24.05508624	8.75493E-08
FAM69C	24.07261957	8.75493E-08
LINC01515	8.000119346	8.75493E-08
MB21D2	24.0836687	8.75493E-08

Continued on next page

Gene	Log2FoldChange	p-adj
TMEM132C	24.06140423	8.75493E-08
TCP11	23.99310047	9.2743E-08
SEPT4	23.95499177	9.62618E-08
IBSP	23.92138275	9.90892E-08
CSPG4	23.88934499	1.0198E-07
GPR12	23.60318781	1.03605E-07
PHLDA3	-22.58916087	1.03605E-07
SELM	23.82560773	1.03605E-07
TMPRSS11A	23.82475941	1.03605E-07
PENK	23.7635116	1.1154E-07
NR3C2	-23.71799701	1.13323E-07
TEX38	-23.7134674	1.13323E-07
TMEM86A	-23.45893499	1.13323E-07
KCNK16	23.6609785	1.20372E-07
RNASE4	23.60881483	1.28765E-07
HSF4	23.56072409	1.36859E-07
MIRLET7D	-8.332317882	1.36859E-07
LINC00200	-23.53375167	1.3891E-07

Table 4: Top 50 differentially expressed genes by DESeq2 between NM and T21 fetal BM MLP. NM: normal, n=5; T21, Trisomy 21, n=4

Table 5: Top 50 differentially expressed genes between NM and T21 fetal BM PreELP/GMP.

Gene	Log2FoldChange	p-adj
SPRYD3	-24.2055381	5.7983E-15
POMK	-29.98307638	9.21191E-15
PVRIG	9.514533613	1.15636E-13
SNCAIP	-29.97394768	2.90902E-12
ZNF285	-29.98727288	2.90902E-12
TPD52	-8.118543687	1.02605E-11
RAI1-AS1	-27.3786212	5.22161E-10
CPM	-8.693890078	2.42631E-09
OVCH2	-26.02670869	4.96912E-09

Continued on next page

Gene	Log2FoldChange	p-adj
MBD4	-2.719250459	1.98933E-08
LOC100506159	-24.99866379	2.76882E-08
HYOU1	3.718351555	4.61338E-08
ADAMTS1	-24.49196534	1.04494E-07
TNRC18	3.158769361	1.33166E-07
C2orf82	10.01487604	1.62053E-07
ARL10	-22.57545053	3.11795E-07
C9orf153	-23.94040721	3.22159E-07
NLRP2	8.868744498	4.48412E-07
ETV5	6.698711488	4.6773E-07
ADARB1	8.748293026	7.61749E-07
SMC2	-3.194045454	7.83716E-07
HPS6	7.566830422	9.56057E-07
TNFSF9	10.18770163	9.92325E-07
MYO5C	-3.668276572	9.97956E-07
MRVI1	-7.02733324	1.05273E-06
ANKRD16	-4.779459817	1.49812E-06
TMEM243	-4.276445576	1.81533E-06
VNN2	-11.42700863	1.81533E-06
CD9	-6.113326596	2.37814E-06
LILRA4	21.51154812	2.37814E-06
TIFA	-3.812545539	2.37814E-06
RERE	2.139729768	2.45401E-06
MROH1	6.925784839	2.50869E-06
PRR14	1.988858578	2.72058E-06
C12orf50	21.29502656	2.95629E-06
TAF1A	-5.566899164	3.66039E-06
ICAM1	6.616112612	3.74999E-06
MSL3P1	-6.095900478	4.40804E-06
CDH15	20.96081477	4.52502E-06
LINC01556	20.8920429	4.92253E-06
MOGS	7.44155488	4.95285E-06
CELF2-AS1	20.58948953	5.09803E-06
SEC16B	20.82401477	5.09803E-06

Continued on next page

Gene	Log2FoldChange	p-adj
ADAMTS2	20.74648928	5.13576E-06
ALDH3A1	20.75989187	5.13576E-06
CAPNS2	20.76957785	5.13576E-06
FBXO5	-2.812485839	5.13576E-06
KRTAP5-9	20.73636944	5.13576E-06
LINC00540	20.73748946	5.13576E-06
AACSP1	20.69178194	5.29135E-06

Table 5: Top 50 differentially expressed genes by DESeq2 between NM and T21 fetal BM Pre/ELPGMP. NM: normal, n=7; T21, Trisomy 21, n=3

Table 6: Top 50 differentially expressed genes between NM and T21 fetal BM ELP.

Gene	Log2FoldChange	p-adj
BLZF1	-6.621641857	3.42425E-16
CTGF	-9.340357562	3.42425E-16
ESCO2	-5.703087351	3.42425E-16
DNTT	-8.701835823	9.41878E-15
RAD18	-7.666177611	1.12874E-14
ACOT9	-8.248941584	1.96066E-13
NT5DC1	-8.00671084	6.10843E-13
BAZ2A	6.954627304	1.2594E-12
RCBTB1	-9.204259758	2.99728E-11
ADPRM	-7.327053914	7.7479E-11
PBK	-8.0610694	8.28334E-11
SMYD2	-6.812538001	8.28334E-11
TECPR1	10.04820803	8.28334E-11
BRCC3	-7.391737655	1.10319E-10
FAM118B	-7.659052472	1.43889E-10
RINT1	-5.397587754	2.13415E-10
RAB6A	-4.193686668	2.41751E-10
DCTN2	-3.984307984	5.3883E-10
TRAPPC11	-4.213057124	7.40157E-10
LEF1	-5.804345682	1.12228E-09
TMEM128	-6.811608845	2.32745E-09

Continued on next page

Gene	Log2FoldChange	p-adj
PANK4	6.77762568	3.49651E-09
BIN3	-6.582926162	4.3819E-09
ZYG11B	-19.83197754	4.3819E-09
MED18	-20.39957327	5.03741E-09
MAML2	-21.03195042	6.30954E-09
THAP1	-6.985614913	6.30954E-09
SNAP47	-6.925591682	7.92816E-09
ZNF549	-20.05878698	8.58488E-09
TIAM2	-20.60070728	1.41407E-08
IGSF10	-21.07313457	1.46322E-08
LY9	-4.600804202	1.46322E-08
C1orf112	-5.081328693	2.1357E-08
NARS2	-4.894161598	2.97126E-08
SOCS4	-7.202961679	3.14254E-08
ZNF90	-21.13520043	3.14254E-08
POC1A	-9.66930057	4.27172E-08
CKAP2L	-4.305767468	4.59692E-08
LCMT2	-20.35629262	4.7501E-08
CYB561D1	-19.29404355	6.05127E-08
ZNF563	-24.55775256	7.16807E-08
PYROXD1	-6.512531861	1.0725E-07
SPNS1	-7.096886765	1.09774E-07
CLK4	-4.242201097	1.43936E-07
PTER	-11.05618285	1.55571E-07
GOLPH3L	-8.66245081	1.69471E-07
HSPB1	4.402142145	1.69471E-07
ARID5B	-5.226743583	3.10675E-07
ZBTB43	6.945795069	4.03356E-07
CYHR1	-6.014600149	4.7996E-07

Table 6: Top 50 differentially expressed genes by DESeq2 between NM and T21 fetal BM ELP. NM: normal, n=9; T21, Trisomy 21, n=3

Table 7: Top 50 differentially expressed genes between NM and T21 fetal BM CLP.

Gene	Log2FoldChange	p-adj
TUSC1	8.290375	2.93135E-13
DTX2	-23.28396917	3.06277E-10
B3GALT4	-21.06650897	1.00743E-09
LMO7	-21.74130118	1.00743E-09
ZNF275	-26.22086015	1.00743E-09
ZNF514	-24.55740316	1.00743E-09
WDFY3	-20.57869338	1.06615E-09
CNKSR2	23.2995597	1.57863E-09
CROT	-23.7326436	2.87536E-09
INCA1	22.5133797	3.13688E-09
ZBTB6	-21.77429273	3.7641E-09
IFT74	-12.18062645	4.10857E-09
ZFYVE27	8.122231088	4.10857E-09
PLOD1	-25.45391518	4.93725E-09
ZNF610	22.68969049	6.0202E-09
ZNF575	-21.09979391	8.68355E-09
DNMBP	22.76810004	1.42352E-08
TUBB2A	-21.12114328	1.42352E-08
ADGRF1	-21.62424159	3.37647E-08
ACSF2	8.284045657	4.71141E-08
LOC100506142	22.59062406	4.71141E-08
PIGO	-24.73241957	8.69572E-08
RPL34-AS1	-22.66463199	8.69572E-08
ZSWIM3	-22.78996951	9.79545E-08
PPP1R14C	22.35246962	1.01644E-07
GP6	22.8728613	1.34898E-07
SMG1P7	-21.86881176	1.34898E-07
ZNF600	-22.82049626	1.34898E-07
ARHGAP11B	-21.82417965	1.39699E-07
ZNF620	-23.43143271	1.39699E-07
CENPI	-23.88235951	1.70893E-07
TLL2	-22.31777289	1.79128E-07

Continued on next page

Gene	Log2FoldChange	p-adj
TNFRSF10D	-20.25894642	1.79492E-07
ADAT3	22.53447459	1.92276E-07
FSIP1	23.42466763	1.92276E-07
LINGO3	-21.13535607	1.92276E-07
MSI2	8.498462123	1.92276E-07
TMC7	23.33382507	2.02185E-07
CEP72	-20.424469	2.51133E-07
MANEA-AS1	-20.91039522	2.5296E-07
RARA	19.74811245	2.5296E-07
SRD5A1	22.51372433	2.5296E-07
LOC729683	21.86033746	2.59896E-07
KCNA5	-21.54670029	2.98396E-07
EPN2-AS1	-21.56838742	3.95079E-07
ZNF155	-22.85384591	5.85917E-07
GBAP1	-22.49960244	7.6743E-07
HCG14	17.77554774	7.73434E-07
KIF18B	-9.691552608	7.93965E-07
MAN1B1-AS1	-22.35829402	7.93965E-07

Table 7: Top 50 differentially expressed genes by DESeq2 between NM and T21 fetal BM CLP. NM: normal, n=9; T21, Trisomy 21, n=3

.2.2 Differentially expressed genes between NM and T21 HSPC on chromosome 21

Gene	log2FoldChange	p-adj
ADAMTS5	12.76867918	0.020939149
ADARB1	5.61485677	0.000153807
BACE2	7.779006009	0.004522161
BRWD1-IT2	6.890507753	0.042279201
C21orf59	0.908963379	0.020939149
CHODL	11.32703155	0.000509995
EVA1C	5.201576341	0.040548055
FAM207A	2.510351913	0.055822523
GART	1.496897489	0.057384777
LINC01547	7.907888379	0.000697205
TCP10L	-7.039776512	0.068947294
TIAM1	4.086571746	0.031958191
TRAPPC10	2.224583768	0.080987391
U2AF1	1.995737032	0.014689462
UBE2G2	1.580688047	0.097095321

Table 8: Differentially expressed genes by DESeq2 between NM and T21 fetal BM HSC on chromosome 21. NM: normal, n=10; T21, Trisomy 21, n=7.

Gene	log2FoldChange	p-adj
ADAMTS1	6.787246335	0.017116711
ADARB1	3.936836484	0.045968324
BRWD1-IT2	5.683615555	0.073339546
C21orf33	1.20516429	0.091827696
C21orf62	8.425610591	0.001080236
COL6A1	8.519612152	0.077076168
HSPA13	2.157496339	0.000401281
ITGB2-AS1	6.791982514	0.002308809
LINC00649	5.857547076	0.052533735
PCBP3	6.660245143	0.012235134
PSMG1	1.048915465	0.041333229
RNA18S5	2.845441366	0.042362034
S100B	6.944659225	0.00672395
SH3BGR	5.673867129	0.001093107
TFF3	23.76720108	5.20554E-09
TRPM2	5.74067622	0.005870415
U2AF1	1.61724037	0.08397829
UBASH3A	8.634760511	0.004231369
UBE2G2	1.434851564	0.032019469

Table 9: Differentially expressed genes by DESeq2 between NM and T21 fetal BM MPP on chromosome 21. NM: normal, n=9; T21, Trisomy 21, n=6.

Gene	log2FoldChange	p-adj
ATP5J	0.945099404	0.031641741
C21orf2	1.563956893	0.019246361
COL6A2	8.83704228	0.00117548
CXADR	8.044740705	0.098005523
DSCR9	6.370607205	0.05941034
HMGN1	0.801035057	0.074102244
LRRC3	15.91873518	0.000434924
PWP2	2.939195148	0.058406822
SOD1	0.929098418	0.050524017
SON	0.976489809	0.033693987
SUMO3	0.686658219	0.098005523

Table 10: Differentially expressed genes by DESeq2 between NM and T21 fetal BM LMPP on chromosome 21. NM: normal, n=6; T21, Trisomy 21, n=3.

Gene	log2FoldChange	p-adj
AGPAT3	2.503004658	0.022168131
LOC101928796	23.00105192	2.45935E-07
SOD1	1.004136956	0.069646945
TCP10L	9.007488111	0.044770912
UMODL1-AS1	-10.11537682	0.007364565

Table 11: Differentially expressed genes by DESeq2 between NM and T21 fetal BM MLP on chromosome 21. NM: normal, n=5; T21, Trisomy 21, n=4.

Gene	log2FoldChange	p-adj
ADAMTS1	-24.49196534	1.04494E-07
ADARB1	8.748293026	7.61749E-07
AGPAT3	5.224314373	0.000974238
AIRE	-9.399451052	0.009216956
C21orf62-AS1	6.849522177	0.026099878
COL6A1	9.57385034	0.0289207
CSTB	1.361663043	0.042393885
ETS2	1.500117131	0.021522528
FAM207A	3.053814277	0.00613837
IL10RB-AS1	8.014560438	0.033858051
LINC01547	9.521366424	0.000204749
LSS	4.30041825	0.042987509
NDUFV3	2.028174189	0.004854561
PCBP3	10.00222447	1.72105E-05
PDXK	1.623575579	0.03420231
POFUT2	3.801412781	0.066063047
PRDM15	4.614985578	0.010918965
RSPH1	5.750633269	0.076770447
RUNX1	1.617762091	0.024055575
SLC19A1	3.362827469	0.056820162
SLC37A1	1.638262252	0.020292411
TRPM2	2.039509505	0.025588444
UBASH3A	8.844282815	0.066991746
UBE2G2	1.419243436	0.060898607

Table 12: Differentially expressed genes by DESeq2 between NM and T21 fetal BM PreELP/GMP on chromosome 21. NM: normal, n=7; T21, Trisomy 21, n=3.

Gene	log2FoldChange	p-adj
ABCG1	4.289037144	6.69266E-05
CBR3	-19.54451739	0.000159594
CRYZL1	-2.152647042	0.024866624
DIP2A	4.110552609	3.65838E-06
DONSON	-2.662537827	0.027329117
ETS2	1.742222798	0.006804657
ITGB2	4.428289185	0.028938519
LINC01426	21.83190716	0.000139854
MCM3AP	2.507411915	0.017004577
MIR155HG	3.049578634	0.007517135
MX2	-19.20815017	0.00314972
PKNOX1	-6.935982187	5.09413E-07
SLC19A1	5.016790703	0.073414276
SON	2.105691891	0.001992864
TRAPPC10	4.864982445	0.021212813
URB1-AS1	2.868810878	0.006804657

Table 13: Differentially expressed genes by DESeq2 between NM and T21 fetal BM ELP on chromosome 21. NM: normal, n=9; T21, Trisomy 21, n=3.

Gene	log2FoldChange	p-adj
HSPA13	4.823817504	0.009047474
MAP3K7CL	6.94602807	0.019748806
MIR99AHG	7.954617649	0.042020458
N6AMT1	5.67991257	0.011648903
NCAM2	8.037123192	0.040645498
PDXK	5.762660995	0.048893312
S100B	9.651388592	0.014591722
TIAM1	7.580802647	0.040773002
UMODL1	6.1667251	0.014284496
URB1	6.094572069	0.062270284

Table 14: Differentially expressed genes by DESeq2 between NM and T21 fetal BM CLP on chromosome 21. NM: normal, n=9; T21, Trisomy 21, n=3.

.2.3 Genes associated with the B lymphopoietic module by WGCNA in NM and T21 fetal BM HSPC

Gene	P-value
VPREB3	1.44805E-56
BLNK	2.15911E-50
CD24	2.55947E-49
CD72	3.1816E-48
P4HA2	1.83199E-47
CD9	2.66868E-47
ARPP21	2.77222E-47
CD79B	3.05405E-47
EBF1	9.6555E-46
TIMP1	6.51204E-45
CD79A	1.71468E-44
POU2AF1	2.3257E-44
MIR5195	9.50765E-44
AKAP12	1.25044E-43
GNG7	1.33776E-43
DTX1	3.88309E-43
VPREB1	1.13308E-40
CD38	2.39174E-40
RAG2	2.79391E-40
MPL	3.06113E-40
ANGPT1	1.28375E-39
ADAM28	5.14706E-39
RAG1	5.31307E-39
NPR3	3.48248E-38
PAX5	1.9875E-37

Table 15: Top 25 genes associated with the B lymphopoietic module identified by WGCNA in NM fetal BM HSPC. P-value calculated by Pearson's Correlation Efficient.

Gene	P-value
CD79B	1.82445E-60
POU2AF1	2.67093E-59
TCL1B	9.61658E-57
MIR5195	4.25673E-55
DTX1	7.48748E-53
CD19	7.89382E-53
CD72	1.53962E-51
VPREB3	3.38084E-51
IGLL5	4.52476E-50
RAG1	2.41095E-48
TMEM243	1.23728E-47
CD24	1.32359E-47
HLA-DRA	3.57289E-47
BLNK	6.65438E-47
PAX5	1.9889E-46
KIAA0226L	5.79693E-44
LOC285766	8.51299E-44
BACH2	4.66355E-43
TCL1A	1.14929E-42
GNG7	4.91906E-41
ISG20	6.97218E-41
CLEC2D	1.52456E-40
CD79A	2.48565E-39
CMTM8	8.94617E-39
HMGA2	2.39091E-38

Table 16: Top 25 genes associated with the B lymphopoietic module identified by WGCNA in T21 fetal BM HSPC. P-value calculated by Pearson's Correlation Efficient.

.3 Differential chromatin accessibility in T21 fetal BM HSPC

Table 17: Differential Chromatin Accessibility between NM and T21 fetal BM HSC.

log2FoldChange	p-adj	CHR	START	END	symbol
1.346576306	1.25376E-05	chr21	36429990	36430390	RUNX1
2.777990787	0.00010964	chr7	4123878	4124278	SDK1
2.09910915	0.000156515	chr12	2616787	2617187	CACNA1C-IT2; CACNA1C
2.579665372	0.000156515	chr6	161829286	161829686	PRKN
2.832909066	0.001370133	chr1	54604572	54604972	CDCP2
2.370258451	0.001547691	chr2	240893469	240893869	NDUFA10
1.393547538	0.007213883	chr21	43939041	43939441	SLC37A1
3.538537085	0.007328689	chr8	74219798	74220198	RDH10
2.548310379	0.007328689	chr1	227934785	227935185	SNAP47
2.95910952	0.007328689	chr21	31087627	31088027	GRIK1
1.365222795	0.008940668	chr7	2698906	2699306	TTYH3
1.582342797	0.008940668	chr3	67655751	67656151	SUCLG2
1.098122363	0.013876331	chr21	36319961	36320361	RUNX1
1.880200116	0.016577963	chr21	37060294	37060694	RUNX1
1.062859941	0.021281512	chr16	53098897	53099297	CHD9
1.569677886	0.022772771	chr21	42097869	42098269	DSCAM
1.014859164	0.022772771	chr4	2262132	2262532	MXD4
1.475272159	0.026472912	chr21	33036418	33036818	SOD1
1.475272159	0.026472912	chr21	33036418	33036818	LOC124900469
1.135106518	0.026472912	chr21	45973648	45974048	TSPEAR
1.403200386	0.027193919	chr21	44297662	44298062	WDR4
0.962049803	0.030725931	chr21	32612362	32612762	TIAM1
2.124786002	0.038375106	chr21	35138734	35139134	ATP5PO
2.124786002	0.038375106	chr21	35138734	35139134	ITSN1
1.601743935	0.049922495	chr21	33101194	33101594	SCAF4
-2.41325988	0.050590498	chrY	2841443	2841843	ZFY
-2.41325988	0.050590498	chrY	2841443	2841843	ZFY-AS1

Continued on next page

log2FoldChange	p-adj	CHR	START	END	symbol
1.794000897	0.050689008	chr17	418443	418843	VPS53
1.284228253	0.055708234	chr21	39388527	39388927	DSCR4
1.838162037	0.055708234	chr21	42616397	42616797	BACE2
1.156374136	0.058305919	chr21	33383118	33383518	HUNK
3.666478974	0.059190613	chr17	18682183	18682583	FBXW10
1.644051002	0.059190613	chr21	31654948	31655348	KRTAP24-1
2.604964217	0.061010769	chr17	18917096	18917496	SLC5A10
1.682798547	0.061986436	chr20	48748017	48748417	PEDS1-UBE2V1
1.682798547	0.061986436	chr20	48748017	48748417	PEDS1
0.883765204	0.062981606	chr21	43728557	43728957	TFF3
1.049361077	0.074886411	chr15	74870015	74870415	ARID3B
3.399887608	0.074886411	chr19	2332363	2332763	LINC02983
3.399887608	0.074886411	chr19	2332363	2332763	SPPL2B
0.933137921	0.074886411	chr21	35026721	35027121	ATP5PO
0.933137921	0.074886411	chr21	35026721	35027121	ITSN1
1.509639668	0.074886411	chr21	41768545	41768945	DSCAM
0.943420013	0.074886411	chr21	42118843	42119243	DSCAM
-1.122239006	0.074886411	chr3	15805723	15806123	ANKRD28
1.935094084	0.085081514	chr20	3716243	3716643	HSPA12B
0.887292941	0.085081514	chr21	37564112	37564512	DOP1B
1.736035182	0.085081514	chr4	8417140	8417540	ACOX3
1.060505288	0.086358101	chr1	9426327	9426727	SPSB1
1.192445778	0.086358101	chr21	37225449	37225849	RUNX1
1.457867635	0.087654146	chr16	57816307	57816707	KIFC3
1.055554443	0.087654146	chr21	46228627	46229027	SUMO3
0.937380303	0.098238308	chr21	36060252	36060652	CLIC6
1.016150043	0.098372029	chr8	22715592	22715992	PEBP4
2.157762722	0.099097626	chr10	6239203	6239603	PFKFB3
2.157762722	0.099097626	chr10	6239203	6239603	PFKFB3-AS1
1.015513656	0.099097626	chr21	34615187	34615587	IFNAR2
4.424619958	0.099097626	chr6	11318319	11318719	NEDD9
2.270240856	0.099857945	chr3	128603772	128604172	ACAD9

Continued on next page

log2FoldChange	p-adj	CHR	START	END	symbol

Table 17: Summary of differentially accessible peaks by DESeq2 between FAC-sorted NM (normal, n=3) and T21 (Trisomy 21, n=4) fetal BM HSC (P-adj <0.1). Peaks 1000bp upstream of or within genes were annotated using ChIPPeakAnno.

Table 18: Differential Chromatin Accessibility between NM and T21 fetal BM MPP.

log2FoldChange	p-adj	CHR	START	END	symbol
3.440682409	7.14297E-05	chr21	37100341	37100741	RUNX1
-2.383663867	0.000439247	chr2	17791444	17791844	VSNL1
1.382733248	0.001748325	chr21	37045164	37045564	RUNX1
3.640207376	0.002869869	chr13	39401676	39402076	FREM2
-2.303608759	0.002869869	chr20	45041572	45041972	ELMO2
-1.458458412	0.003206687	chr17	7350110	7350510	CHRNB1
1.584185159	0.003899769	chr2	54422020	54422420	ACYP2
1.206650063	0.003899769	chr21	33641748	33642148	MIS18A
3.021122788	0.00487524	chr7	138147030	138147430	TRIM24
1.020670854	0.006631016	chr21	29024740	29025140	LINC01673
2.3796382	0.006631016	chr3	32114532	32114932	OSBPL10
-1.633532047	0.007401788	chr6	20978293	20978693	CDKAL1
-2.267908168	0.009437454	chr20	34938451	34938851	DLGAP4
-1.634409361	0.010404844	chr5	168585074	168585474	SLIT3
-2.003306337	0.010999081	chr1	84245757	84246157	LOC101927560; LINC01725
1.350967462	0.011187704	chr7	4123878	4124278	SDK1
-1.352749153	0.012006756	chr11	121464489	121464889	SORL1
2.635861602	0.013699131	chr19	6721777	6722177	C3
-1.537384701	0.013699131	chr3	150606041	150606441	MINDY4B
-2.501456044	0.014380254	chr7	111029680	111030080	IMMP2L
-1.739934318	0.01814801	chr7	146661399	146661799	CNTNAP2
-1.917124985	0.021941188	chr7	80082199	80082599	CD36
0.963815721	0.021941188	chr21	37267363	37267763	RUNX1
2.007731668	0.021941188	chr21	44980626	44981026	HSF2BP
-1.23184593	0.021941188	chr4	81421426	81421826	CFAP299
-2.243499113	0.022919677	chr11	128772790	128773190	KCNJ5
-2.243499113	0.022919677	chr11	128772790	128773190	KCNJ5-AS1
2.347872437	0.025997175	chr13	113164501	113164901	TUBGCP3

Continued on next page

log2FoldChange	p-adj	CHR	START	END	symbol
-1.700442862	0.026761525	chr1	207282063	207282463	C4BPA
2.023979117	0.026761525	chr19	2325142	2325542	LINC02983
2.023979117	0.026761525	chr19	2325142	2325542	LSM7
1.070363663	0.028181099	chr21	42188219	42188619	DSCAM
1.918573127	0.029514861	chr15	72785388	72785788	ARIH1
-1.603987295	0.030117824	chr7	72405386	72405786	POM121
-2.260334271	0.033616417	chr6	82882575	82882975	IBTK
2.690801491	0.033616417	chr7	102671574	102671974	FBXL13
3.22274855	0.034052974	chr22	31876145	31876545	DRG1
3.22274855	0.034052974	chr22	31876145	31876545	EIF4ENIF1
-1.682567812	0.036141478	chr5	13766176	13766576	DNAH5
-1.499335058	0.036496154	chr6	5672513	5672913	FARS2
-1.74708228	0.036496154	chr6	6284197	6284597	F13A1
-1.210202853	0.036496154	chr17	46291234	46291634	SKAP1
2.776704947	0.036496154	chr2	36689036	36689436	CRIM1
-1.792522916	0.036496154	chr4	79210206	79210606	FRAS1
1.150577317	0.040228662	chr21	17454461	17454861	MIR99AHG
-2.115983152	0.043571558	chr1	84847355	84847755	SAMD13
2.952127837	0.048817447	chr9	133256833	133257233	HMCN2
1.002546413	0.04946186	chr15	77910533	77910933	LINGO1
1.571363865	0.050972163	chr11	2467306	2467706	KCNQ1
2.791943183	0.05350568	chr3	17774570	17774970	TBC1D5
-1.537723789	0.05350568	chr5	151059873	151060273	SPARC
-1.47430078	0.053943327	chr20	59004955	59005355	MIR646HG; LOC729296
1.080515952	0.056017148	chr11	46671005	46671405	ATG13
-1.515263205	0.05817257	chr20	20412794	20413194	RALGAPA2
0.874329935	0.05817257	chr21	42892993	42893393	LOC124905021; TMPRSS2
-1.216943103	0.058626748	chr3	66472616	66473016	LRIG1
1.583378234	0.058795921	chr14	102298676	102299076	PPP2R5C
1.852510898	0.060297832	chr20	51643394	51643794	TSHZ2
1.585093451	0.063985125	chr21	22421411	22421811	NCAM2
-1.365365809	0.064058938	chr1	218473485	218473885	RRP15
1.696902577	0.064373088	chr2	219109436	219109836	ARPC2
1.760347211	0.064373088	chr6	157510768	157511168	ARID1B

Continued on next page

log2FoldChange	p-adj	CHR	START	END	symbol
-1.372840641	0.065473528	chr15	25761973	25762373	LINC02250
-1.231925289	0.067854018	chr18	35039095	35039495	CELF4
-1.894899253	0.068295249	chr8	40579730	40580130	ZMAT4
-1.753817254	0.070764087	chr7	133563277	133563677	EXOC4
-2.060414115	0.072001159	chr8	104864519	104864919	RIMS2
0.950581785	0.072642649	chr21	46606067	46606467	ADARB1
-1.357678843	0.076107493	chr7	27698003	27698403	HIBADH
-1.236826251	0.079521469	chr13	98974102	98974502	FARP1
0.862400327	0.079521469	chr21	34908390	34908790	GART
1.625017018	0.079521469	chr21	34911262	34911662	GART
-1.296425636	0.081128353	chr7	131235678	131236078	PODXL
-1.948834861	0.081128353	chr2	40471401	40471801	SLC8A1-AS1
-1.948834861	0.081128353	chr2	40471401	40471801	SLC8A1
1.506966331	0.083066345	chr9	133371392	133371792	ASS1
-1.918510645	0.083459462	chr16	57235276	57235676	RSPRY1
-1.238593314	0.084545013	chr11	76657034	76657434	ACER3
-1.672468014	0.085208097	chr1	231106253	231106653	TTC13
1.575396141	0.08792171	chr12	28583852	28584252	CCDC91
-1.224371444	0.08792171	chr3	99825251	99825651	CMSS1
-1.224371444	0.08792171	chr3	99825251	99825651	FILIP1L
-1.779918516	0.088514888	chr8	38957510	38957910	ADAM9
-1.602686715	0.089057425	chr3	159978379	159978779	IFT80
0.90841726	0.090010437	chr21	39349237	39349637	DSCR4
1.643065632	0.090394799	chr18	13112993	13113393	CEP192
-1.362993111	0.090418982	chr14	33045784	33046184	AKAP6
-1.343587419	0.091363796	chr1	12376744	12377144	VPS13D
1.506379676	0.091890821	chr16	70018296	70018696	NPIPB14P
-1.383727681	0.091890821	chr17	55067746	55068146	SCPEP1
-1.982004197	0.092763121	chr1	202586433	202586833	SYT2
0.902090794	0.092763121	chr3	75435223	75435623	EVA1CP5
-1.751065322	0.094348114	chr11	73957511	73957911	PPME1
0.995023203	0.094716487	chr21	43834548	43834948	UBASH3A
1.393608224	0.095087081	chr20	46240046	46240446	NCOA3
1.757605609	0.096386297	chr3	148525759	148526159	CPB1
-1.272886837	0.09645637	chr12	11809735	11810135	ETV6
-1.818597816	0.098222919	chr9	16626666	16627066	BNC2

Continued on next page

log2FoldChange	p-adj	CHR	START	END	symbol
0.886043532	0.098222919	chr21	46323850	46324250	ITGB2
0.942590858	0.099177683	chr21	37225449	37225849	RUNX1
1.96326836	0.099177683	chr6	159077161	159077561	SYTL3

Table 18: Summary of differentially accessible peaks by DESeq2 between FAC-sorted NM (normal, n=3) and T21 (Trisomy 21, n=4) fetal BM MPP (P-adj <0.1). Peaks 1000bp upstream of or within genes were annotated using ChIPPeakAnno.

Table 19: Differential Chromatin Accessibility between NM and T21 fetal BM LMPP.

log2FoldChange	p-adj	CHR	START	END	symbol
2.439745775	6.03483E-07	chr7	138147030	138147430	TRIM24
2.873717932	2.60766E-05	chr21	41717875	41718275	DSCAM
-3.094916473	6.5043E-05	chr7	16268895	16269295	CRPPA
-3.094916473	6.5043E-05	chr7	16268895	16269295	CRPPA-AS1
1.630317155	6.5043E-05	chr16	50666794	50667194	NKD1
1.212518789	6.5043E-05	chr21	42614877	42615277	BACE2
1.720951806	6.5043E-05	chr21	43346006	43346406	C2CD2
1.198996682	6.5043E-05	chr21	43939041	43939441	SLC37A1
2.833383861	6.59098E-05	chr18	29897864	29898264	GAREM1
2.067422388	0.000184321	chr3	10284541	10284941	IRAK2
2.038428747	0.000357941	chr8	102886929	102887329	NCALD
2.292394762	0.000357941	chr22	31876145	31876545	DRG1
2.292394762	0.000357941	chr22	31876145	31876545	EIF4ENIF1
-1.790976951	0.000400711	chr17	7350110	7350510	CHRNB1
2.182821223	0.00040866	chr15	34018228	34018628	RYR3
-1.436126293	0.000774795	chr14	53571996	53572396	DDHD1
1.656658337	0.001639398	chr8	48949553	48949953	UBE2V2
-1.960017047	0.001820141	chr4	123976322	123976722	AFG2A
1.741926728	0.002036117	chr21	42193169	42193569	DSCAM
1.425197852	0.002036117	chr21	45308787	45309187	AGPAT3
1.078052525	0.002523931	chr21	36060252	36060652	CLIC6
1.070626809	0.004094559	chr21	31654948	31655348	KRTAP24-1
1.671228508	0.004094559	chr22	30940838	30941238	MTMR3
1.671228508	0.004094559	chr22	30940838	30941238	SEC14L6

Continued on next page

log2FoldChange	p-adj	CHR	START	END	symbol
-1.848320731	0.004394781	chr4	41647066	41647466	LIMCH1
0.909530447	0.00444245	chr21	29024740	29025140	LINC01673
0.969580391	0.00444245	chr21	32727895	32728295	TIAM1
1.862349996	0.004588298	chr5	156672274	156672674	ITK
2.985157446	0.004625377	chr8	3112883	3113283	CSMD1
0.930236197	0.004986304	chr21	42107870	42108270	DSCAM
0.948242045	0.006022798	chr21	42839590	42839990	LOC124905021; TMPRSS2
1.026016077	0.007528749	chr21	46606067	46606467	ADARB1
1.434831184	0.007528749	chr6	159077161	159077561	SYTL3
-2.485604544	0.007822201	chr13	35603625	35604025	NBEA
0.933398694	0.008342327	chr21	37267363	37267763	RUNX1
0.933847991	0.008558331	chr21	31731948	31732348	KRTAP13-2
0.822312871	0.008558331	chr21	42118843	42119243	DSCAM
1.133350718	0.008790772	chr21	33059482	33059882	SCAF4
0.977474055	0.009046978	chr21	37225449	37225849	RUNX1
-1.623359581	0.00977697	chr1	58149288	58149688	DAB1
1.548887174	0.01022069	chr6	40436657	40437057	LRFN2
-1.534734537	0.01022069	chr7	133563277	133563677	EXOC4
0.884745881	0.01022069	chr21	32612362	32612762	TIAM1
-1.604707965	0.01049513	chr17	70987855	70988255	SLC39A11
-2.230401627	0.010859603	chr8	141289217	141289617	TRAPPC9
1.131284791	0.010859603	chr21	45140352	45140752	PDXK
0.830807227	0.010955829	chr21	44845999	44846399	SIK1
-1.697503932	0.011079182	chr8	20009074	20009474	SLC18A1
1.283292661	0.011589623	chr3	32114532	32114932	OSBPL10
0.871536441	0.013243011	chr21	32569671	32570071	TIAM1
1.885871371	0.013761029	chr13	98044320	98044720	MBNL2
-1.809919337	0.014104832	chr2	188919817	188920217	LINC01090
0.972960247	0.014214228	chr21	42188219	42188619	DSCAM
0.915272012	0.014319277	chr21	42009901	42010301	DSCAM
1.607845644	0.015882221	chr11	12717887	12718287	TEAD1
0.980283222	0.015971039	chr21	33067461	33067861	SCAF4
1.065010166	0.015971039	chr21	43975444	43975844	SLC37A1

Continued on next page

log2FoldChange	p-adj	CHR	START	END	symbol
0.988982241	0.017425444	chr21	37045164	37045564	RUNX1
1.94446152	0.018319892	chr14	106355897	106356297	FAM30A
1.32367834	0.018319892	chr3	45915827	45916227	LZTFL1
-1.072709035	0.019051913	chr8	38957510	38957910	ADAM9
-2.09538682	0.019231908	chr2	166792865	166793265	TTC21B
0.813466588	0.019231908	chr21	35026721	35027121	ATP5PO
0.813466588	0.019231908	chr21	35026721	35027121	ITSN1
1.53073708	0.019231908	chr21	41671782	41672182	DSCAM
-1.41969983	0.019337834	chr7	155239673	155240073	EN2-DT
0.846820986	0.019990546	chr21	36319961	36320361	RUNX1
-1.407322202	0.020587758	chr9	123687275	123687675	TRAF1
1.471390826	0.020826581	chr16	11114788	11115188	CLEC16A
2.952725933	0.021427367	chr6	37962727	37963127	ZFAND3
1.663828165	0.023193092	chr1	17588421	17588821	PADI3
0.869997767	0.023481621	chr21	35051251	35051651	ATP5PO
0.869997767	0.023481621	chr21	35051251	35051651	ITSN1
1.052971888	0.023547092	chr21	42145505	42145905	DSCAM
1.83583658	0.024039144	chr13	93151213	93151613	GPC5
-1.275516744	0.024039144	chr2	187510067	187510467	ITGAV
1.016105774	0.024039144	chr21	43834548	43834948	UBASH3A
0.797326017	0.024039144	chr21	44353273	44353673	NDUFV3
-2.019563916	0.025388533	chr3	182525369	182525769	ATP11B
1.480134282	0.027613153	chr19	39297982	39298382	LGALS4
0.917335055	0.027956894	chr21	42746881	42747281	MX2
0.951722103	0.028850425	chr21	45287782	45288182	AGPAT3
0.865215848	0.029211123	chr21	39388527	39388927	DSCR4
0.830270461	0.029629081	chr21	46323850	46324250	ITGB2
1.440191471	0.029712681	chr19	16876815	16877215	NWD1
0.794910517	0.030105497	chr21	37208048	37208448	RUNX1
0.86926375	0.03028084	chr21	37220959	37221359	RUNX1
0.897010036	0.033594878	chr21	43728557	43728957	TFF3
2.716119944	0.033594878	chr5	179212860	179213260	MAML1
1.914308899	0.034715993	chr12	131528628	131529028	ADGRD1
-1.766311098	0.034715993	chr13	46745713	46746113	LCP1

Continued on next page

log2FoldChange	p-adj	CHR	START	END	symbol
0.737942544	0.034715993	chr21	39349237	39349637	DSCR4
1.082296357	0.034840392	chr21	37530949	37531349	DOP1B
-1.438346294	0.034840392	chr3	64945205	64945605	ADAMTS9-AS2
-1.417100176	0.035965494	chr10	80090125	80090525	LINC00856; LINC00595
1.369774378	0.035965494	chr21	34987175	34987575	ATP5PO
1.369774378	0.035965494	chr21	34987175	34987575	CRYZL1
-1.773016413	0.036774858	chr20	47876491	47876891	ZNFX1
1.799122134	0.036774858	chr21	44968107	44968507	HSF2BP
-2.160848148	0.041430967	chr5	93278330	93278730	ARB2A
0.800509662	0.043880136	chr21	39183472	39183872	KCNJ6
-1.452265962	0.045058006	chr12	57726093	57726493	R3HDM2
0.771947755	0.045058006	chr21	42892993	42893393	LOC124905021; TMPRSS2
0.973790574	0.045058006	chr21	43338921	43339321	C2CD2
1.119404908	0.045502973	chr21	36173843	36174243	RUNX1
-0.972023824	0.048097909	chr17	46291234	46291634	SKAP1
0.870448894	0.051826329	chr21	17512528	17512928	MIR99AHG
1.154705462	0.051826329	chr21	45535391	45535791	PWP2
-1.262131114	0.052862592	chr10	24622963	24623363	KIAA1217
1.106524317	0.052862592	chr1	2434267	2434667	PLCH2
1.479206937	0.053322211	chr3	140770960	140771360	SPSB4
0.87761238	0.05343687	chr19	2332363	2332763	LINC02983
0.87761238	0.05343687	chr19	2332363	2332763	SPPL2B
0.952874965	0.054524166	chr21	43810785	43811185	TMPRSS3
1.044037712	0.057687454	chr2	36689036	36689436	CRIM1
1.034000887	0.058016456	chr13	111189155	111189555	RAB20
2.354439833	0.058016456	chr19	1998926	1999326	BTBD2
-1.249260085	0.059911225	chr2	112784343	112784743	MERTK
-1.540067983	0.061589107	chr9	100282272	100282672	TMOD1
1.486641749	0.061982177	chr7	156612896	156613296	LMBR1
-1.685977214	0.062784778	chr1	66494476	66494876	PDE4B
-1.353140753	0.062784778	chr15	52419506	52419906	GNB5

Continued on next page

log2FoldChange	p-adj	CHR	START	END	symbol
-1.605623621	0.062784778	chr17	64344188	64344588	PRKCA
0.897582873	0.062784778	chr21	41283236	41283636	PCP4
-1.710002848	0.065123111	chr6	6284197	6284597	F13A1
0.836452323	0.065123111	chr21	43719017	43719417	ABCG1
0.797950412	0.066466867	chr21	44297662	44298062	WDR4
1.379740264	0.06697233	chr5	33850065	33850465	ADAMTS12
0.795964164	0.068414213	chr21	38805503	38805903	DYRK1A
1.817608504	0.068414213	chr21	44836685	44837085	SIK1
0.89191792	0.069039741	chr10	100510978	100511378	HPSE2
0.775587059	0.069039741	chr21	46369448	46369848	SLX9
1.002887251	0.069039741	chr5	114858017	114858417	FEM1C
-1.566562592	0.069479382	chr8	40579730	40580130	ZMAT4
1.12308568	0.070514608	chr4	7828307	7828707	AFAP1
-1.482328141	0.071948798	chr11	82932549	82932949	ANKRD42
1.649902559	0.072712685	chr11	118342579	118342979	KMT2A
1.110645229	0.072712685	chr4	113355635	113356035	ALPK1
-1.607001431	0.074373607	chr11	73957511	73957911	PPME1
0.759346781	0.074974248	chr21	42879387	42879787	LOC124905021; TMPRSS2
1.044095977	0.075092989	chr9	133371392	133371792	ASS1
0.785033618	0.075092989	chr21	33265679	33266079	HUNK
-1.182032346	0.076582011	chr6	20575359	20575759	CDKAL1
-1.56508512	0.07712151	chr16	67652760	67653160	CTCF
-1.867234161	0.07712151	chr2	112869511	112869911	TMEM87B
0.738207604	0.079506942	chr21	45152309	45152709	PDXK
2.100721105	0.079506942	chr1	243596326	243596726	SDCCAG8
2.085594639	0.080447018	chr10	1475082	1475482	ADARB2
2.141859111	0.080447018	chr13	113607367	113607767	MCF2L
-1.420248276	0.080447018	chr19	41135573	41135973	LTBP4
-1.347830834	0.082734961	chr3	11363761	11364161	ATG7
-1.335145308	0.085500962	chrX	113906141	113906541	HTR2C
-1.019845855	0.087752042	chr22	30743585	30743985	MTMR3
-1.019845855	0.087752042	chr22	30743585	30743985	SF3A1
-1.085992164	0.087752042	chr3	9946384	9946784	IL17RE

Continued on next page

log2FoldChange	p-adj	CHR	START	END	symbol
-1.341540982	0.089475244	chr1	6935406	6935806	CAMTA1
1.443546066	0.089475244	chr10	856716	857116	LARP4B
1.447242626	0.089475244	chr16	4384249	4384649	GLIS2
0.757537451	0.089475244	chr21	42117381	42117781	DSCAM
1.4181339	0.089475244	chr6	168355889	168356289	AFDN
1.23452923	0.090010028	chr10	83680473	83680873	NRG3
0.800050369	0.090284123	chr21	46057200	46057600	TSPEAR
0.800050369	0.090284123	chr21	46057200	46057600	KRTAP10-10
1.740528793	0.090866205	chr6	168367230	168367630	AFDN
-1.223815006	0.092119216	chr12	31645921	31646321	DENND5B
-1.790914721	0.092627997	chr3	58892537	58892937	CFAP20DC
-1.790914721	0.092627997	chr3	58892537	58892937	CFAP20DC-AS1
-0.83144503	0.096095573	chr5	43603505	43603905	NNT
0.700739834	0.09900259	chr21	38831418	38831818	DYRK1A
-1.215396302	0.099258497	chr1	180611267	180611667	XPR1
2.408872317	0.099258497	chr5	83662576	83662976	EDIL3

Table 19: Summary of differentially accessible peaks by DESeq2 between FAC-sorted NM (normal, n=5) and T21 (trisomy 21, n=4) fetal BM LMPP (P-adj <0.1). Peaks 1000bp upstream of or within genes were annotated using ChIPPeakAnno.

.4 Differential gene expression in fetal BM MSC

Table 20: Differential gene expression between NM and T21 fetal BM MSC.

Gene	log2FoldChange	p-adj	Comment
LPPR4	2.1040648	3.27E-02	
NMNAT2	1.7412278	9.12E-02	
LHX9	2.081844	7.14E-03	
VSTM4	0.7558809	2.87E-02	
LINC01468	5.185768	6.44E-02	
C10orf11	-1.985281	9.40E-02	
OLR1	3.3081078	7.63E-02	
C2CD5	-0.3585052	7.36E-03	
FGD4	2.1256018	8.08E-02	
OAS2	3.2402162	7.87E-02	Involved in interferon response.
RNASE1	-23.6006663	1.06E-10	
NYNRIN	0.7011426	9.12E-02	
SSTR1	1.7809667	8.08E-02	
TTC9	1.9471373	1.92E-02	
IFI27	3.9179441	5.65E-03	Involved in interferon response.
SLC12A6	1.1717018	1.92E-02	
ICE2	-0.3450377	9.84E-02	
TMEM8A	0.5667377	3.52E-05	
NOMO1	0.4848218	4.30E-02	
CES1	-5.6512339	1.02E-02	
PDP2	-0.3886134	3.87E-02	Regulates carbohydrate metabolism [747]
CCDC144B	-2.181937	5.81E-02	
AOC2	3.2993727	1.65E-02	
SLC44A2	0.7289145	9.62E-03	
APLP1	1.016338	3.67E-02	
EMP3	0.3691576	1.70E-02	
ZNF578	0.7726787	8.87E-02	
GALNT5	1.3174933	7.63E-02	
GRB14	2.3536908	9.40E-02	
HECW2	1.6379669	8.08E-02	
DES	-2.6716271	2.90E-02	
HSPA13	0.6124705	2.05E-02	Chr 21 gene that encodes a heat shock protein
BTG3	0.6041468	8.08E-02	Chr 21 gene that functions as a negative regulator of the cell cycle[335, 748]. A prognostic marker of T-ALL[749].
ATP5J	0.6319067	3.70E-02	Chr 21 mitochondrial gene

Continued on next page

Gene	Log2FoldChange	P-adj	Comment
GABPA	0.5158887	1.58E-02	on Chr 21. A regulator of pluripotency[750]. In HSPC, GABPA plays a role in HSPC maintenance and differentiation[751], especially into myeloid lineages[598] and B lymphoid maturation[597].
LTN1	0.5254104	3.30E-02	on Chr 21. Maintains protein homeostasis, mediates ribosome degradation[752, 753]; plays a role in regulating the inflammatory response to viral infection[754].
USP16	0.4634345	1.60E-03	on Chr 21. Regulates *HOX* gene expression. Increased *USP16* expression been linked to decreased proliferation in fibroblasts in T21[755]. In HSPC, USP16 plays a role in murine HSC function and lymphopoiesis[756].
SOD1	0.6948912	2.20E-03	on Chr 21. Protects against oxidative stress, oxidative stress impairs adipogenesis [757] Part of Hallmark Adipogenesis.
URB1	0.7939386	9.54E-02	on Chr 21, RNA binding gene
C21orf59	0.5847393	1.92E-02	on Chr 21, plays a role in motile cilia function
SYNJ1	0.8081915	8.92E-02	on Chr 21, involved in membrane trafficking
IFNAR1	0.7564055	3.85E-05	on Chr 21. IFNα receptor, involved in IFN response.
IFNGR2	0.5928279	1.65E-02	on Chr 21. IFNγ receptor, involved in IFN response.
ITSN1	0.6968588	9.24E-08	on Chr 21. Involved in insulin secretion [758], part of Hallmark Adipogenesis.
SLC5A3	1.9730768	2.03E-03	on Chr 21, a solute carrier protein, can transport monosaccharides across the cell membrane.
MRPS6	1.4344776	2.03E-03	on Chr 21, a mitochondrial ribosomal protein.
CBR1	0.6974741	7.36E-03	on Chr 21, an NADPH reductase, involved in the metabolism of glucocorticoids and prostaglandins.
CBR3	0.5766584	7.17E-03	on Chr 21, an NADPH reductase, involved in the metabolism of glucocorticoids and prostaglandins

Continued on next page

Gene	Log2FoldChange	P-adj	Comment
MORC3	0.4490186	2.33E-02	on Chr 21, a negative regulator of the interferon response[759]
HLCS	0.8036806	2.18E-06	on Chr 21, plays a role in fatty acid synthesis [760]
PIGP	0.9755093	4.52E-02	on Chr 21, plays a role in membrane glycolipid synthesis
DSCR3	0.6672207	2.81E-06	on Chr 21, an endosomal protein
DYRK1A	0.6406623	3.29E-06	on Chr 21. kinase involved in regulating cell cycle; implicated in skeletal abnormalities in Down Syndrome[492]. In HSPC, it has been linked to inhibiting B cell proliferation [591], autoimmunity[592] and leukaemia[592, 593].
PSMG1	0.588752	2.90E-02	on Chr 21, a chaperone protein for proteasome assembly.
BRWD1	0.589165	6.26E-05	on Chr 21, regulates chromatin remodelling in mice
HMGN1	0.5152939	2.90E-02	on Chr 21. Involved in chromatin remodelling, plays a role in white adipose tissue formation [761]. Overexpression recapitulates T21 B lymphoid phenotype in T21 models[380, 532].
MX1	3.84949	1.47E-02	on Chr 21. Involved in interferon response.
RIPK4	2.7593354	1.01E-04	on Chr , a protein kinase that can activate inflammatory transcription factor NFκB[762]
C2CD2	0.8270818	2.20E-03	on Chr 21
PDXK	0.6122467	7.13E-03	on Chr 21, involved in metabolism, phosphorylates vitamin B6
CSTB	0.5894049	7.21E-02	on Chr 21, involved in preventing proteases leaking from lysosomes.
AGPAT3	0.5410332	2.20E-04	on Chr 21. Involved in lipid synthesis[763], part of Hallmark Adipogenesis.
TRAPPC10	0.7500334	1.70E-02	on Chr 21, involved in vesicle-mediated protein transport.
PFKL	0.838384	2.49E-06	on Chr 21. Plays a role in glycolysis, glycolytic intermediates promote adipogenesis [764]. Part of Hallmark Adipogenesis.
C21orf2	0.9178305	9.62E-03	on Chr 21, mitochondrial protein.
UBE2G2	0.6284777	1.38E-02	on Chr 21, a ubiquitin conjugating enzyme.

Continued on next page

Gene	Log2FoldChange	P-adj	Comment
SUMO3	0.4423854	2.10E-02	on Chr 21, a ubiquitin-like protein that can be attached to other proteins post-translation.
PTTG1IP	0.790697	5.31E-04	on Chr 21, facilitates translocation of transcription factor pituitary tumor transforming protein into the nucleus.
POFUT2	0.9086167	8.61E-12	on Chr 21, an enzyme that can post translationally modify proteins.
LOC642852	0.8186982	1.84E-04	on Chr 21, non-protein coding.
MCM3AP	0.5860516	2.05E-02	on Chr 21, involved in DNA replication.
DIP2A	0.6463877	3.27E-02	on Chr 21, involved in axon patterning in the nervous system.
PRMT2	0.7328711	1.84E-04	on Chr 21, an enzyme that methylates arginine residues.
CYB5R3	0.5300228	8.08E-02	Part of mitochondrial electron transfer chain
CELSR3	1.169353	2.35E-05	
TNNC1	2.2299249	3.27E-02	
UPK1B	5.6970785	2.81E-06	
FGFR3	2.7825562	7.13E-02	
S100P	4.8889486	2.17E-02	
LIMCH1	2.1887834	2.10E-02	
NAAA	0.9510516	3.93E-02	Part of lipid metabolism, can hydrolyse bioactive lipids [630]
PCDH10	2.4389412	1.92E-02	
PCDHB2	1.1611482	9.06E-02	
FGF1	1.7664984	9.40E-02	Seceted ligand, negative regulator of BMP signalling[670]
BMP6	3.2596338	4.68E-03	Secreted ligand, Involved in osteogenesis[676], impairs B lymphopoiesis *in vitro*[677].
HIST1H4C	-2.2276178	3.30E-02	
SLC17A5	0.6675097	8.08E-02	
FGL2	5.2470066	1.70E-02	
STEAP1	-1.0177513	2.90E-02	
WNT16	2.6721577	6.24E-02	Secreted ligand, implicated in promoting MSC differentiation and regulating balance between osteoblastic / adipocytic fate [765][671][672]
LINC01605	-0.7675191	2.03E-03	
VPS13B	0.4299656	4.30E-02	
FAM83H	1.2339848	1.65E-02	

Continued on next page

Gene	Log2FoldChange	P-adj	Comment
PTGES	1.4481263	2.32E-02	Prostaglandin E Synthase, PGE2 implicated in transition between white and brown adipose tissue[766]
GPR107	0.269266	8.96E-02	

Table 20: Summary of differentially expressed genes by DESeq2 between derived NM (n=7) and T21 (n=5) fetal BM MSC (P-adj <0.1). Chromosome 21 genes are highlighted in red text.

References

[1] William Bloom and G. W. Bartelmez. “Hematopoiesis in young human embryos”. In: *American Journal of Anatomy* 67.1 (July 1940), pp. 21–53.

[2] T. Fukuda. “Fetal hemopoiesis”. In: *Virchows Archiv B Cell Pathology* 14.1 (Dec. 1973), p. 197.

[3] Richard C.V. Tyser et al. “Single-cell transcriptomic characterization of a gastrulating human embryo”. In: *Nature* 600.7888 (Dec. 2021), pp. 285–289.

[4] James Palis. “Hematopoietic stem cell-independent hematopoiesis: emergence of erythroid, megakaryocyte, and myeloid potential in the mammalian embryo”. In: *FEBS Letters* 590.22 (Nov. 2016), pp. 3965–3974.

[5] Valerie Wittamer and Julien Y. Bertrand. “Yolk sac hematopoiesis: does it contribute to the adult hematopoietic system?” In: *Cellular and Molecular Life Sciences* 77.20 (Oct. 2020), pp. 4081–4091.

[6] Igor M. Samokhvalov, Natalia I. Samokhvalova, and Shin-ichi Nishikawa. “Cell tracing shows the contribution of the yolk sac to adult haematopoiesis”. In: *Nature* 446.7139 (Apr. 2007), pp. 1056–1061.

[7] Natalie DeWitt. “Inside the Paper: Rewriting in blood: blood stem cells may have a surprising origin”. In: *Nature Reports Stem Cells* (June 2007).

[8] Kiyoshi Takahashi, Fumie Yamamura, and Makoto Naito. “Differentiation, Maturation, and Proliferation of Macrophages in the Mouse Yolk Sac: A Light-Microscopic, Enzyme-Cytochemical, Immunohistochemical, and Ultrastructural Study”. In: *Journal of Leukocyte Biology* 45.2 (Feb. 1989), pp. 87–96.

[9] Lynn Morris, Christopher F. Graham, and Siamon Gordon. “Macrophages in haemopoietic and other tissues of the developing mouse detected by the monoclonal antibody F4/80”. In: *Development* 112.2 (June 1991), pp. 517–526.

[10] Elisa Gomez Perdiguero et al. “Tissue-resident macrophages originate from yolk-sac-derived erythro-myeloid progenitors”. In: *Nature* 518.7540 (Feb. 2015), pp. 547–551.

[11] Florent Ginhoux et al. “Fate Mapping Analysis Reveals That Adult Microglia Derive from Primitive Macrophages”. In: *Science* 330.6005 (Nov. 2010), pp. 841–845.

[12] Kathleen E. McGrath, Jenna M. Frame, and James Palis. “Early hematopoiesis and macrophage development”. In: *Seminars in Immunology* 27.6 (Dec. 2015), pp. 379–387.

[13] Manuela Tavian, Marie-France Hallais, and Bruno Péault. “Emergence of intraembryonic hematopoietic precursors in the pre-liver human embryo”. In: *Development* 126.4 (Feb. 1999), pp. 793–803.

[14] Zhilei Bian et al. “Deciphering human macrophage development at single-cell resolution”. In: *Nature* 582.7813 (June 2020), pp. 571–576.

[15] Vincenzo Calvanese and Hanna K A Mikkola. “The genesis of human hematopoietic stem cells”. In: *Blood* 142.6 (Aug. 2023), pp. 519–532.

[16] Michael J. Chen et al. “Runx1 is required for the endothelial to haematopoietic cell transition but not thereafter”. In: *Nature* 457.7231 (Feb. 2009), pp. 887–891.

[17] Tsukasa Okuda et al. “AML1, the Target of Multiple Chromosomal Translocations in Human Leukemia, Is Essential for Normal Fetal Liver Hematopoiesis”. In: *Cell* 84.2 (Jan. 1996), pp. 321–330.

[18] Dorin Mirel Popescu et al. “Decoding human fetal liver haematopoiesis”. In: *Nature* 574.7778 (Oct. 2019), pp. 365–371.

[19] P. G. Holt and C. A. Jones. “The development of the immune system during pregnancy and early life”. In: *Allergy* 55.8 (Aug. 2000), pp. 688–697.

[20] Sorcha O’Byrne et al. “Discovery of a CD10-negative B-progenitor in human fetal life identifies unique ontogeny-related developmental programs”. In: *Blood* 134 (Sept. 2019), pp. 1059–1071.

[21] Anindita Roy et al. “Transitions in lineage specification and gene regulatory networks in hematopoietic stem/progenitor cells over human development”. In: *Cell Reports* 36.11 (Sept. 2021).

[22] Elisabeth R. Krow-Lucal and Joseph M. McCune. “Distinct Functional Programs in Fetal T and Myeloid Lineages”. In: *Frontiers in Immunology* 5 (July 2014).

[23] Trevor D. Burt and Joseph M. McCune. “Human fetal T cells: Insights into developmental specialization and mechanisms of lineage transition”. In: *Immunological Reviews* 315.1 (May 2023), pp. 126–153.

[24] Leonore A. Herzenberg and Leonard A. Herzenberg. “Toward a layered immune system”. In: *Cell* 59.6 (Dec. 1989), pp. 953–954.

[25] Ramy Elsaid et al. “Hematopoiesis: A Layered Organization Across Chordate Species”. In: *Frontiers in Cell and Developmental Biology* 8 (Dec. 2020).

[26] Brandon Hadland and Momoko Yoshimoto. “Many layers of embryonic hematopoiesis: new insights into B-cell ontogeny and the origin of hematopoietic stem cells”. In: *Experimental Hematology* 60 (Apr. 2018), pp. 1–9.

[27] Kenneth Dorshkind and Gay Crooks. “Layered immune system development in mice and humans”. In: *Immunological Reviews* 315.1 (May 2023), pp. 5–10.

[28] Ryan Mack et al. “The Fetal-to-Adult Hematopoietic Stem Cell Transition and its Role in Childhood Hematopoietic Malignancies”. In: *Stem Cell Reviews and Reports* 17.6 (Dec. 2021), pp. 2059–2080.

[29] Daniel G. Bunis et al. “Single-Cell Mapping of Progressive Fetal-to-Adult Transition in Human Naive T Cells”. In: *Cell Reports* 34.1 (Jan. 2021).

[30] Mikael N. E. Sommarin et al. “Single-cell multiomics of human fetal hematopoiesis define a developmental-specific population and a fetal signature”. In: *Blood Advances* 7.18 (Sept. 2023), pp. 5325–5340.

[31] P M Lansdorp, W Dragowska, and H Mayani. “Ontogeny-related changes in proliferative potential of human hematopoietic cells.” In: *The Journal of experimental medicine* 178.3 (Sept. 1993), pp. 787–791.

[32] M O Muench et al. “Expression of CD33, CD38, and HLA-DR on CD34+ human fetal liver progenitors with a high proliferative potential.” In: *Blood* 83.11 (June 1994), pp. 3170–81.

[33] M. B. Bowie et al. “Hematopoietic stem cells proliferate until after birth and show a reversible phase-specific engraftment defect”. In: *Journal of Clinical Investigation* 116.10 (Oct. 2006), pp. 2808–2816.

[34] Michael R. Copley et al. “The Lin28b–let-7–Hmga2 axis determines the higher self-renewal potential of fetal haematopoietic stem cells”. In: *Nature Cell Biology* 15.8 (Aug. 2013), pp. 916–925.

[35] Michael R Copley and Connie J Eaves. “Developmental changes in hematopoietic stem cell properties”. In: *Experimental & Molecular Medicine* 45.11 (Nov. 2013), e55–e55.

[36] Laura Jardine et al. “Blood and immune development in human fetal bone marrow and Down syndrome”. In: *Nature* 598.7880 (Oct. 2021), pp. 327–331.

[37] Claudia Benz et al. “Hematopoietic Stem Cell Subtypes Expand Differentially during Development and Display Distinct Lymphopoietic Programs”. In: *Cell Stem Cell* 10.3 (Mar. 2012), pp. 273–283.

[38] Ping Lan et al. “Reconstitution of a functional human immune system in immunodeficient mice through combined human fetal thymus/liver and CD34+ cell transplantation”. In: *Blood* 108.2 (July 2006), pp. 487–492.

[39] C C Fraser et al. “Human allogeneic stem cell maintenance and differentiation in a long-term multilineage SCID-hu graft.” In: *Blood* 86.5 (Sept. 1995), pp. 1680–93.

[40] Naoyuki Uchida et al. “Transplantable hematopoietic stem cells in human fetal liver have a CD34+ side population (SP) phenotype”. In: *Journal of Clinical Investigation* 108.7 (Oct. 2001), pp. 1071–1077.

[41] Tessa L Holyoake, Franck E Nicolini, and Connie J Eaves. “Functional differences between transplantable human hematopoietic stem cells from fetal liver, cord blood, and adult marrow”. In: *Experimental Hematology* 27.9 (Sept. 1999), pp. 1418–1427.

[42] Pierre Rollini et al. “Phenotypic and Functional Analysis of Human Fetal Liver Hematopoietic Stem Cells in Culture”. In: *Stem Cells and Development* 16.2 (Apr. 2007), pp. 281–296.

[43] D DiGiusto et al. “Human fetal bone marrow early progenitors for T, B, and myeloid cells are found exclusively in the population expressing high levels of CD34.” In: *Blood* 84.2 (July 1994), pp. 421–32.

[44] B P Chen et al. “Engraftment of human hematopoietic precursor cells with secondary transfer potential in SCID-hu mice.” In: *Blood* 84.8 (Oct. 1994), pp. 2497–505.

[45] Zhaofeng Zheng et al. “Uncovering the emergence of HSCs in the human fetal bone marrow by single-cell RNA-seq analysis”. In: *Cell Stem Cell* 29.11 (Nov. 2022), pp. 1562–1579.

[46] Sean J. Morrison et al. “Identification of a lineage of multipotent hematopoietic progenitors”. In: *Development* 124.10 (May 1997), pp. 1929–1939.

[47] Ravindra Majeti, Christopher Y Park, and Irving L Weissman. “Identification of a hierarchy of multipotent hematopoietic progenitors in human cord blood.” In: *Cell stem cell* 1.6 (Dec. 2007), pp. 635–45.

[48] Ana Cvejic. “Mechanisms of fate decision and lineage commitment during haematopoiesis”. In: *Immunology and Cell Biology* 94.3 (Mar. 2016), pp. 230–235.

[49] Nicola K. Wilson et al. “Combined Single-Cell Functional and Gene Expression Analysis Resolves Heterogeneity within Stem Cell Populations”. In: *Cell Stem Cell* 16.6 (June 2015), pp. 712–724.

[50] Roy Drissen et al. “Identification of two distinct pathways of human myelopoiesis”. In: *Sci. Immunol* 4 (2019), p. 7148.

[51] Faiyaz Notta et al. “Distinct routes of lineage development reshape the human blood hierarchy across ontogeny”. In: *Science* 351.6269 (Jan. 2016), pp. 139–148.

[52] Bethan Psaila and Adam J. Mead. “Single-cell approaches reveal novel cellular pathways for megakaryocyte and erythroid differentiation”. In: *Blood* 133.13 (2019), pp. 1427–1435.

[53] Timm Schroeder. “Cytokines Instruct Hematopoietic Lineage Choice”. In: *Blood* 116.21 (Nov. 2010), SCI-13-SCI–13.

[54] Anne Galy et al. “Human T, B, natural killer, and dendritic cells arise from a common bone marrow progenitor cell subset”. In: *Immunity* 3.4 (Oct. 1995), pp. 459–473.

[55] Marit E. Hystad et al. “Characterization of Early Stages of Human B Cell Development by Gene Expression Profiling”. In: *The Journal of Immunology* 179.6 (Sept. 2007), pp. 3662–3671.

[56] Sören Boller and Rudolf Grosschedl. “The regulatory network of B-cell differentiation: A focused view of early B-cell factor 1 function”. In: *Immunological Reviews* 261.1 (2014), pp. 102–115.

[57] Tomohiko Tamura, Daisuke Kurotaki, and Shin ichi Koizumi. “Regulation of myelopoiesis by the transcription factor IRF8”. In: *International Journal of Hematology* 101.4 (Apr. 2015), pp. 342–351.

[58] Joachim L. Schultze, Elvira Mass, and Andreas Schlitzer. “Emerging Principles in Myelopoiesis at Homeostasis and during Infection and Inflammation”. In: *Immunity* 50.2 (Feb. 2019), pp. 288–301.

[59] David Lara-Astiaso et al. “In vivo screening characterizes chromatin factor functions during normal and malignant hematopoiesis”. In: *Nature Genetics* 55.9 (Sept. 2023), pp. 1542–1554.

[60] Anna Maria Ranzoni et al. “Integrative Single-Cell RNA-Seq and ATAC-Seq Analysis of Human Developmental Hematopoiesis”. In: *Cell Stem Cell* 28.3 (Mar. 2021), pp. 472–487.

[61] Stuart H Orkin. "Priming the Hematopoietic Pump". In: *Immunity* 19.5 (Nov. 2003), pp. 633–634.

[62] M Hu et al. "Multilineage gene expression precedes commitment in the hemopoietic system." In: *Genes & Development* 11.6 (Mar. 1997), pp. 774–785.

[63] Guoji Guo et al. "Mapping cellular hierarchy by single-cell analysis of the cell surface repertoire". In: *Cell Stem Cell* 13.4 (Oct. 2013), pp. 492–505.

[64] Elinore M. Mercer et al. "Multilineage Priming of Enhancer Repertoires Precedes Commitment to the B and Myeloid Cell Lineages in Hematopoietic Progenitors". In: *Immunity* 35.3 (Sept. 2011), pp. 413–425.

[65] Lisa A Kohn et al. "Lymphoid priming in human bone marrow begins before expression of CD10 with upregulation of L-selectin". In: *Nature Immunology* 13.10 (Oct. 2012), pp. 963–971.

[66] Sidinh Luc, Natalija Buza-Vidas, and Sten Eirik W. Jacobsen. "Biological and Molecular Evidence for Existence of Lymphoid-Primed Multipotent Progenitors". In: *Annals of the New York Academy of Sciences* 1106.1 (June 2007), pp. 89–94.

[67] Sergei Doulatov et al. "Revised map of the human progenitor hierarchy shows the origin of macrophages and dendritic cells in early lymphoid development". In: *Nature Immunology* 11.7 (July 2010), pp. 585–593.

[68] Dimitris Karamitros et al. "Single-cell analysis reveals the continuum of human lympho-myeloid progenitor cells". In: *Nature Immunology* 19.1 (Jan. 2018), pp. 85–97.

[69] Anindita Roy et al. "Perturbation of fetal liver hematopoietic stem and progenitor cell development by trisomy 21". In: *Proceedings of the National Academy of Sciences of the United States of America* 109.43 (Oct. 2012), pp. 17579–17584.

[70] Sorcha O'byrne. "Human fetal B-lymphopoiesis and acute lymphoblastic leukaemia: the impact of trisomy 21". PhD thesis. Oxford: University of Oxford, 2019.

[71] Nicolas Goardon et al. "Coexistence of LMPP-like and GMP-like Leukemia Stem Cells in Acute Myeloid Leukemia". In: *Cancer Cell* 19.1 (Jan. 2011), pp. 138–152.

[72] Wendy W. Pang et al. "Human bone marrow hematopoietic stem cells are increased in frequency and myeloid-biased with age". In: *Proceedings of the National Academy of Sciences of the United States of America* 108.50 (Dec. 2011), pp. 20012–20017.

[73] Motonari Kondo, Irving L. Weissman, and Koichi Akashi. "Identification of Clonogenic Common Lymphoid Progenitors in Mouse Bone Marrow". In: *Cell* 91.5 (Nov. 1997), pp. 661–672.

[74] Robert Mansson et al. "Single-cell analysis of the common lymphoid progenitor compartment reveals functional and molecular heterogeneity". In: *Blood* 115.13 (Apr. 2010), pp. 2601–2609.

[75] Maryam Ghaedi et al. "Common-Lymphoid-Progenitor-Independent Pathways of Innate and T Lymphocyte Development". In: *Cell Reports* 15.3 (Apr. 2016), pp. 471–480.

[76] R Haddad et al. “Molecular characterization of early human T/NK and B-lymphoid progenitor cells in umbilical cord blood”. In: *Blood* 104.13 (Dec. 2004), pp. 3918–3926.

[77] Qian-Lin Hao et al. “Identification of a novel, human multilymphoid progenitor in cord blood”. In: *Blood* 97.12 (June 2001), pp. 3683–3690.

[78] Thomas R. Jackson, Rebecca E. Ling, and Anindita Roy. “The Origin of B-cells: Human Fetal B Cell Development and Implications for the Pathogenesis of Childhood Acute Lymphoblastic Leukemia”. In: *Frontiers in Immunology* 12 (Feb. 2021).

[79] Kenneth Dorshkind and Encarnacion Montecino-Rodriguez. “Fetal B-cell lymphopoiesis and the emergence of B-1-cell potential”. In: *Nature Reviews Immunology* 7.3 (Mar. 2007), pp. 213–219.

[80] Charlotta Böiers et al. “A Human IPS Model Implicates Embryonic B-Myeloid Fate Restriction as Developmental Susceptibility to B Acute Lymphoblastic Leukemia-Associated ETV6-RUNX1”. In: *Developmental Cell* 44.3 (Feb. 2018), pp. 362–377.

[81] Kutaiba Alhaj Hussen et al. “Multimodal cartography of human lymphopoiesis reveals B and T/NK/ILC lineages are subjected to differential regulation”. In: *iScience* 26.10 (Oct. 2023).

[82] Kutaiba Alhaj Hussen et al. “Molecular and Functional Characterization of Lymphoid Progenitor Subsets Reveals a Bipartite Architecture of Human Lymphopoiesis”. In: *Immunity* 47.4 (Oct. 2017), pp. 680–696.

[83] Seydou Keita et al. “Distinct subsets of multi-lymphoid progenitors support ontogeny-related changes in human lymphopoiesis”. In: *Cell Reports* 42.6 (June 2023), p. 112618.

[84] Elze Rackaityte and Joanna Halkias. “Mechanisms of Fetal T Cell Tolerance and Immune Regulation”. In: *Frontiers in Immunology* 11 (Apr. 2020).

[85] Ellen V. Rothenberg. “Transcriptional control of early T and B cell developmental choices”. In: *Annual Review of Immunology* 32 (Mar. 2014), pp. 283–321.

[86] Bianca Blom and Hergen Spits. “DEVELOPMENT OF HUMAN LYMPHOID CELLS”. In: *Annual Review of Immunology* 24.1 (Apr. 2006), pp. 287–320.

[87] Stephen L. Nutt and Barbara L. Kee. *The Transcriptional Regulation of B Cell Lineage Commitment*. June 2007.

[88] Julita Ramirez, Kara Lukin, and James Hagman. “From hematopoietic progenitors to B cells: mechanisms of lineage restriction and commitment.” In: *Current opinion in immunology* 22.2 (Apr. 2010), pp. 177–84.

[89] Sasan Zandi, David Bryder, and Mikael Sigvardsson. “Load and lock: the molecular mechanisms of B-lymphocyte commitment”. In: *Immunological Reviews* 238.1 (Nov. 2010), pp. 47–62.

[90] Christian A J Voßhenrich et al. “Thymic stromal-derived lymphopoietin distinguishes fetal from adult B cell development”. In: *Nature Immunology* 4.8 (Aug. 2003), pp. 773–779.

[91] O J Borge et al. “Lymphoid-restricted development from multipotent candidate murine stem cells: distinct and complimentary functions of the c-kit and flt3-ligands.” In: *Blood* 94.11 (Dec. 1999), pp. 3781–90.

[92] Kazu Kikuchi et al. “IL-7 receptor signaling is necessary for stage transition in adult B cell development through up-regulation of EBF”. In: *The Journal of Experimental Medicine* 201.8 (Apr. 2005), pp. 1197–1203.

[93] Kazu Kikuchi et al. “IL-7 Specifies B Cell Fate at the Common Lymphoid Progenitor to Pre-ProB Transition Stage by Maintaining Early B Cell Factor Expression”. In: *The Journal of Immunology* 181.1 (July 2008), pp. 383–392.

[94] Panagiotis Tsapogas et al. “IL-7 mediates Ebf-1–dependent lineage restriction in early lymphoid progenitors”. In: *Blood* 118.5 (Aug. 2011), pp. 1283–1290.

[95] Sheila Dias et al. “Interleukin-7 is necessary to maintain the B cell potential in common lymphoid progenitors”. In: *The Journal of Experimental Medicine* 201.6 (Mar. 2005), pp. 971–979.

[96] Anne Puel et al. “Defective IL7R expression in T-B+NK+ severe combined immunodeficiency”. In: *Nature Genetics* 20.4 (Dec. 1998), pp. 394–397.

[97] Silvia Giliani et al. “Interleukin-7 receptor α (IL-7Rα) deficiency: cellular and molecular bases. Analysis of clinical, immunological, and molecular features in 16 novel patients”. In: *Immunological Reviews* 203.1 (Feb. 2005), pp. 110–126.

[98] Yasmin Khan Parrish et al. “IL-7 Dependence in Human B Lymphopoiesis Increases during Progression of Ontogeny from Cord Blood to Bone Marrow”. In: *The Journal of Immunology* 182.7 (Apr. 2009), pp. 4255–4266.

[99] Eva Sanz et al. “Human cord blood CD34+Pax-5+ B-cell progenitors: single-cell analyses of their gene expression profiles”. In: *Blood* 101.9 (May 2003), pp. 3424–3430.

[100] Nely Rodriguez-Zhurbenko et al. “Human B-1 Cells and B-1 Cell Antibodies Change With Advancing Age”. In: *Frontiers in Immunology* 10 (Mar. 2019).

[101] Momoko Yoshimoto et al. “Embryonic day 9 yolk sac and intra-embryonic hemogenic endothelium independently generate a B-1 and marginal zone progenitor lacking B-2 potential”. In: *Proceedings of the National Academy of Sciences* 108.4 (Jan. 2011), pp. 1468–1473.

[102] Nanette Solvason, Agnès Lehuen, and John F. Kearney. “An embryonic source of Ly1 but not conventional B cells”. In: *International Immunology* 3.6 (1991), pp. 543–550.

[103] Belén de Andrés et al. “The first 3 days of B-cell development in the mouse embryo”. In: *Blood* 100.12 (Dec. 2002), pp. 4074–4081.

[104] Encarnacion Montecino-Rodriguez and Kenneth Dorshkind. “B-1 B cell development in the fetus and adult.” In: *Immunity* 36.1 (Jan. 2012), pp. 13–21.

[105] K Hayakawa et al. “Progenitors for Ly-1 B cells are distinct from progenitors for other B cells.” In: *The Journal of experimental medicine* 161.6 (June 1985), pp. 1554–1568.

[106] Encarnacion Montecino-Rodriguez, Hyosuk Leathers, and Kenneth Dorshkind. “Identification of a B-1 B cell–specified progenitor”. In: *Nature Immunology* 7.3 (Mar. 2006), pp. 293–301.

[107] Daniel O. Griffin, Nichol E. Holodick, and Thomas L. Rothstein. "Human B1 cells in umbilical cord and adult peripheral blood express the novel phenotype CD20+CD27+CD43+CD70". In: *Journal of Experimental Medicine* 208.1 (Jan. 2011), pp. 67–80.

[108] C Bueno et al. "Immunophenotypic analysis and quantification of B-1 and B-2 B cells during human fetal hematopoietic development". In: *Leukemia* 30.7 (July 2016), pp. 1603–1606.

[109] Chenqu Suo et al. "Mapping the developing human immune system across organs". In: *Science* 376.6597 (June 2022).

[110] Marc Descatoire et al. "A human equivalent of mouse B-1 cells?" In: *Journal of Experimental Medicine* 208.13 (Dec. 2011), pp. 2563–2564.

[111] Tâm D Quách et al. "Distinctions among Circulating Antibody-Secreting Cell Populations, Including B-1 Cells, in Human Adult Peripheral Blood". In: *The Journal of Immunology* 196.3 (Feb. 2016), pp. 1060–1069.

[112] F M Uckun and J A Ledbetter. "Immunobiologic differences between normal and leukemic human B-cell precursors." In: *Proceedings of the National Academy of Sciences* 85.22 (Nov. 1988), pp. 8603–8607.

[113] ER Grumayer et al. "Identification of novel B-lineage cells in human fetal bone marrow that coexpress CD7". In: *Blood* 77.1 (Jan. 1991), pp. 64–68.

[114] Anindita Roy et al. "High resolution IgH repertoire analysis reveals fetal liver as the likely origin of life-long, innate B lymphopoiesis in humans". In: *Clinical Immunology* 183 (Oct. 2017), pp. 8–16.

[115] Damien Reynaud et al. "Regulation of B cell fate commitment and immunoglobulin heavy-chain gene rearrangements by Ikaros". In: *Nature Immunology* 9.8 (Aug. 2008), pp. 927–936.

[116] H W Schroeder and J Y Wang. "Preferential utilization of conserved immunoglobulin heavy chain variable gene segments during human fetal life." In: *Proceedings of the National Academy of Sciences* 87.16 (Aug. 1990), pp. 6146–6150.

[117] Harry W. Schroeder et al. "Developmental Regulation of the Human Antibody Repertoire". In: *Annals of the New York Academy of Sciences* 764.1 (Sept. 1995), pp. 242–260.

[118] M. Margarida Souto-Carneiro et al. "Developmental Changes in the Human Heavy Chain CDR3". In: *The Journal of Immunology* 175.11 (Dec. 2005), pp. 7425–7436.

[119] J H Van Es et al. "Expression pattern of the most JH-proximal human VH gene segment (VH6) in the B cell and antibody repertoire suggests a role of VH6-encoded IgM antibodies in early ontogeny." In: *The Journal of Immunology* 150.1 (Jan. 1993), pp. 161–168.

[120] F.E. Bertrand et al. "Ig DH Gene Segment Transcription and Rearrangement Before Surface Expression of the Pan-B–Cell Marker CD19 in Normal Human Bone Marrow". In: *Blood* 90.2 (July 1997), pp. 736–744.

[121] Encarnacion Montecino-Rodriguez et al. "Distinct Genetic Networks Orchestrate the Emergence of Specific Waves of Fetal and Adult B-1 and B-2 Development". In: *Immunity* 45.3 (Sept. 2016), pp. 527–539.

[122] Joan Yuan et al. “Lin28b Reprograms Adult Bone Marrow Hematopoietic Progenitors to Mediate Fetal-Like Lymphopoiesis”. In: *Science* 335.6073 (Mar. 2012), pp. 1195–1200.

[123] Rebecca Ling et al. *The fetal specific gene LIN28B is essential for human fetal B-lymphopoiesis and initiation of KMT2A::AFF1 infant leukemia.* Sept. 2024. URL: http://biorxiv.org/lookup/doi/10.1101/2024.09.18.613730.

[124] Ashley P. Ng et al. “An Erg-driven transcriptional program controls B cell lymphopoiesis”. In: *Nature Communications* 11.1 (Dec. 2020).

[125] Mayuri Tanaka-Yano et al. *Dynamic activity of Erg promotes aging of the hematopoietic system.* Tech. rep. bioRxiv, Jan. 2025. URL: http://biorxiv.org/lookup/doi/10.1101/2025.01.23.634563.

[126] Dahai Wang et al. “Developmental maturation of the hematopoietic system controlled by a Lin28b-let-7-Cbx2 axis”. In: *Cell Reports* 39.1 (Apr. 2022), p. 110587.

[127] T L Carvalho et al. “Arrested B lymphopoiesis and persistence of activated B cells in adult interleukin 7(-/)- mice.” In: *The Journal of experimental medicine* 194.8 (Oct. 2001), pp. 1141–50.

[128] Christina T. Jensen et al. “FLT3 ligand and not TSLP is the key regulator of IL-7 independent B-1 and B-2 B lymphopoiesis”. In: *Blood* 112.6 (Sept. 2008), pp. 2297–2304.

[129] Christian A. J. Vosshenrich et al. “Pre-B cell receptor expression is necessary for thymic stromal lymphopoietin responsiveness in the bone marrow but not in the liver environment”. In: *Proceedings of the National Academy of Sciences* 101.30 (July 2004), pp. 11070–11075.

[130] Stephane Chappaz et al. “Increased TSLP availability restores T- and B-cell compartments in adult IL-7 deficient mice.” In: *Blood* 110.12 (Dec. 2007), pp. 3862–70.

[131] Terry Ann M. Milford et al. “TSLP or IL-7 provide an IL-7Rα signal that is critical for human B lymphopoiesis”. In: *European Journal of Immunology* 46.9 (Sept. 2016), pp. 2155–2161.

[132] Ferenc A. Scheeren et al. “Thymic stromal lymphopoietin induces early human B-cell proliferation and differentiation”. In: *European Journal of Immunology* 40.4 (Apr. 2010), pp. 955–965.

[133] Victoria Michaels et al. “Co-Transplantation of Barcoded Lymphoid-Primed Multipotent (LMPP) and Common Lymphocyte (CLP) Progenitors Reveals a Major Contribution of LMPP to the Lymphoid Lineage”. In: *International Journal of Molecular Sciences* 24.5 (Mar. 2023).

[134] Edward L.Y. Chen, Patrycja K. Thompson, and Juan Carlos Zúñiga-Pflücker. “RBPJ-dependent Notch signaling initiates the T cell program in a subset of thymus-seeding progenitors”. In: *Nature Immunology* 20.11 (Nov. 2019), pp. 1456–1468.

[135] Daniel A Zlotoff et al. “CCR7 and CCR9 together recruit hematopoietic progenitors to the adult thymus”. In: *Blood* 115 (2010), pp. 1897–1905.

[136] Emmanuelle M. Six et al. “A human postnatal lymphoid progenitor capable of circulating and seeding the thymus”. In: *The Journal of Experimental Medicine* 204.13 (Dec. 2007), pp. 3085–3093.

[137] Martijn Cordes et al. “Single-cell immune profiling reveals thymus-seeding populations, T cell commitment, and multilineage development in the human thymus”. In: *Science Immunology* 7.77 (Nov. 2022).

[138] Freddy Radtke et al. “Deficient T Cell Fate Specification in Mice with an Induced Inactivation of Notch1”. In: *Immunity* 10.5 (May 1999), pp. 547–558.

[139] Thorsten B. Feyerabend et al. “Deletion of Notch1 Converts Pro-T Cells to Dendritic Cells and Promotes Thymic B Cells by Cell-Extrinsic and Cell-Intrinsic Mechanisms”. In: *Immunity* 30.1 (Jan. 2009), pp. 67–79.

[140] Brittany Nicole Weber et al. “A critical role for TCF-1 in T-lineage specification and differentiation”. In: *Nature* 476.7358 (Aug. 2011), pp. 63–69.

[141] Kristine Germar et al. “T-cell factor 1 is a gatekeeper for T-cell specification in response to Notch signaling”. In: *Proceedings of the National Academy of Sciences of the United States of America* 108.50 (Dec. 2011), pp. 20060–20065.

[142] Marcos E Garcia-Ojeda et al. “GATA-3 promotes T-cell specification by repressing B-cell potential in pro-T cells in mice”. In: *Blood* 121.10 (Mar. 2013), pp. 1749–1759.

[143] Deirdre D. Scripture-Adams et al. “GATA-3 Dose-Dependent Checkpoints in Early T Cell Commitment”. In: *The Journal of Immunology* 193.7 (Oct. 2014), pp. 3470–3491.

[144] Inge Van De Walle et al. “GATA3 induces human T-cell commitment by restraining Notch activity and repressing NK-cell fate”. In: *Nature Communications* 7 (Apr. 2016).

[145] Brendan W. MacNabb and Ellen V. Rothenberg. “Speed and navigation control of thymocyte development by the fetal T-cell gene regulatory network”. In: *Immunological Reviews* 315.1 (May 2023), pp. 171–196.

[146] Juan Carlos Zúñiga-Pflücker. “T-cell development made simple”. In: *Nature Reviews Immunology* 4.1 (Jan. 2004), pp. 67–72.

[147] Brahma V. Kumar, Thomas J. Connors, and Donna L. Farber. “Human T Cell Development, Localization, and Function throughout Life”. In: *Immunity* 48.2 (Feb. 2018), pp. 202–213.

[148] B F Haynes and C S Heinly. “Early human T cell development: analysis of the human thymus at the time of initial entry of hematopoietic stem cells into the fetal thymic microenvironment.” In: *The Journal of experimental medicine* 181.4 (Apr. 1995), pp. 1445–58.

[149] Alison M. Farley et al. “Dynamics of thymus organogenesis and colonization in early human development”. In: *Development (Cambridge)* 140.9 (May 2013), pp. 2015–2026.

[150] B F Haynes et al. “Early events in human T cell ontogeny. Phenotypic characterization and immunohistologic localization of T cell precursors in early human fetal tissues.” In: *The Journal of experimental medicine* 168.3 (Sept. 1988), pp. 1061–1080.

[151] Jeff E Mold et al. “Maternal alloantigens promote the development of tolerogenic fetal regulatory T cells in utero.” In: *Science (New York, N.Y.)* 322.5907 (Dec. 2008), pp. 1562–5.

[152] Tom Cupedo et al. “Development and activation of regulatory Tcells in the human fetus”. In: *European Journal of Immunology* 35.2 (Feb. 2005), pp. 383–390.

[153] Michela Frascoli et al. “Alloreactive fetal T cells promote uterine contractility in preterm labor via IFN-γ and TNF-α.” In: *Science translational medicine* 10.438 (Apr. 2018).

[154] Cesar M. Rueda et al. “Effect of chorioamnionitis on regulatory T cells in moderate/late preterm neonates”. In: *Human Immunology* 76.1 (Jan. 2015), pp. 65–73.

[155] PJ Duggan et al. “Intrauterine T-cell activation and increased proinflammatory cytokine concentrations in preterm infants with cerebral lesions”. In: *The Lancet* 358.9294 (Nov. 2001), pp. 1699–1700.

[156] Steven D. Scoville, Aharon G. Freud, and Michael A. Caligiuri. “Modeling Human Natural Killer Cell Development in the Era of Innate Lymphoid Cells”. In: *Frontiers in Immunology* 8 (Mar. 2017).

[157] Nicolas Serafini, Christian A.J. Vosshenrich, and James P. Di Santo. “Transcriptional regulation of innate lymphoid cell fate”. In: *Nature Reviews Immunology* 15.7 (July 2015), pp. 415–428.

[158] Wei Xu et al. “NFIL3 Orchestrates the Emergence of Common Helper Innate Lymphoid Cell Precursors”. In: *Cell Reports* 10.12 (Mar. 2015), pp. 2043–2054.

[159] Duncan M. Gascoyne et al. “The basic leucine zipper transcription factor E4BP4 is essential for natural killer cell development”. In: *Nature Immunology* 10.10 (2009), pp. 1118–1124.

[160] Shintaro Kamizono et al. “Nfil3/E4bp4 is required for the development and maturation of NK cells in vivo”. In: *Journal of Experimental Medicine* 206.13 (Dec. 2009), pp. 2977–2986.

[161] Yoshifumi Yokota et al. “Development of peripheral lymphoid organs and natural killer cells depends on the helix–loop–helix inhibitor Id2”. In: *Nature* 397.6721 (Feb. 1999), pp. 702–706.

[162] Markus D. Boos et al. “Mature natural killer cell and lymphoid tissue-inducing cell development requires Id2-mediated suppression of E protein activity”. In: *Journal of Experimental Medicine* 204.5 (May 2007), pp. 1119–1130.

[163] Kenneth H. Grabstein et al. “Cloning of a T Cell Growth Factor that Interacts with the β Chain of the Interleukin-2 Receptor”. In: *Science* 264.5161 (May 1994), pp. 965–968.

[164] Mary K. Kennedy et al. “Reversible Defects in Natural Killer and Memory Cd8 T Cell Lineages in Interleukin 15–Deficient Mice”. In: *The Journal of Experimental Medicine* 191.5 (Mar. 2000), pp. 771–780.

[165] Christian A. J. Vosshenrich et al. “Roles for Common Cytokine Receptor γ-Chain-Dependent Cytokines in the Generation, Differentiation, and Maturation of NK Cell Precursors and Peripheral NK Cells in Vivo”. In: *The Journal of Immunology* 174.3 (Feb. 2005), pp. 1213–1221.

[166] Haruhiko Suzuki et al. "Abnormal Development of Intestinal Intraepithelial Lymphocytes and Peripheral Natural Killer Cells in Mice Lacking the IL-2 Receptor β Chain". In: *The Journal of Experimental Medicine* 185.3 (Feb. 1997), pp. 499–506.

[167] E Mrozek, P Anderson, and MA Caligiuri. "Role of interleukin-15 in the development of human CD56+ natural killer cells from CD34+ hematopoietic progenitor cells". In: *Blood* 87.7 (Apr. 1996), pp. 2632–2640.

[168] Haixin Yu et al. "Flt3 Ligand Promotes the Generation of a Distinct CD34+Human Natural Killer Cell Progenitor That Responds to Interleukin-15". In: *Blood* 92.10 (Nov. 1998), pp. 3647–3657.

[169] Nicholas D. Huntington et al. "IL-15 trans-presentation promotes human NK cell development and differentiation in vivo". In: *Journal of Experimental Medicine* 206.1 (Jan. 2009), pp. 25–34.

[170] E E Rosmaraki et al. "Identification of committed NK cell progenitors in adult murine bone marrow." In: *European journal of immunology* 31.6 (June 2001), pp. 1900–9.

[171] Yoshimitsu Taguchi et al. "Interleukin-2-induced survival of natural killer (NK) cells involving phosphatidylinositol-3 kinase-dependent reduction of ceramide through acid sphingomyelinase, sphingomyelin synthase, and glucosylceramide synthase". In: *Blood* 104.10 (Nov. 2004), pp. 3285–3293.

[172] C A Biron, H A Young, and M T Kasaian. "Interleukin 2-induced proliferation of murine natural killer cells in vivo." In: *The Journal of experimental medicine* 171.1 (Jan. 1990), pp. 173–188.

[173] Brian Becknell and Michael A Caligiuri. *Interleukin-2, Interleukin-15, and Their Roles in Human Natural Killer Cells*. Tech. rep.

[174] D A Weigent, G J Stanton, and H M Johnson. "Interleukin 2 enhances natural killer cell activity through induction of gamma interferon". In: *Infection and Immunity* 41.3 (Sept. 1983), pp. 992–997.

[175] Dylan E. Cherrier, Nicolas Serafini, and James P. Di Santo. "Innate Lymphoid Cell Development: A T Cell Perspective". In: *Immunity* 48.6 (June 2018), pp. 1091–1103.

[176] Laura S. Angelo et al. "Practical NK cell phenotyping and variability in healthy adults". In: *Immunologic Research* 62.3 (July 2015), pp. 341–356.

[177] Megan A Cooper, Todd A Fehniger, and Michael A Caligiuri. "The biology of human natural killer-cell subsets". In: *Trends in Immunology* 22.11 (Nov. 2001), pp. 633–640.

[178] Emily M Mace. "Human natural killer cells: Form, function, and development." In: *The Journal of allergy and clinical immunology* 151.2 (Feb. 2023), pp. 371–385.

[179] Difeng Fang and Jinfang Zhu. "Dynamic balance between master transcription factors determines the fates and functions of CD4 T cell and innate lymphoid cell subsets". In: *Journal of Experimental Medicine* 214.7 (July 2017), pp. 1861–1876.

[180] Ana C. Jaleco et al. "Differential Effects of Notch Ligands Delta-1 and Jagged-1 in Human Lymphoid Differentiation". In: *The Journal of Experimental Medicine* 194.7 (Oct. 2001), pp. 991–1002.

[181] Patricia Chaves et al. “Loss of Canonical Notch Signaling Affects Multiple Steps in NK Cell Development in Mice”. In: *The Journal of Immunology* 201.11 (Dec. 2018), pp. 3307–3319.

[182] Kyoko Haraguchi et al. “Notch activation induces the generation of functional NK cells from human cord blood CD34-positive cells devoid of IL-15.” In: *Journal of immunology* 182.10 (May 2009), pp. 6168–78.

[183] Alex M. Abel et al. *Natural killer cells: Development, maturation, and clinical utilization*. Aug. 2018.

[184] Frank Cichocki, Bartosz Grzywacz, and Jeffrey S. Miller. “Human NK Cell Development: One Road or Many?” In: *Frontiers in Immunology* 10 (Aug. 2019).

[185] Steven D Scoville, Aharon G Freud, and Michael A Caligiuri. “Cellular pathways in the development of human and murine innate lymphoid cells”. In: *Current Opinion in Immunology* 56 (Feb. 2019), pp. 100–106.

[186] Erin C. Zook and Barbara L. Kee. *Development of innate lymphoid cells*. June 2016.

[187] Virginie M. Renoux et al. “Identification of a Human Natural Killer Cell Lineage-Restricted Progenitor in Fetal and Adult Tissues”. In: *Immunity* 43.2 (Aug. 2015), pp. 394–407.

[188] J H Phillips et al. “Ontogeny of human natural killer (NK) cells: fetal NK cells mediate cytolytic function and express cytoplasmic CD3 epsilon,delta proteins.” In: *The Journal of experimental medicine* 175.4 (Apr. 1992), pp. 1055–1066.

[189] Martin A Ivarsson et al. “Differentiation and functional regulation of human fetal NK cells.” In: *The Journal of clinical investigation* 123.9 (Sept. 2013), pp. 3889–901.

[190] Carissa Dege et al. “Potently Cytotoxic Natural Killer Cells Initially Emerge from Erythro-Myeloid Progenitors during Mammalian Development.” In: *Developmental cell* 53.2 (Apr. 2020), pp. 229–239.

[191] Manuela Tavian et al. “The Human Embryo, but Not Its Yolk Sac, Generates Lympho-Myeloid Stem Cells”. In: *Immunity* 15.3 (Sept. 2001), pp. 487–495.

[192] Iyadh Douagi et al. “Identification of the earliest prethymic bipotent T/NK progenitor in murine fetal liver”. In: *Blood* 99.2 (Jan. 2002), pp. 463–471.

[193] Hans-Reimer Rodewald et al. “A population of early fetal thymocytes expressing FcγRIIIII contains precursors of T lymphocytes and natural killer cells”. In: *Cell* 69.1 (Apr. 1992), pp. 139–150.

[194] Yuichi Wakabayashi et al. “Bcl11b is required for differentiation and survival of $\alpha\beta$ T lymphocytes”. In: *Nature Immunology* 4.6 (June 2003), pp. 533–539.

[195] Tomokatsu Ikawa et al. “An Essential Developmental Checkpoint for Production of the T Cell Lineage”. In: *Science* 329.5987 (July 2010), pp. 93–96.

[196] Long Li, Mark Leid, and Ellen V. Rothenberg. “An Early T Cell Lineage Commitment Checkpoint Dependent on the Transcription Factor Bcl11b”. In: *Science* 329.5987 (July 2010), pp. 89–93.

[197] Peng Li et al. “Reprogramming of T Cells to Natural Killer–Like Cells upon Bcl11b Deletion”. In: *Science* 329.5987 (July 2010), pp. 85–89.

[198] Bartosz Grzywacz et al. “Natural killer–cell differentiation by myeloid progenitors”. In: *Blood* 117.13 (Mar. 2011), pp. 3548–3558.

[199] Qingfeng Chen et al. “Delineation of Natural Killer Cell Differentiation from Myeloid Progenitors in Human”. In: *Scientific Reports* 5.1 (Oct. 2015), p. 15118.

[200] Laura S. Angelo et al. “CXCR6+ NK Cells in Human Fetal Liver and Spleen Possess Unique Phenotypic and Functional Capabilities”. In: *Frontiers in Immunology* 10 (Mar. 2019).

[201] Scott R Mckercher et al. “Targeted disruption of the PU. 1 gene results in multiple hematopoietic abnormalities”. In: *The EMBO Journal* 15.20 (1996), pp. 5647–5658.

[202] Edward W. Scott et al. “Requirement of Transcription Factor PU.1 in the Development of Multiple Hematopoietic Lineages”. In: *Science* 265.5178 (Sept. 1994), pp. 1573–1577.

[203] Aleksandar Dakic et al. “PU.1 regulates the commitment of adult hematopoietic progenitors and restricts granulopoiesis”. In: *The Journal of Experimental Medicine* 201.9 (May 2005), pp. 1487–1502.

[204] Hiromi Iwasaki et al. “Distinctive and indispensable roles of PU.1 in maintenance of hematopoietic stem cells and their differentiation”. In: *Blood* 106.5 (Sept. 2005), pp. 1590–1600.

[205] Rodney P. DeKoter and Harinder Singh. “Regulation of B Lymphocyte and Macrophage Development by Graded Expression of PU.1”. In: *Science* 288.5470 (May 2000), pp. 1439–1441.

[206] Hiromi Iwasaki et al. “GATA-1 Converts Lymphoid and Myelomonocytic Progenitors into the Megakaryocyte/Erythrocyte Lineages”. In: *Immunity* 19.3 (Sept. 2003), pp. 451–462.

[207] C Nerlov et al. “GATA-1 interacts with the myeloid PU.1 transcription factor and represses PU.1-dependent transcription.” In: *Blood* 95.8 (Apr. 2000), pp. 2543–51.

[208] N. Rekhtman et al. “Direct interaction of hematopoietic transcription factors PU.1 and GATA-1: functional antagonism in erythroid cells”. In: *Genes & Development* 13.11 (June 1999), pp. 1398–1411.

[209] Pu Zhang et al. “Negative cross-talk between hematopoietic regulators: GATA proteins repress PU.1”. In: *Proceedings of the National Academy of Sciences* 96.15 (July 1999), pp. 8705–8710.

[210] Thomas Graf and Tariq Enver. “Forcing cells to change lineages”. In: *Nature* 462.7273 (Dec. 2009), pp. 587–594.

[211] Philipp S. Hoppe et al. “Early myeloid lineage choice is not initiated by random PU.1 to GATA1 protein ratios”. In: *Nature* 535.7611 (July 2016), pp. 299–302.

[212] Koichi Akashi et al. “A clonogenic common myeloid progenitor that gives rise to all myeloid lineages”. In: *Nature* 404.6774 (Mar. 2000), pp. 193–197.

[213] Jörgen Adolfsson et al. “Identification of Flt3+ lympho-myeloid stem cells lacking erythro-megakaryocytic potential: A revised road map for adult blood lineage commitment”. In: *Cell* 121.2 (Apr. 2005), pp. 295–306.

[214] Serena Belluschi et al. “Myelo-lymphoid lineage restriction occurs in the human haematopoietic stem cell compartment before lymphoid-primed multipotent progenitors”. In: *Nature Communications* 9.1 (Dec. 2018).

[215] Renée F. de Pooter et al. “Cutting Edge: Lymphomyeloid-Primed Progenitor Cell Fates Are Controlled by the Transcription Factor Tal1”. In: *The Journal of Immunology* 202.10 (May 2019), pp. 2837–2842.

[216] Louis C. Doré and John D. Crispino. “Transcription factor networks in erythroid cell and megakaryocyte development”. In: *Blood* 118.2 (July 2011), pp. 231–239.

[217] Christiaan J. Stavast, Pieter J.M. Leenen, and Stefan J. Erkeland. “The interplay between critical transcription factors and microRNAs in the control of normal and malignant myelopoiesis”. In: *Cancer Letters* 427 (July 2018), pp. 28–37.

[218] Pu Zhang et al. “Enhancement of hematopoietic stem cell repopulating capacity and self-renewal in the absence of the transcription factor C/EBPα”. In: *Immunity* 21.6 (Dec. 2004), pp. 853–863.

[219] Ou Ma et al. “Granulopoiesis requires increased C/EBPα compared to monopoiesis, correlated with elevated Cebpa in immature G-CSF receptor versus M-CSF receptor expressing cells.” In: *PloS one* 9.4 (2014), e95784.

[220] Daisuke Kurotaki et al. “Essential role of the IRF8-KLF4 transcription factor cascade in murine monocyte differentiation”. In: *Blood* 121.10 (2013), pp. 1839–1849.

[221] Sophie Hambleton et al. “IRF8 Mutations and Human Dendritic-Cell Immunodeficiency”. In: *New England Journal of Medicine* 365.2 (July 2011), pp. 127–138.

[222] Linda J. Bendall and Kenneth F. Bradstock. “G-CSF: From granulopoietic stimulant to bone marrow stem cell mobilizing agent”. In: *Cytokine & Growth Factor Reviews* 25.4 (Aug. 2014), pp. 355–367.

[223] Christina V Jones and Sharon D Ricardo. “Macrophages and CSF-1”. In: *Organogenesis* 9.4 (Oct. 2013), pp. 249–260.

[224] James W. Swann, Oakley C. Olson, and Emmanuelle Passegué. “Made to order: emergency myelopoiesis and demand-adapted innate immune cell production”. In: *Nature Reviews Immunology* 24.8 (Aug. 2024), pp. 596–613.

[225] Amélie Collins et al. “Maternal inflammation regulates fetal emergency myelopoiesis”. In: *Cell* 187.6 (Mar. 2024), pp. 1402–1421.

[226] Hanna K. A. Mikkola and Stuart H. Orkin. “The journey of developing hematopoietic stem cells”. In: *Development* 133.19 (Oct. 2006), pp. 3733–3744.

[227] Matthew A. Martin and Mickie Bhatia. “Analysis of the Human Fetal Liver Hematopoietic Microenvironment”. In: *Stem Cells and Development* 14.5 (Oct. 2005), pp. 493–504.

[228] Kazunobu Sasaki and Yuji Sonoda. “Histometrical and Three-Dimensional Analyses of Liver Hematopoiesis in the Mouse Embryo.” In: *Archives of Histology and Cytology* 63.2 (2000), pp. 137–146.

[229] Daisuke Sugiyama et al. “Hepatoblasts comprise a niche for fetal liver erythropoiesis through cytokine production”. In: *Biochemical and Biophysical Research Communications* 410.2 (July 2011), pp. 301–306.

[230] Cheng Cheng Zhang and Harvey F. Lodish. "Insulin-like growth factor 2 expressed in a novel fetal liver cell population is a growth factor for hematopoietic stem cells". In: *Blood* 103.7 (Apr. 2004), pp. 2513–2521.

[231] Cheng Cheng Zhang et al. "Angiopoietin-like proteins stimulate ex vivo expansion of hematopoietic stem cells". In: *Nature Medicine* 12.2 (Mar. 2006), pp. 240–245.

[232] Song Chou and Harvey F. Lodish. "Fetal liver hepatic progenitors are supportive stromal cells for hematopoietic stem cells". In: *Proceedings of the National Academy of Sciences of the United States of America* 107.17 (Apr. 2010), pp. 7799–7804.

[233] Yeojin Lee et al. "Hematopoietic stem cells temporally transition to thrombopoietin dependence in the fetal liver". In: *Sci. Adv* 8 (2022), p. 7688.

[234] Thomas R.L. Klei et al. "From the cradle to the grave: The role of macrophages in erythropoiesis and erythrophagocytosis". In: *Frontiers in Immunology* 8.73 (Feb. 2017).

[235] Wei Li et al. "Identification and transcriptome analysis of erythroblastic island macrophages". In: *Blood* 134.5 (Aug. 2019), pp. 480–491.

[236] Yanfang Lu et al. "Spatial transcriptome profiling by MERFISH reveals fetal liver hematopoietic stem cell niche architecture". In: *Cell Discovery* 7.1 (Dec. 2021).

[237] Jalal A. Khan et al. "Fetal liver hematopoietic stem cell niches associate with portal vessels". In: *Science* 351.6269 (Jan. 2016), pp. 176–180.

[238] Dimas T. Covas et al. "Multipotent mesenchymal stromal cells obtained from diverse human tissues share functional properties and gene-expression profile with CD146+ perivascular cells and fibroblasts". In: *Experimental Hematology* 36.5 (May 2008), pp. 642–654.

[239] Jörg C. Gerlach et al. "Perivascular Mesenchymal Progenitors in Human Fetal and Adult Liver". In: *Stem Cells and Development* 21.18 (Dec. 2012), pp. 3258–3269.

[240] Mirko Corselli et al. "Perivascular support of human hematopoietic stem/progenitor cells". In: *Blood* 121.151 (Apr. 2013), pp. 2891–2901.

[241] Yi Yu et al. "Human fetal liver MSCs are more effective than adult bone marrow MSCs for their immunosuppressive, immunomodulatory, and Foxp3+ T reg induction capacity." In: *Stem cell research & therapy* 12.1 (Feb. 2021), p. 138.

[242] Ye Fan et al. "Human Fetal Liver Mesenchymal Stem Cell-Derived Exosomes Impair Natural Killer Cell Function". In: *Stem Cells and Development* 28.1 (Jan. 2019), pp. 44–55.

[243] C Götherström et al. "Immunomodulatory effects of human foetal liver-derived mesenchymal stem cells". In: *Bone Marrow Transplantation* 32.3 (Aug. 2003), pp. 265–272.

[244] Massimo Giuliani et al. "Long-Lasting Inhibitory Effects of Fetal Liver Mesenchymal Stem Cells on T-Lymphocyte Proliferation". In: *PLoS ONE* 6.5 (May 2011), e19988.

[245] Wen Hao Neo et al. "Cell-extrinsic hematopoietic impact of Ezh2 inactivation in fetal liver endothelial cells". In: *Blood* 131.20 (May 2018), pp. 2223–2233.

[246] Julia Fröbel et al. “The Hematopoietic Bone Marrow Niche Ecosystem”. In: *Frontiers in Cell and Developmental Biology* 9 (July 2021).

[247] Yang Liu et al. “A specialized bone marrow microenvironment for fetal haematopoiesis”. In: *Nature Communications* 13.1 (Dec. 2022).

[248] Lei Ding and Sean J. Morrison. “Haematopoietic stem cells and early lymphoid progenitors occupy distinct bone marrow niches”. In: *Nature* 495.7440 (Mar. 2013), pp. 231–235.

[249] Sandra Pinho et al. “Lineage-Biased Hematopoietic Stem Cells Are Regulated by Distinct Niches”. In: *Developmental Cell* 44.5 (Mar. 2018), pp. 634–641.

[250] Ioannis Mitroulis et al. “Regulation of the Bone Marrow Niche by Inflammation”. In: *Frontiers in Immunology* 11 (July 2020).

[251] Myriam L.R. Haltalli et al. “Manipulating niche composition limits damage to haematopoietic stem cells during Plasmodium infection”. In: *Nature Cell Biology* 22.12 (Dec. 2020), pp. 1399–1410.

[252] Simón Méndez-Ferrer et al. “Bone marrow niches in haematological malignancies”. In: *Nature Reviews Cancer* 20.5 (May 2020), pp. 285–298.

[253] Anastasia M. Hughes et al. “The Bone Marrow Microenvironment in B-Cell Development and Malignancy”. In: *Cancers* 14.9 (May 2022).

[254] Mark J. Kiel et al. “SLAM family receptors distinguish hematopoietic stem and progenitor cells and reveal endothelial niches for stem cells”. In: *Cell* 121.7 (July 2005), pp. 1109–1121.

[255] Lei Ding et al. “Endothelial and perivascular cells maintain haematopoietic stem cells”. In: *Nature* 481.7382 (Jan. 2012), pp. 457–462.

[256] Cristina Lo Celso et al. “Live-animal tracking of individual haematopoietic stem/progenitor cells in their niche”. In: *Nature* 457.7225 (Jan. 2009), pp. 92–96.

[257] Melih Acar et al. “Deep imaging of bone marrow shows non-dividing stem cells are mainly perisinusoidal”. In: *Nature* 526.7571 (Oct. 2015), pp. 126–130.

[258] Bo O. Zhou et al. “Leptin-receptor-expressing mesenchymal stromal cells represent the main source of bone formed by adult bone marrow”. In: *Cell Stem Cell* 15.2 (Aug. 2014), pp. 154–168.

[259] Yuya Kunisaki et al. “Arteriolar niches maintain haematopoietic stem cell quiescence”. In: *Nature* 502.7473 (2013), pp. 637–643.

[260] Noboru Asada et al. “Differential cytokine contributions of perivascular haematopoietic stem cell niches”. In: *Nature Cell Biology* 19.3 (Mar. 2017), pp. 214–223.

[261] Stefano Comazzetto et al. “Restricted Hematopoietic Progenitors and Erythropoiesis Require SCF from Leptin Receptor+ Niche Cells in the Bone Marrow”. In: *Cell Stem Cell* 24.3 (Mar. 2019), pp. 477–486.

[262] Bo Shen et al. “A mechanosensitive peri-arteriolar niche for osteogenesis and lymphopoiesis”. In: *Nature* 591.7850 (Mar. 2021), pp. 438–444.

[263] Jizhou Zhang et al. “In situ mapping identifies distinct vascular niches for myelopoiesis”. In: *Nature* 590.7846 (Feb. 2021), pp. 457–462.

[264] David Stegner et al. “Thrombopoiesis is spatially regulated by the bone marrow vasculature”. In: *Nature Communications* 8.1 (Dec. 2017).

[265] Huichun Zhan and Kenneth Kaushansky. “Megakaryocytes as the Regulator of the Hematopoietic Vascular Niche”. In: *Frontiers in Oncology* 12 (June 2022).

[266] Meng Zhao et al. “N-Cadherin-Expressing Bone and Marrow Stromal Progenitor Cells Maintain Reserve Hematopoietic Stem Cells.” In: *Cell reports* 26.3 (Jan. 2019), pp. 652–669.

[267] Tatsuki Sugiyama et al. “Maintenance of the Hematopoietic Stem Cell Pool by CXCL12-CXCR4 Chemokine Signaling in Bone Marrow Stromal Cell Niches”. In: *Immunity* 25.6 (Dec. 2006), pp. 977–988.

[268] Russell S Taichman, Marcelle J Reilly, and Stephen G Emerson. “Human Osteoblasts Support Human Hematopoietic Progenitor Cells in In Vitro Bone Marrow Cultures”. In: *Blood* 87.2 (Jan. 1994).

[269] Jiwang Zhang et al. “Identification of the haematopoietic stem cell niche and control of the niche size”. In: *Nature* 425.6960 (Oct. 2003), pp. 836–841.

[270] Fumio Arai et al. “Tie2/angiopoietin-1 signaling regulates hematopoietic stem cell quiescence in the bone marrow niche.” In: *Cell* 118.2 (July 2004), pp. 149–61.

[271] Hiroki Yoshihara et al. “Thrombopoietin/MPL signaling regulates hematopoietic stem cell quiescence and interaction with the osteoblastic niche.” In: *Cell stem cell* 1.6 (Dec. 2007), pp. 685–97.

[272] Andrea T Hooper et al. “Engraftment and reconstitution of hematopoiesis is dependent on VEGFR2-mediated regeneration of sinusoidal endothelial cells.” In: *Cell stem cell* 4.3 (Mar. 2009), pp. 263–74.

[273] Jochen Grassinger et al. “Phenotypically identical hemopoietic stem cells isolated from different regions of bone marrow have different biologic potential”. In: *Blood* 116.17 (Oct. 2010), pp. 3185–3196.

[274] Dora Visnjic et al. “Hematopoiesis is severely altered in mice with an induced osteoblast deficiency”. In: *Blood* 103.9 (May 2004), pp. 3258–3264.

[275] Jiang Zhu et al. “Osteoblasts support B-lymphocyte commitment and differentiation from hematopoietic stem cells”. In: 109 (2007), pp. 3706–3712.

[276] Joy Y Wu et al. “Osteoblastic regulation of B lymphopoiesis is mediated by G s-dependent signaling pathways”. In: *Proceedings of the National Academy of Sciences of the United States of America* 105.44 (Nov. 2008), pp. 16976–16981.

[277] D. G. Osmond et al. “In Vivo Localization of B Lymphoctye Progenitor Cells in Mouse Bone Marrow”. In: *Adv Exp Med Biol* 237 (1988), pp. 45–51.

[278] M H Hermans, H Hartsuiker, and D Opstelten. “An in situ study of B-lymphocytopoiesis in rat bone marrow. Topographical arrangement of terminal deoxynucleotidyl transferase-positive cells and pre-B cells.” In: *Journal of immunology (Baltimore, Md. : 1950)* 142.1 (Jan. 1989), pp. 67–73.

[279] Takahiro Hara et al. “Identification of IL-7–Producing Cells in Primary and Secondary Lymphoid Organs Using IL-7–GFP Knock-In Mice”. In: *The Journal of Immunology* 189.4 (Aug. 2012), pp. 1577–1584.

[280] Armin Ehninger and Andreas Trumpp. “The bone marrow stem cell niche grows up: mesenchymal stem cells and macrophages move in”. In: *Journal of Experimental Medicine* 208.3 (Mar. 2011), pp. 421–428.

[281] Shovik Bandyopadhyay et al. “Mapping the cellular biogeography of human bone marrow niches using single-cell transcriptomics and proteomic imaging”. In: *Cell* (May 2024).

[282] Benedetto Sacchetti et al. “Self-Renewing Osteoprogenitors in Bone Marrow Sinusoids Can Organize a Hematopoietic Microenvironment”. In: *Cell* 131.2 (Oct. 2007), pp. 324–336.

[283] Charles K. F. Chan et al. “Endochondral ossification is required for haematopoietic stem-cell niche formation”. In: *Nature* 457.7228 (Jan. 2009), pp. 490–494.

[284] Koji Tokoyoda et al. “Cellular Niches Controlling B Lymphocyte Behavior within Bone Marrow during Development”. In: *Immunity* 20 (June 2004), pp. 707–718.

[285] Marielle Balzano et al. “Nidogen-1 Contributes to the Interaction Network Involved in Pro-B Cell Retention in the Peri-sinusoidal Hematopoietic Stem Cell Niche”. In: *Cell Reports* 26.12 (Mar. 2019), pp. 3257–3271.

[286] Malay Mandal et al. “CXCR4 signaling directs Igk recombination and the molecular mechanisms of late B lymphopoiesis”. In: *Nature Immunology* 20.10 (Oct. 2019), pp. 1393–1403.

[287] Anjali P. Kusumbe et al. “Age-dependent modulation of vascular niches for haematopoietic stem cells”. In: *Nature* 532.7599 (Apr. 2016), pp. 380–384.

[288] Chiara Baccin et al. “Combined single-cell and spatial transcriptomics reveal the molecular, cellular and spatial bone marrow niche organization”. In: *Nature Cell Biology* 22.1 (Jan. 2020), pp. 38–48.

[289] Yoshiki Omatsu et al. “The Essential Functions of Adipo-osteogenic Progenitors as the Hematopoietic Stem and Progenitor Cell Niche”. In: *Immunity* 33.3 (Sept. 2010), pp. 387–399.

[290] Adam Greenbaum et al. “CXCL12 in early mesenchymal progenitors is required for haematopoietic stem-cell maintenance”. In: *Nature* 495.7440 (Mar. 2013), pp. 227–230.

[291] Hongzhe Li et al. “Isolation and characterization of primary bone marrow mesenchymal stromal cells”. In: *Annals of the New York Academy of Sciences* 1370.1 (Apr. 2016), pp. 109–118.

[292] Ariane Tormin et al. “CD146 expression on primary nonhematopoietic bone marrow stem cells is correlated with in situ localization.” In: *Blood* 117.19 (May 2011), pp. 5067–77.

[293] M. Dominici et al. “Minimal criteria for defining multipotent mesenchymal stromal cells. The International Society for Cellular Therapy position statement”. In: *Cytotherapy* 8.4 (Aug. 2006), pp. 315–317.

[294] Ping Zhang et al. “Characterization of mesenchymal stem cells in human fetal bone marrow by single-cell transcriptomic and functional analysis”. In: *Signal Transduction and Targeted Therapy* 8.1 (Dec. 2023).

[295] Alanna C. Green et al. *Mesenchymal lineage cells and their importance in B lymphocyte niches*. Feb. 2019.

[296] H.T. Hassan and A. Zander. "Stem Cell Factor as a Survival and Growth Factor in Human Normal and Malignant Hematopoiesis". In: *Acta Haematologica* 95.3-4 (1996), pp. 257–262.

[297] Virginia C Broudy. "Stem Cell Factor and Hematopoiesis". In: *Blood* 90.4 (Aug. 1997), pp. 1345–1364.

[298] Ana Cordeiro Gomes et al. "Hematopoietic Stem Cell Niches Produce Lineage-Instructive Signals to Control Multipotent Progenitor Differentiation". In: *Immunity* 45.6 (Dec. 2016), pp. 1219–1231.

[299] Steven A. Corfe and Christopher J. Paige. "The many roles of IL-7 in B cell development; Mediator of survival, proliferation and differentiation". In: *Seminars in Immunology* 24.3 (June 2012), pp. 198–208.

[300] Marcus R. Clark et al. "Orchestrating B cell lymphopoiesis through interplay of IL-7 receptor and pre-B cell receptor signalling". In: *Nature Reviews Immunology* 14.2 (Feb. 2014), pp. 69–80.

[301] J E Aubin. "Regulation of osteoblast formation and function." In: *Reviews in endocrine & metabolic disorders* 2.1 (Jan. 2001), pp. 81–94.

[302] Christa Maes et al. "Osteoblast Precursors, but Not Mature Osteoblasts, Move into Developing and Fractured Bones along with Invading Blood Vessels". In: *Developmental Cell* 19.2 (Aug. 2010), pp. 329–344.

[303] Ying-Hua Cheng et al. "Impact of maturational status on the ability of osteoblasts to enhance the hematopoietic function of stem and progenitor cells." In: *Journal of bone and mineral research* 26.5 (May 2011), pp. 1111–21.

[304] Cristina Panaroni and Joy Y. Wu. "Interactions between b lymphocytes and the osteoblast lineage in bone marrow". In: *Calcified Tissue International* 93.3 (Sept. 2013), pp. 261–268.

[305] L. M. Calvi et al. "Osteoblastic cells regulate the haematopoietic stem cell niche". In: *Nature* 425.6960 (Oct. 2003), pp. 841–846.

[306] Younghun Jung et al. "Cell-to-cell contact is critical for the survival of hematopoietic progenitor cells on osteoblasts". In: *Cytokine* 32.3-4 (Nov. 2005), pp. 155–162.

[307] Asuka Terashima et al. "Sepsis-Induced Osteoblast Ablation Causes Immunodeficiency". In: *Immunity* 44.6 (June 2016), pp. 1434–1443.

[308] Cristina Panaroni et al. "PTH Signaling in Osteoprogenitors Is Essential for B-Lymphocyte Differentiation and Mobilization". In: *Journal of Bone and Mineral Research* 30.12 (Dec. 2015), pp. 2273–2286.

[309] Vionnie W.C. Yu et al. "Distinctive Mesenchymal-Parenchymal Cell Pairings Govern B Cell Differentiation in the Bone Marrow". In: *Stem Cell Reports* 7.2 (Aug. 2016), pp. 220–235.

[310] Anastasia N. Tikhonova et al. "The bone marrow microenvironment at single-cell resolution". In: *Nature* 569.7755 (May 2019), pp. 222–228.

[311] Tomoko Taguchi et al. “Involvement of insulin-like growth factor-I and insulin-like growth factor binding proteins in pro–B-cell development”. In: *Experimental Hematology* 34.4 (Apr. 2006), pp. 508–518.

[312] Thomas H Ambrosi et al. “Adipocyte Accumulation in the Bone Marrow during Obesity and Aging Impairs Stem Cell-Based Hematopoietic and Bone Regeneration.” In: *Cell stem cell* 20.6 (June 2017), pp. 771–784.

[313] Vincent Cuminetti and Lorena Arranz. “Bone marrow adipocytes: The enigmatic components of the hematopoietic stem cell niche”. In: *Journal of Clinical Medicine* 8.5 (May 2019).

[314] Urban Švajger, Patrik Milić, and Primož J. Rožman. “Bone Marrow Niche Aging: Are Adipocytes Detrimental Cells in the Bone Marrow?” In: *Cells* 14.11 (June 2025).

[315] Benjamin J Adler et al. “High fat diet rapidly suppresses B lymphopoiesis by disrupting the supportive capacity of the bone marrow niche.” In: *PloS one* 9.3 (2014), e90639.

[316] Fareena A. Bilwani and Katherine L. Knight. “Adipocyte-Derived Soluble Factor(s) Inhibits Early Stages of B Lymphopoiesis”. In: *The Journal of Immunology* 189.9 (Nov. 2012), pp. 4379–4386.

[317] Domenick E. Kennedy and Katherine L. Knight. “Inhibition of B Lymphopoiesis by Adipocytes and IL-1–Producing Myeloid-Derived Suppressor Cells”. In: *The Journal of Immunology* 195.6 (Sept. 2015), pp. 2666–2674.

[318] Domenick E. Kennedy and Katherine L. Knight. “Inflammatory Changes in Bone Marrow Microenvironment Associated with Declining B Lymphopoiesis”. In: *The Journal of Immunology* 198.9 (May 2017), pp. 3471–3479.

[319] Saravana K. Ramasamy. “Structure and Functions of Blood Vessels and Vascular Niches in Bone”. In: *Stem Cells International* 2017 (2017), pp. 1–10.

[320] A Solanilla et al. “Expression of Flt3-ligand by the endothelial cell”. In: *Leukemia* 14.1 (Jan. 2000), pp. 153–162.

[321] Ewa Sitnicka et al. “Complementary Signaling through flt3 and Interleukin-7 Receptor α Is Indispensable for Fetal and Adult B Cell Genesis”. In: *The Journal of Experimental Medicine* 198.10 (Nov. 2003), pp. 1495–1506.

[322] Ewa Sitnicka et al. “Critical role of FLT3 ligand in IL-7 receptor–independent T lymphopoiesis and regulation of lymphoid-primed multipotent progenitors”. In: *Blood* 110.8 (Oct. 2007), pp. 2955–2964.

[323] Kilian Sottoriva and Kostandin V. Pajcini. “Notch Signaling in the Bone Marrow Lymphopoietic Niche”. In: *Frontiers in Immunology* 12 (July 2021).

[324] Christian E. Jacome-Galarza et al. “Developmental origin, functional maintenance and genetic rescue of osteoclasts”. In: *Nature* 568.7753 (Apr. 2019), pp. 541–545.

[325] Tomi Lazarov et al. “Physiology and diseases of tissue-resident macrophages”. In: *Nature* 618.7966 (June 2023), pp. 698–707.

[326] Matthew D. Park et al. “Macrophages in health and disease”. In: *Cell* 185.23 (Nov. 2022), pp. 4259–4279.

[327] Paul D. Kingsley et al. “Tissue-Resident Macrophages in the Bone Marrow Comprise a Diverse Cellular Population Derived from Hematopoietic Stem Cells”. In: *Blood* 142.Supplement 1 (Nov. 2023), pp. 3910–3910.

[328] Gülce Perçin et al. “Embryonic macrophages orchestrate niche cell homeostasis for the establishment of the definitive hematopoietic stem cell pool”. In: *Nature Communications* 16.1 (May 2025), p. 4428.

[329] M Bessis. “Erythroblastic island, functional unity of bone marrow”. In: *Revue d'hematologie* 13.1 (1958), pp. 8–11.

[330] S H Lee et al. “Isolation and immunocytochemical characterization of human bone marrow stromal macrophages in hemopoietic clusters.” In: *The Journal of experimental medicine* 168.3 (Sept. 1988), pp. 1193–1198.

[331] Mette Kristiansen et al. “Identification of the haemoglobin scavenger receptor”. In: *Nature* 409.6817 (Jan. 2001), pp. 198–201.

[332] Babs O. Fabriek et al. “The macrophage CD163 surface glycoprotein is an erythroblast adhesion receptor”. In: *Blood* 109.12 (June 2007), pp. 5223–5229.

[333] Rebecca N. Jacobsen, Andrew C. Perkins, and Jean-Pierre Levesque. “Macrophages and regulation of erythropoiesis”. In: *Current Opinion in Hematology* 22.3 (May 2015), pp. 212–219.

[334] Andrew Chow et al. “Bone marrow CD169+ macrophages promote the retention of hematopoietic stem and progenitor cells in the mesenchymal stem cell niche”. In: *Journal of Experimental Medicine* 208.2 (Feb. 2011), pp. 261–271.

[335] G. Sebastiaan Winkler. “The mammalian anti-proliferative BTG/Tob protein family”. In: *Journal of Cellular Physiology* 222.1 (Jan. 2010), pp. 66–72.

[336] Lena Batoon et al. “CD169+ macrophages are critical for osteoblast maintenance and promote intramembranous and endochondral ossification during bone repair.” In: *Biomaterials* 196 (Mar. 2019), pp. 51–66.

[337] Ming K Chang et al. “Osteal Tissue Macrophages Are Intercalated throughout Human and Mouse Bone Lining Tissues and Regulate Osteoblast Function In Vitro and In Vivo 1”. In: *The Journal of Immunology* 181 (July 2008), pp. 1232–1244.

[338] Kyung Hee Chang et al. “p62 Is Required for Stem Cell/Progenitor Retention through Inhibition of IKK/NF-κB/Ccl4 Signaling at the Bone Marrow Macrophage-Osteoblast Niche”. In: *Cell Reports* 9.6 (Dec. 2014), pp. 2084–2097.

[339] Simon Yona et al. “Fate Mapping Reveals Origins and Dynamics of Monocytes and Tissue Macrophages under Homeostasis”. In: *Immunity* 38.1 (Jan. 2013), pp. 79–91.

[340] Charles D. Mills et al. “M-1/M-2 Macrophages and the Th1/Th2 Paradigm”. In: *The Journal of Immunology* 164.12 (June 2000), pp. 6166–6173.

[341] Peter J. Murray. “Macrophage Polarization”. In: *Annual Review of Physiology* 79.1 (Feb. 2017), pp. 541–566.

[342] Min Luo et al. “Macrophage polarization: an important role in inflammatory diseases”. In: *Frontiers in Immunology* 15 (Apr. 2024).

[343] Yi Luo et al. "M1 and M2 macrophages differentially regulate hematopoietic stem cell self-renewal and ex vivo expansion". In: *Blood Advances* 2.8 (Apr. 2018), pp. 859–870.

[344] Masayuki Yamashita and Emmanuelle Passegué. "TNF-α Coordinates Hematopoietic Stem Cell Survival and Myeloid Regeneration". In: *Cell Stem Cell* 25.3 (Sept. 2019), pp. 357–372.

[345] Yumi Sasaki et al. "IL-6 Generated from Human Hematopoietic Stem and Progenitor Cells through TLR4 Signaling Promotes Emergency Granulopoiesis by Regulating Transcription Factor Expression". In: *The Journal of Immunology* 207.4 (Aug. 2021), pp. 1078–1086.

[346] Kenichiro Maeda et al. "Interleukin-6 aborts lymphopoiesis and elevates production of myeloid cells in systemic lupus erythematosus-prone B6.Sle1.Yaa animals". In: *Blood* 113.19 (2009), pp. 4534–4540.

[347] Eric M Pietras et al. "Chronic interleukin-1 exposure drives haematopoietic stem cells towards precocious myeloid differentiation at the expense of self-renewal." In: *Nature cell biology* 18.6 (June 2016), pp. 607–18.

[348] Daniela Flores-Gomez et al. "Interleukin-1β induces trained innate immunity in human hematopoietic progenitor cells in vitro". In: *Stem Cell Reports* 19.12 (Dec. 2024), pp. 1651–1664.

[349] Jennifer M. Broughan et al. "Cohort profile: the National Congenital Anomaly Registration Dataset in England". In: *BMJ Open* 14.1 (Jan. 2024), e077743.

[350] *NCARDRS Congenital Anomaly Official Statistics Report*. Tech. rep. NCARDRS, Mar. 2024. URL: `https://digital.nhs.uk/data-and-information/publications/statistical/ncardrs-congenital-anomaly-statistics-annual-data/ncardrs-congenital-anomaly-statistics-report-2021/prevalence-of-t21-t18-t13`.

[351] JLH Down. "Observations on an Ethnic Classification of Idiots". In: *London Hospital Reports* 3 (1866), pp. 259–262.

[352] Jérôme Lejeune. "Human chromosomes in tissue culture". In: *Comptes rendus hebdomadaires des seances de l'Academie des sciences* 602 (1959), pp. 602–602.

[353] Marilyn J. Bull. "Down Syndrome". In: *New England Journal of Medicine* 382.24 (June 2020). Ed. by Allan H. Ropper, pp. 2344–2352.

[354] Henrik Hasle, Inge Haunstrup Clemmensen, and Margareta Mikkelsen. "Risks of leukaemia and solid tumours in individuals with Down's syndrome". In: *The Lancet* 355.9199 (Jan. 2000), pp. 165–169.

[355] Henrik Hasle. "Pattern of malignant disorders in individuals with Down's syndrome". In: *THE LANCET Oncology* 2 (2001), p. 429.

[356] Henrik Hasle et al. "Low risk of solid tumors in persons with Down syndrome". In: *Genetics in Medicine* 18.11 (Nov. 2016), pp. 1151–1157.

[357] Stylianos E. Antonarakis. "Parental Origin of the Extra Chromosome in Trisomy 21 as Indicated by Analysis of DNA Polymorphisms". In: *New England Journal of Medicine* 324.13 (Mar. 1991), pp. 872–876.

[358] Stylianos E. Antonarakis et al. "Down syndrome". In: *Nature Reviews Disease Primers* 6.1 (Jan. 2020).

[359] Stylianos E. Antonarakis et al. “Mitotic errors in somatic cells cause trisomy 21 in about 4.5% of cases and are not associated with advanced maternal age”. In: *Nature Genetics* 3.2 (Feb. 1993), pp. 146–150.

[360] Maria Chiara Pelleri et al. “Systematic reanalysis of partial trisomy 21 cases with or without Down syndrome suggests a small region on 21q22.13 as critical to the phenotype.” In: *Human molecular genetics* 25.12 (June 2016), pp. 2525–2538.

[361] Robert Lyle et al. “Genotype-phenotype correlations in Down syndrome identified by array CGH in 30 cases of partial trisomy and partial monosomy chromosome 21”. In: *European Journal of Human Genetics* 17.4 (2009), pp. 454–466.

[362] Gillian M Barlow et al. “Down syndrome congenital heart disease: A narrowed region and a candidate gene”. In: *Genetics in Medicine* 3.2 (Mar. 2001), pp. 91–101.

[363] Sarah C Dyer et al. “Ensembl 2025”. In: *Nucleic Acids Research* 53.D1 (Jan. 2025), pp. D948–D957.

[364] Yae-Huei Liou et al. “Adipocyte IL-15 Regulates Local and Systemic NK Cell Development”. In: *The Journal of Immunology* 193.4 (Aug. 2014), pp. 1747–1758.

[365] Eduardo M. Torres. “Consequences of gaining an extra chromosome”. In: *Chromosome Research* 31.3 (Aug. 2023), p. 24.

[366] Maria Chiara Pelleri et al. “Partial trisomy 21 with or without highly restricted Down syndrome critical region (HR-DSCR): report of two new cases and reanalysis of the genotype–phenotype association”. In: *BMC Medical Genomics* 15.1 (Dec. 2022).

[367] Meenal Gupta, A. Ranjitha Dhanasekaran, and Katheleen J. Gardiner. “Mouse models of Down syndrome: gene content and consequences”. In: *Mammalian Genome* 27.11-12 (Dec. 2016), pp. 538–555.

[368] Jason P. Weick et al. “Deficits in human trisomy 21 iPSCs and neurons”. In: *Proceedings of the National Academy of Sciences* 110.24 (June 2013), pp. 9962–9967.

[369] Jean-Maurice Delabar et al. “Molecular Mapping of Twenty-Four Features of Down Syndrome on Chromosome 21”. In: *European Journal of Human Genetics* 1.2 (1993), pp. 114–124.

[370] L. E. Olson et al. “A chromosome 21 critical region does not cause specific down syndrome phenotypes”. In: *Science* 306.5696 (Oct. 2004), pp. 687–690.

[371] Jan O Korbel et al. “The genetic architecture of Down syndrome phenotypes revealed by high-resolution analysis of human segmental trisomies”. In: *Proceedings of the National Academy of Sciences* 106.29 (2009).

[372] J R Korenberg et al. “Down syndrome phenotypes: the consequences of chromosomal imbalance.” In: *Proceedings of the National Academy of Sciences* 91.11 (May 1994), pp. 4997–5001.

[373] Ryotaro Hashizume et al. “Trisomic rescue via allele-specific multiple chromosome cleavage using CRISPR-Cas9 in trisomy 21 cells”. In: *PNAS Nexus* 4.2 (Feb. 2025).

[374] Jen Chieh Chiang et al. “Trisomy silencing by XIST normalizes Down syndrome cell pathogenesis demonstrated for hematopoietic defects in vitro”. In: *Nature Communications* 9.1 (Dec. 2018).

[375] Maite Mendioroz et al. “Trans effects of chromosome aneuploidies on DNA methylation patterns in human Down syndrome and mouse models”. In: *Genome Biology* 16.1 (Nov. 2015).

[376] Kristi Kerkel et al. “Altered DNA methylation in leukocytes with trisomy 21”. In: *PLoS Genetics* 6.11 (Nov. 2010).

[377] Maria Giulia Bacalini et al. “Identification of a DNA methylation signature in blood cells from persons with Down Syndrome”. In: *AGING* 7.2 (Feb. 2015), pp. 82–93.

[378] Peter Henneman et al. “Widespread domain-like perturbations of DNA methylation in whole blood of Down syndrome neonates”. In: *PLoS ONE* 13.3 (Mar. 2018).

[379] Ivo S. Muskens et al. “The genome-wide impact of trisomy 21 on DNA methylation and its implications for hematopoiesis”. In: *Nature Communications* 12.1 (Dec. 2021).

[380] Andrew A. Lane et al. “Triplication of a 21q22 region contributes to B cell transformation through HMGN1 overexpression and loss of histone H3 Lys27 trimethylation”. In: *Nature Genetics* 46.6 (2014), pp. 618–623.

[381] Audrey Letourneau et al. “Domains of genome-wide gene expression dysregulation in Down’s syndrome”. In: *Nature* 508.7496 (2014), pp. 345–350.

[382] M. Reza Sailani et al. “DNA-methylation patterns in trisomy 21 using cells from monozygotic twins”. In: *PLoS ONE* 10.8 (Aug. 2015).

[383] Binbin Liu et al. “Stem and progenitor cell dysfunction in human trisomies”. In: *EMBO reports* 16.1 (Jan. 2015), pp. 44–62.

[384] Micah G. Donovan et al. “Variegated overexpression of chromosome 21 genes reveals molecular and immune subtypes of Down syndrome”. In: *Nature Communications* 15.1 (Dec. 2024).

[385] G. Ram and J. Chinen. “Infections and immunodeficiency in Down syndrome”. In: *Clinical and Experimental Immunology* 164 (Apr. 2011), pp. 9–16.

[386] Annika Englund et al. “Changes in mortality and causes of death in the Swedish Down syndrome population”. In: *American Journal of Medical Genetics* 161.4 (Apr. 2013), pp. 642–649.

[387] Oliver Tunstall-Pedoe et al. “Abnormalities in the myeloid progenitor compartment in Down syndrome fetal liver precede acquisition of GATA1 mutations”. In: *Blood* 112.12 (Dec. 2008).

[388] Andrew R. Marderstein et al. “Single-cell multi-omics map of human fetal blood in Down syndrome”. In: *Nature* (Oct. 2024).

[389] Sorcha Isabella O’Byrne et al. “Trisomy 21 Driven Pro-Inflammatory Signalling in Fetal Bone Marrow May Play a Role in Perturbed B-Lymphopoiesis and Acute Lymphoblastic Leukemia of Down Syndrome”. In: *Blood* 134.Supplement_1 (Nov. 2019), pp. 1206–1206.

[390] Glenn A. MacLean et al. “Downregulation of Endothelin Receptor B Contributes to Defective B Cell Lymphopoiesis in Trisomy 21 Pluripotent Stem Cells”. In: *Scientific Reports* 8.1 (Dec. 2018).

[391] Glenn A. MacLean et al. “Altered hematopoiesis in trisomy 21 as revealed through in vitro differentiation of isogenic human pluripotent cells”. In: *Proceedings of the National Academy of Sciences of the United States of America* 109.43 (Oct. 2012), pp. 17567–17572.

[392] Baskaran Thilaganathan, Dennis Tsakonas, and Kypros Nicolaides. “Abnormal fetal immunological development in Down’s syndrome”. In: *British Journal of Obstetrics and Gynaecology* 100.1 (1993), pp. 60–62.

[393] Zdenek Zizka et al. “Prenatally Diagnosable Differences in the Cellular Immunity of Fetuses with Down’s and Edwards’ Syndrome”. In: *Fetal Diagnosis and Therapy* 21.6 (2006), pp. 510–514.

[394] Dean Huggard, Derek G. Doherty, and Eleanor J. Molloy. “Immune Dysregulation in Children With Down Syndrome”. In: *Frontiers in Pediatrics* 8 (Feb. 2020).

[395] Meredith Ramba and Dusan Bogunovic. “The immune system in Down Syndrome: Autoimmunity and severe infections”. In: *Immunological Reviews* 322.1 (Mar. 2024), pp. 300–310.

[396] Irene Roberts et al. “GATA1-mutant clones are frequent and often unsuspected in babies with Down syndrome: identification of a population at risk of leukemia”. In: (2013).

[397] Irene Roberts and Shai Izraeli. “Haematopoietic development and leukaemia in Down syndrome”. In: *British Journal of Haematology* 167.5 (Dec. 2014), pp. 587–599.

[398] M A A Kusters et al. “Intrinsic defect of the immune system in children with Down syndrome: a review”. In: *Clinical and Experimental Immunology* 156.2 (Apr. 2009), pp. 189–193.

[399] Yvette C.M. de Hingh et al. “Intrinsic Abnormalities of Lymphocyte Counts in Children with Down Syndrome”. In: *The Journal of Pediatrics* 147.6 (Dec. 2005), pp. 744–747.

[400] Ayse Nazli Seckin et al. “Age-related alterations of the CD19 complex and memory B cells in children with Down syndrome”. In: *Clinical and Experimental Medicine* 18.1 (Feb. 2018), pp. 125–131.

[401] Rita Carsetti et al. “Reduced numbers of switched memory B cells with high terminal differentiation potential in Down syndrome”. In: *European Journal of Immunology* 45.3 (Mar. 2015), pp. 903–914.

[402] Ruud H.J. Verstegen et al. “Defective B-cell memory in patients with Down syndrome”. In: *Journal of Allergy and Clinical Immunology* 134.6 (Dec. 2014), pp. 1346–1353.

[403] Louise Malle et al. “Autoimmunity in Down’s syndrome via cytokines, CD4 T cells and CD11c+ B cells”. In: *Nature* (2023).

[404] Katherine A. Waugh et al. “Mass Cytometry Reveals Global Immune Remodeling with Multi-lineage Hypersensitivity to Type I Interferon in Down Syndrome”. In: *Cell Reports* 29.7 (Nov. 2019), pp. 1893–1908.

[405] Katharina Lambert et al. “Deep immune phenotyping reveals similarities between aging, Down syndrome, and autoimmunity”. In: *Sci. Transl. Med* 14.627 (Jan. 2022).

[406] Yannick Dieudonné et al. “Immune Defect in Adults With Down Syndrome: Insights Into a Complex Issue”. In: *Frontiers in Immunology* 11 (May 2020).

[407] Diletta Valentini et al. “Generation of switched memory B cells in response to vaccination in Down syndrome children and their siblings”. In: *Vaccine* 33.48 (Nov. 2015), pp. 6689–6696.

[408] Ruud H J Verstegen et al. “Down Syndrome B-Lymphocyte Subpopulations, Intrinsic Defect or Decreased T-Lymphocyte Help”. In: *Pediatric Research* 67.5 (May 2010), pp. 563–569.

[409] Jodi L. Karnell et al. “Role of CD11c + T-bet + B cells in human health and disease”. In: *Cellular Immunology* 321 (Nov. 2017), pp. 40–45.

[410] Beatrijs L.P. Bloemers et al. “Distinct Abnormalities in the Innate Immune System of Children with Down Syndrome”. In: *Journal of Pediatrics* 156.5 (2010).

[411] S. Cetiner et al. “Analysis of peripheral blood T-cell subsets, natural killer cells and serum levels of cytokines in children with Down syndrome”. In: *International Journal of Immunogenetics* 37.4 (Aug. 2010), pp. 233–237.

[412] Justine Schoch et al. “Quantitative, Phenotypical, and Functional Characterization of Cellular Immunity in Children and Adolescents With Down Syndrome”. In: *The Journal of Infectious Diseases* 215.10 (May 2017), pp. 1619–1628.

[413] A Cossarizza et al. “Age-related expansion of functionally inefficient cells with markers of natural killer activity in Down’s syndrome.” In: *Blood* 77.6 (Mar. 1991), pp. 1263–70.

[414] Phyllis Jean Linton and Kenneth Dorshkind. “Age-related changes in lymphocyte development and function”. In: *Nature Immunology* 5.2 (Feb. 2004), pp. 133–139.

[415] D. A. Devenny et al. “Cued recall in early-stage dementia in adults with Down’s syndrome”. In: *Journal of Intellectual Disability Research* 46.6 (Sept. 2002), pp. 472–483.

[416] Warren B. Zigman. “Atypical aging in Down syndrome”. In: *Developmental Disabilities Research Reviews* 18.1 (Nov. 2013), pp. 51–67.

[417] Homayoun Vaziri et al. “Loss of Telomeric DNA during Aging of Normal and Trisomy 21 Human Lymphocytes”. In: *The American Journal of Human Genetics.* 52 (1993), pp. 661–667.

[418] Steve Horvath et al. “Accelerated epigenetic aging in Down syndrome”. In: *Aging Cell* 14.3 (June 2015), pp. 491–495.

[419] Keren Xu et al. “Accelerated epigenetic aging in newborns with Down syndrome”. In: *Aging Cell* 21.7 (July 2022).

[420] Maria BF Trotta et al. “Inflammatory and Immunological parameters in adults with Down syndrome”. In: *Immunity & Ageing* 8.4 (Dec. 2011).

[421] Mauro G. Carta et al. "Chemokines and Pro-Inflammatory Cytokines in Down's Syndrome: An Early Marker for Alzheimer-Type Dementia?" In: *Psychotherapy and Psychosomatics* 71.4 (2002), pp. 233–236.

[422] M. Florencia Iulita et al. "An inflammatory and trophic disconnect biomarker profile revealed in Down syndrome plasma: Relation to cognitive decline and longitudinal evaluation". In: *Alzheimer's & Dementia* 12.11 (Nov. 2016), pp. 1132–1148.

[423] Mahmoud Nateghi Rostami et al. "Altered serum pro-inflammatory cytokines in children with Down's syndrome". In: *European Cytokine Network* 23.2 (June 2012), pp. 64–67.

[424] Rodrigo Rodrigues et al. "Alterations of ectonucleotidases and acetylcholinesterase activities in lymphocytes of Down syndrome subjects: Relation with inflammatory parameters". In: *Clinica Chimica Acta* 433 (June 2014), pp. 105–110.

[425] Kelly D. Sullivan et al. "Trisomy 21 causes changes in the circulating proteome indicative of chronic autoinflammation". In: *Scientific Reports* 7.1 (Dec. 2017).

[426] Yan Zhang et al. "Aberrations in circulating inflammatory cytokine levels in patients with Down syndrome: a meta-analysis". In: *Oncotarget* 8.48 (2017), pp. 84489–84496.

[427] M. Hattori et al. "The DNA sequence of human chromosome 21". In: *Nature* 405.6784 (May 2000), pp. 311–319.

[428] Kelly D Sullivan et al. "Trisomy 21 consistently activates the interferon response". In: *eLife* 5 (July 2016).

[429] Y. H. Tan et al. "Human Chromosome 21 Dosage: Effect on the Expression of the Interferon Induced Antiviral State". In: *Science* 186.4158 (Oct. 1974), pp. 61–63.

[430] Rani K. Powers et al. "Trisomy 21 activates the kynurenine pathway via increased dosage of interferon receptors". In: *Nature Communications* 10.1 (Dec. 2019).

[431] Louise Malle et al. "Excessive negative regulation of type I interferon disrupts viral control in individuals with Down syndrome". In: *Immunity* 55.11 (Nov. 2022), pp. 2074–2084.

[432] Katherine A. Waugh et al. "Triplication of the interferon receptor locus contributes to hallmarks of Down syndrome in a mouse model". In: *Nature Genetics* (June 2023).

[433] Maria Krivega et al. "Genotoxic stress in constitutive trisomies induces autophagy and the innate immune response via the cGAS-STING pathway". In: *Communications Biology* 4.1 (Dec. 2021).

[434] M J Goldacre. "Cancers and immune related diseases associated with Down's syndrome: a record linkage study". In: *Archives of Disease in Childhood* 89.11 (Nov. 2004), pp. 1014–1017.

[435] Kathleen M. Gillespie et al. "Islet Autoimmunity in Children With Down's Syndrome". In: *Diabetes* 55.11 (Nov. 2006), pp. 3185–3188.

[436] R. Bergholdt et al. "Increased prevalence of Down's syndrome in individuals with type 1 diabetes in Denmark: a nationwide population-based study". In: *Diabetologia* 49.6 (June 2006), pp. 1179–1182.

[437] Isabella Friis Jørgensen et al. "Comorbidity landscape of the Danish patient population affected by chromosome abnormalities". In: *Genetics in Medicine* 21.11 (Nov. 2019), pp. 2485–2495.

[438] Brian Hom et al. "Down Syndrome and Autoimmune Disease". In: *Clinical Reviews in Allergy and Immunology* 66.3 (June 2024), pp. 261–273.

[439] Shirley Ramos da Rosa Utiyama et al. "Autoantibodies in patients with Down syndrome: early senescence of the immune system or precocious markers for immunological diseases?" In: *Journal of paediatrics and child health* 44.4 (Apr. 2008), pp. 182–6.

[440] Emily C. Marlow et al. "Leukemia Risk in a Cohort of 3.9 Million Children with and without Down Syndrome". In: *The Journal of Pediatrics* 234 (July 2021), pp. 172–180.

[441] Irene Roberts. "Leukemogenesis in infants and young children with trisomy 21". In: *American Society of Hematology* (2022).

[442] André Baruchel et al. "Down syndrome and leukemia: from basic mechanisms to clinical advances". In: *Haematologica* 108.10 (Oct. 2023), pp. 2570–2581.

[443] Joseph D. Khoury et al. "The 5th edition of the World Health Organization Classification of Haematolymphoid Tumours: Myeloid and Histiocytic/Dendritic Neoplasms". In: *Leukemia* 36.7 (July 2022), pp. 1703–1719.

[444] Jan-Henning Klusmann et al. "Treatment and prognostic impact of transient leukemia in neonates with Down syndrome". In: *Blood* 111.6 (Mar. 2008), pp. 2991–2998.

[445] Alan S. Gamis et al. "Natural history of transient myeloproliferative disorder clinically diagnosed in Down syndrome neonates: a report from the Children's Oncology Group Study A2971". In: *Blood* 118.26 (Dec. 2011), pp. 6752–6759.

[446] Luciana M Hollanda et al. "An inherited mutation leading to production of only the short isoform of GATA-1 is associated with impaired erythropoiesis". In: *Nature Genetics* 38.7 (July 2006), pp. 807–812.

[447] Henrik Hasle et al. "Germline GATA1s-generating mutations predispose to leukemia with acquired trisomy 21 and Down syndrome-like phenotype". In: *Blood* 139.21 (May 2022), pp. 3159–3165.

[448] Sara Parrella et al. "Loss of GATA-1 full length as a cause of Diamond–Blackfan anemia phenotype". In: *Pediatric Blood & Cancer* 61.7 (July 2014), pp. 1319–1321.

[449] Alvin Zipursky. "Transient leukaemia – a benign form of leukaemia in newborn infants with trisomy 21". In: *British Journal of Haematology* 120.6 (Mar. 2003), pp. 930–938.

[450] Joshua Wechsler et al. "Acquired mutations in GATA1 in the megakaryoblastic leukemia of Down syndrome". In: *Nature Genetics* 32.1 (Sept. 2002), pp. 148–152.

[451] Gina Mundschau et al. "Mutagenesis of GATA1 is an initiating event in Down syndrome leukemogenesis". In: *Blood* 101.11 (June 2003), pp. 4298–4300.

[452] Marta Byrska-Bishop et al. "Pluripotent stem cells reveal erythroid-specific activities of the GATA1 N-terminus". In: *Journal of Clinical Investigation* 125.3 (Mar. 2015), pp. 993–1005.

[453] Te Ling et al. “Chromatin occupancy and epigenetic analysis reveal new insights into the function of the GATA1 N terminus in erythropoiesis”. In: *Blood* 134.19 (Nov. 2019), pp. 1619–1631.

[454] Zhe Li et al. “Developmental stage–selective effect of somatically mutated leukemogenic transcription factor GATA1”. In: *Nature Genetics* 37.6 (June 2005), pp. 613–619.

[455] Zahra Kadri et al. “Direct Binding of pRb/E2F-2 to GATA-1 Regulates Maturation and Terminal Cell Division during Erythropoiesis”. In: *PLoS Biology* 7.6 (June 2009), e1000123.

[456] L. Rainis. “Mutations in exon 2 of GATA1 are early events in megakaryocytic malignancies associated with trisomy 21”. In: *Blood* 102.3 (Apr. 2003), pp. 981–986.

[457] M. Ahmed. “Natural history of GATA1 mutations in Down syndrome”. In: *Blood* 103.7 (Apr. 2004), pp. 2480–2489.

[458] J A Tamblyn et al. “Prenatal therapy in transient abnormal myelopoiesis: a systematic review”. In: *Archives of Disease in Childhood - Fetal and Neonatal Edition* 101.1 (Jan. 2016), pp. 67–71.

[459] Natalina Elliott et al. “Clinical significance of preleukemic somatic GATA1 mutations in children with Down syndrome”. In: *Blood* (June 2025). URL: `http://ashpublications.org/blood/article-pdf/doi/10.1182/blood.2025029250/2382608/blood.2025029250.pdf`.

[460] Kenichi Yoshida et al. “The landscape of somatic mutations in Down syndrome–related myeloid disorders”. In: *Nature Genetics* 45.11 (Nov. 2013), pp. 1293–1299.

[461] Maurice Labuhn et al. “Mechanisms of Progression of Myeloid Preleukemia to Transformed Myeloid Leukemia in Children with Down Syndrome”. In: *Cancer Cell* 36.2 (Aug. 2019), pp. 123–138.

[462] Oliver Tunstall et al. “Guidelines for the investigation and management of Transient Leukaemia of Down Syndrome”. In: *British Journal of Haematology* 182.2 (July 2018), pp. 200–211.

[463] Austin C Boucher et al. “Clinical and biological aspects of myeloid leukemia in Down syndrome.” In: *Leukemia* 35.12 (Dec. 2021), pp. 3352–3360.

[464] C Bohnstedt et al. “Physicians compliance during maintenance therapy in children with Down syndrome and acute lymphoblastic leukemia”. In: *Leukemia* 27.4 (Apr. 2013), pp. 866–870.

[465] Trudy D Buitenkamp et al. “Acute lymphoblastic leukemia in children with Down syndrome: a retrospective analysis from the Ponte di Legno study group”. In: *Blood* 123.1 (Jan. 2014), pp. 70–77.

[466] P. Lee et al. “The biology, pathogenesis and clinical aspects of acute lymphoblastic leukemia in children with Down syndrome”. In: *Leukemia* 30.9 (Sept. 2016), pp. 1816–1823.

[467] Yousif Matloub et al. “Excellent long-term survival of children with Down syndrome and standard-risk ALL: a report from the Children’s Oncology Group.” In: *Blood advances* 3.11 (June 2019), pp. 1647–1656.

[468] C H Pui et al. “Immunophenotypes and karyotypes of leukemic cells in children with Down syndrome and acute lymphoblastic leukemia.” In: *Journal of Clinical Oncology* 11.7 (July 1993), pp. 1361–1367.

[469] Bernward Zeller et al. “Acute leukaemia in children with Down syndrome: a population-based Nordic study”. In: *British Journal of Haematology* 128.6 (Mar. 2005), pp. 797–804.

[470] Maurizio Arico et al. “Acute lymphoblastic leukemia and Down syndrome”. In: *Cancer* 113.3 (Aug. 2008), pp. 515–521.

[471] Charles G. Mullighan et al. “Rearrangement of CRLF2 in B-progenitor-and Down syndrome-associated acute lymphoblastic leukemia”. In: *Nature Genetics* 41.11 (Nov. 2009), pp. 1243–1246.

[472] Lisa J. Russell et al. “Deregulated expression of cytokine receptor gene, CRLF2, is involved in lymphoid transformation in B-cell precursor acute lymphoblastic leukemia”. In: *Blood* 114.13 (Sept. 2009), pp. 2688–2698.

[473] Akinori Yoda et al. “Functional screening identifies CRLF2 in precursor B-cell acute lymphoblastic leukemia”. In: *Proceedings of the National Academy of Sciences* 107.1 (Jan. 2010), pp. 252–257.

[474] Libi Hertzberg et al. “Down syndrome acute lymphoblastic leukemia, a highly heterogeneous disease in which aberrant expression of CRLF2 is associated with mutated JAK2: a report from the International BFM Study Group”. In: *Blood* 115.5 (Feb. 2010), pp. 1006–1017.

[475] Yrina Rochman et al. “Thymic stromal lymphopoietin-mediated STAT5 phosphorylation via kinases JAK1 and JAK2 reveals a key difference from IL-7-induced signaling.” In: *Proceedings of the National Academy of Sciences of the United States of America* 107.45 (Nov. 2010), pp. 19455–60.

[476] Mel Greaves. “A causal mechanism for childhood acute lymphoblastic leukaemia”. In: *Nature Reviews Cancer* 18.8 (Aug. 2018), pp. 471–484.

[477] Adam J. de Smith et al. “Backtracking to the future: unraveling the origins of childhood leukemia”. In: *Leukemia* 38.2 (Feb. 2024), pp. 416–419.

[478] Maria Morak et al. “Small sizes and indolent evolutionary dynamics challenge the potential role of P2RY8-CRLF2–harboring clones as main relapse-driving force in childhood ALL”. In: *Blood* 120.26 (Dec. 2012), pp. 5134–5142.

[479] Karlijn A.L. Hasaart et al. “Mutation accumulation and developmental lineages in normal and Down syndrome human fetal haematopoiesis”. In: *Scientific Reports* 10.1 (Dec. 2020).

[480] Slobodan V Jovanovic, Debbie Clements, and Kent MacLeod. “Biomarkers of oxidative stress are significantly elevated in Down syndrome”. In: *Free Radical Biology and Medicine* 25.9 (Dec. 1998), pp. 1044–1048.

[481] C. Piccoli et al. “Chronic pro-oxidative state and mitochondrial dysfunctions are more pronounced in fibroblasts from Down syndrome foeti with congenital heart defects”. In: *Human Molecular Genetics* 22.6 (Mar. 2013), pp. 1218–1232.

[482] Pablo Helguera et al. “Adaptive Downregulation of Mitochondrial Function in Down Syndrome”. In: *Cell Metabolism* 17.1 (Jan. 2013), pp. 132–140.

[483] Antonella Izzo et al. “Metformin restores the mitochondrial network and reverses mitochondrial dysfunction in Down syndrome cells”. In: *Human Molecular Genetics* (Jan. 2017), p. ddx016.

[484] Daniela Valenti et al. “Deficit of complex I activity in human skin fibroblasts with chromosome 21 trisomy and overproduction of reactive oxygen species by mitochondria: involvement of the cAMP/PKA signalling pathway”. In: *Biochemical Journal* 435.3 (May 2011), pp. 679–688.

[485] Marzia Perluigi and D. Allan Butterfield. “Oxidative Stress and Down Syndrome: A Route toward Alzheimer-Like Dementia”. In: *Current Gerontology and Geriatrics Research* 2012 (2012), pp. 1–10.

[486] Antonella Izzo et al. “Mitochondrial dysfunction in down syndrome: molecular mechanisms and therapeutic targets”. In: *Molecular Medicine* 24.1 (Dec. 2018), p. 2.

[487] Kajsa Paulsson et al. “The genomic landscape of high hyperdiploid childhood acute lymphoblastic leukemia”. In: *Nature Genetics* 47.6 (June 2015), pp. 672–676.

[488] Anouchka P. Laurent, Rishi S. Kotecha, and Sébastien Malinge. “Gain of chromosome 21 in hematological malignancies: lessons from studying leukemia in children with Down syndrome”. In: *Leukemia* 34.8 (Aug. 2020), pp. 1984–1999.

[489] David O’connor. “The role of the fetal microenvironment in abnormal fetal haematopoiesis in Down syndrome”. PhD thesis. Imperial College London, 2014.

[490] Agnieszka A. Wendorff et al. “Niche Requirements of Transient Leukemia Cells in Down Syndrome”. In: *Blood* 120.21 (Nov. 2012), pp. 1753–1753.

[491] Emerald Butko, Claire Pouget, and David Traver. “Complex regulation of HSC emergence by the Notch signaling pathway”. In: *Developmental Biology* 409.1 (Jan. 2016), pp. 129–138.

[492] Jared R. Thomas and Randall J. Roper. *Current Analysis of Skeletal Phenotypes in Down Syndrome*. June 2021.

[493] A. Carfì et al. “Bone mineral density in adults with Down syndrome”. In: *Osteoporosis International* 28.10 (Oct. 2017), pp. 2929–2934.

[494] Joshua D. Blazek et al. “Rescue of the abnormal skeletal phenotype in Ts65Dn Down syndrome mice using genetic and therapeutic modulation of trisomic Dyrk1a”. In: *Human Molecular Genetics* 24.20 (Oct. 2015), pp. 5687–5696.

[495] Kirby M. Sherman et al. “Low bone mass and impaired fracture healing in mouse models of Trisomy21 (Down syndrome)”. In: *Bone* 162 (Sept. 2022), p. 116471.

[496] Grimwood et al. “Histological assessment of vertebral bone in a Down’s syndrome adult with osteoporosis”. In: *Histopathology* 36.3 (Mar. 2000), pp. 279–280.

[497] Tristan W. Fowler et al. “Low bone turnover and low BMD in down syndrome: Effect of intermittent PTH treatment”. In: *PLoS ONE* 7.8 (Aug. 2012).

[498] R. J.M. Snijders et al. “Femur length and trisomy 21: Impact of gestational age on screening efficiency”. In: *Ultrasound in Obstetrics and Gynecology* 16.2 (2000), pp. 142–145.

[499] Bryann Bromley et al. “The Genetic Sonogram”. In: *Journal of Ultrasound in Medicine* 21.10 (Oct. 2002), pp. 1087–1096.

[500] W M Hern. “Correlation of fetal age and measurements between 10 and 26 weeks of gestation.” In: *Obstetrics and gynecology* 63.1 (Jan. 1984), pp. 26–32.

[501] Sofie Van Gassen et al. “FlowSOM: Using self-organizing maps for visualization and interpretation of cytometry data”. In: *Cytometry Part A* 87.7 (July 2015), pp. 636–645.

[502] Malgorzata Nowicka et al. “CyTOF workflow: differential discovery in high-throughput high-dimensional cytometry datasets”. In: *F1000Research* 6 (May 2019), p. 748.

[503] Florian Hahne et al. “flowCore: a Bioconductor package for high throughput flow cytometry”. In: *BMC Bioinformatics* 10.1 (Dec. 2009), p. 106.

[504] K Itoh et al. “Reproducible establishment of hemopoietic supportive stromal cell lines from murine bone marrow.” In: *Experimental hematology* 17.2 (Feb. 1989), pp. 145–53.

[505] Shigeru Tsuchiya et al. “Establishment and characterization of a human acute monocytic leukemia cell line (THP-1)”. In: *International Journal of Cancer* 26.2 (Aug. 1980), pp. 171–176.

[506] Simone Picelli et al. “Full-length RNA-seq from single cells using Smart-seq2”. In: *Nature Protocols* 9.1 (Jan. 2014), pp. 171–181.

[507] Alba Rodriguez-Meira et al. “TARGET-Seq: A Protocol for High-Sensitivity Single-Cell Mutational Analysis and Parallel RNA Sequencing”. In: *STAR Protocols* 1.3 (Dec. 2020).

[508] S Andrews. *FastQC: A Quality Control Tool for High Throughput Sequence Data*. 2010. URL: `http://www.bioinformatics.babraham.ac.uk/projects/fastqc/`.

[509] F Krueger. *Trim Galore!* 2019. URL: `https://www.bioinformatics.babraham.ac.uk/projects/trim_galore/`.

[510] Alexander Dobin et al. “STAR: ultrafast universal RNA-seq aligner”. In: *Bioinformatics* 29.1 (Jan. 2013), pp. 15–21.

[511] Yang Liao, Gordon K. Smyth, and Wei Shi. “featureCounts: an efficient general purpose program for assigning sequence reads to genomic features”. In: *Bioinformatics* 30.7 (Apr. 2014), pp. 923–930.

[512] Matthew E. Ritchie et al. “limma powers differential expression analyses for RNA-sequencing and microarray studies”. In: *Nucleic Acids Research* 43.7 (Apr. 2015), e47–e47.

[513] Michael I Love, Wolfgang Huber, and Simon Anders. “Moderated estimation of fold change and dispersion for RNA-seq data with DESeq2”. In: *Genome Biology* 15.12 (Dec. 2014), p. 550.

[514] Aravind Subramanian et al. “Gene set enrichment analysis: A knowledge-based approach for interpreting genome-wide expression profiles”. In: *Proceedings of the National Academy of Sciences* 102.43 (Oct. 2005), pp. 15545–15550.

[515] Peter Langfelder and Steve Horvath. “WGCNA: an R package for weighted correlation network analysis”. In: *BMC Bioinformatics* 9.1 (Dec. 2008), p. 559.

[516] Simon Anders, Alejandro Reyes, and Wolfgang Huber. "Detecting differential usage of exons from RNA-seq data". In: *Genome Research* 22.10 (Oct. 2012), pp. 2008–2017.

[517] Ben Langmead and Steven L Salzberg. "Fast gapped-read alignment with Bowtie 2". In: *Nature Methods* 9.4 (Apr. 2012), pp. 357–359.

[518] Petr Danecek et al. "Twelve years of SAMtools and BCFtools". In: *GigaScience* 10.2 (Jan. 2021).

[519] Yong Zhang et al. "Model-based Analysis of ChIP-Seq (MACS)". In: *Genome Biology* 9.9 (Sept. 2008), R137.

[520] Caryn S. Ross-Innes et al. "Differential oestrogen receptor binding is associated with clinical outcome in breast cancer". In: *Nature* 481.7381 (Jan. 2012), pp. 389–393.

[521] Lihua J Zhu et al. "ChIPpeakAnno: a Bioconductor package to annotate ChIP-seq and ChIP-chip data". In: *BMC Bioinformatics* 11.1 (Dec. 2010), p. 237.

[522] Sven Heinz et al. "Simple combinations of lineage-determining transcription factors prime cis-regulatory elements required for macrophage and B cell identities." In: *Molecular cell* 38.4 (May 2010), pp. 576–89.

[523] Fidel Ramírez et al. "deepTools2: a next generation web server for deep-sequencing data analysis". In: *Nucleic Acids Research* 44.W1 (July 2016), W160–W165.

[524] Daniel R Zerbino et al. "WiggleTools: parallel processing of large collections of genome-wide datasets for visualization and statistical analysis." In: *Bioinformatics (Oxford, England)* 30.7 (Apr. 2014), pp. 1008–9.

[525] Yuhan Hao et al. "Dictionary learning for integrative, multimodal and scalable single-cell analysis". In: *Nature Biotechnology* 42.2 (Feb. 2024), pp. 293–304.

[526] Ilya Korsunsky et al. "Fast, sensitive and accurate integration of single-cell data with Harmony". In: *Nature Methods* 16.12 (Dec. 2019), pp. 1289–1296.

[527] George C. Linderman et al. "Zero-preserving imputation of single-cell RNA-seq data". In: *Nature Communications* 13.1 (Dec. 2022).

[528] Cole Trapnell et al. "The dynamics and regulators of cell fate decisions are revealed by pseudotemporal ordering of single cells". In: *Nature Biotechnology* 32.4 (2014), pp. 381–386.

[529] Suoqin Jin et al. "Inference and analysis of cell-cell communication using CellChat". In: *Nature Communications* 12.1 (Dec. 2021).

[530] Alireza Khatamian et al. "SJARACNe: A scalable software tool for gene network reverse engineering from big data". In: *Bioinformatics* 35.12 (June 2019), pp. 2165–2166.

[531] Xinran Dong et al. "NetBID2 provides comprehensive hidden driver analysis". In: *Nature Communications* 14.1 (Dec. 2023).

[532] Cody T. Mowery et al. "Trisomy of a Down Syndrome Critical Region Globally Amplifies Transcription via HMGN1 Overexpression". In: *Cell Reports* 25.7 (Nov. 2018), pp. 1898–1911.

[533] Ewa Sitnicka et al. “Ly-through their corresponding receptors c-kit and c-mpl man and Jacobsen”. In: *Immunity* 17 (Oct. 2002), pp. 463–472.

[534] Katrin Mackarehtschian et al. “Targeted Disruption of the flk2/flt3 Gene Leads to Deficiencies in Primitive Hematopoietic Progenitors”. In: *Immunity* 3 (July 1995), pp. 147–161.

[535] Alya Zriwil et al. “Direct role of FLT3 in regulation of early lymphoid progenitors”. In: *British Journal of Haematology* 183.4 (Nov. 2018), pp. 588–600.

[536] Ebtehal Al Sheikh et al. “TCF3 Dominant Negative Variant Causes an Early Block in B-Lymphopoiesis and Agammaglobulinemia”. In: *Journal of Clinical Immunology* 41.6 (Aug. 2021), pp. 1391–1394.

[537] Meriem Ben-Ali et al. “Homozygous transcription factor 3 gene (TCF3) mutation is associated with severe hypogammaglobulinemia and B-cell acute lymphoblastic leukemia”. In: *Journal of Allergy and Clinical Immunology* 140.4 (Oct. 2017), pp. 1191–1194.

[538] Laura Bou-Maroun et al. “Heterozygous TCF3-Related Disease Presenting as X-linked Agammaglobulinemia Mimicry in a Male Toddler with B-cell Aplasia, Agammaglobulinemia, and Severe Neutropenia”. In: *Clinical Immunology* 250 (May 2023), p. 109487.

[539] J. Hagman, A. Travis, and R. Grosschedl. “A novel lineage-specific nuclear factor regulates mb-1 gene transcription at the early stages of B cell differentiation.” In: *The EMBO Journal* 10.11 (Nov. 1991), pp. 3409–3417.

[540] Charles E. Bullerwell et al. “EBF1 drives hallmark B cell gene expression by enabling the interaction of PAX5 with the MLL H3K4 methyltransferase complex”. In: *Scientific Reports* 11.1 (Dec. 2021).

[541] Jagan M.R. Pongubala et al. “Transcription factor EBF restricts alternative lineage options and promotes B cell fate commitment independently of Pax5”. In: *Nature Immunology* 9.2 (Feb. 2008), pp. 203–215.

[542] Lisa Borghesi et al. “B Lineage–specific Regulation of V(D)J Recombinase Activity Is Established in Common Lymphoid Progenitors”. In: *The Journal of Experimental Medicine* 199.4 (Feb. 2004), pp. 491–502.

[543] David G. Schatz and Yanhong Ji. “Recombination centres and the orchestration of V(D)J recombination”. In: *Nature Reviews Immunology* 11.4 (Apr. 2011), pp. 251–263.

[544] Sophie M. Lehar et al. “Notch ligands Delta1 and Jagged1 transmit distinct signals to T-cell precursors”. In: *Blood* 105.4 (Feb. 2005), pp. 1440–1447.

[545] Anne Wilson, H Robson Macdonald, and Freddy Radtke. “Notch 1–deficient Common Lymphoid Precursors Adopt a B Cell Fate in the Thymus”. In: *J. Exp. Med* 194.7 (Oct. 2001), pp. 1003–1012.

[546] Hua Han et al. “Inducible gene knockout of transcription factor recombination signal binding protein-J reveals its essential role in T versus B lineage decision”. In: *International Immunology* 14.6 (June 2002), pp. 637–645.

[547] John C Pui et al. “Notch1 Expression in Early Lymphopoiesis Influences B versus T Lineage Determination”. In: *Immunity* 11 (Sept. 1999), pp. 299–308.

[548] Rose C. Beck et al. “The Notch Ligands Jagged2, Delta1, and Delta4 Induce Differentiation and Expansion of Functional Human NK Cells from CD34+ Cord Blood Hematopoietic Progenitor Cells”. In: *Biology of Blood and Marrow Transplantation* 15.9 (Sept. 2009), pp. 1026–1037.

[549] Clarisse Benne et al. “Notch increases T/NK potential of human hematopoietic progenitors and inhibits B cell differentiation at a pro-B stage”. In: *Stem Cells* 27.7 (2009), pp. 1676–1685.

[550] Qi Yang et al. “TCF-1 upregulation identifies early innate lymphoid progenitors in the bone marrow”. In: *Nature Immunology* 16.10 (Sept. 2015), pp. 1044–1050.

[551] Chao-Nan Ting et al. “Transcription factor GATA-3 is required for development of the T-cell lineage”. In: *Nature* 384.6608 (Dec. 1996), pp. 474–478.

[552] R W Hendriks et al. “Expression of the transcription factor GATA-3 is required for the development of the earliest T cell progenitors and correlates with stages of cellular proliferation in the thymus.” In: *European journal of immunology* 29.6 (June 1999), pp. 1912–8.

[553] Alaa Kassim Ali et al. “NK Cell–Specific Gata3 Ablation Identifies the Maturation Program Required for Bone Marrow Exit and Control of Proliferation”. In: *The Journal of Immunology* 196.4 (Feb. 2016), pp. 1753–1767.

[554] Sandrine I Samson et al. “GATA-3 Promotes Maturation, IFN-Production, and Liver-Specific Homing of NK Cells”. In: *Immunity* 19 (Nov. 2003), pp. 701–711.

[555] Catherine Frelin et al. “GATA-3 regulates the self-renewal of long-term hematopoietic stem cells.” In: *Nature immunology* 14.10 (Oct. 2013), pp. 1037–44.

[556] Chia-Jui Ku et al. “GATA-3 regulates hematopoietic stem cell maintenance and cell-cycle entry.” In: *Blood* 119.10 (Mar. 2012), pp. 2242–51.

[557] R Barndt, M F Dai, and Y Zhuang. “A novel role for HEB downstream or parallel to the pre-TCR signaling pathway during alpha beta thymopoiesis.” In: *Journal of immunology (Baltimore, Md. : 1950)* 163.6 (Sept. 1999), pp. 3331–43.

[558] Yuan Zhuang, Peifeng Cheng, and Harold Weintraub. “B-Lymphocyte Development Is Regulated by the Combined Dosage of Three Basic Helix-Loop-Helix Genes, E2A , E2-2 , and HEB”. In: *Molecular and Cellular Biology* 16.6 (June 1996), pp. 2898–2905.

[559] Eva Welinder et al. “The transcription factors E2A and HEB act in concert to induce the expression of FOXO1 in the common lymphoid progenitor”. In: *Proceedings of the National Academy of Sciences* 108.42 (Oct. 2011), pp. 17402–17407.

[560] Marsela Braunstein and Michele K. Anderson. “HEB in the Spotlight: Transcriptional Regulation of T-Cell Specification, Commitment, and Developmental Plasticity”. In: *Clinical and Developmental Immunology* 2012 (2012), pp. 1–15.

[561] Lesly Calderón and Thomas Boehm. “Three chemokine receptors cooperatively regulate homing of hematopoietic progenitors to the embryonic mouse thymus”. In: *Proceedings of the National Academy of Sciences of the United States of America* 108.18 (May 2011), pp. 7517–7522.

[562] Joonsoo Kang and Nidhi Malhotra. "Transcription factor networks directing the development, function, and evolution of innate lymphoid effectors". In: *Annual Review of Immunology* 33 (Mar. 2015), pp. 505–538.

[563] Cyril Seillet et al. "Deciphering the Innate Lymphoid Cell Transcriptional Program". In: *Cell Reports* 17.2 (Oct. 2016), pp. 436–447.

[564] Victoria Male et al. "The transcription factor E4bp4/Nfil3 controls commitment to the NK lineage and directly regulates Eomes and Id2 expression". In: *Journal of Experimental Medicine* 211.4 (2014), pp. 635–642.

[565] Parinaz Aliahmad, Brian De La Torre, and Jonathan Kaye. "Shared dependence on the DNA-binding factor TOX for the development of lymphoid tissue-inducer cell and NK cell lineages". In: *Nature Immunology* 11.10 (Oct. 2010), pp. 945–952.

[566] Melissa A Thal et al. "Ebf1-mediated down-regulation of Id2 and Id3 is essential for specification of the B cell lineage". In: *Proceedings of the National Academy of Sciences of the United States of America* 106.2 (Jan. 2009), pp. 552–557.

[567] Xiaofei Yu et al. "The basic leucine zipper transcription factor NFIL3 directs the development of a common innate lymphoid cell precursor". In: *eLife* 3 (Oct. 2014).

[568] Michael J Townsend et al. "T-bet Regulates the Terminal Maturation and Homeostasis of NK and VA14i NKT Cells". In: *Immunity* 20 (Apr. 2004), pp. 477–494.

[569] Scott M. Gordon et al. "The Transcription Factors T-bet and Eomes Control Key Checkpoints of Natural Killer Cell Maturation". In: *Immunity* 36.1 (Jan. 2012), pp. 55–67.

[570] Rodney P. DeKoter, Meghana B. Kamath, and Isaac B. Houston. "Analysis of concentration-dependent functions of PU.1 in hematopoiesis using mouse models". In: *Blood Cells, Molecules, and Diseases* 39.3 (Nov. 2007), pp. 316–320.

[571] Nai-dy Wang et al. "Impaired Energy Homeostasis in C/EBPα Knockout Mice". In: *Science* 269.5227 (Aug. 1995), pp. 1108–1112.

[572] Dong-Er Zhang et al. "Absence of granulocyte colony-stimulating factor signaling and neutrophil development in CCAAT enhancer binding proteinα-deficientmice". In: *Proceedings of the National Academy of Sciences* 94.2 (Jan. 1997), pp. 569–574.

[573] Georg F Weber et al. "Interleukin-3 amplifies acute inflammation and is a potential therapeutic target in sepsis". In: *Science* 247.6227 (Mar. 2015), pp. 1260–1264.

[574] Daisuke Kurotaki, Haruka Sasaki, and Tomohiko Tamura. "Transcriptional control of monocyte and macrophage development". In: *International Immunology* 29.3 (Mar. 2017), pp. 97–107.

[575] Alberto Yañez et al. "IRF8 acts in lineage-committed rather than oligopotent progenitors to control neutrophil vs monocyte production". In: *Blood* 125.9 (2015), pp. 1452–1459.

[576] Daisuke Kurotaki et al. *Epigenetic control of early dendritic cell lineage specification by the transcription factor IRF8 in mice*. Tech. rep. 17. 2019, pp. 1803–1813.

[577] Hannah R. Moorman et al. "IRF8: Mechanism of Action and Health Implications". In: *Cells* 11.17 (Sept. 2022).

[578] Michael A. Rieger et al. “Hematopoietic Cytokines Can Instruct Lineage Choice”. In: *Science* 325.5937 (July 2009), pp. 217–218.

[579] Max Endele et al. “CSF-1-induced Src signaling can instruct monocytic lineage choice Key Points”. In: *Blood* 129.12 (Mar. 2017), pp. 1961–1701.

[580] A. D. Friedman. “Transcriptional control of granulocyte and monocyte development”. In: *Oncogene* 26.47 (Oct. 2007), pp. 6816–6828.

[581] Hrishikesh M. Mehta and Seth J. Corey. “G-CSF, the guardian of granulopoiesis”. In: *Seminars in Immunology* 54 (Apr. 2021).

[582] Alexa Triot et al. “Inherited biallelic CSF3R mutations in severe congenital neutropenia”. In: *Blood* 123.24 (June 2014), pp. 3811–3817.

[583] Richard E Person et al. “Mutations in proto-oncogene GFI1 cause human neutropenia and target ELA2”. In: *Nature Genetics* 34.3 (July 2003), pp. 308–312.

[584] Holger Karsunky et al. “Inflammatory reactions and severe neutropenia in mice lacking the transcriptional repressor GFi1”. In: *Nature Genetics* 30.3 (2002), pp. 295–300.

[585] Hui Zeng et al. “Transcription factor Gfi1 regulates self-renewal and engraftment of hematopoietic stem cells”. In: *EMBO Journal* 23.20 (Oct. 2004), pp. 4116–4125.

[586] Xiaoqing Xie et al. “Dose-dependent effect of GFI1 expression in the reconstitution and the differentiation capacity of HSCs”. In: *Frontiers in Cell and Developmental Biology* 11 (2023).

[587] L. T. Van Der Meer, J. H. Jansen, and B. A. Van Der Reijden. “Gfi1 and Gfi1b: Key regulators of hematopoiesis”. In: *Leukemia* 24.11 (Nov. 2010), pp. 1834–1843.

[588] Tarik Möröy and Cyrus Khandanpour. “Growth factor independence 1 (Gfi1) as a regulator of lymphocyte development and activation”. In: *Seminars in Immunology* 23.5 (Oct. 2011), pp. 368–378.

[589] Maria Chiara Pelleri et al. “Partial trisomy 21 map: Ten cases further supporting the highly restricted Down syndrome critical region (HR-DSCR) on human chromosome 21”. In: *Molecular Genetics & Genomic Medicine* 7.8 (Aug. 2019).

[590] Ari Itoh-Nakadai et al. “The transcription repressors Bach2 and Bach1 promote B cell development by repressing the myeloid program”. In: *Nature Immunology* 15.12 (Nov. 2014), pp. 1171–1180.

[591] Liat Stoler-Barak et al. “B cell class switch recombination is regulated by DYRK1A through MSH6 phosphorylation”. In: *Nature Communications* 14.1 (Dec. 2023).

[592] Yanchuan Li et al. “DYRK1a mediates BAFF-induced noncanonical NF-κB activation to promote autoimmunity and B-cell leukemogenesis”. In: *Blood* 138.23 (Dec. 2021), pp. 2360–2371.

[593] Rahul S. Bhansali et al. “DYRK1A regulates B cell acute lymphoblastic leukemia through phosphorylation of FOXO1 and STAT3”. In: *Journal of Clinical Investigation* 131.1 (Jan. 2021).

[594] Esteban J. Rozen, Robin D. Dowell, and Mary A. Allen. “DYRK1A in blood and immune function: implications in leukemia, inflammatory disorders, infection and Down syndrome”. In: *Frontiers in Cell and Developmental Biology* 13 (May 2025).

[595] Monika J. Stankiewicz and John D. Crispino. "ETS2 and ERG promote megakaryopoiesis and synergize with alterations in GATA-1 to immortalize hematopoietic progenitor cells". In: *Blood* 113.14 (Apr. 2009), pp. 3337–3347.

[596] C. T. Stankey et al. "A disease-associated gene desert directs macrophage inflammation through ETS2". In: *Nature* 630.8016 (June 2024), pp. 447–456.

[597] Hai Hui Xue et al. "The Transcription Factor GABP Is a Critical Regulator of B Lymphocyte Development". In: *Immunity* 26.4 (Apr. 2007), pp. 421–431.

[598] Zhong Fa Yang et al. "GABP transcription factor is required for myeloid differentiation, in part, through its control of Gfi-1 expression". In: *Blood* 118.8 (Aug. 2011), pp. 2243–2253.

[599] Katie A. Matatall et al. "Type II interferon promotes differentiation of myeloid-biased hematopoietic stem cells". In: *Stem Cells* 32.11 (Nov. 2014), pp. 3023–3030.

[600] Matthew B. Buechler et al. "Cutting Edge: Type I IFN Drives Emergency Myelopoiesis and Peripheral Myeloid Expansion during Chronic TLR7 Signaling". In: *The Journal of Immunology* 190.3 (Feb. 2013), pp. 886–891.

[601] Amanda McCabe et al. "Interleukin-10 Signaling in Hematopoietic Stem and Progenitor Cells Maintains Stem Cell Function and Regulates Inflammation-Induced Myeloid Cell Output". In: *Blood* 132.Supplement 1 (Nov. 2018), pp. 2407–2407.

[602] Finlay McNab et al. "Type I interferons in infectious disease". In: *Nature Reviews Immunology* 15.2 (Jan. 2015), pp. 87–103.

[603] Alexander Zaslavsky et al. "The calcineurin-NFAT pathway negatively regulates megakaryopoiesis". In: *Blood* 121.16 (Nov. 2013).

[604] Katherine R Martin et al. "Upregulation of RCAN1 causes Down syndrome-like immune dysfunction". In: *Journal of Medical Genetics* 50.7 (July 2013), pp. 444–454.

[605] Wooseok Seo et al. "Runx1-Cbfβ facilitates early B lymphocyte development by regulating expression of Ebf1". In: *Journal of Experimental Medicine* 209.7 (July 2012), pp. 1255–1262.

[606] Birte Niebuhr et al. "Runx1 is essential at two stages of early murine B-cell development". In: *Blood* 122.3 (July 2013), pp. 413–423.

[607] Sofia Gialesaki et al. "RUNX1 isoform disequilibrium promotes the development of trisomy 21-associated myeloid leukemia". In: *Blood* 141.10 (Mar. 2023), pp. 1105–1118.

[608] Yoh-suke Mukouyama et al. "The AML1 Transcription Factor Functions to Develop and Maintain Hematogenic Precursor Cells in the Embryonic Aorta–Gonad–Mesonephros Region". In: *Developmental Biology* 220.1 (Apr. 2000), pp. 27–36.

[609] G. Lacaud. "Runx1 is essential for hematopoietic commitment at the hemangioblast stage of development in vitro". In: *Blood* 100.2 (June 2002), pp. 458–466.

[610] Tomomasa Yokomizo et al. "Requirement of Runx1/AML1/PEBP2αB for the generation of haematopoietic cells from endothelial cells". In: *Genes to Cells* 6.1 (Jan. 2001), pp. 13–23.

[611] Elaine Dzierzak and Anna Bigas. "Blood Development: Hematopoietic Stem Cell Dependence and Independence". In: *Cell Stem Cell* 22.5 (May 2018), pp. 639–651.

[612] Marella de Bruijn and Elaine Dzierzak. "Runx transcription factors in the development and function of the definitive hematopoietic system". In: *Blood* 129.15 (Apr. 2017), pp. 2061–2069.

[613] Joseph D. Growney et al. "Loss of Runx1 perturbs adult hematopoiesis and is associated with a myeloproliferative phenotype". In: *Blood* 106.2 (July 2005), pp. 494–504.

[614] Dana C Bellissimo and Nancy A Speck. "RUNX1 Mutations in Inherited and Sporadic Leukemia." In: *Frontiers in cell and developmental biology* 5 (2017), p. 111.

[615] Liying Guan et al. "RUNX1 Isoforms Regulate RUNX1 and Target-Genes Differentially in Platelets-Megakaryocytes: Association with Clinical Cardiovascular Events". In: *Journal of Thrombosis and Haemostasis* (Dec. 2024).

[616] Remko Schotte et al. "The transcription factor Spi-B is expressed in plasmacytoid DC precursors and inhibits T-, B-, and NK-cell development". In: *Blood* 101 (2003), pp. 1015–1023.

[617] Chia-Lin Hsu et al. "Antagonistic effect of CCAAT enhancer-binding protein-and Pax5 in myeloid or lymphoid lineage choice in common lymphoid progenitors". In: *Proceedings of the National Academy of Sciences of the United States of America* 103.3 (Jan. 2006), pp. 672–577.

[618] Koichiro Miyamoto et al. "Inhibitory effect of interleukin 3 on early development of human B-lymphopoiesis". In: *British Journal of Haematology* 114.3 (2001), pp. 690–697.

[619] Ross Okamura et al. *Redundant Regulation of T Cell Differentiation and TCR Gene Expression by the Transcription Factors LEF-1 and TCF-1*. Tech. rep. 1998.

[620] Saria Mcheik et al. "Coexpression of CCR7 and CXCR4 During B Cell Development Controls CXCR4 Responsiveness and Bone Marrow Homing". In: *Frontiers in Immunology* 10 (Dec. 2019).

[621] Milena Brunner et al. "Transcriptome analysis identifies CCR7 and cell adhesion molecules as mediators of B cell migration to the bursa of Fabricius during chicken embryonic development". In: *BMC Genomics* 26.1 (Dec. 2025).

[622] Benyu Liu et al. "Yeats4 drives ILC lineage commitment via activation of Lmo4 transcription". In: *Journal of Experimental Medicine* 216.11 (Nov. 2019), pp. 2653–2668.

[623] Izumi Sasaki et al. "Spi-B is critical for plasmacytoid dendritic cell function and development". In: *Blood* 120.24 (Dec. 2012), pp. 4733–4743.

[624] P. Burda, P. Laslo, and T. Stopka. "The role of PU.1 and GATA-1 transcription factors during normal and leukemogenic hematopoiesis". In: *Leukemia* 24.7 (June 2010), pp. 1249–1257.

[625] Tomasz Kostrzewski et al. “Multiple Levels of Control Determine How E4bp4/Nfil3 Regulates NK Cell Development”. In: *The Journal of Immunology* 200.4 (Feb. 2018), pp. 1370–1381.

[626] Ai Ping Mao et al. “Multiple layers of transcriptional regulation by PLZF in NKT-cell development”. In: *Proceedings of the National Academy of Sciences of the United States of America* 113.27 (July 2016), pp. 7602–7607.

[627] Tamara Goldfarb et al. “NCBI RefSeq: reference sequence standards through 25 years of curation and annotation.” In: *Nucleic acids research* 53.D1 (Jan. 2025), pp. D243–D257.

[628] Matthew S Hayden and Sankar Ghosh. “Regulation of NF-κB by TNF family cytokines.” In: *Seminars in immunology* 26.3 (June 2014), pp. 253–66.

[629] John D. Woronicz et al. “IκB Kinase-β: NF-κB Activation and Complex Formation with IκB Kinase-α and NIK”. In: *Science* 278.5339 (Oct. 1997), pp. 866–870.

[630] Yoshihiro Ueda et al. “Inflammation Controls B Lymphopoiesis by Regulating Chemokine CXCL12 Expression”. In: *Journal of Experimental Medicine* 199.1 (Jan. 2004), pp. 47–57.

[631] Andrea Paun, Estefania Claudio, and Ulrich K. Siebenlist. “Constitutive activation of NF-kB during early bone marrow development results in loss of B cells at the pro-B-cell stage”. In: *Blood Advances* 5.3 (Feb. 2021), pp. 745–755.

[632] Paula Araya et al. “Trisomy 21 dysregulates T cell lineages toward an autoimmunity-prone state associated with interferon hyperactivity”. In: *Proceedings of the National Academy of Sciences of the United States of America* 116.48 (Nov. 2019), pp. 24231–24241.

[633] M Murphy et al. “Tumor necrosis factor-alpha and IFN-gamma expression in human thymus. Localization and overexpression in Down syndrome (trisomy 21).” In: *Journal of immunology* 149.7 (Oct. 1992), pp. 2506–12.

[634] Alan D. Friedman. “C/EBPα in normal and malignant myelopoiesis”. In: *International Journal of Hematology* 101.4 (Apr. 2015), pp. 330–341.

[635] Cyril Seillet et al. “Nfil3 is required for the development of all innate lymphoid cell subsets”. In: *Journal of Experimental Medicine* 211.9 (2014), pp. 1733–1740.

[636] Mohamad F. Al Sayed et al. “T-cell–secreted TNFa induces emergency myelopoiesis and myeloid-derived suppressor cell differentiation in cancer”. In: *Cancer Research* 79.2 (Jan. 2019), pp. 346–359.

[637] Vionnie W.C. Yu and David T. Scadden. “Heterogeneity of the bone marrow niche”. In: *Current Opinion in Hematology* 23.4 (July 2016), pp. 331–338.

[638] Sandra Pinho and Paul S. Frenette. “Haematopoietic stem cell activity and interactions with the niche”. In: *Nature Reviews Molecular Cell Biology* 20.5 (May 2019), pp. 303–320.

[639] Laura M Calvi and Daniel C Link. “The hematopoietic stem cell niche in homeostasis and disease”. In: *Blood* 126.22 (Nov. 2015), pp. 2443–23451.

[640] Marc H.G.P. Raaijmakers et al. “Bone progenitor dysfunction induces myelodysplasia and secondary leukaemia”. In: *Nature* 464.7290 (Apr. 2010), pp. 852–857.

[641] Patrick M. Helbling et al. "Global Transcriptomic Profiling of the Bone Marrow Stromal Microenvironment during Postnatal Development, Aging, and Inflammation". In: *Cell Reports* 29.10 (Dec. 2019), pp. 3313–3330.

[642] Aysegul V Ergen, Nathan C Boles, and Margaret A Goodell. "Rantes/Ccl5 influences hematopoietic stem cell subtypes and causes myeloid skewing". In: *Blood* 119.11 (Mar. 2012), pp. 2500–2509.

[643] M L Wolf et al. "Development of a bone marrow culture for maintenance and growth of normal human B cell precursors." In: *Journal of immunology* 147.10 (Nov. 1991), pp. 3324–30.

[644] J R Pribyl, B N Dittel, and T W LeBien. "In vitro studies of human B lymphopoiesis." In: *Annals of the New York Academy of Sciences* 764 (Sept. 1995), pp. 9–18.

[645] Daitaro Kurosaka, Tucker W Lebien, and Julie A R Pribyl. "Comparative studies of different stromal cell microenvironments in support of human B-cell development". In: *Experimental Hematology* 27.8 (Aug. 1999), pp. 1271–1281.

[646] Michiko Ichii et al. "Regulation of human B lymphopoiesis by the transforming growth factor-β superfamily in a newly established coculture system using human mesenchymal stem cells as a supportive microenvironment". In: *Experimental Hematology* 36.5 (May 2008), pp. 587–597.

[647] Satoshi Yoshioka et al. "C/EBPβ expressed By Bone Marrow Mesenchymal Stromal Cells Is Indispensable For Precursor B-Cell Lymphopoiesis". In: *Blood* 122.21 (Nov. 2013), pp. 1213–1213.

[648] Soraya Tabera et al. "The effect of mesenchymal stem cells on the viability, proliferation and differentiation of B-lymphocytes". In: *Haematologica* 93.9 (Sept. 2008), pp. 1301–1309.

[649] Robert P Stephan, Colette R Reilly, and Pamela L Witte. "Impaired Ability of Bone Marrow Stromal Cells to Support B-Lymphopoiesis With Age". In: *Blood* (Jan. 1998), pp. 75–88.

[650] J Barker and C M Verfaillie. "A novel in vitro model of early human adult B lymphopoiesis that allows proliferation of pro-B cells and differentiation to mature B lymphocytes". In: *Leukemia* 14 (2000), pp. 1614–1620.

[651] Jeffrey S Miller et al. "Single Adult Human CD34 /Lin /CD38 Progenitors Give Rise to Natural Killer Cells, B-Lineage Cells, Dendritic Cells, and Myeloid Cells". In: *Blood* 93.1 (1999), pp. 96–106.

[652] Anne-Catherine Fluckiger et al. "In Vitro Reconstitution of Human B-Cell Ontogeny: From CD34 Multipotent Progenitors to Ig-Secreting Cells". In: *Blood* 92 (Dec. 1998), pp. 4509–4520.

[653] David J Rawlings et al. "Long-term culture system for selective growth of human B-cell progenitors". In: *Immunology* 92 (Feb. 1995), pp. 1570–1574.

[654] Simona Valletta et al. "Micro-environmental sensing by bone marrow stroma identifies IL-6 and TGFβ1 as regulators of hematopoietic ageing". In: *Nature Communications* 11.1 (Dec. 2020).

[655] J-I Ohkawara et al. “Culture system for extensive production of CD19 + IgM + cells by human cord blood CD34 + progenitors”. In: *Leukemia* 12 (Jan. 1998), pp. 764–771.

[656] Simon E. Richardson et al. “In vitro differentiation of human pluripotent stem cells into the B lineage using OP9-MS5 co-culture”. In: *STAR Protocols* 2.2 (June 2021).

[657] Sonja E Johnson et al. “Murine and Human IL-7 Activate STAT5 and Induce Proliferation of Normal Human Pro-B Cells 1”. In: *Journal of Immunology* 175.11 (Dec. 2005), pp. 7325–7331.

[658] J J Peschon et al. “Early lymphocyte expansion is severely impaired in interleukin 7 receptor-deficient mice.” In: *The Journal of experimental medicine* 180.5 (Nov. 1994), pp. 1955–1960.

[659] U von Freeden-Jeffry et al. “Lymphopenia in interleukin (IL)-7 gene-deleted mice identifies IL-7 as a nonredundant cytokine.” In: *The Journal of experimental medicine* 181.4 (Apr. 1995), pp. 1519–1526.

[660] Mana Momenilandi et al. “FLT3L governs the development of partially overlapping hematopoietic lineages in humans and mice”. In: *Cell* 187.11 (May 2024), pp. 2817–2837.

[661] Irwin D Bernstein, Robert G Andrews, and Krisztina M Zsebo. “Recombinant Human Stem Cell Factor Enhances the Formation of Colonies by CD34’ and CD34’lin-Cells, and the Generation of Colony-Forming Cell Progeny From CD34’lin-Cells Cultured With Interleukin-3, Granulocyte Colony-Stimulating Factor, or Granulocyte-Macrophage Colony-Stimulating Factor”. In: *Blood* 77.11 (June 1991), pp. 2316–2321.

[662] N Nishi et al. “Granulocyte-colony stimulating factor and stem cell factor are the crucial factors in long-term culture of human primitive hematopoietic cells supported by a murine stromal cell line.” In: *Experimental hematology* 24.11 (Sept. 1996), pp. 1312–21.

[663] Rafael F. Duarte and David A. Frank. “The synergy between stem cell factor (SCF) and granulocyte colony-stimulating factor (G-CSF): Molecular basis and clinical relevance”. In: *Leukemia and Lymphoma* 43.6 (2002), pp. 1179–1187.

[664] TR Ulich et al. “Stem cell factor in combination with granulocyte colony-stimulating factor (CSF) or granulocyte-macrophage CSF synergistically increases granulopoiesis in vivo”. In: *Blood* 78.8 (Oct. 1991), pp. 1954–1962.

[665] Nicolas Hipp et al. “IL-2 imprints human naive B cell fate towards plasma cell through ERK/ELK1-mediated BACH2 repression”. In: *Nature Communications* 8.1 (Dec. 2017).

[666] K. Taga, Akira Yamauchi, and E. T. Bloom. “Target cell-induced apoptosis in IL-2-activated human natural killer cells”. In: *Leukemia and Lymphoma* 32.5-6 (1999), pp. 451–458.

[667] Kimberly C Gilmour et al. “Defective expression of the interleukin-2/interleukin-15 receptor subunit leads to a natural killer cell-deficient form of severe combined immunodeficiency”. In: *Blood* 98.3 (Aug. 2001), pp. 877–879.

[668] Yavor K. Bozhilov et al. “In Vitro Human Haematopoietic Stem Cell Expansion and Differentiation”. In: *Cells* 12.6 (Mar. 2023).

[669] Aaron W. James. “Review of Signaling Pathways Governing MSC Osteogenic and Adipogenic Differentiation”. In: *Scientifica* 2013 (2013), pp. 1–17.

[670] Claire Pouget et al. “FGF signalling restricts haematopoietic stem cell specification via modulation of the BMP pathway”. In: *Nature Communications* 5 (2014).

[671] David J. Cohen et al. “Non-Canonical Wnt16 and microRNA-145 Mediate the Response of Human Bone Marrow Stromal Cells to Additively Manufactured Porous 3-Dimensional Biomimetic Titanium–Aluminum–Vanadium Constructs”. In: *Cells* 14.3 (Feb. 2025).

[672] Michael B. Berger et al. “Wnt16 Increases Bone-to-Implant Contact in an Osteopenic Rat Model by Increasing Proliferation and Regulating the Differentiation of Bone Marrow Stromal Cells”. In: *Annals of Biomedical Engineering* 52.6 (June 2024), pp. 1744–1762.

[673] Guiqian Chen, Chuxia Deng, and Yi Ping Li. “TGF-β and BMP signaling in osteoblast differentiation and bone formation”. In: *International Journal of Biological Sciences* 8.2 (Jan. 2012), pp. 272–288.

[674] Mengrui Wu et al. “The roles and regulatory mechanisms of TGF-β and BMP signaling in bone and cartilage development, homeostasis and disease”. In: *Cell Research* 34.2 (Feb. 2024), pp. 101–123.

[675] Petra Simic et al. “Systemically administered bone morphogenetic protein-6 restores bone in aged ovariectomized rats by increasing bone formation and suppressing bone resorption”. In: *Journal of Biological Chemistry* 281.35 (Sept. 2006), pp. 25509–25521.

[676] Mark J. Solloway et al. “Mice lacking Bmp6 function”. In: *Developmental Genetics* 22.4 (1998), pp. 321–339.

[677] Christian Kersten et al. “BMP-6 inhibits human bone marrow B lymphopoiesis - Upregulation of Id1 and Id3”. In: *Experimental Hematology* 34.1 (Jan. 2006), pp. 72–81.

[678] Rui Benedito et al. “The Notch Ligands Dll4 and Jagged1 Have Opposing Effects on Angiogenesis”. In: *Cell* 137.6 (June 2009), pp. 1124–1135.

[679] Douglas A. Johnston, Bamboo Dong, and Christopher C.W. Hughes. “TNF induction of jagged-1 in endothelial cells is NFκB-dependent”. In: *Gene* 435.1-2 (Apr. 2009), pp. 36–44.

[680] Rita Fragoso et al. “VEGF signaling on hematopoietic precursors restricts B-lymphoid commitment in vitro and in vivo”. In: *Experimental Hematology* 36.10 (2008).

[681] Nathan M. Novotny et al. “Differential IL-6 and VEGF secretion in adult and neonatal mesenchymal stem cells: Role of NFkB”. In: *Cytokine* 43.2 (Aug. 2008), pp. 215–219.

[682] Luigi Tarani et al. “Neuroinflammatory Markers in the Serum of Prepubertal Children with down Syndrome”. In: *Journal of Immunology Research* 2020 (2020).

[683] Akira Shimada et al. “Pro-inflammatory cytokinemia is frequently found in Down syndrome patients with hematological disorders.” In: *Leukemia research* 31.9 (Sept. 2007), pp. 1199–203.

[684] Ninib Baryawno et al. “A Cellular Taxonomy of the Bone Marrow Stroma in Homeostasis and Leukemia”. In: *Cell* 177.7 (June 2019), pp. 1915–1932.

[685] S. Chen et al. “Massive parallel RNA sequencing of highly purified mesenchymal elements in low-risk MDS reveals tissue-context-dependent activation of inflammatory programs”. In: *Leukemia* 30.9 (Sept. 2016), pp. 1938–1942.

[686] Lei Wang et al. “Inflammatory Bone Marrow Mesenchymal Stem Cells in Multiple Myeloma: Transcriptional Signature and In Vitro Modeling”. In: *Cancers* 15.21 (Nov. 2023).

[687] Yuqi Shen et al. *comBO: A combined human bone and lympho-myeloid bone marrow organoid for pre-clinical modelling of haematopoietic disorders*. Feb. 2025. URL: http://biorxiv.org/lookup/doi/10.1101/2025.02.16.638505.

[688] Matthew J. Kim, Rodrigo J. Valderrábano, and Joy Y. Wu. “Osteoblast Lineage Support of Hematopoiesis in Health and Disease”. In: *Journal of Bone and Mineral Research* 37.10 (Oct. 2022), pp. 1823–1842.

[689] Takafumi Yokota et al. “Adiponectin, a Fat Cell Product, Influences the Earliest Lymphocyte Precursors in Bone Marrow Cultures by Activation of the Cyclooxygenase-Prostaglandin Pathway in Stromal Cells”. In: *The Journal of Immunology* 171 (2003), pp. 5091–5099.

[690] Daniel L. Coutu et al. “Three-dimensional map of nonhematopoietic bone and bone-marrow cells and molecules”. In: *Nature Biotechnology* 35.12 (2017), pp. 1202–1210.

[691] Ireneusz Stolarek et al. “Dimensionality reduction by UMAP for visualizing and aiding in classification of imaging flow cytometry data”. In: *iScience* 25.10 (Oct. 2022), p. 105142.

[692] Siyu Zhu et al. *Cell signaling and transcriptional regulation of osteoblast lineage commitment, differentiation, bone formation, and homeostasis*. Dec. 2024.

[693] Hui-Xi Zhang et al. “Imputation of Human Primary Osteoblast Single Cell RNA-Seq Data Identified Three Novel Osteoblastic Subtypes”. In: *Frontiers in Bioscience-Landmark* 27.10 (Oct. 2022).

[694] Mark F. Pittenger et al. “Multilineage Potential of Adult Human Mesenchymal Stem Cells”. In: *Science* 284.5411 (Apr. 1999), pp. 143–147.

[695] Andrew R Marderstein et al. “Single-cell multi-omics map of human foetal blood in Down’s Syndrome”. In: ().

[696] T Komori, H Yagi, and S Nomura. *Targeted Disruption of Cbfa1 Results in a Complete Lack of Bone Formation owing to Maturational Arrest of Osteoblasts*. Tech. rep. 1997, pp. 755–764.

[697] Hirayuki Enomoto et al. “Induction of Osteoclast Differentiation by Runx2 through Receptor Activator of Nuclear Factor-κB Ligand (RANKL) and Osteoprotegerin Regulation and Partial Rescue of Osteoclastogenesis in Runx2–/– Mice by RANKL Transgene”. In: *Journal of Biological Chemistry* 278.26 (June 2003), pp. 23971–23977.

[698] Kazuhisa Nakashima et al. "The Novel Zinc Finger-Containing Transcription Factor Osterix Is Required for Osteoblast Differentiation and Bone Formation". In: *Cell* 108 (Jan. 2002), pp. 17–29.

[699] Karissa Ludwig et al. "Dominant osteogenesis imperfecta with low bone turnover caused by a heterozygous SP7 variant". In: *Bone* 160 (July 2022).

[700] Cuidi Xu et al. "ZEB1 Mediates Bone Marrow Mesenchymal Stem Cell Osteogenic Differentiation Partly via Wnt/β-Catenin Signaling". In: *Frontiers in Molecular Biosciences* 8 (May 2021).

[701] Carine Gubelmann et al. "Identification of the transcription factor ZEB1 as a central component of the adipogenic gene regulatory network". In: *eLife* 3.August2014 (Aug. 2014), pp. 1–30.

[702] Rana K. Gupta et al. "Transcriptional control of preadipocyte determination by Zfp423". In: *Nature* 464.7288 (Mar. 2010), pp. 619–623.

[703] Julie M. Quach et al. "Zinc finger protein 467 is a novel regulator of osteoblast and adipocyte commitment". In: *Journal of Biological Chemistry* 286.6 (Feb. 2011), pp. 4186–4198.

[704] Martina Gluscevic et al. "Functional expression of ZNF467 and PCBP2 supports adipogenic lineage commitment in adipose-derived mesenchymal stem cells". In: *Gene* 737 (May 2020).

[705] Sona Kang et al. "Regulation of Early Adipose Commitment by Zfp521". In: *PLoS Biology* 10.11 (Nov. 2012).

[706] William N. Addison et al. "Direct Transcriptional Repression of Zfp423 by Zfp521 Mediates a Bone Morphogenic Protein-Dependent Osteoblast versus Adipocyte Lineage Commitment Switch". In: *Molecular and Cellular Biology* 34.16 (Aug. 2014), pp. 3076–3085.

[707] Emanuela Chiarella et al. "ZNF521 Has an Inhibitory Effect on the Adipogenic Differentiation of Human Adipose-Derived Mesenchymal Stem Cells". In: *Stem Cell Reviews and Reports* 14.6 (Dec. 2018), pp. 901–914.

[708] Evan D. Rosen et al. "C/EBPα induces adipogenesis through PPARγ: A unified pathway". In: *Genes and Development* 16.1 (Jan. 2002), pp. 22–26.

[709] N. Salma, H. Xiao, and Anthony N. Imbalzano. "Temporal recruitment of CCAAT/enhancer-binding proteins to early and late adipogenic promoters in vivo". In: *Journal of Molecular Endocrinology* 36.1 (Feb. 2006), pp. 139–151.

[710] Stephen L Clarke, Claudius E Robinson, and Jeffrey M Gimble. "CAAT/Enhancer Binding Proteins Directly Modulate Transcription from the Peroxisome Proliferator- Activated Receptor Gamma2 Promoter". In: *Biochemical and Biophysical Research Communications* 240 (Sept. 1997), pp. 99–103.

[711] Zhaodan Cao, Robert M Umek, and Steven L Mcknight. "Regulated expression of three C/EBP lsoforms during adipose conversion of 3T3-L1 cells". In: *Genes and Development* 5 (June 1991), pp. 1538–1552.

[712] Fang-tsyr Lin and M Daniel Lane. "CCAAT/enhancer binding protein a is sufficient to initiate the 3T3-L1 adipocyte differentiation program". In: *Proceedings of the National Academy of Sciense, USA* 91 (May 1994), pp. 8757–8761.

[713] S. R. Farmer. "Regulation of PPARγ activity during adipogenesis". In: *International Journal of Obesity* 29 (2005), S13–S16.

[714] Hirohito Minami et al. "CXCL12–CXCR4 Axis Is Required for Contact-Mediated Human B Lymphoid and Plasmacytoid Dendritic Cell Differentiation but Not T Lymphoid Generation". In: *The Journal of Immunology* 199.7 (Oct. 2017), pp. 2343–2355.

[715] Reem Dowery, David Benhamou, and E Benchetrit. "Peripheral B cells repress B-cell regeneration in aging through a TNF-α/IGFBP-1/IGF-1 immune-endocrine axis". In: *Blood* 136.19 (Nov. 2020), pp. 2125–2132.

[716] KS Landreth, R Narayanan, and K Dorshkind. "Insulin-like growth factor-I regulates pro-B cell differentiation". In: *Blood* 80.5 (Sept. 1992), pp. 1207–1212.

[717] Laura F Gibson, Debra Piktel, and Kenneth S Landreth. "Insulin-Like Growth Factor-1 Potentiates Expansion of Interleukin-7-Dependent Pro-B Cells". In: *Blood* 82.10 (Nov. 1993), pp. 3005–3011.

[718] Zahia Hamidouche et al. "Crosstalks between integrin alpha 5 and IGF2/IGFBP2 signalling trigger human bone marrow-derived mesenchymal stromal osteogenic differentiation". In: *BMC Cell Biology* 11 (2010), p. 44.

[719] Sylvie Nathalie Hardouin et al. "Impaired mesenchymal stem cell differentiation and osteoclastogenesis in mice deficient for Igf2-P2 transcripts." In: *Development (Cambridge, England)* 138.2 (Jan. 2011), pp. 203–13.

[720] Yu Shi et al. "Hedgehog signaling activates a positive feedback mechanism involving insulin-like growth factors to induce osteoblast differentiation". In: *Proceedings of the National Academy of Sciences* 112.15 (Apr. 2015), pp. 4678–4683.

[721] Maria I Mascarenhas et al. "Identification of novel regulators of hematopoietic stem cell development through refinement of stem cell localization and expression profiling". In: *Blood* 114.21 (Nov. 2009), pp. 4645–45653.

[722] Vilma Barroca et al. "Paternal Insulin-like Growth Factor 2 (Igf2) Regulates Stem Cell Activity During Adulthood". In: *EBioMedicine* 15 (Feb. 2017), pp. 150–162.

[723] Isabelle Hansenne et al. "Dendritic Cell Differentiation and Immune Tolerance to Insulin-Related Peptides in Igf2-Deficient Mice". In: *The Journal of Immunology* 176.8 (Feb. 2006), pp. 4651–4657.

[724] Hanna Hanna, Lluis M. Mir, and Franck M. Andre. "In vitro osteoblastic differentiation of mesenchymal stem cells generates cell layers with distinct properties". In: *Stem Cell Research & Therapy* 9.1 (Dec. 2018), p. 203.

[725] Alexander Rasch et al. "Evaluation of bone allograft processing methods: Impact on decellularization efficacy, biocompatibility and mesenchymal stem cell functionality." In: *PloS one* 14.6 (2019), e0218404.

[726] Yi-Hsiung Lin et al. "Enhancement of Bone Marrow-Derived Mesenchymal Stem Cell Osteogenesis and New Bone Formation in Rats by Obtusilactone A." In: *International journal of molecular sciences* 18.11 (Nov. 2017).

[727] Yochai Wolf et al. "Autonomous TNF is critical for in vivo monocyte survival in steady state and inflammation". In: *Journal of Experimental Medicine* 214.4 (Apr. 2017), pp. 905–917.

[728] Christophe Caux et al. *Tumor Necrosis Factor-alpha Strongly Potentiates Interleukin-3 and Granulocyte-Macrophage Colony-Stimulating Factor-Induced Proliferation of Human CD34+ Hematopoietic Progenitor Cells*. Tech. rep. 1990.

[729] Hal E Broxmeyer et al. "The suppressive influences of human tumor necrosis factors on bone marrow hematopoietic progenitor cells from normal donors and patients with leukemia". In: *THE JOURNAL OF IMMUNOLOGY* 136.12 (June 1986), pp. 4487–4495.

[730] *Rheumatoid arthritis in adults: management NICE guideline*. Tech. rep. July 2018. URL: `www.nice.org.uk/guidance/ng100`.

[731] Liang Ma et al. "Reduced numbers of regulatory B cells are negatively correlated with disease activity in patients with new-onset rheumatoid arthritis". In: *Clinical Rheumatology* 33.2 (Feb. 2014), pp. 187–195.

[732] P. Conigliaro et al. "Restoration of peripheral blood natural killer and B cell levels in patients affected by rheumatoid and psoriatic arthritis during etanercept treatment". In: *Clinical and Experimental Immunology* 177.1 (July 2014), pp. 234–243.

[733] Zhe Li et al. "Anti-Tumor Necrosis Factor Therapy Restores Peripheral Blood B-cell Subsets and CD40 Expression in Inflammatory Bowel Diseases". In: *Inflammatory Bowel Diseases* 21.12 (Aug. 2015), pp. 2787–2796.

[734] Caterina Defendenti et al. "Anti-tumour necrosis factor-α antibodies and B cell homeostasis in human inflammatory bowel diseases". In: *International Immunopharmacology* 54 (Jan. 2018), pp. 329–335.

[735] Roy A. Black et al. "A metalloproteinase disintegrin that releases tumour-necrosis factor-α from cells". In: *Nature* 385.6618 (Feb. 1997), pp. 729–733.

[736] Marcia L. Moss et al. "Cloning of a disintegrin metalloproteinase that processes precursor tumour-necrosis factor-α". In: *Nature* 385.6618 (Feb. 1997), pp. 733–736.

[737] Geert van Loo and Mathieu J.M. Bertrand. "Death by TNF: a road to inflammation". In: *Nature Reviews Immunology* 23.5 (May 2023), pp. 289–303.

[738] Joan D. Pellegrini et al. "Membrane TNF-α/TNFR ratio correlates to MODS score and mortality". In: *Shock* 6.6 (Dec. 1996), pp. 389–396.

[739] Hiroki Mitoma et al. "Mechanisms for cytotoxic effects of anti–tumor necrosis factor agents on transmembrane tumor necrosis factor α–expressing cells: Comparison among infliximab, etanercept, and adalimumab". In: *Arthritis & Rheumatism* 58.5 (May 2008), pp. 1248–1257.

[740] Takahiko Horiuchi et al. "Transmembrane TNF-α: Structure, function and interaction with anti-TNF agents". In: *Rheumatology* 49.7 (Mar. 2010), pp. 1215–1228.

[741] Matthias Grell et al. "The transmembrane form of tumor necrosis factor is the prime activating ligand of the 80 kDa tumor necrosis factor receptor". In: *Cell* 83.5 (Dec. 1995), pp. 793–802.

[742] Audrey Moatti and José L. Cohen. *The TNF-α/TNFR2 Pathway: Targeting a Brake to Release the Anti-tumor Immune Response*. Oct. 2021.

[743] Takashi Nagasawa. "CXCL12/SDF-1 and CXCR4". In: *Frontiers in Immunology* 6 (June 2015).

[744] Dominic Chih-Cheng Voon, Yit Teng Hor, and Yoshiaki Ito. "The RUNX complex: reaching beyond haematopoiesis into immunity." In: *Immunology* 146.4 (Dec. 2015), pp. 523–36.

[745] Maria Rosaria Imperato et al. "The RUNX1–PU.1 axis in the control of hematopoiesis". In: *International Journal of Hematology* 101.4 (Apr. 2015), pp. 319–329.

[746] Jared R. Thomas et al. "Interaction of sexual dimorphism and gene dosage imbalance in skeletal deficits associated with Down syndrome". In: *Bone* 136 (July 2020).

[747] Boli Huang et al. "Isoenzymes of Pyruvate Dehydrogenase Phosphatase". In: *Journal of Biological Chemistry* 273.28 (July 1998), pp. 17680–17688.

[748] Yi-Hung Ou et al. "The candidate tumor suppressor BTG3 is a transcriptional target of p53 that inhibits E2F1". In: *The EMBO Journal* 26.17 (Sept. 2007), pp. 3968–3980.

[749] Nicholas G. Gottardo et al. "Identification of novel molecular prognostic markers for paediatric T-cell acute lymphoblastic leukaemia". In: *British Journal of Haematology* 137.4 (May 2007), pp. 319–328.

[750] Chengjie Zhou et al. "The transcription factor GABPA is a master regulator of naive pluripotency". In: *Nature Cell Biology* 27.1 (Jan. 2025), pp. 48–58.

[751] Shuyang Yu et al. "GABP controls a critical transcription regulatory module that is essential for maintenance and differentiation of hematopoietic stem/progenitor cells". In: *Blood* 117.7 (Feb. 2011), pp. 2166–2178.

[752] Batool Ossareh-Nazari et al. "Ubiquitylation by the Ltn1 E3 ligase protects 60S ribosomes from starvation-induced selective autophagy". In: *Journal of Cell Biology* 204.6 (Mar. 2014), pp. 909–917.

[753] Jessie Chu et al. "A mouse forward genetics screen identifies LISTERIN as an E3 ubiquitin ligase involved in neurodegeneration." In: *Proceedings of the National Academy of Sciences of the United States of America* 106.7 (Feb. 2009), pp. 2097–103.

[754] Fei Qin et al. "LTN1 promotes RLR degradation to inhibit immune response to RNA virus through the ESCRT pathway". In: *Autophagy* 20.6 (June 2024), pp. 1270–1285.

[755] Maddalena Adorno et al. "Usp16 contributes to somatic stem-cell defects in Down's syndrome". In: *Nature* 501.7467 (Sept. 2013), pp. 380–384.

[756] Yue Gu et al. "The histone H2A deubiquitinase Usp16 regulates hematopoiesis and hematopoietic stem cell function". In: *Proceedings of the National Academy of Sciences* 113.1 (Jan. 2016).

[757] Raquel Fernando et al. "Low steady-state oxidative stress inhibits adipogenesis by altering mitochondrial dynamics and decreasing cellular respiration". In: *Redox Biology* 32 (May 2020).

[758] Queelim Ch'ng, Derek Sieburth, and Joshua M. Kaplan. "Profiling synaptic proteins identifies regulators of insulin secretion and lifespan". In: *PLoS Genetics* 4.11 (Nov. 2008).

[759] Moritz M. Gaidt et al. “Self-guarding of MORC3 enables virulence factor-triggered immunity”. In: *Nature* 600.7887 (Dec. 2021), pp. 138–142.

[760] Lei Qin et al. “Mechanism of holocarboxylase synthetase and biotin supplementation in promoting adipose development”. In: *Journal of Animal Science and Technology* (Apr. 2025).

[761] Ravikanth Nanduri et al. “Epigenetic regulation of white adipose tissue plasticity and energy metabolism by nucleosome binding HMGN proteins”. In: *Nature Communications* 13.1 (Dec. 2022).

[762] Jian-Ye Liu et al. “RIPK4 promotes bladder urothelial carcinoma cell aggressiveness by upregulating VEGF-A through the NF-κB pathway”. In: *British Journal of Cancer* 118.12 (June 2018), pp. 1617–1627.

[763] Hongyi Zhou et al. “AGPAT3 deficiency impairs adipocyte differentiation and leads to a lean phenotype in mice”. In: *American Journal of Physiology - Endocrinology and Metabolism* 327.1 (July 2024), E69–E80.

[764] Mengli Yang et al. “Bta-miR-6517 promotes proliferation and inhibits differentiation of pre-adipocytes by targeting PFKL”. In: *Journal of Animal Physiology and Animal Nutrition* 106.6 (Nov. 2022), pp. 1197–1207.

[765] Jia Shen et al. “Effects of WNT3A and WNT16 on the Osteogenic and Adipogenic Differentiation of Perivascular Stem/Stromal Cells”. In: *Tissue Engineering - Part A* 24.1-2 (Jan. 2018), pp. 68–80.

[766] Verónica García-Alonso and Joan Clária. “Prostaglandin E 2 signals white-to-brown adipogenic differentiation”. In: *Adipocyte* 3.4 (2014), pp. 290–296.